

Universiteit
Leiden
The Netherlands

Synthetic tools to study ubiquitin biology

Shahul Hameed, D.A.

Citation
Shahul Hameed, D. A. (2020, June 23). *Synthetic tools to study ubiquitin biology*. Retrieved from https://hdl.handle.net/1887/123181

Version:	Publisher's Version
License:	Licence agreement concerning inclusion of doctoral thesis in the Institutional Repository of the University of Leiden
Downloaded from:	https://hdl.handle.net/1887/123181

Note: To cite this publication please use the final published version (if applicable).

Cover Page



Universiteit Leiden



The handle http://hdl.handle.net/1887/123181 holds various files of this Leiden University dissertation.

Author: Shahul Hameed D.A.
Title: Synthetic tools to study ubiquitin biology
Issue Date: 2020-06-23

Synthetic tools to study ubiquitin biology

Dharjath Ahamed Shahul Hameed

The research described in this thesis was performed at the Department of Cell Biology II at the Netherlands Cancer Institute in Amsterdam, the Netherlands, as well as at the Department of Chemical Immunology and the Department of Cell and Chemical Biology at Leiden University Medical Center in Leiden, the Netherlands. The work was financially supported by funding from Ubicode, the Dutch Research Council (NWO) and Oncode Institute.

ISBN: 978-94-6402-142-4

Author: D.A. Shahul Hameed
Front Cover: Yvonne Meeuwsen
Back Cover: Aysegul Sapmaz
Financial support: The Netherlands Cancer Institute and Leiden University
Printed by: Gildeprint B.V.

Copyright © 2020 by D.A.Shahul Hameed. All rights reserved. No part of this publication may be reproduced or transmitted in any form or by any means without prior written permission of the author, or where appropriate, of the publisher of the articles.

Synthetic tools to study ubiquitin biology

Proefschrift

ter verkrijging van
de graad van Doctor aan de Universiteit Leiden,
op gezag van Rector Magnificus prof. mr. C.J.J.M. Stolker,
volgens besluit van het College voor Promoties
te verdedigen op dinsdag 23 juni 2020
klokke 15:00 uur

door

Dharjath Ahamed Shahul Hameed

Geboren te Ambattur, India
Op 19 december 1984

Promotores
Prof. dr. H. Ovaa
Prof. dr. J.J.C. Neefjes
Co-promotor
Dr. A. Sapmaz

Leden promotiecommissie
Prof. dr. F. van Leeuwen – Nederlands Kanker Instituit
Prof. dr. N. Martin
Prof. dr. P. ten Dijke
Prof. dr. M. Vermeulen – Radboud Universiteit
Prof. dr. R. C. Hoeben
Dr. S. I. van Kasteren
Dr. L. Heitman

யாதானும் நாடாமால் ஊராமால் என்னொருவன்
சாந்துணையுங் கல்லாத வாறு.

-Thiruvalluvar (Thirukkural 397)

The learned make each land their own, in every city find a home;
Who, till they die; learn nought, along what weary ways they roam!

Meaning:

How is it that anyone can remain without learning, even to his death, when (to the learned man) every country is his own (country), and every town his own (town)?

In memory of my beloved father, A.Shahul Hameed and my beloved supervisor, Prof.dr.Huib Ovaa

Dedicated to all mothers

TABLE OF CONTENTS

Chapter 1 – *General Introduction* *9*

Chapter 2 – *Synthesis of isopeptide-linked diubiquitin chains* *31*

Chapter 3 – *Diubiquitin-based NMR analysis* *59*

Chapter 4 – *Development of a ubiquitin-based probe for metalloprotease deubiquitinases* *99*

Chapter 5 – *Enhanced delivery of synthetic labelled ubiquitin into live cells* *135*

Chapter 6 – *A Ub-derived cyclic peptide inhibitor for UCHL5* *155*

Chapter 7 – *Summary and Outlook* *173*

Nederlandse samenvatting *185*

List of publications *187*

Curriculum vitae *189*

Acknowledgements *191*

Chapter 1

General Introduction: How chemical synthesis of ubiquitin conjugates helps to understand ubiquitin signal transduction

Adapted from:
Hameed, D.S., A. Sapmaz, and H. Ovaa, *How Chemical Synthesis of Ubiquitin Conjugates Helps To Understand Ubiquitin Signal Transduction*. Bioconjug Chem, 2017. 28(3): p. 805-815

Summary

Ubiquitin (Ub) is a small post-translational modifier protein involved in a myriad of biochemical processes including DNA damage repair, proteasomal proteolysis, and cell cycle control. Ubiquitin signalling pathways have not been completely deciphered due to the complex nature of the enzymes involved in ubiquitin conjugation and deconjugation. Hence, probes and assay reagents are important to get a better understanding of this pathway. Recently, improvements have been made in synthesis procedures of Ub derivatives. In this perspective, we explain various research reagents available and how chemical synthesis has made an important contribution to Ub research.

Introduction

Ubiquitin (Ub) is a small 76 amino acid protein that can be covalently attached to a target protein in a process called ubiquitination in order to regulate protein function or lifespan. Three different classes of enzymes E1 (ubiquitin-activating enzyme), E2 (ubiquitin-conjugating enzyme) and E3 (ubiquitin ligase) facilitate different types of ubiquitination of a target protein. [1, 2] E1 activates ubiquitin as a thioester of the active site cysteine residue at the expense of ATP. The activated ubiquitin molecule is then transferred to an E2 enzyme by the formation of a new thioester with the catalytic cysteine residue of an E2 enzyme. From the E2 enzyme, ubiquitin can either be transferred to the catalytic cysteine residue of HECT or RBR classes of E3 enzymes or the E2-Ub loaded complex binds to RING class E3 enzymes forming an Ub-E2-E3 complex (Figure 1A). Finally, an isopeptide bond is formed between the C-terminal glycine residue (Gly76) and ε-NH_2 of a lysine residue of a substrate protein. Target specificity is determined by precise E2/E3 combinations to regulate the fate of a substrate. Ubiquitination can be reversed by the removal of ubiquitin from target proteins by deubiquitinating enzymes (DUBs) (Figure 1B). More than 90 DUBs are encoded in the human genome. [3]

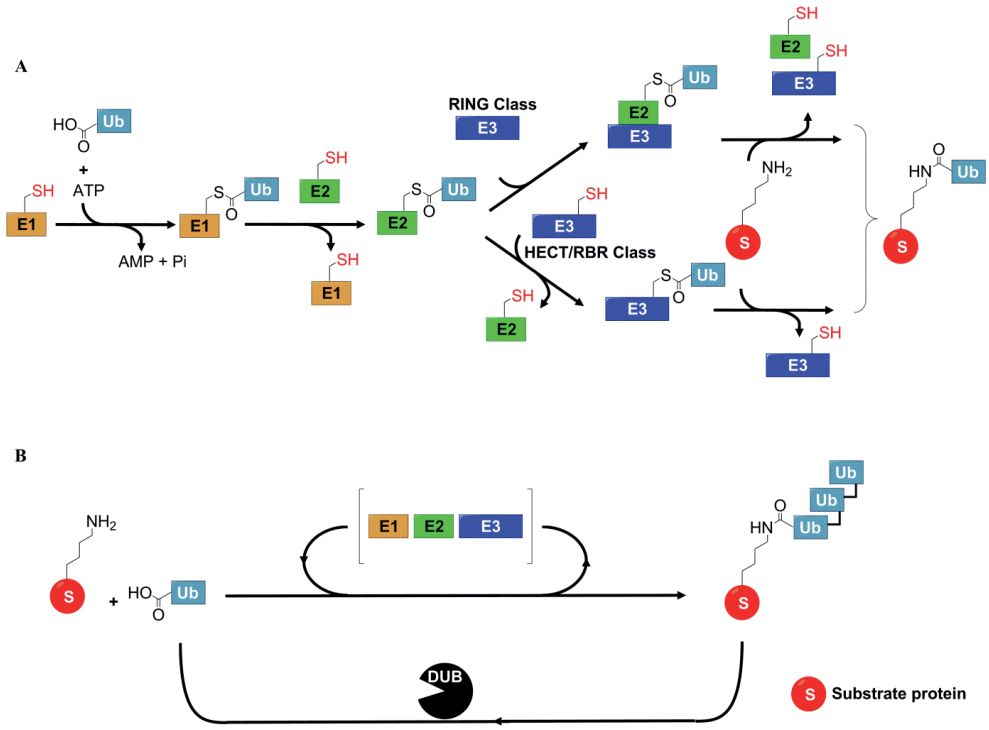


Figure 1: Schematic overview of the ubiquitin machinery. ***A***. *The ubiquitin conjugation pathway starts with the activation of ubiquitin as a thioester by a ubiquitin-activating enzyme E1, followed by transfer to a ubiquitin-conjugating enzyme (E2) and finally onto the target with the help of an E3 ligase.* ***B***. *Different types of ubiquitin chains are conjugated by the concerted action of different E1, E2 and E3 enzyme combinations. Ubiquitin removal is carried out by deubiquitinating enzymes (DUBs).*

Target proteins can be modified by monoubiquitination, multi-monoubiquitination or polyubiquitination. Ubiquitin contains an N-terminal methionine residue and seven internal lysine residues at positions 6, 11, 27, 29, 33, 48 and 63 which are all involved in the formation of different ubiquitin chains. [4, 5] Different types of ubiquitin chains are involved in many cellular events including proteasomal degradation, cell-cycle regulation, DNA repair and vesicle transport. The most well-studied Ub chains are the K48- and K63-linked polyUb chains. After the discovery that the degradation of proteins in the cell can be carried out by ubiquitin-mediated proteolysis, it was shown that cell cycle progression and protein degradation processes are abolished when the lysine 48 (K48) residue in Ub is changed to an arginine (R) residue suggesting that K48-linked polyubiquitin chains target proteins for proteasomal degradation. [6, 7] The K63-linked polyUb is important for other processes including DNA damage repair. [8] Furthermore, K11-linked polyUb has been associated with endoplasmic reticulum-associated degradation (ERAD)[9] and proteasomal degradation. [10]

DUBs are classified into USP, UCH, OTU and Josephin domain-containing proteases that belong to cysteine proteases class. A fifth DUB family, the JAMM/MPN+ domain-containing

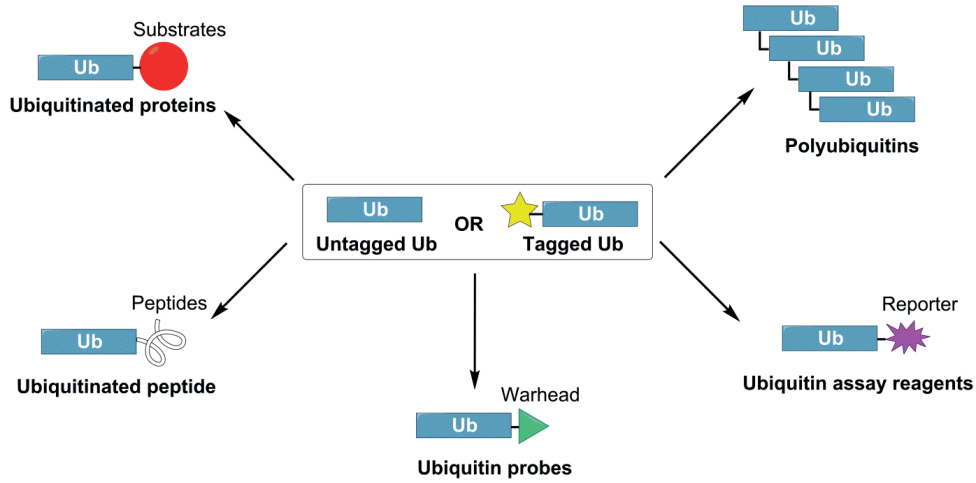


Figure 2: Overview of different DUB activity reporters*. Ub is chemically synthesized as tagged or untagged protein which can be further chemically modified into different Ub-conjugates, each used in different assays for DUB activity.*

proteins, is a family of metalloproteases. In the cysteine protease class of DUBs, the thiol group of the active site cysteine residue acts as a nucleophile that attacks the carbonyl group of the isopeptide bond between ubiquitin and the lysine residue of a target protein. [11] In the case of the JAMM/MPN+ metalloprotease class of DUBs, the active site contains a water molecule that is activated by a zinc atom coordinated by two histidine residues and a glutamate residue near the active site. This water molecule hydrolyzes the isopeptide bond thereby deconjugating ubiquitin from the target protein. [12, 13]

Defects in components of the ubiquitination process can contribute to disease pathogenesis, especially cancer and neurodegeneration. This makes them of interest as potential therapeutic targets. [14, 15] For example, the E3 ligase MDM2 ubiquitinates the tumour suppressor p53, regulating its levels in the cell by targeting them for proteasomal degradation. [16] The DUB USP7, in turn, regulates the stability of p53 by deubiquitination of both MDM2 and p53. [17]

Many ubiquitin-like modifiers (UBLs) have been identified as well. These UBLs include NEDD8, SUMO, ISG15, FAT10, Ufm1 and URM1. Although they are similar to Ub in sequence and structure, they have different functions. These UBL modifiers are attached to the target protein *via* their own dedicated E1, E2 and E3 enzymes and dedicated proteases recognize and deconjugate UBLs from the target although often crosstalk with enzymes from the ubiquitin machinery is observed. [18]

Ubiquitin-based probes and assay reagents are important as they help to provide insight into enzymatic activity and substrate recognition. Also, they have been important in the discovery of various new enzymes involved in the Ub machinery. Initially, reagents were generated by reversed proteolysis and later by intein chemistry. Various Ub conjugates have also been generated by chemical synthesis in order to study different components of the Ub signalling cascade (Figure 2). Such tools help in determining the kinetic properties and substrate specificity of the enzymes involved in the ubiquitination pathway, which in turn helps in the identification and characterization of interesting therapeutic targets.

Table 1A

Ub-based assay reagents	Applications	References
Ub-AMC	Fluorogenic assay reagent used to identify small molecule inhibitors for UCHL5 (see Figure 3A) (AMC: λ_{ex} 365nm; λ_{em} 440nm)	[19]
DiUb-AMC	Non-hydrolysable diUb molecule linked to AMC at the C-terminal end; Used to characterize special DUBs that have an additional Ub binding site (see Figure 3B) (AMC: λ_{ex} 365nm; λ_{em} 440nm)	[20]
Ub-Rho	Fluorogenic assay reagent with spectral properties not overlapping with most small molecule inhibitors (see Figure 3C) (Rho110: λ_{ex} 490nm; λ_{em} 550nm). An improved derivative based on morpholinecarbonyl-rhodamine 110 [21] is commercially available.	[22]
Ub-Lys-TAMRA-Gly	A fluorogenic reagent that is linked by an isopeptide bond; used in Fluorescence polarization assays (see Figure 3D) (TAMRA: λ_{ex} 550nm; λ_{em} 590nm)	[23]
Ub-(pep)TAMRA	Similar to Ub-Lys-TAMRA-Gly, but with substrate specificity for the DUBs determined by the peptide (see Figure 3E)	[23, 24]
Ub-Luc	Bioluminescence-based assay reagent with low background noise - suited for DUBs that require high substrate concentrations (see Figure 4)	[25]
diUb-based FRET pair	FRET-based assay reagents used to identify Ub linkage specificity of DUBs (see Figure 5A)	[26-29]
Tb-Ub/Fl-Ub	Ub with different fluorescently labelled dyes for FRET-based assays, used in characterizing UBC13, an E2 enzyme (see Figure 5B)	[30]

Table 1B

Activity-based probes with a Ub backbone	Applications	References
Ub-VS	An α,β unsaturated sulfone at the C-terminal end of Ub that can label DUBs. It was used to identify USP14 as a proteasome-associated DUB (see Figure 6A)	[31]

Ub-VME	An α,β unsaturated ester at the C-terminal end of Ub that can covalently react with many of the known cysteine protease DUBs (see Figure 6B)	[32, 33]
Ub-PRG	Relatively stable Ub-based probe for cysteine protease DUBs with an alkyne functionality as warhead at the C-terminal end of Ub (see Figure 6C)	[34]
DiUb-based DUB probes	DiUb molecules of different linkages equipped with a warhead positioned either between two Ub molecules or at the C-terminal end of the diUb to identify linkage-specific DUBs (see Figure 7)	[20, 35-39]
Ub-based E1/E2/E3 probe	Ub based probe containing a warhead at the C-terminal end of Ub that can target E1, E2 and E3 enzymes (see Figure 8)	[40-44]

***Table 1: Overview of currently available Ub-based assay reagents and active-site directed probes**. **A**. Representative Ub-based assay reagents to study DUB activity. **B**. Activity-based probes used to study different DUBs and E1, E2 and E3 enzymes.*

Various Ub-based probes and assay reagents are available especially for the cysteine protease class of DUBs and for conjugating enzymes. Examples are given in Table 1. In this review, we will discuss the development of Ub-based probes and activity reporters and how chemical synthesis has contributed to the current understanding of Ub signal transduction.

In-vitro generated ubiquitinated proteins and peptides

The fate of a ubiquitinated protein in a cell depends on the site and the type of ubiquitination involved. Polyubiquitination can lead to different responses based on the position of the isopeptide bond and the number of ubiquitin molecules attached to the target protein. K48- and K63-linked polyubiquitin chains are the best-studied chains. The functions of other polyubiquitin chains (lysine 6, 11, 27, 29, 33 and the methionine 1 linked chains) have been explored more recently. Not all enzymes that make specific polyubiquitin chains are currently known, but fortunately, several non-enzymatic methods have been recently developed to make well-defined ubiquitin conjugates.

Polyubiquitin chains bind to specific elements in "reader" proteins leading to different Ub signalling transduction events. To prevent premature chain cleavage, non-hydrolyzable ubiquitin conjugates that are resistant to DUB activity can be used. In 2000, Yin *et al.* reported the biochemical synthesis of non-hydrolyzable Ub dimers where Ub molecules containing cysteine residues at specific sites were cross-linked using dichloroacetone. [45] Recently, Lewis *et al.* used a similar approach to cross-link Ub with α-Synuclein and studied their mechanism of aggregation. [46] The triazole linkage is another example of a non-hydrolyzable link that can be formed by a click reaction between an alkyne and an azido group and serves as a good isostere of the naturally occurring peptide bond. In 2010, Eger *et al.* were able to incorporate an alkyne and an azide functionality in ubiquitin using orthogonal tRNA/tRNA synthetase pair in a bacterial expression system and made non-hydrolyzable ubiquitin dimers. *[47]* Similarly, Wiekart *et al.* were able to incorporate an alkyne functionality in SUMO and made non-hydrolyzable SUMO-peptide conjugates. *[48]* However, the use of a bacterial expression system limits the number of possible modifications. To overcome this problem, chemical synthesis of polypeptides provides an

attractive alternative. Jung *et al.* were able to incorporate a non-hydrolyzable thioether functionality in a lysine 63-linked diubiquitin molecule. *[49]* Shanmugham *et al.* incorporated an oxime functionality between the C-terminus of ubiquitin and specific lysine positions on polypeptides derived from PCNA, PTEN, H2A and H2B. *[50]* Such non-hydrolysable ubiquitin conjugates can be used for determining the substrate selectivity of certain DUBs.

Chemical synthesis of ubiquitin to make ubiquitin conjugates

The efficiency of the chemical synthesis of a polypeptide depends highly on the number of amino acid couplings carried out during synthesis. This makes the linear synthesis of proteins challenging. The first chemical synthesis of ubiquitin was reported in 1989 by Briand *et al.* and Ramage *et al.* [51] [52] Over the years, technologies for the synthesis of long polypeptides have improved allowing for an increase in the yield and purity of the produced polypeptides. Ubiquitin has been synthesized in a linear fashion using an optimized procedure[53] or in a step-wise modular fashion using native chemical ligation (NCL)[54] and subsequent desulfurization. [55] Chemical synthesis has the advantage that site-specific incorporation of unnatural amino acids, labels and pull-down handles is possible in virtually any position.

Using Fmoc-based solid-phase peptide synthesis (SPPS), the N-terminal end of Ub can be coupled to short peptide epitope tags like Human influenza hemagglutinin (HA), His_6 or Biotin. Such modified Ub molecules can be used in Western Blots (WB) or pull-down assays. Modifications of the internal residues of Ub, especially at one of the seven Lys position, are useful to chemically make Ub conjugates. This may involve a native chemical ligation handle or a 'click' handle instead of lysine. The C-terminal end of Ub can be modified by mild cleavage of the fully protected Ub from a trityl resin, followed by global deprotection and purification. In this manner, fluorogenic molecules or reactive moieties may be introduced that can selectively target enzymes involved in the ubiquitination pathway.

The site-specific incorporation of the unnatural amino acid thiolysine has allowed the synthesis of ubiquitinated reagents including ubiquitinated peptides, polyubiquitin chains and diubiquitin molecules. [53, 55] The synthesis and use of such conjugates have been reviewed extensively. [56-58] One development is the synthesis of diubiquitin-based reagents that have made it possible to monitor the chain specificity of DUBs including the USP enzymes[59] and the OTU proteases. [60, 61] Other diUb-based linkage specific reagents have been developed recently using chemical means which revealed the mechanism of action for specific DUBs. [20, 29] Also, these diubiquitin molecules have been used to determine the linkage specificity of specific DUBs and for the characterization of DUB inhibitors using mass spectrometry. [61] Polyubiquitin chains synthesized from recombinant proteins through click linkages have been used to study interactions with binding domains. [47, 62] Also, ubiquitinated peptides have also been generated to the study substrate-specificity of DUBs. [24]

Ubiquitin conjugates: activity-based probes and activity reporters based on ubiquitin

Ubiquitin conjugated to reporter molecules has been used to study the biochemical properties of many DUBs. Initially, such molecules were synthesized by purifying expressed Ub and introducing reporter molecules by reverse trypsinolysis. [63] Later, intein chemistry was used to generate Ub as an activated thioester. [31] More recently, chemical synthesis has provided an efficient route to such reagents. [24, 53, 55]

Ubiquitin assay reagents

Ub-based assay reagents consist of Ub attached to a reporter molecule at the C-terminal end. DUBs recognize Ub and cleave the reporter molecules that can be fluorogenic or bioluminescent. In case of DUBs that are specific for a particular Ub linkage, unlabeled chains can be used in a gel-based assay, or a labelled diUb-based reagent can be used for measuring enzyme kinetics. Sometimes, two different sets of fluorescent Ub molecules can be assembled using ubiquitinating enzymes and the resulting FRET readout can be used to characterize such enzymes. [30]

Fluorogenic ubiquitin reagents

Fluorogenic assay reagents based on Ub contain a fluorogenic molecule attached *via* an amide bond at the C-terminal end of Ub. DUBs recognize Ub and hydrolyze the amide linkage at the C-terminal glycine residue in Ub, releasing a fluorescent reporter molecule, which can be used to measure the DUB activity over time (Figure 3).

One of the earliest reported fluorogenic substrates for DUBs is Ub amidomethyl coumarin (UbAMC) by Dang *et al.* (Figure 3A). [19] They were able to synthesize Ub-AMC using a transpeptidation reaction involving Ub, GlyGlyAMC and trypsin. This substrate was used to characterize UCH-L3 and Isopeptidase T enzyme kinetics. In addition, they were able to test the inhibition kinetics of Ubiquitin aldehyde, a DUB inhibitor. UbAMC can now be easily prepared by chemical synthesis. [53] Recently, Flierman *et al.* reported a fluorogenic assay reagent based on AMC where non-hydrolysable diUb molecules of different linkages were attached to AMC at their C-terminal end. [20] These reagents serve as a specific substrate for DUBs that have an additional Ub binding site (S2 binding site) (Figure 3B). Another fluorogenic substrate called Ub-Rho110 (Figure 3C) was first described by Hassiepen *et al*. [22] It was used in the screening of inhibitors for UCHL3 and USP2. Both Ub-AMC and Ub-Rho110 contains a peptide bond at the C-terminal end of Ub. However, the majority of naturally occurring Ub conjugates have an isopeptide bond instead. Although many DUBs cleave a normal peptide bond at the C-terminal end of Ub, an isopeptide linked Ub assay reagent would be a more relevant substrate for DUBs. The earliest report on an isopeptide-linked ubiquitin assay reagent was by Tirat *et al.* who used fluorescent polarization assays to study the biochemistry of DUBs. [23] They generated a short peptide sequence surrounding the K48 position in Ub by SPPS. A fluorescent molecule (TAMRA) was attached to the N-terminus of the peptide. Full-length ubiquitin, E1 and E2 enzymes were then added to this peptide to yield a fluorescent ubiquitin-peptide conjugate. Changes in the fluorescence polarization occur when a DUB cleaves the isopeptide bond between ubiquitin and a TAMRA-labelled peptide (Figure 3D). This reagent was used to validate the enzyme kinetics of UCHL3 and USP2. However, this technique requires the use of both E1 and E2 enzymes, which limits the nature of the peptide that can be conjugated to Ub.

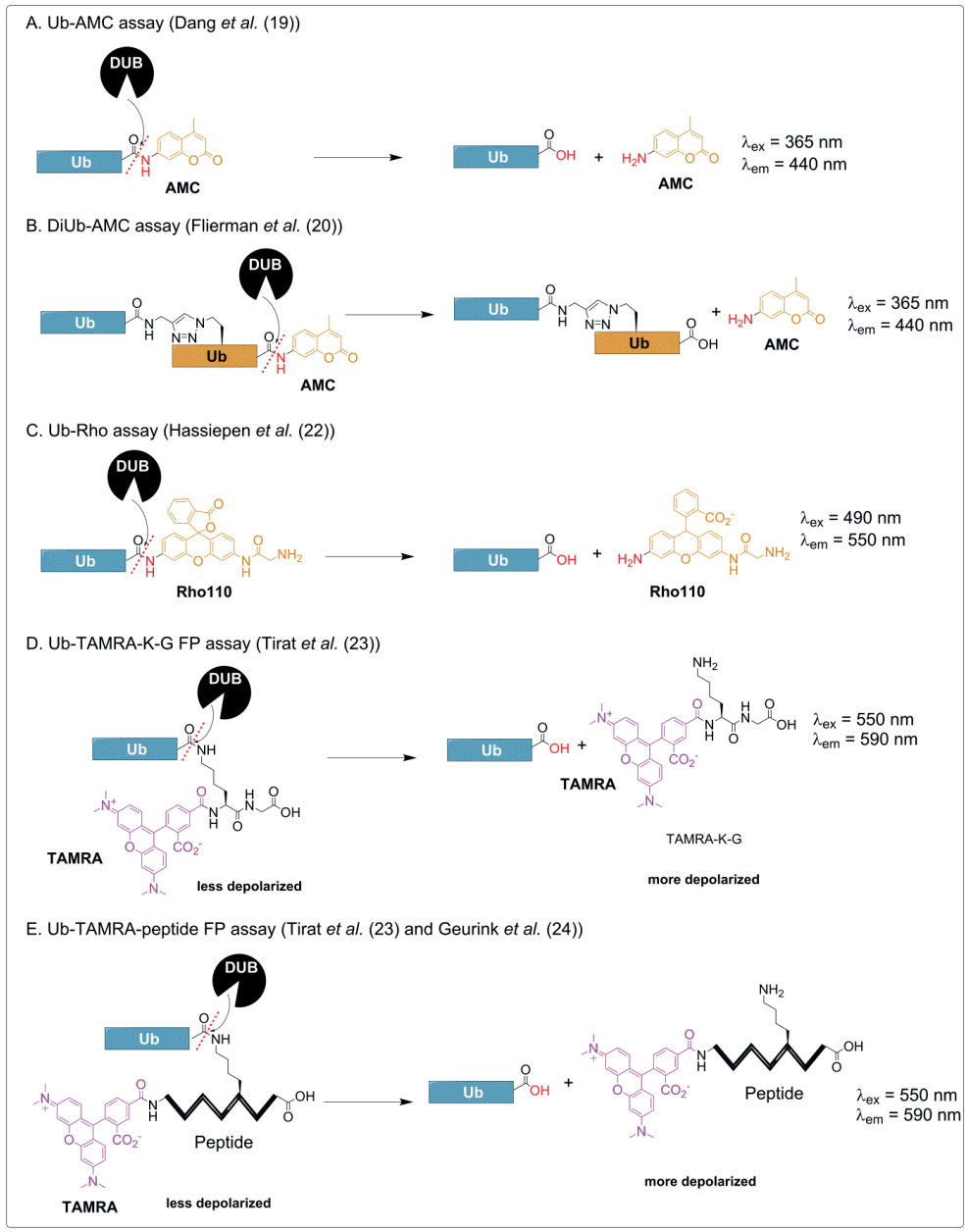


Figure 3: Ubiquitin-based assay reagents. A. *Ub-AMC,* ***B.*** *non-hydrolysable diUb-AMC and* ***C.*** *Ub-Rho assay reagents, all work on the principle of increase in fluorescence upon DUB cleavage.* ***D and E.*** *Fluorescent Polarization (FP) assay reagents. These reagents consist of a TAMRA-linked peptide attached to the C-terminal end of Ub by an isopeptide bond. Upon DUB-mediated cleavage, the TAMRA-containing peptide is released, and its fluorescence polarization is measured.*

In 2012, Geurink *et al.* synthesized a fluorescent Ub-peptide and UBL-peptide assay reagents using SPPS and subsequent NCL and desulfurization (Figure 3E). [24] Ub or UBL were activated as a thioester using E1 and MESNa (sodium 2-mercaptoethanesulfonate) in the presence of thiolysine containing peptides. The NCL products were then desulfurized and used in cleavage assays. Site-specific incorporation of the thiolysine handle by SPPS has expanded the choice of peptides that can be conjugated to Ub and also allows the generation of reagents based on UBLs like NEDD8 and SUMO-1, -2 and -3.

Bioluminescent ubiquitin reagents

Some of the DUBs have lower affinity for their substrates due to which a higher substrate concentration is needed in a DUB assay. This often results in more background noise causing problems with the measurement. To avoid this problem, Orcutt *et al.* designed a bioluminescence-based assay to study DUBs at lower concentrations. [25]

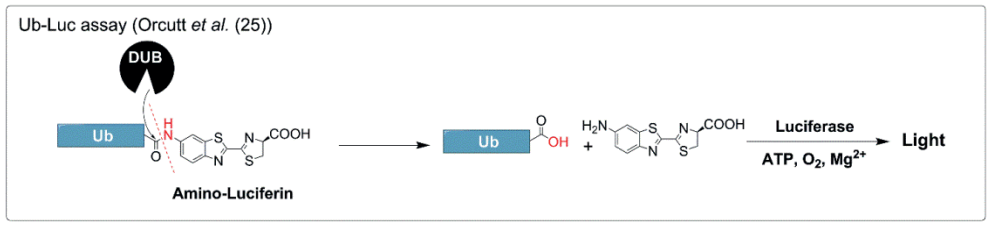


Figure 4: Ub-based bioluminescent assay reagent. *DUBs act on the Ub-Luc reagent which releases free amino-luciferin. Luciferase, that is already present in the reaction mix, acts on this amino-luciferin which leads to bioluminescence.*

The bioluminescent assay reagent consists of a Ub molecule linked to amino-luciferin at its C-terminal end (Ub-Luc). The DUB acts on the Ub-Luc releasing free amino-luciferin (Figure 4). Since amino-luciferin is not luminescent by itself, background noise is almost absent. Then, luciferase enzyme acts on the free luciferin in the presence of ATP and Mg^{2+}, leading to oxidation of aminoluciferin, thereby releasing photons. This technique was used to assay a panel of DUBs and in high throughput screening (HTS). However, care must be taken while using this reagent in an HTS assay because the small molecules may also inhibit luciferase.

FRET-based ubiquitin assay reagents

In order to study the Ub-linkage specificity of DUBs and their enzyme kinetics, labelled diUb-based assay reagents are used. In 2012, Ohayon *et al*. reported the chemical synthesis of a ubiquitinated peptide that was used in a FRET-based assay in HTS to identify small molecule inhibitors for UCHL3. [26] Later on, Ye *et al*. reported the enzymatic approach to make FRET-pair diUb reagents that were used to characterize ubiquitin-binding domains and DUBs. [27] Arnst *et al.* also used such a reagent in a Fluorescence Resonance Energy Transfer (FRET)-based assay in order to characterize the K63 linkage-specific metalloprotease-DUB AMSH (Figure 5A). *[28]* They used a diUb molecule in which two fluorescently labelled Ub modules were linked at position K63. Due to the proximity of the two fluorescent dyes, a FRET signal is observed. Upon adding AMSH, the FRET signal decreases over time. More recently, Geurink *et al.* have made a panel of all seven isopeptide-linked diUb-based FRET assay reagent using chemical synthesis. [29] The diUb-based FRET assay reagents were prepared by native chemical ligation using Rhodamine-Ub (FRET-

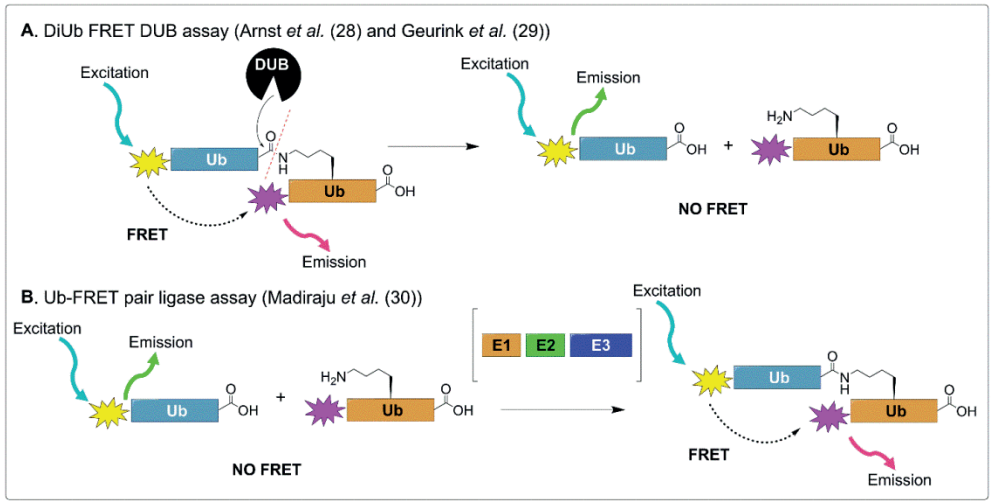


Figure 5: Ubiquitin-based assay FRET assay reagents A. *DiUb FRET assay reagent in which two different fluorescently labelled Ub molecules are linked by a native isopeptide bond. Upon DUB activity, the diUb-based reagent is cleaved, and the FRET signal decreases over time.* ***B.*** *FRET-based Ub ligase assays where two different fluorescently labelled Ub molecules form a diUb with the help of a specific E1, E2 and E3 enzyme combination. When the two fluorescent dyes are in close proximity, the FRET signal increases.*

donor) and TAMRA Ub (FRET-acceptor). The changes in the FRET signal upon DUB activity can be used to quantify the enzyme kinetics.The FRET-based assay can also be used to characterize ubiquitination enzymes. In 2012, Madiraju *et al.* used this technique to characterize the E2 enzyme UBC13-UEV1A (Figure 5B). [30] In this study, terbium-labelled Ub and fluorescein-Ub were used in a reaction containing E1 and UBC13-UEV1A (E2). Upon Ub chain formation and elongation due to the E1-E2 enzyme activity, the FRET signal between terbium and fluorescein is increased. This gives a real-time measurement of enzyme activity. The technique was used primarily in a high throughput screen for small molecules that can inhibit UBC13. In all these cases, the inherent nature of ubiquitin recognition by a DUB is used. However, DUBs often are specific to polyubiquitin chains, or ubiquitinated substrates. Hence the processing capacity of a DUB for these ubiquitin-small molecule conjugate assay reagents may not reflect the true activity of these enzymes. To measure the activity of a DUB more specific reagents are often needed.

Ubiquitin-based probes for the covalent capture of DUBs

Most of the DUBs are cysteine proteases, containing a catalytically active cysteine residue. Ub-based DUB probes can be used to visualize such DUBs in biochemical assays using SDS PAGE-based readouts. A thiol-reactive functionality is positioned in the probe in such a way that a covalent adduct with the active site cysteine residue of the DUB is formed. Such probes have been reviewed extensively by Ekkebus *et al.* [64] In this review, we give only a brief account of the different probes reported so far.

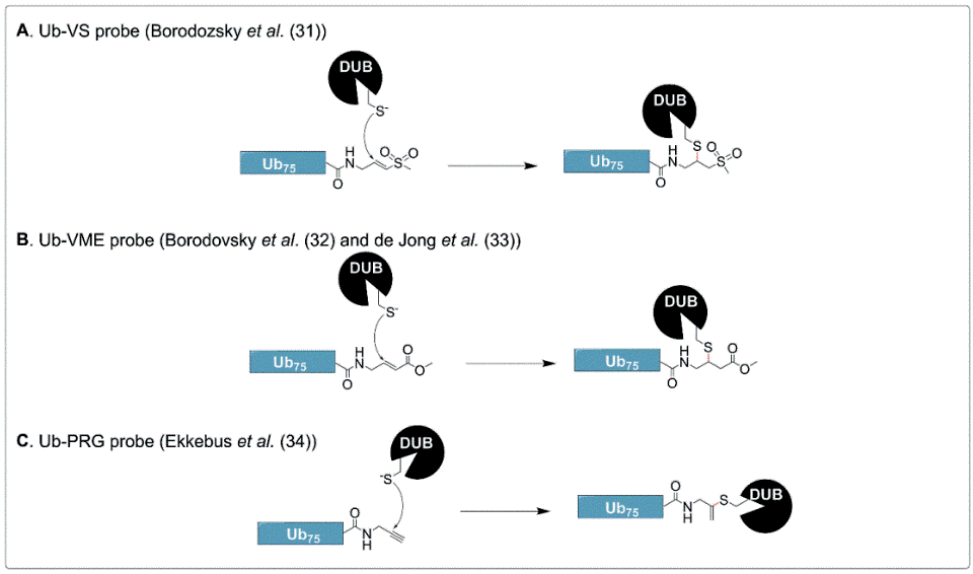


Figure 6: Monoubiquitin-based probes for cysteine protease class of DUB. A. *Ub-vinyl sulfone (UbVS) probe. In this monoUb-based probe, a vinyl sulfone Michael acceptor is positioned at the C-terminal end of Ub and used to capture DUBs at their active site.* ***B.*** *Ub-vinyl methyl ester (UbVME) probe. In this reagent, a vinyl methyl ester is used to covalently trap the active site of DUBs.* ***C.*** *Ub-propargyl (Ub-PRG) probe. The Michael acceptor is a terminal alkyne that can form a covalent adduct with the active site of DUBs.*

Many types of Ub-based DUB probes (Figure 6) have been developed using intein-fusions, including ubiquitin vinyl sulfone (Ub-VS)[31] and several derivatives including ubiquitin vinyl methyl ester (Ub-VME). [32] Using intein chemistry ubiquitin-like probes can also be prepared. [65] One of the main advantages of such covalent inhibitors is the use of epitope-tagging at the N-terminal end of ubiquitin allowing retrieval and detection or identification of DUBs. This includes tags that can be used in western blot and pull-down assays or fluorescent molecules that can be used to visualize DUBs in an SDS-PAGE protein gel. In 2012, de Jong *et al.* reported the total chemical synthesis of Ub-based probes. [33] In this method, a reactive vinyl methyl ester (VME) moiety was coupled to the C-terminus of ubiquitin by chemical synthesis. The free N-terminus was then labelled with a fluorescent dye like TAMRA, or peptide epitope tag such as HA. In 2013, Ekkebus *et al.* reported another activity-based DUB probe based on the unexpected reactivity of a propargyl group incorporated at the C-terminus of ubiquitin. [34] Sommer *et al.* independently reported the development of a SUMO-based propargyl probe for SUMO-specific proteases. [66] In this case, the SUMO protein was expressed as an intein-fusion and then modified with a terminal alkyne. To characterize DUBs that specifically hydrolyze different lysine-linked ubiquitin chains,[59, 61, 67] diUb-based probes have been used. In such probes, both the Ub moieties can bind to linkage-specific DUBs. Generally, in a diUb molecule, the Ub that is linked at its C-terminal end is called distal Ub while the lysine-linked Ub is called proximal Ub. In a diubiquitin-based probe, a reactive group is positioned at the site of action of the DUB, which can be either between the two ubiquitin moieties or at the C-terminal end of the diubiquitin molecule (Figure 7).

Iphofer *et al.* reported the first linkage-specific DUB probe where the C-terminus of a distal ubiquitin is linked to short peptides surrounding K48 or K63 of another ubiquitin and a reactive Michael acceptor is positioned instead of the isopeptide bond between the two Ub modules (Figure 7B). [35] This reacts specifically with DUBs that recognize this linkage by forming a covalent adduct at the active site of the DUB. This technique can be extended to other peptides derived from different substrates of DUBs. Later on, McGouran *et al.* developed a diubiquitin based probe containing the reactive trap at the site of isopeptide bond between two full-length Ub molecules that are linked by a non-hydrolyzable triazole moiety (Figure 7C). [36] Later on, different versions of a diUb-based probe were developed independently by Li *et al.*[37] (Figure 7D) who used a vinyl amide warhead positioned between two ubiquitin molecules and Haj-Yahya *et al.*[38] (Figure 7E) who used a dehydroalanine group. In 2014, Mulder *et al.* reported another diUb-based DUB probe that can be prepared in large quantities (Figure 7F). [39] Here, native chemical ligation was used to synthesize a diubiquitin molecule in which the subsequent elimination of a thiol residue resulted in the formation of a Michael acceptor warhead positioned at the appropriate site for reaction with a cysteine residue in the DUB catalytic site. These probes form a stable covalent interaction with the DUBs, which can be further used for structural studies. More recently, Flierman *et al.* reported another diUb-based probe with a propargyl warhead positioned at the C-terminal end of the proximal Ub (Figure 7G). [20] With this reagent, DUBs that have an additional Ub-binding site (S2) in poly-Ub chains can be characterized.

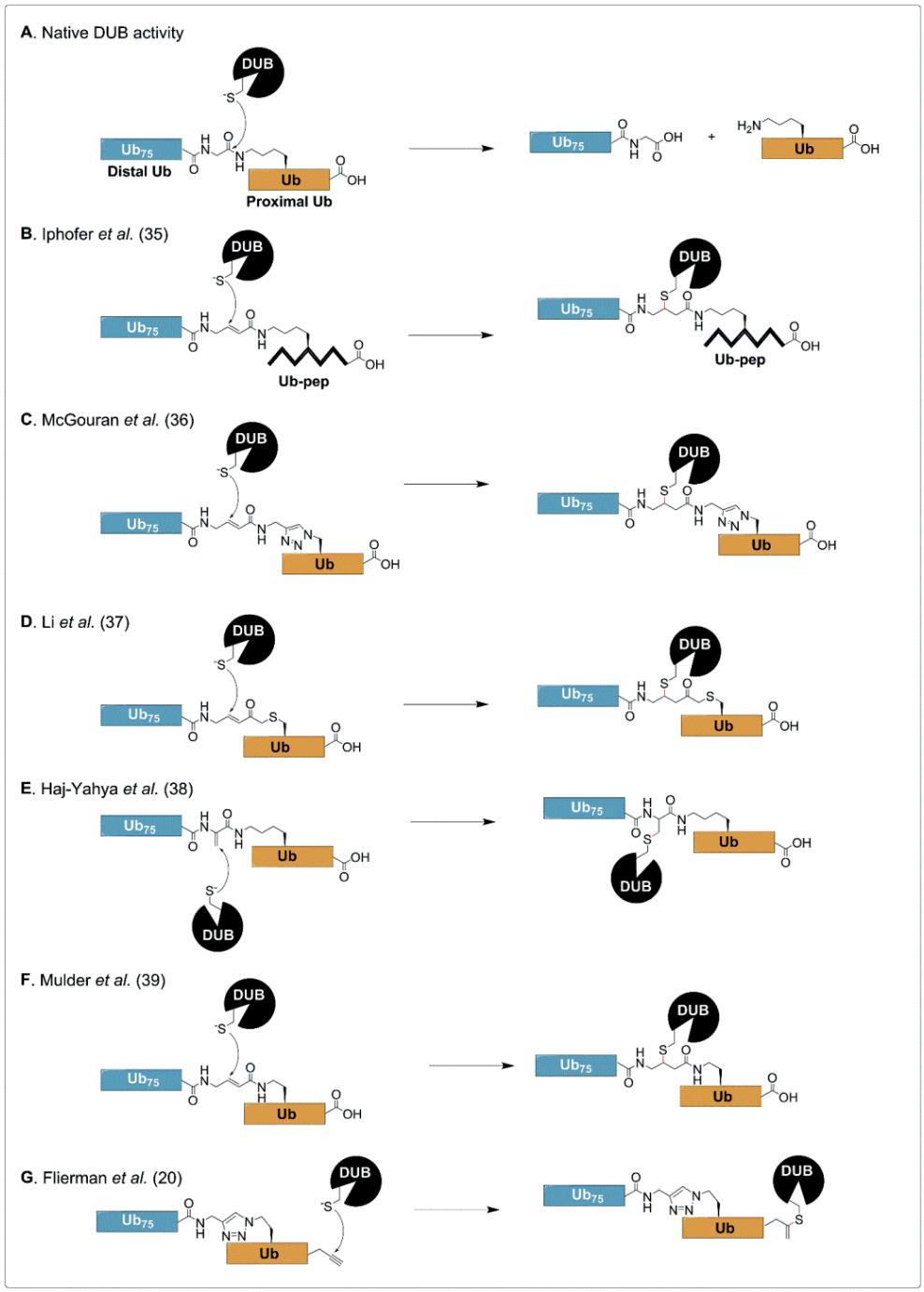

A. Native DUB activity
DUB
Ub75
Distal Ub
Ub
Proximal Ub
B. Iphofer et al. (35)
Ub-pep
C. McGouran et al. (36)
D. Li et al. (37)
E. Haj-Yahya et al. (38)
F. Mulder et al. (39)
G. Flierman et al. (20)

Figure 7: Diubiquitin-based probes. ***A.*** *Mechanism of diUb cleavage. The active site cysteine of a DUB acts on the carbonyl group of the C-terminal glycine residue in the distal Ub module. This makes the bond scissile and the resulting thioester intermediate is hydrolysed by a water molecule.* ***B.*** *Substrate-specific DUB probe using Ub and a short peptide derived from a substrate protein with an electrophilic centre positioned in between.* ***C–F.*** *Various diUb-probes using different types of Michael acceptors positioned between the distal and the proximal Ub.* ***G.*** *DiUb-based DUB probe where an alkyne group is positioned at the C-terminal end of the proximal Ub module.*

Ubiquitin-based probes for E1, E2 and E3 enzymes

Although several Ub-based probes have been developed for DUBs, probes that can target the ubiquitination enzymes (E1, E2 and E3) are challenging to make, due to the sequential trans-thioesterification reactions in the ligation cascade (Figure 8A). In particular, UbE1 activates Ub as a Ub-adenylate intermediate at the expense of ATP. This is then exchanged for the thiol in the active site of E1 to form an E1-Ub thioester complex. Upon subsequent trans-thioesterification by E2 and E3 (HECT/BRB class) or with the help of a RING E3 ligase, Ub is transferred onto a substrate protein forming a peptide or an isopeptide bond between them. However, few Ub-based probes for such enzyme cascade have been reported very recently. Among the earliest Ub-based probes for E1 are the Ub-AMP mimics. In 2010, Lu *et al.* have shown that a non-hydrolyzable Ub/UBL-adenylate mimic could be used to covalently trap the E1 enzyme (Figure 8B). [40] Later on, An and Statsyuk reported a mechanism-based AMP-derived compound that mimics the Ub/UBL-adenylate upon reacting with the E1-Ub/UBL thioester, which was used as an activity-based probe for E1 enzymes for Ub and different UBLs and as selective inhibitors (Figure 8C). [41] More recently, the same authors reported a dehydroalanine analogue of the adenylate mimic in order to study the structural dynamics of the E1 during the activation of Ub (Figure 8D). [42]

In 2016, Pao *et al.* reported a specific E2-loaded Ub probe that can target nucleophiles in E3 ligases. [43] In this technique, Ub containing thioacrylate and thioacrylamide electrophiles are loaded onto E2 and then incubated with their corresponding E3. The resulting bisthioether of Ub with both E2 and E3 can be used to characterize the enzyme kinetics of an E3 ligase (Figure 8E). Recently, Mulder *et al.* reported the synthesis and use of a transferable Ub-based probe where the C-terminal glycine is replaced with a dehydroalanine moiety which can either form a covalently trapped enzyme intermediate (Figure 8F, a', c', e') or a transferable thioester intermediate with the enzymes that are then transferred to subsequent enzymes in the cascade (Figure 8F, b', d', f'). [44]

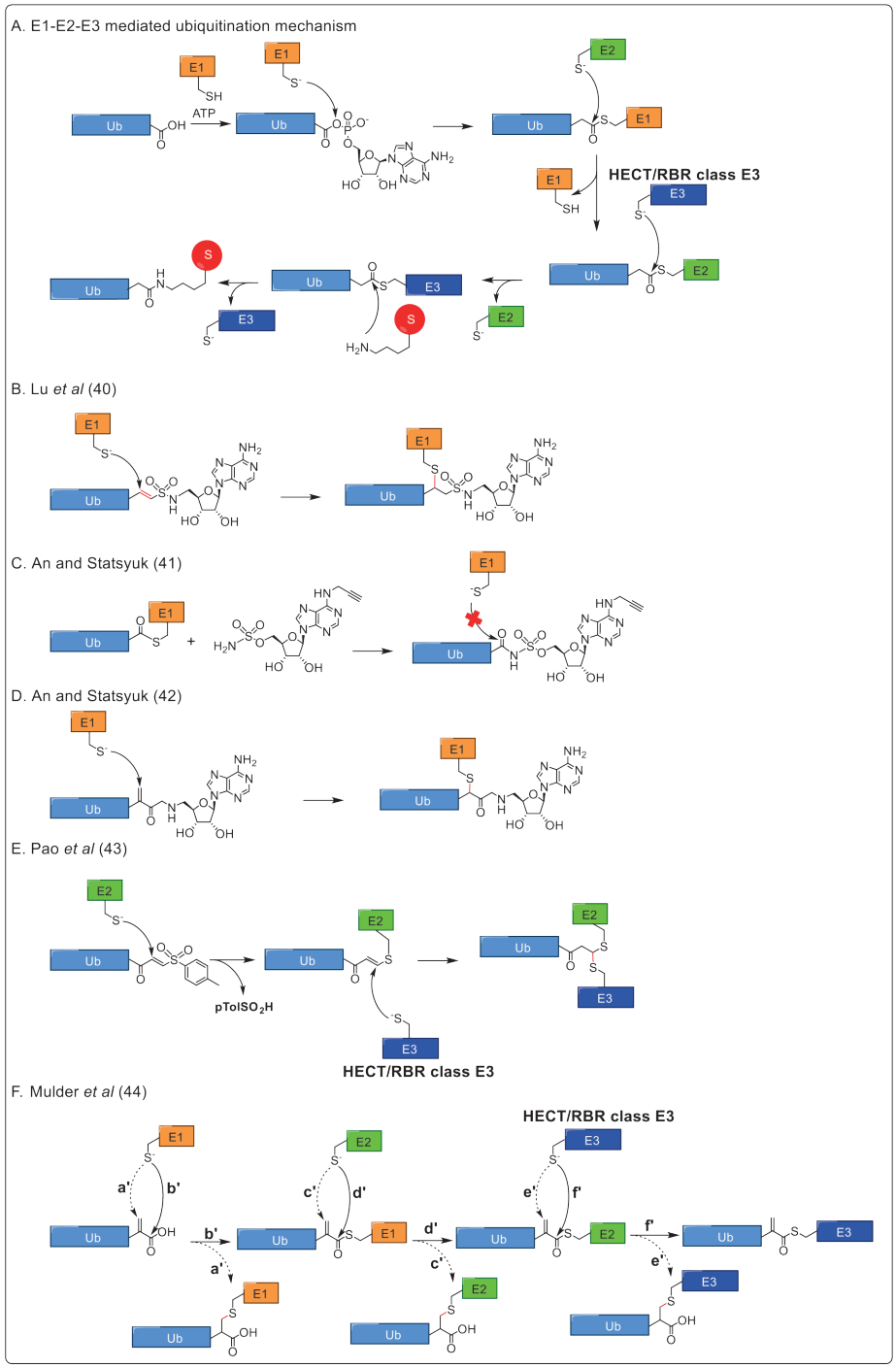

A. E1-E2-E3 mediated ubiquitination mechanism
E1
SH
ATP
Ub
OH
E2
HECT/RBR class E3
E3
S
B. Lu et al (40)
C. An and Statsyuk (41)
D. An and Statsyuk (42)
E. Pao et al (43)
pTolSO2H
HECT/RBR class E3
F. Mulder et al (44)
HECT/RBR class E3
a
b'
c'
d'
e'
f'

Figure 8: Ub-based probes for E1, E2 and E3 enzymes A. *General mechanism of ubiquitin activation by E1 and subsequent action leading to the formation of a ubiquitinated protein.* ***B-D.*** *Ub-based E1 probes that mimic the Ub-adenylate intermediate thereby inhibiting UbE1 enzyme.* ***E.*** *E2-Ub conjugate probe that can react covalently with the corresponding E3 using a Michael acceptor between the C-terminal end of Ub and the E2 enzyme. This probe can capture both E2-E3 in complex with Ub.* ***F.*** *Ub containing a dehydroalanine moiety instead of the terminal glycine is used to either trap the ubiquitinating enzymes or form a transferable Ub-based probe that can be transferred to subsequent enzymes in the cascade pathway.*

Conclusions

The chemical synthesis of ubiquitin has accelerated research in the ubiquitin field. Due to the availability of different assay reagents and probes, many DUBs have been characterized and studied. The next step in the chemical synthesis of reagents is to synthesize an assay reagent or a probe specific for a single DUB. This facilitates enzyme-specific characterization in a cellular environment. This can rely on the identification of ubiquitin mutants that are very specific to a particular DUB. Ernst *et al.* elegantly reported the use of such a Ub mutant library to specifically modulate DUBs, E2/ E3 ligase activity and to develop high-affinity Ub binders for DUBs and Ubiquitin Binding Domains (UBDs). [68] Zhang *et al.* also used a Ub mutant library to develop high-affinity Ub variants for USP7. [69]

Ub-based probes for the cysteine protease class of DUBs have revealed much information on mechanisms of their identity and enzymatic action. However, a different class of probes is needed to study the DUB metalloprotease family because, unlike the cysteine proteases, they contain a Zn^{2+} ion coordinated in their active site. Due to this, the development of a probe is challenging.

Recently, ubiquitin has shown to be phosphorylated at specific sites. Such post-translational modifications on Ub plays regulatory roles in ubiquitin chain processing and chain recognition. [70] At this point, many reagents can be quickly designed and tailored for specific applications.

Acknowledgements

We thank Guido Janssen for critical reading of the manuscript and suggestions. Work in the Ovaa lab is supported by the European Research Council (ERC) and the Netherlands Organisation for Scientific Research (NWO).

References

1. Hochstrasser, M., *Ubiquitin-dependent protein degradation.* Annu Rev Genet, 1996. **30**: p. 405-39.
2. Hershko, A. and A. Ciechanover, *The ubiquitin system.* Annu Rev Biochem, 1998. **67**: p. 425-79.
3. Komander, D., M.J. Clague, and S. Urbe, *Breaking the chains: structure and function of the deubiquitinases.* Nat Rev Mol Cell Biol, 2009. **10**(8): p. 550-63.
4. Meierhofer, D., X. Wang, L. Huang, and P. Kaiser, *Quantitative analysis of global ubiquitination in HeLa cells by mass spectrometry.* J Proteome Res, 2008. **7**(10): p. 4566-76.
5. Akutsu, M., I. Dikic, and A. Bremm, *Ubiquitin chain diversity at a glance.* Journal of Cell Science, 2016. **129**(5): p. 875-880.
6. Hershko, A., E. Eytan, A. Ciechanover, and A.L. Haas, *Immunochemical analysis of the turnover of ubiquitin-protein conjugates in intact cells. Relationship to the breakdown of abnormal proteins.* J Biol Chem, 1982. **257**(23): p. 13964-70.
7. Chau, V., J.W. Tobias, A. Bachmair, D. Marriott, D.J. Ecker, D.K. Gonda, and A. Varshavsky, *A multiubiquitin chain is confined to specific lysine in a targeted short-lived protein.* Science, 1989. **243**(4898): p. 1576-83.
8. Hoege, C., B. Pfander, G.L. Moldovan, G. Pyrowolakis, and S. Jentsch, *RAD6-dependent DNA repair is linked to modification of PCNA by ubiquitin and SUMO.* Nature, 2002. **419**(6903): p. 135-41.
9. Xu, P., D.M. Duong, N.T. Seyfried, D. Cheng, Y. Xie, J. Robert, J. Rush, M. Hochstrasser, D. Finley, and J. Peng, *Quantitative proteomics reveals the function of unconventional ubiquitin chains in proteasomal degradation.* Cell, 2009. **137**(1): p. 133-45.
10. Jin, L., A. Williamson, S. Banerjee, I. Philipp, and M. Rape, *Mechanism of ubiquitin-chain formation by the human anaphase-promoting complex.* Cell, 2008. **133**(4): p. 653-65.
11. Kessler, B.M., *Putting proteomics on target: activity-based profiling of ubiquitin and ubiquitin-like processing enzymes.* Expert Rev Proteomics, 2006. **3**(2): p. 213-21.
12. Ambroggio, X.I., D.C. Rees, and R.J. Deshaies, *JAMM: a metalloprotease-like zinc site in the proteasome and signalosome.* PLoS Biol, 2004. **2**(1): p. 113-119.
13. Komander, D., *Mechanism, specificity and structure of the deubiquitinases.* Subcell Biochem, 2010. **54**: p. 69-87.
14. Shanmugham, A. and H. Ovaa, *DUBs and disease: activity assays for inhibitor development.* Curr Opin Drug Discov Devel, 2008. **11**(5): p. 688-96.
15. Lim, K.H. and K.H. Baek, *Deubiquitinating enzymes as therapeutic targets in cancer.* Curr Pharm Des, 2013. **19**(22): p. 4039-52.
16. Wade, M., Y.C. Li, and G.M. Wahl, *MDM2, MDMX and p53 in oncogenesis and cancer therapy.* Nat Rev Cancer, 2013. **13**(2): p. 83-96.
17. Reverdy, C., S. Conrath, R. Lopez, C. Planquette, C. Atmanene, V. Collura, J. Harpon, V. Battaglia, V. Vivat, W. Sippl, and F. Colland, *Discovery of specific inhibitors of human USP7/HAUSP deubiquitinating enzyme.* Chem Biol, 2012. **19**(4): p. 467-77.
18. Kerscher, O., R. Felberbaum, and M. Hochstrasser, *Modification of proteins by ubiquitin and ubiquitin-like proteins.* Annu Rev Cell Dev Biol, 2006. **22**: p. 159-80.
19. Dang, L.C., F.D. Melandri, and R.L. Stein, *Kinetic and mechanistic studies on the hydrolysis of ubiquitin C-terminal 7-amido-4-methylcoumarin by deubiquitinating enzymes.* Biochemistry, 1998. **37**(7): p. 1868-79.

20. Flierman, D., Gerbrand J. van der Heden van Noort, R. Ekkebus, Paul P. Geurink, Tycho E.T. Mevissen, Manuela K. Hospenthal, D. Komander, and H. Ovaa, *Non-hydrolyzable Diubiquitin Probes Reveal Linkage-Specific Reactivity of Deubiquitylating Enzymes Mediated by S2 Pockets.* Cell Chemical Biology.
21. Terentyeva, T.G., W. Van Rossom, M. Van der Auweraer, K. Blank, and J. Hofkens, *Morpholinecarbonyl-Rhodamine 110 based substrates for the determination of protease activity with accurate kinetic parameters.* Bioconjug Chem, 2011. **22**(10): p. 1932-8.
22. Hassiepen, U., U. Eidhoff, G. Meder, J.F. Bulber, A. Hein, U. Bodendorf, E. Lorthiois, and B. Martoglio, *A sensitive fluorescence intensity assay for deubiquitinating proteases using ubiquitin-rhodamine110-glycine as substrate.* Anal Biochem, 2007. **371**(2): p. 201-7.
23. Tirat, A., A. Schilb, V. Riou, L. Leder, B. Gerhartz, J. Zimmermann, S. Worpenberg, U. Eidhoff, F. Freuler, T. Stettler, L. Mayr, J. Ottl, B. Leuenberger, and I. Filipuzzi, *Synthesis and characterization of fluorescent ubiquitin derivatives as highly sensitive substrates for the deubiquitinating enzymes UCH-L3 and USP-2.* Anal Biochem, 2005. **343**(2): p. 244-55.
24. Geurink, P.P., F. El Oualid, A. Jonker, D.S. Hameed, and H. Ovaa, *A general chemical ligation approach towards isopeptide-linked ubiquitin and ubiquitin-like assay reagents.* Chembiochem, 2012. **13**(2): p. 293-7.
25. Orcutt, S.J., J. Wu, M.J. Eddins, C.A. Leach, and J.E. Strickler, *Bioluminescence assay platform for selective and sensitive detection of Ub/Ubl proteases.* Biochim Biophys Acta, 2012. **1823**(11): p. 2079-86.
26. Ohayon, S., L. Spasser, A. Aharoni, and A. Brik, *Targeting deubiquitinases enabled by chemical synthesis of proteins.* J Am Chem Soc, 2012. **134**(6): p. 3281-9.
27. Ye, Y., G. Blaser, M.H. Horrocks, M.J. Ruedas-Rama, S. Ibrahim, A.A. Zhukov, A. Orte, D. Klenerman, S.E. Jackson, and D. Komander, *Ubiquitin chain conformation regulates recognition and activity of interacting proteins.* Nature, 2012. **492**(7428): p. 266-70.
28. Arnst, J.L., C.W. Davies, S.M. Raja, C. Das, and A. Natarajan, *High-throughput compatible fluorescence resonance energy transfer-based assay to identify small molecule inhibitors of AMSH deubiquitinase activity.* Anal Biochem, 2013. **440**(1): p. 71-7.
29. Geurink, P.P., B.D. van Tol, D. van Dalen, P.J. Brundel, T.E. Mevissen, J.N. Pruneda, P.R. Elliott, G.B. van Tilburg, D. Komander, and H. Ovaa, *Development of Diubiquitin-Based FRET Probes To Quantify Ubiquitin Linkage Specificity of Deubiquitinating Enzymes.* Chembiochem, 2016.
30. Madiraju, C., K. Welsh, M.P. Cuddy, P.H. Godoi, I. Pass, T. Ngo, S. Vasile, E.A. Sergienko, P. Diaz, S. Matsuzawa, and J.C. Reed, *TR-FRET-based high-throughput screening assay for identification of UBC13 inhibitors.* J Biomol Screen, 2012. **17**(2): p. 163-76.
31. Borodovsky, A., B.M. Kessler, R. Casagrande, H.S. Overkleeft, K.D. Wilkinson, and H.L. Ploegh, *A novel active site-directed probe specific for deubiquitylating enzymes reveals proteasome association of USP14.* EMBO J, 2001. **20**(18): p. 5187-96.
32. Borodovsky, A., H. Ovaa, N. Kolli, T. Gan-Erdene, K.D. Wilkinson, H.L. Ploegh, and B.M. Kessler, *Chemistry-based functional proteomics reveals novel members of the deubiquitinating enzyme family.* Chem Biol, 2002. **9**(10): p. 1149-59.
33. de Jong, A., R. Merkx, I. Berlin, B. Rodenko, R.H. Wijdeven, D. El Atmioui, Z. Yalcin, C.N. Robson, J.J. Neefjes, and H. Ovaa, *Ubiquitin-based probes prepared by total*

synthesis to profile the activity of deubiquitinating enzymes. Chembiochem, 2012. **13**(15): p. 2251-8.
34. Ekkebus, R., S.I. van Kasteren, Y. Kulathu, A. Scholten, I. Berlin, P.P. Geurink, A. de Jong, S. Goerdayal, J. Neefjes, A.J. Heck, D. Komander, and H. Ovaa, *On terminal alkynes that can react with active-site cysteine nucleophiles in proteases.* J Am Chem Soc, 2013. **135**(8): p. 2867-70.
35. Iphofer, A., A. Kummer, M. Nimtz, A. Ritter, T. Arnold, R. Frank, J. van den Heuvel, B.M. Kessler, L. Jansch, and R. Franke, *Profiling ubiquitin linkage specificities of deubiquitinating enzymes with branched ubiquitin isopeptide probes.* Chembiochem, 2012. **13**(10): p. 1416-20.
36. McGouran, J.F., S.R. Gaertner, M. Altun, H.B. Kramer, and B.M. Kessler, *Deubiquitinating enzyme specificity for ubiquitin chain topology profiled by di-ubiquitin activity probes.* Chem Biol, 2013. **20**(12): p. 1447-55.
37. Li, G., Q. Liang, P. Gong, A.H. Tencer, and Z. Zhuang, *Activity-based diubiquitin probes for elucidating the linkage specificity of deubiquitinating enzymes.* Chem Commun (Camb), 2014. **50**(2): p. 216-8.
38. Haj-Yahya, N., H.P. Hemantha, R. Meledin, S. Bondalapati, M. Seenaiah, and A. Brik, *Dehydroalanine-based diubiquitin activity probes.* Org Lett, 2014. **16**(2): p. 540-3.
39. Mulder, M.P., F. El Oualid, J. ter Beek, and H. Ovaa, *A native chemical ligation handle that enables the synthesis of advanced activity-based probes: diubiquitin as a case study.* Chembiochem, 2014. **15**(7): p. 946-9.
40. Lu, X., S.K. Olsen, A.D. Capili, J.S. Cisar, C.D. Lima, and D.S. Tan, *Designed semisynthetic protein inhibitors of Ub/Ubl E1 activating enzymes.* J Am Chem Soc, 2010. **132**(6): p. 1748-9.
41. An, H. and A.V. Statsyuk, *Development of activity-based probes for ubiquitin and ubiquitin-like protein signaling pathways.* J Am Chem Soc, 2013. **135**(45): p. 16948-62.
42. An, H. and A.V. Statsyuk, *Facile synthesis of covalent probes to capture enzymatic intermediates during E1 enzyme catalysis.* Chem Commun (Camb), 2016. **52**(12): p. 2477-80.
43. Pao, K.C., M. Stanley, C. Han, Y.C. Lai, P. Murphy, K. Balk, N.T. Wood, O. Corti, J.C. Corvol, M.M. Muqit, and S. Virdee, *Probes of ubiquitin E3 ligases enable systematic dissection of parkin activation.* Nat Chem Biol, 2016.
44. Mulder, M.P., K. Witting, I. Berlin, J.N. Pruneda, K.P. Wu, J.G. Chang, R. Merkx, J. Bialas, M. Groettrup, A.C. Vertegaal, B.A. Schulman, D. Komander, J. Neefjes, F. El Oualid, and H. Ovaa, *A cascading activity-based probe sequentially targets E1-E2-E3 ubiquitin enzymes.* Nat Chem Biol, 2016. **12**(7): p. 523-30.
45. Yin, L., B. Krantz, N.S. Russell, S. Deshpande, and K.D. Wilkinson, *Nonhydrolyzable diubiquitin analogues are inhibitors of ubiquitin conjugation and deconjugation.* Biochemistry, 2000. **39**(32): p. 10001-10.
46. Lewis, Y.E., T. Abeywardana, Y.H. Lin, A. Galesic, and M.R. Pratt, *Synthesis of a Bis-thio-acetone (BTA) Analogue of the Lysine Isopeptide Bond and its Application to Investigate the Effects of Ubiquitination and SUMOylation on alpha-Synuclein Aggregation and Toxicity.* ACS Chem Biol, 2016.
47. Eger, S., M. Scheffner, A. Marx, and M. Rubini, *Synthesis of defined ubiquitin dimers.* J Am Chem Soc, 2010. **132**(46): p. 16337-9.
48. Weikart, N.D. and H.D. Mootz, *Generation of site-specific and enzymatically stable conjugates of recombinant proteins with ubiquitin-like modifiers by the Cu(I)-catalyzed azide-alkyne cycloaddition.* Chembiochem, 2010. **11**(6): p. 774-7.

49. Jung, J.E., H.P. Wollscheid, A. Marquardt, M. Manea, M. Scheffner, and M. Przybylski, *Functional ubiquitin conjugates with lysine-epsilon-amino-specific linkage by thioether ligation of cysteinyl-ubiquitin peptide building blocks.* Bioconjug Chem, 2009. **20**(6): p. 1152-62.
50. Shanmugham, A., A. Fish, M.P. Luna-Vargas, A.C. Faesen, F. El Oualid, T.K. Sixma, and H. Ovaa, *Nonhydrolyzable ubiquitin-isopeptide isosteres as deubiquitinating enzyme probes.* J Am Chem Soc, 2010. **132**(26): p. 8834-5.
51. Briand, J.P., A. Van Dorsselaer, B. Raboy, and S. Muller, *Total chemical synthesis of ubiquitin using BOP reagent: biochemical and immunochemical properties of the purified synthetic product.* Pept Res, 1989. **2**(6): p. 381-8.
52. Ramage, R., J. Green, and O.M. Ogunjobi, *Solid phase peptide synthesis of ubiquitin.* Tetrahedron Letters, 1989. **30**(16): p. 2149-2152.
53. El Oualid, F., R. Merkx, R. Ekkebus, D.S. Hameed, J.J. Smit, A. de Jong, H. Hilkmann, T.K. Sixma, and H. Ovaa, *Chemical synthesis of ubiquitin, ubiquitin-based probes, and diubiquitin.* Angew Chem Int Ed Engl, 2010. **49**(52): p. 10149-53.
54. Dawson, P.E., T.W. Muir, I. Clark-Lewis, and S.B. Kent, *Synthesis of proteins by native chemical ligation.* Science, 1994. **266**(5186): p. 776-9.
55. Kumar, K.S., L. Spasser, L.A. Erlich, S.N. Bavikar, and A. Brik, *Total chemical synthesis of di-ubiquitin chains.* Angew Chem Int Ed Engl, 2010. **49**(48): p. 9126-31.
56. Hemantha, H.P. and A. Brik, *Non-enzymatic synthesis of ubiquitin chains: where chemistry makes a difference.* Bioorg Med Chem, 2013. **21**(12): p. 3411-20.
57. Meledin, R., S.M. Mali, and A. Brik, *Pushing the Boundaries of Chemical Protein Synthesis: The Case of Ubiquitin Chains and Polyubiquitinated Peptides and Proteins.* Chem Rec, 2016. **16**: p. 509-519.
58. Pham, G.H. and E.R. Strieter, *Peeling away the layers of ubiquitin signaling complexities with synthetic ubiquitin-protein conjugates.* Curr Opin Chem Biol, 2015. **28**: p. 57-65.
59. Faesen, A.C., M.P. Luna-Vargas, P.P. Geurink, M. Clerici, R. Merkx, W.J. van Dijk, D.S. Hameed, F. El Oualid, H. Ovaa, and T.K. Sixma, *The differential modulation of USP activity by internal regulatory domains, interactors and eight ubiquitin chain types.* Chem Biol, 2011. **18**(12): p. 1550-61.
60. Licchesi, J.D., J. Mieszczanek, T.E. Mevissen, T.J. Rutherford, M. Akutsu, S. Virdee, F. El Oualid, J.W. Chin, H. Ovaa, M. Bienz, and D. Komander, *An ankyrin-repeat ubiquitin-binding domain determines TRABID's specificity for atypical ubiquitin chains.* Nat Struct Mol Biol, 2012. **19**(1): p. 62-71.
61. Ritorto, M.S., R. Ewan, A.B. Perez-Oliva, A. Knebel, S.J. Buhrlage, M. Wightman, S.M. Kelly, N.T. Wood, S. Virdee, N.S. Gray, N.A. Morrice, D.R. Alessi, and M. Trost, *Screening of DUB activity and specificity by MALDI-TOF mass spectrometry.* Nat Commun, 2014. **5**: p. 4763.
62. Rosner, D., T. Schneider, D. Schneider, M. Scheffner, and A. Marx, *Click chemistry for targeted protein ubiquitylation and ubiquitin chain formation.* Nat Protoc, 2015. **10**(10): p. 1594-611.
63. Wilkinson, K.D., M.J. Cox, A.N. Mayer, and T. Frey, *Synthesis and characterization of ubiquitin ethyl ester, a new substrate for ubiquitin carboxyl-terminal hydrolase.* Biochemistry, 1986. **25**(21): p. 6644-9.
64. Ekkebus, R., D. Flierman, P.P. Geurink, and H. Ovaa, *Catching a DUB in the act: novel ubiquitin-based active site directed probes.* Curr Opin Chem Biol, 2014. **23**: p. 63-70.
65. Hemelaar, J., A. Borodovsky, B.M. Kessler, D. Reverter, J. Cook, N. Kolli, T. Gan-Erdene, K.D. Wilkinson, G. Gill, C.D. Lima, H.L. Ploegh, and H. Ovaa, *Specific and*

covalent targeting of conjugating and deconjugating enzymes of ubiquitin-like proteins. Mol Cell Biol, 2004. **24**(1): p. 84-95.
66. Sommer, S., N.D. Weikart, U. Linne, and H.D. Mootz, *Covalent inhibition of SUMO and ubiquitin-specific cysteine proteases by an in situ thiol-alkyne addition.* Bioorg Med Chem, 2013. **21**(9): p. 2511-7.
67. Mevissen, T.E., M.K. Hospenthal, P.P. Geurink, P.R. Elliott, M. Akutsu, N. Arnaudo, R. Ekkebus, Y. Kulathu, T. Wauer, F. El Oualid, S.M. Freund, H. Ovaa, and D. Komander, *OTU deubiquitinases reveal mechanisms of linkage specificity and enable ubiquitin chain restriction analysis.* Cell, 2013. **154**(1): p. 169-84.
68. Ernst, A., G. Avvakumov, J. Tong, Y. Fan, Y. Zhao, P. Alberts, A. Persaud, J.R. Walker, A.M. Neculai, D. Neculai, A. Vorobyov, P. Garg, L. Beatty, P.K. Chan, Y.C. Juang, M.C. Landry, C. Yeh, E. Zeqiraj, K. Karamboulas, A. Allali-Hassani, M. Vedadi, M. Tyers, J. Moffat, F. Sicheri, L. Pelletier, D. Durocher, B. Raught, D. Rotin, J. Yang, M.F. Moran, S. Dhe-Paganon, and S.S. Sidhu, *A strategy for modulation of enzymes in the ubiquitin system.* Science, 2013. **339**(6119): p. 590-5.
69. Zhang, Y., L. Zhou, L. Rouge, A.H. Phillips, C. Lam, P. Liu, W. Sandoval, E. Helgason, J.M. Murray, I.E. Wertz, and J.E. Corn, *Conformational stabilization of ubiquitin yields potent and selective inhibitors of USP7.* Nat Chem Biol, 2013. **9**(1): p. 51-8.
70. Wauer, T., K.N. Swatek, J.L. Wagstaff, C. Gladkova, J.N. Pruneda, M.A. Michel, M. Gersch, C.M. Johnson, S.M. Freund, and D. Komander, *Ubiquitin Ser65 phosphorylation affects ubiquitin structure, chain assembly and hydrolysis.* EMBO J, 2015. **34**(3): p. 307-25.

Chapter 2

Synthesis of isopeptide-linked diubiquitin chains

Adapted from:

Oualid, F.E., **D.S. Hameed**, D.E. Atmioui, H. Hilkmann, and H. Ovaa, *Synthesis of atypical diubiquitin chains.* Methods Mol Biol, 2012. 832: p. 597-609.

El Oualid, F., R. Merkx, R. Ekkebus, **D.S. Hameed**, J.J. Smit, A. de Jong, H. Hilkmann, T.K. Sixma, and H. Ovaa, *Chemical synthesis of ubiquitin, ubiquitin-based probes, and diubiquitin*. Angew Chem Int Ed Engl, 2010. 49(52): p. 10149-53.

Summary

Ubiquitination is an important post-translational modification that determines the fate of a target protein. Proteins can be modified with a single ubiquitin (Ub) or polyUb chains involving one of seven internal lysines or the N-terminal methionine of Ub. The concerted action of three enzymes (i.e., E1, E2 and E3) specify the target protein and also determine the type of ubiquitination involved. Access to all but K48 and K63 chains have been hampered due to the lack of specific E2 enzymes. We present native chemical ligation as an alternative to overcome the tedious biological enzyme ligation. In our approach, we used a thiolysine handle to mimic the property of E2 enzymes and facilitate diubiquitin (DiUb) synthesis. This way, we generated all seven iso-peptide linked diUb molecules.

Introduction

Diubiquitin synthesis using enzymes

Ubiquitination is the process of covalent modification of a target protein by another small protein called ubiquitin (Ub). It involves the concerted action of a specific E1 activating enzyme, an E2 ligase and an E3 conjugating enzyme leading to the formation of different types of ubiquitin conjugates. Targeted proteins can be modified with a single Ub or a polyubiquitin (polyUb) chain where Ub is self-conjugated onto itself via one of its seven internal lysine residues or the N-terminal methionine. Although functions of K48 and K63 linked Ub chains have been studied extensively, the lack of enzyme combinations has hampered access to other lysine-linked chains called the atypical chains.[1-3]

E1 enzymes activate Ub by forming a stable Ub-E1 thioester at the expense of an ATP molecule. In the presence of E2 enzymes, the Ub-E1 thioester undergoes trans-thioesterification to form Ub-E2 thioester. Subsequently, depending on the types of the E3 enzyme, Ub can be directly or indirectly transferred to a substrate protein to form the isopeptide link between the lysine of the target protein and the C-terminus of Ub (Figure 1). PolyUb chains are also formed by these enzyme combinations and lead to specific Ub signaling pathway.[4, 5] Also, mixed linkage polyUb chains have also been identified in cells.[6] The entire process of ubiquitination is reversed by enzymes called deubiquitinases (DUBs) that break down Ub conjugates releasing Ub monomers.[7]

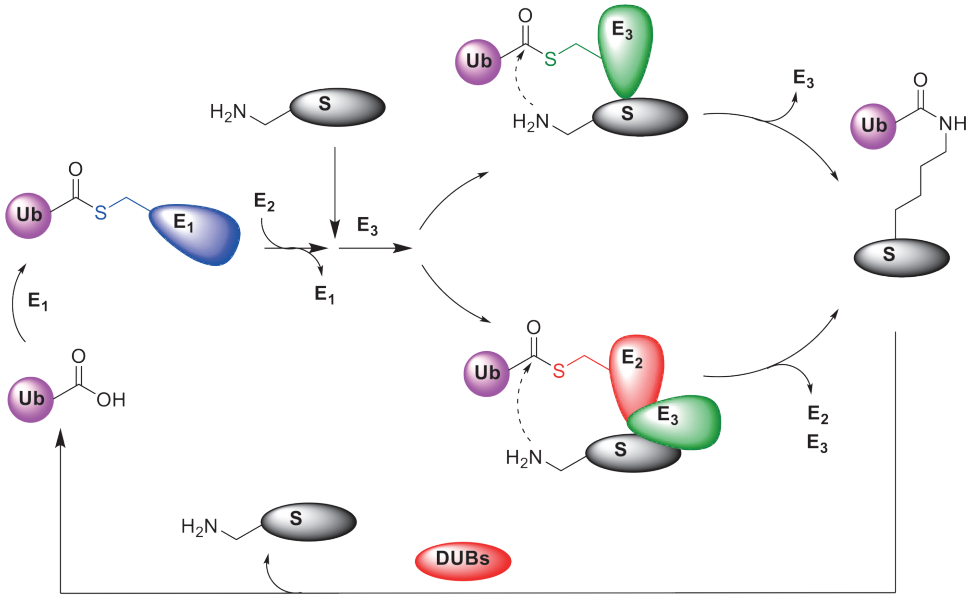


Figure 1: Schematic representation of Ubiquitination and deubiquitination. *Free Ub is activated by UbE1, which is then transferred via E2 and E3 onto a target protein, constituting the process of ubiquitination. On the other hand, Ub monomers are released from conjugates using deubiquitinases (DUBs).*

Enzymatic synthesis of Ub chains has been reported for all but K27 linked chains.[8] In general, K48 and K63 chains are easily generated using specific E2/E3 enzymes.[9] However, for the synthesis of atypical chains like K6, K11, K29 and K33, the enzymes are generally mutated to increase their fidelity to form only one type of chain.[10-15] However, the specificity of these enzymes is limited and there is still a minuscule formation of chains of other linkage types. Normally, these contaminating linkages are eliminated by the use of DUBs that are specific for the unwanted chains.[13, 15] Though enzymatic synthesis yield native isopeptide linked polyUb chains, the use of mutated enzymes and DUBs makes the whole process expensive and less yielding. Secondly, although it is possible to separate polyUb chains of different lengths, it is, however, difficult to restrict the chain-length using enzymatic synthesis approach. Hence, alternative ways to generate ubiquitin chains of specific length is needed. For many *in-vitro* assays to ascertain the linkage specificity of certain DUBs, a simple diubiquitin would be sufficient.[16] This diubiquitin has the basic components of a polyUb chain, containing both the distal and proximal ubiquitin and the different isopeptide linkages between them.

Native Chemical ligation as an alternative to enzymatic synthesis

Native chemical ligation was a technique introduced for the total or a semi-synthesis of a polypeptide.[17] Generally, this technique employs the use of an activated thioester-containing peptide and an N-terminal cysteine-containing peptide. When both peptides are added at neutral or slightly basic pH, the thioester-peptide would undergo trans-thioesterification to form a thioester with the cysteine of the second peptide. This then undergoes intramolecular rearrangement through the nucleophilic attack of the N-terminal

amino group in cysteine residue, thereby forming an irreversible and a stable peptide bond at this site. The kinetics of this reaction is dependent on the type of thioester linkage and the pH of the buffer.

In addition to cysteine which forms a peptide bond in a typical NCL, a novel unnatural amino acid called thiolysine is used in places where an isopeptide bond is needed.[18-20] In this case, a thiol handle is attached at either the δ or γ position of the lysine residue. During NCL, the thioester peptide undergoes trans-thioesterification and with thiolysine. This is followed by an S-N acyl transfer resulting in the intramolecular rearrangement to form the isopeptide bond at the ε amino group of the lysine residue. The thiol handle in thiolysine is then removed by radical-based desulfurization techniques. Thiolysines have been used in the synthesis of ubiquitinated peptides where the position of thiolysine determines the site of isopeptide linkage.[21] We have extended this technique to the synthesis of all seven isopeptide-linked diubiquitins (diUbs).

Chemical synthesis of ubiquitin mutants to facilitate diubiquitin synthesis

Ub has been synthesized using Fmoc-solid-phase peptide chemistry (Fmoc-SPPS) in both linear and modular fashions. Linear synthesis offers the advantage of yielding the desired product directly and in parallel. In particular, the use of dipeptides at a specific location during the linear synthesis of Ub has been instrumental in improving the yield and preventing the formation of aggregated intermediates during synthesis (Figure 2). [22]

One of the major advantages of chemical synthesis of Ub is the ability to specifically incorporate any amino acid at virtually any position. Among the unnatural amino acids, thiolysine has been useful in carrying our native chemical ligations where an isopeptide bond could be made specifically at a certain position.[18-20, 23, 24] For this purpose, Fmoc thiolysines were synthesized and incorporated into the Ub sequence by SPPS. This way, thiolysines was incorporated into positions 6, 11, 27, 29, 33, 48 and 63 thereby making synthetic mutant Ubs.

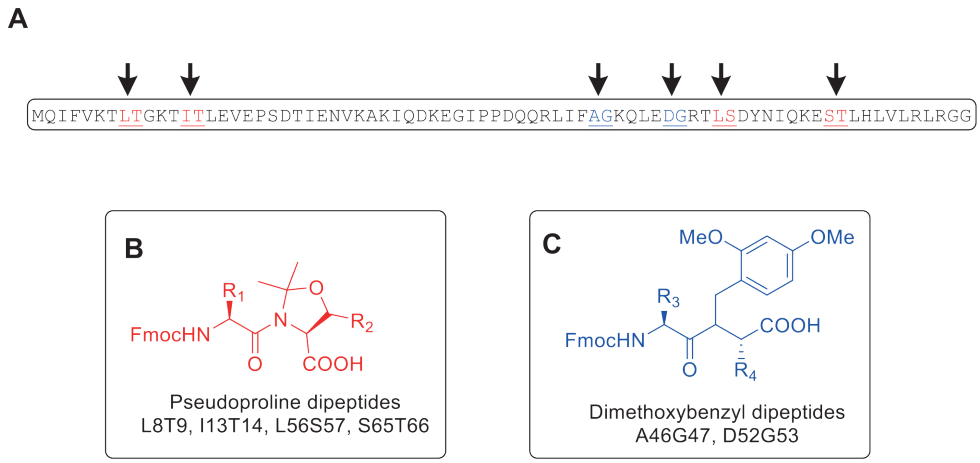


***Figure 2: Fmoc-SPPS strategy to make Ubiquitin**. **A:** Sequence of Ub with positions of dipeptides indicated by black arrow head. **B:** Pseudoproline dipeptides were used in four different positions as indicated. **C:** Dimethoxybenzyl dipeptides were used in two positions in the sequence.*

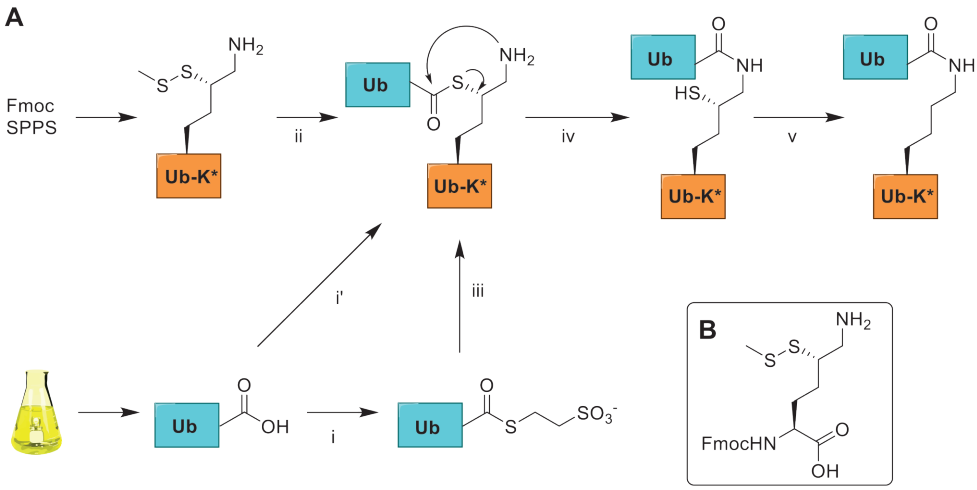


Figure 3: Schematic representation of diubiquitin synthesis*. **A:** The distal Ub is obtained from bacterial expression system, while the proximal Ub is obtained from Fmoc-SPPS. i) UbE1, MESNa, ATP, $MgCl_2$, Sodium phosphate buffer pH 8.0 and then pH 6.5 after reaction is completed ; i') UbE1, MESNa, MPAA, ATP, $MgCl_2$, Sodium phosphate buffer pH 8.0; ii) TCEP, 6M Gnd.HCl pH 8.0; iii) MPAA, Gnd.HCl pH 8.0; iv) N→C acyl transfer; v) V-50, TCEP, Gnd.HCl pH 7.0; **B:** Structure of Fmoc δ-thiolysine used in the synthesis.*

Diubiquitin ligation reaction was carried out according to a native chemical ligation scheme described in figure 3. On one hand, Ub was synthesized or expressed as a full-length protein and activated as a thioester using the UbE1 enzyme and MESNa. This thioester can be generated *in-situ* during NCL by using UbE1 or isolated to yield Ub-MESNa thioester which is stable under acidic conditions. On the other hand, mutant Ub containing thiolysines at specific lysine positions was synthesized exclusively by SPPS. A native chemical ligation between the two-ubiquitin species formed a diubiquitin molecule with an isopeptide bond at the desired lysine position. A subsequent desulfurization step resulted in the removal of the thiol handle in lysine, leading to the formation of native isopeptide linked diubiquitin molecules.[25, 26]

Potential applications in assay of DUBs

Generally, diubiquitins can be used in characterizing the DUB preference for a particular linkage, especially in the context of polyubiquitin chains attached to a target protein.[27-29] DUBs normally fall under two categories – cysteine protease and metalloprotease class.[28, 30] The Cysteine protease class of DUBs is sub-divided into four families based on the conserved domains. These DUBs can either be specific for a substrate protein or non-specific where only the distal Ub is sufficient to invoke the DUB activity.[28] Also, linkage specificity is also attributed to DUBs. However, the linkage preference of the DUBs has been characterized only to a certain extent, and so it is important to know which DUB cleaves which kind of ubiquitin chain. This can also be used for establishing the functional role of DUBs in cells and thereby facilitating the development of therapeutic agents that can target a particular DUB based on its linkage specificity and functions.[31-33]

Results and Discussion

Expression of Ub and UbE1

Ub was expressed as a fully functional protein using a bacterial expression system. In our case, we expressed Ub in BL21 Rosetta cells. Harvesting Ub without any purification handle was possible due to its thermal stability. The expressed cells were simply heated up to 90 °C and then centrifuged to isolate Ub with more than 80% purity. Further purifications using FPLC followed by HPLC yielded lyophilized Ub (Figure S1).

Ub activating enzyme, E1 was also expressed in a bacterial expression system. Hexa-His-tagged UbE1 protein was expressed at 18 °C using IPTG induction and then the cells were lysed and spun down. Then, UbE1 in the supernatant was isolated by metal affinity chromatography using TALON beads followed by the removal of imidazole by buffer exchange using Amicon spin columns (Figure S2). Finally, the enzyme was concentrated and used in native chemical ligation experiments.

Solid Phase synthesis of Ub thiolysine

We have developed a high-yielding linear Fmoc-SPPS of Ub that allows the incorporation of desired tags and mutations as well as both the C- and N-terminal modifications. As linear syntheses yield desired products directly and in parallel, a significant advantage over modular approaches, we revisited the linear chemical synthesis of Ub. We decided to incorporate pseudoproline building blocks and dimethoxybenzyl (DMB) dipeptides (Figure 1A), which prevented the formation of folded and/or aggregated intermediates on-resin, resulting in a high yielding linear synthesis of Ub and Ub mutants.

We used Fmoc δ-thiolsyine that is protected in the free thiol as a methyl disulfide. This way, Fmoc thiolysine was incorporated in positions 6, 11, 27, 29, 33, 48 and 63 during the linear synthesis of Ub. After synthesis, these mutant Ub molecules are purified by FPLC and HPLC to yield the desired thiolysine-Ub molecule for native chemical ligation.

Native Chemical ligations and desulfurization

The native chemical ligation (NCL) reactions were carried out in both native buffer conditions and in denaturing buffer conditions. For reactions in the native buffer, UbE1 was added directly to the ligation mix containing Ub, ATP, $MgSO_4$ and the thiolysine-containing Ub. However, in such reactions, the thiolysine-Ub can also form thioester with E1 and result in the formation of polyUb chains. To avoid this, we used a mutant thiolysine-Ub that contained valine instead of glycine at position 76. This way, only the Ub w.t. that doesn't have the thiolysine handle, would form the activated Ub-thioester and react specifically with the thiolysine containing Ub. Initial experiments with E1 using only Ub and Ub thiolysine (G76V) also formed diubiquitins. However, positions 27 and 29 were difficult to make, owing to the inaccessibility to the enzyme-Ub intermediate (Figure 4A).

For NCL under denaturing conditions, it is necessary to make a stable Ub-thioester molecule. For that purpose, the addition of E1 along with Ub, ATP, MgCl2 and MESNa formed the Ub-MESNa thioester. After the reaction was complete, the Ub-MESNa thioester was kept stable under acidic conditions and purified as a lyophilized powder. This resulted in the formation of all seven isopeptide linked diubiquitin chains with a yield of around 15% (Figure 4B-I, S3).

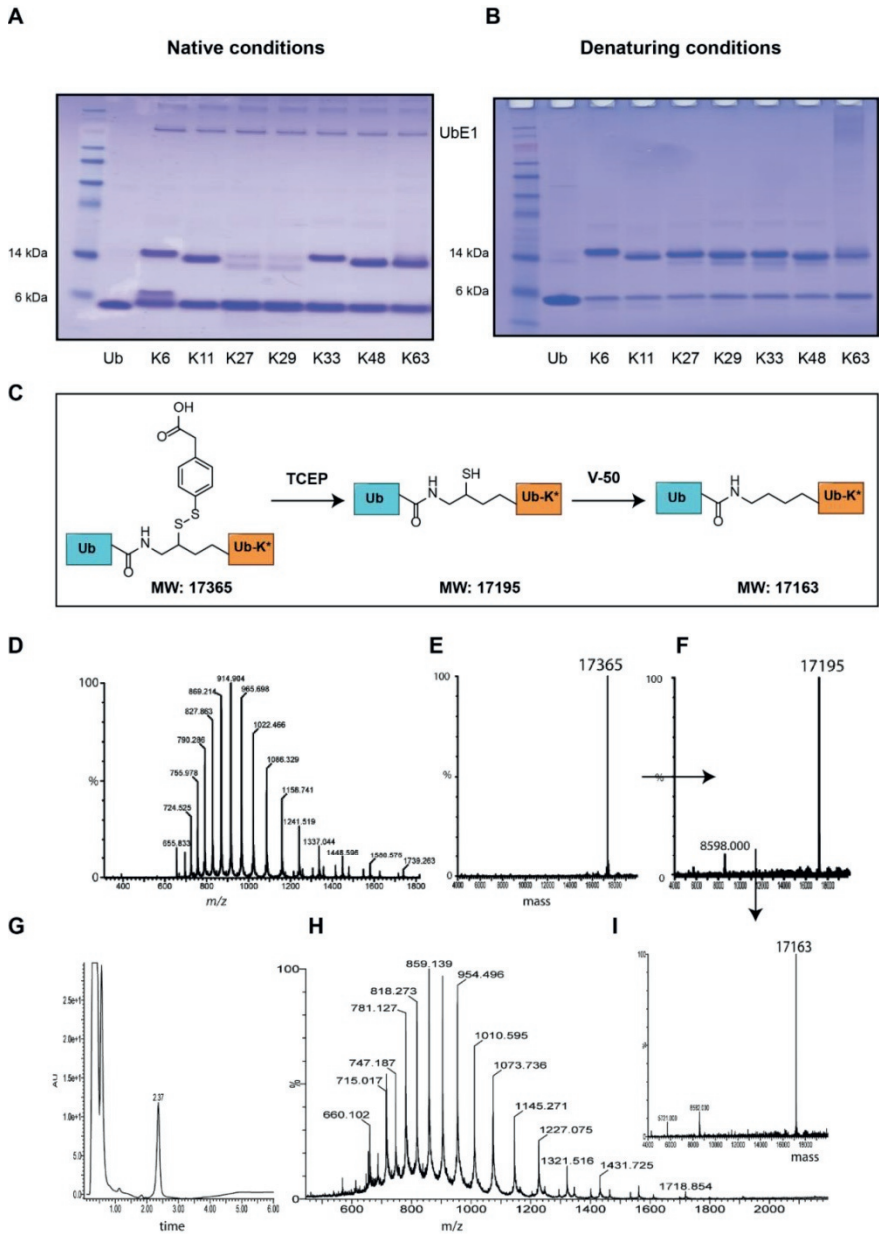


***Figure 4**: **A:** diUb synthesis under native buffer conditions using UbE1 enzyme; **B:** diUb synthesis under denaturing conditions using purified Ub-MESNa thioester; **C:** Schematic representation of desulphurization of diubiquitin using V-50; **D**: Mass spectra of K33 diUb showing the protein envelope; **E:** deconvoluted spectra showing MPAA adduct of K33 diUb; **F:** deconvoluted spectra of K33 diUb after reduction of MPAA using TCEP; **G:** UV chromatogram of desulfurized K33 diUb; **H:** Mass spectra of K33 diUb after desulfurization; **I:** deconvoluted mass spectrum of desulfurized K33 diUb showing removal of thiol (-32 Da).*

Purifications and validation

Normally, ubiquitins are purified using reverse-phase HPLC. Due to their efficient refolding capacity, the proteins can be lyophilized and subsequently refolded from DMSO into water or buffer of choice. However, separating diubiquitins from mono ubiquitin was difficult owing to similar hydrophobicity of both the molecules. However, the use of a 300 Å pore sized C18 columns in HPLC provided sufficient resolution to isolate diubiquitins from mono ubiquitin, as observed by SDS PAGE and validated using LCT-MS (Figures S4-S10).

Synthetic diUbs are validated for their biological function by assessing their recognition by DUBs. As mentioned earlier, DUBs can cleave ubiquitin chains based on the type of linkage.[28, 30] This requires recognition elements on the surface of DUBs which were identified using diUb probes. [34] To characterize the specificity of DUBs, diUb reagents are used. For example, an exclusive analysis of the linkage specificity of the USP family of DUBs has been done using our diUb reagents.[35] Moreover, our diUb reagents were also used to identify linkage specificity of an ovarian tumor (OTU) domain DUB called TRABID.[36] Very recently, our reagents were used to identify the specificity of USP7 and their role in cellular stress.[37]

Conclusions

We were able to synthesize diUbs from Ub precursors which were partly made synthetically. Ub expression was optimized to a yield higher quantity of protein and their purification was made easy due to the thermal stability of Ub to higher temperatures. UbE1 was also expressed by the auto-induction procedure yielding a higher quantity of active enzymes. These were used to successfully make Ub-thioester which can either be purified or used *in-situ*. Synthetic Ub containing thiolysine at specific sites were made using SPPS with high yield and efficiency due to the use of dipeptides in positions that are deemed difficult.

The synthesis of Ub thiolysine was instrumental in making all isopeptide linked diUbs without the need for E2 and E3 enzymes. This also restricts the synthesis to diUb and not the higher-order Ub chains which are one of the drawbacks when using the enzymatic route. This way, we synthesized all seven isopeptide linked diUb molecules.

Finally, we used these synthetic diUbs to establish the functional properties of enzymes from the USP family of DUBs. We observed that these DUBs preferred linkages that are easily accessible while there was some hydrolysis observed for the difficult linkages. These linkages were found in lysine positions that are hidden in the alpha-helix structure of the proximal Ub.

Experimental section

General

All aqueous solutions are prepared with ultrapure water (milliQ, prepared by purifying deionized water to attain a sensitivity of 18 MΩ cm at 25°C) and analytical grade reagents. Unless indicated otherwise, reagents are prepared and stored at room temperature. Unless indicated otherwise, chemicals are obtained commercially of the highest available grade. Fmoc-δ-thiolysine-OH (**D**, Fig. 1) was prepared as reported.[38] Solid Phase Peptide Synthesis was performed on a Syro II MultiSyntech Automated Peptide synthesizer. LC-MS measurements were made on a Waters 2795 Separation Module (Alliance HT) and Waters 2996 Photodiode Array Detector (190-750 nm) using the following conditions: Flowrate was at 0.8 mL/min for 6 min, using 2 mobile phases: A= 1% CH_3CN, 0.1% formic acid in water and B= 1% water and 0.1% formic acid in CH_3CN. Preparative cation-chromatography was used to purify Ub and Ub thiolysine at 4°C with an ÄKTA Unichromat 1500- "PRO" system

(15x185 mm column packed with Workbeads 40S™) using 2 mobile phases: 50 mM NaOAc, pH 4.5, and 1M NaCl in 50 mM NaOAc, pH 4.5. Flowrate is 5 mL/min. Purification of Ub and thiolysine-Ubs were performed on preparative reverse-phase HPLC purifications on a Shimadzu Prominence system using 2 mobile phases: A= 0.05% TFA in water and B= 0.05% TFA in CH_3CN. The column temperature was set at 40°C, flowrate was 7.5 mL/min and the UV-detection was performed at 230 and 254 nm. Quality analysis of the mass of synthesized Ub was done on the analytical column: Phenomenex Kinetex C18, (2.1x50 mm, 2.6 μM), the column at T= 40°C. For this, the following gradient was used: 0→0.5 min: 5% B; 0.5→4 min: 5 to 95%B gradient; 4→5.5 min: 95% B. Data processing was performed using Waters MassLynx Mass Spectrometry Software 4.1 (deconvolution with Maxent 1 function).

Solid Phase Peptide Synthesis (SPPS) Ubiquitin polypeptide

SPPS reagents and standard fluorenylmethyloxycarbonyl (Fmoc) protected amino acid building blocks like benzotriazol-1-yl-oxytripyrrolidinophosphonium hexafluorophosphate [PyBOP], diisopropylethylamine [DiPEA], 1-hydroxybenzotriazole (HOBt), acetic anhydride (Ac_2O), piperidine, trifluoroacetic acid [TFA] were obtained from Biosolve, Sigma-Aldrich and Novabiochem. Fmoc protected pseudoproline and dimethoxybenzyl (DMB) protected dipeptides like Fmoc-L-Ser(*t*Bu)-L-Thr($\Psi^{Me,Me}$pro)-OH, Fmoc-L-Leu-L-Ser($\Psi^{Me,Me}$pro)-OH, Fmoc-L-Ile-L-Thr($\Psi^{Me,Me}$pro)-OH; Fmoc-L-Leu-L-Thr($\Psi^{Me,Me}$pro)-OH, Fmoc-L-Asp(O*t*Bu)-(Dmb)Gly-OH and Fmoc-L-Ala-(Dmb)Gly-OH were bought from Novabiochem. Wang type resin pre-loaded with 0.2 mmol/g Fmoc-Gly-OH were obtained from Applied Biosystems. Peptide synthesis grade organic solvents that include *N*-methylpyrrolidinone [NMP]) were bought from Biosolve (*see* **Note 1**). Work-up solvents like phenol, triisopropylsilane [iPr_3SiH], diethyl ether [Et_2O], *n*-pentane were obtained from Aldrich. Two sets of cocktail mixtures were used for the synthesis. Cocktail A (TFA cleavage mix): TFA, H_2O, Phenol, iPr_3SiH (90.5/5/2.5/2 v/v/v/v). Cocktail B (Freeze dry mix): H_2O, CH_3CN, HOAc (65/25/10 v/v/v)

All Fmoc-protected amino acid building blocks were dried overnight under high vacuum (*see* **Note 8**). We used Fmoc-Gly-Wang resin (25 μmol) for Fmoc SPPS in NMP using PyBOP (4 equiv) and DiPEA (8 equiv). The following settings are applied:

For the first 30 cycles: a) single couplings for 45 min using 4 equiv of standard Fmoc amino acids; b) The Fmoc-δ-thiolysine-OH building block (Figure 3B) is coupled using 3 equiv; c) Fmoc removal with 20% piperidine in NMP for 2x 2 min and 1x 5 min;

After the first 30 cycles: a) extend the coupling time to 60 min; b) Fmoc deprotection with 20% piperidine in NMP for 4x 3 min; c) Thr12, Glu18 and Pro37 are attached with double couplings and elongated reaction times (90 min);

From cycle 40 to the final cycle, capping is performed with a mixture of Ac_2O/DiPEA/HOBt in NMP at 500, 125 and 15 mM respectively (2x 2 min and 1x 5 min). This solution is prepared fresh on the ice every 2 days. After the completion of all cycles in SPPS, the resins were washed with diethylether and dried under high vacuum. Following this, the resin was transferred to a 50 mL falcon tube. Cocktail A was degassed for 5 min with nitrogen and 5 mL of this was added to the resin. The resin was mixed with the TFA cleavage mix by rotation for 3 h at RT. After incubating with the TFA cleavage mix, the resin was filtered using syringe filter units and the mix was collected in a falcon tube containing a mixture of dry-ice cold Et_2O, *n*-pentane (3:1 v/v) (40 mL). The resulting pellet was precipitated by slow centrifugation (10 min at 2,000 rpm). The Et_2O, *n*-pentane mixture was removed by decantation, and the pellet was taken up in fresh Et_2O, *n*-pentane (3:1 v/v) (40 mL) at room temperature and centrifuged. This step was repeated twice. The pellet was

dissolved in 5 mL cocktail B and lyophilized. In general, a 25 μmol scale SPPS afforded ±120 mg of crude material.

LC-MS, cation-exchange FPLC, and HPLC

Liquid chromatography-mass spectrometry (LC-MS)-grade solvents like Formic acid and ULC/MS-grade water was obtained from Biosolve. Fast protein liquid chromatography (FPLC)-eluents like 50 mM sodium acetate, pH 4.5, and 1M NaCl, 50 mM sodium acetate, pH 4.5 were prepared according to the standard procedure to make buffers and salt solutions. High-performance liquid chromatography (HPLC-S)-grade solvents like acetonitrile [CH_3CN] were bought from Biosolve.

The crude lyophilized thiolysine Ub mutant (white powder, ±120 mg) was dissolved in DMSO (1 - 4 mL) and then added dropwise to 50 mM NaOAc, pH 4.5 (45 mL) (*see* **Note 10**). This solution was loaded onto an FPLC column (15x185 mm) packed with Workbeads 40S™. The Ub mutant was purified using a gradient of 0 to 1 M NaCl over 5 column volumes in 50 mM NaOAc, pH 4.5. The fractions containing the desired product was analysed by LC-MS (±0.2 M NaCl). The NaCl and NaOAc in the pure fractions can be removed by RP-HPLC or by exchanging it for milliQ water by spin-filtration over 3 kDa cutoff membrane filters (Amicon Ultra-15 Centrifugal Filter Units). For RP-HPLC, the crude lyophilized thiolysine Ub mutant (white powder, ±25 mg) was dissolved in DMSO (1 mL) and 2-3 drops of TFA was added and vortexed mixture for 5 min. Then, Ub mutant was purified by RP-HPLC (Atlantis C18 column, 10x150 mm, 5 μM) using a protocol that starts with a gradient of 3 min from 5% to 25% CH_3CN followed by a gradient of 11 min from 25% to 43% CH_3CN (in water containing 0.05% TFA). The Ub-(δ-thiolysine) mutant elutes from 15 to 16 min. Pure fractions were analysed in LC/MS and pooled together. These were lyophilized, and the resulting powder was lyophilized again after dissolving in 10 mL cocktail B. The overall yields of the Ub-(δ-thiolsyine) mutants varied between 15-20%. For MS analysis of synthesized Ub and diUbs, we used Kinetex C18 LC-MS column (2.1x50 mm, 2.6 μm) from Phenomenex. For HPLC purification of diUbs, we used Atlantis® dC_{18} OBD™ preparative RP-HPLC column (19x250 mm, 10 μM) and Atlantis® Prep T3, C18 column (10x150 mm, 5 μM) from Waters. For cation exchange FPLC purification of Ub, we used Work Beads™ 40 S from Bio-Works.

Ubiquitin-E1 expression and purification

Ubiquitin (Ub) and Ub activating enzyme (UbE1) were expressed in a bacterial expression system and purified. UbE1 was expressed from Rosetta BL21 cells by growing the cells in a 5 mL starter culture at 37 °C for 4 hours until the cells were grown till saturation. After this, they were transferred to a 2 L LB medium at a dilution rate of 100 x and grown until the OD reached 0.6. Then, 1 mM IPTG was added to this medium and the temperature was reduced to 18 °C for the cells to express UbE1 overnight. The following day, the cells were spun down at 2500xG for 5 min and the supernatant was removed. UbE1 cell pellets was homogenized in lysis buffer containing 20 mM Tris-HCl, 5 mM β-mercaptoethanol, 250 mM NaCl, 1 mM PhenylMethaneSulphonyl Fluoride (PMSF) and 1 Protease-inhibitor tablets (EDTA-free) for 50 mL lysis buffer at 4°C. The cell lysate was then subjected to lysis by the French press applying a final pressure between 5000-10,000 psi at 4 °C. The cells were lysed twice in the French press to ensure complete extraction of protein. Finally, the cell lysate was centrifuged at 22,000 rpm for 30 minutes at 4°C in an ultracentrifuge. The supernatant was then collected in a separate tube and imidazole was added to a final concentration of 25 mM. Pre-washed TALON beads were then added to the tube in a ratio of 1:20 (v:v) and left at 4 °C for 15 minutes in a rotor to ensure homogenization of the lysate. The solution was then transferred to a column packed with a glass filter and pressure was applied using a syringe

set-up. The filtrate flow-through was collected and stored separately. The column was then washed twice with 5 bed volumes of wash buffer. Elution buffer containing 20 mM Tris-HCl, 5 mM β-Mercaptoethanol, 250 mM NaCl and 250 mM Imidazole was added up to four times the bed volume to the column and homogenized by repeated pipetting. It was left at 4 ºC for 10 minutes. Pressure was applied to collect the filtrate containing the UbE1 enzyme. A portion of this filtrate was used for SDS-PAGE analysis to confirm the presence of UbE1.

The rest of the sample was loaded into a centrifugal filter with a molecular cut-off of 25 KDa. It was spun for 60 minutes at 4000 rpm at 4 ºC in a centrifuge to concentrate the enzyme. Dilution buffer (20 mM Tris-HCl pH 8.0, 5 mM β-Mercaptoethanol, 250 mM NaCl) was then added to the tube until the final volume was about 10 ml and centrifuged again for 60 minutes at 4000 rpm at 4 ºC. The supernatant was finally diluted with dilution buffer to a final volume of 10 ml and aliquoted into 250 µl per vial, immediately frozen in liquid nitrogen and stored at -80ºC.

Ubiquitin expression and purification

UbE1 was expressed by transforming Ub w.t. pET 15 plasmid (*Amp*+) into Rosetta cells and growing the cells in 5 mL starter culture in LB medium at 37 °C for 4 hours until the cells were grown till saturation. In the meanwhile, auto induction medium was prepared using the following components:

ZY medium (1L)

- 10 g Tryptone
- 5 g yeast extract
- 5 g NaCl
- MQ water was added to make up the final volume upto 1 L
- The medium was autoclaved at 121ºC for 15 minutes

NPS buffer (20×)

Component	mol/liter
dd H_2O	-
$(NH_4)_2SO_4$	0.5 M
KH_2PO_4	1 M
Na_2HPO_4	1 M

***Table 1: NPS buffer in 20x concentration**. The solution was prepared by adding the components in the sequence mentioned and stirred until they are completely dissolved. The pH of 20-fold dilution in water was around 6.75. The solution was autoclaved at 121ºC for 15 minutes.*

5052 (50×):

Component	concentration
Glycerol 100% solution	0.5 %
Glucose	0.05 %
α-lactose	0.2 %

***Table 2: 5052 addendum in 50x concentration**. The solution was prepared by adding the components in the sequence mentioned and stirred until they are completely dissolved.If necessary, the solution was snap heated in microwave (90ºC for about 30 seconds in intervals) until dissolved. The solution was autoclaved at 121ºC for 15 minutes.*

1 M $MgSO_4$

- 9.86 g $MgSO_4 \cdot 7H_2O$
- MQ water was added up to 40 ml
- Sterilization was performed using membrane filter (0.22 µm)

40% glucose (w/v)

- Glucose was added to the beaker filled with water and constantly stirred with a magnetic stirrer
- If necessary, the solution was snap heated in microwave (90ºC for about 30 seconds in intervals) until dissolved

ZYP-0.8G

Component	Concentration
ZY	-
1 M $MgSO_4$	1 mM
40% glucose	0.8%
20× NPS	1×
chloramphenicol (34 mg/mL)	34 µg/mL
ampicillin (50 mg/mL)	50 µg/mL

Table 3: ZYP 0.8G medium used for cell growth*. The 1M $MgSO_4$ was added before adding the 20x NPS to prevent precipitation of the medium. The saturated culture in ZYP 0.8G medium was slightly acidic around pH 6.0. The solution was autoclaved at 121ºC for 15 minutes.*

ZYP-5052 rich medium for auto-induction

Component	Concentration
ZY	-
1 M $MgSO_4$	1 mM
50x 5052	1×
20x NPS	1×
chloramphenicol (34 mg/mL)	34 µg/mL
ampicillin (50 mg/mL)	50 µg/mL

Table 4: ZYP 5052 medium used for autoinduction*. The 1M $MgSO_4$ was added before adding the 20x NPS to prevent precipitation of the medium. The solution was autoclaved at 121ºC for 15 minutes.*

After the starter culture reached saturation, 100 µl from this cell culture is inoculated in a 250 ml **ZYP-5052** medium supplemented with ampicillin in 2 L Erlenmeyer flask. They were left in the shaker at 300 rpm or more at 37ºC overnight. The next day (usually after 20-24 hours) when the OD_{600} was around 10, the cells were pelleted at 4000 rpm for 20 minutes. The supernatant was removed, and the cell pellet was resuspended in MQ containing protease inhibitor tablet. After homogenization, the cells were heated in a heating block at 90 °C for 30 minutes. After this, the cells were cooled down and DNAse I supplemented with 10 mM MgSO4 was added. After incubating for 15 min at 4 °C, the cells were heated again at 90 C for another 30 minutes and the lysate was then spun down at 20000 rpm for 30 minutes at 4 ºC. The supernatant was then used for purification using cation exchange chromatography followed by RP-HPLC using conditions mentioned in general methods. Finally, Ub was obtained as a lyophilized powder with a yield of 1 G per liter of cell culture.

For the synthesis of Ub-MESNa thioester, a buffer containing 0.2 M magnesium(II) chloride ($MgCl_2$), 0.5 M adenosine triphosphate (ATP), 2.0 M 2-mercaptoethane sulfonate sodium salt (MESNa), 50 mM sodium phosphate buffer, pH 8.0 were prepared according to standard procedure. To synthesize Ub-MESNa, 10 mg of ubiquitin was dissolved in 0.5 mL DMSO and then into 10.2 mL 50 mM sodium phosphate buffer, pH 8.0. To this was added 0.59 mL $MgCl_2$ (0.2 M; final conc. 10 mM), 0.59 mL MESNa (2.0 M; final conc. 100 mM) and finally 0.23 mL ATP (0.5 M; final conc. 10 mM). The pH was adjusted to pH 8.0 using 1N NaOH. Then 75 µL of Ub activating enzyme E1 (39 µM; final conc. 0.25 µM) was added and incubated at 37 °C for 3 hours (final Ub conc is now 100 µM) (*see* **Note 11**). The resulting Ub-MESNa thioester was purified by RP-HPLC (Atlantis C18 column, 10x150 mm, 5 µM) using an 18 min gradient from 10% to 60% CH_3CN in water containing 0.05% TFA. The conversion was almost 100 % and the final yield was approximately 85 % pure.

Native Chemical Ligation

Native chemical ligation (NCL) in the native buffer as performed in 0.2 M sodium phosphate buffer, containing 50 mM NaCl at pH 8. For this, 200 ηM of UbE1 was added to 100 µM of Ub w.t. and 100 µM of Ub(G76V) thiolysine (of each linkage type) in the presence of 6 mM ATP, 6 mM MgSO4 and 50 mM MESNa at 37 °C overnight.

In the case of NCL under denaturing conditions, Cocktail C buffer containing 6 M guanidine-HCl (Gdn·HCl) in 0.2 M sodium phosphate buffer at pH 7.0 (*see* **Note 3**) containing 50 mM tris(2-carboxyethyl)phosphine-HCl, pH 7.0 (TCEP) (Piercenet, *see* **Note 5**) and 100 mM 4-mercaptophenylacetic acid at pH 8.0 (MPAA) (AlfaAesar, *see* **Note 4**) was prepared. For the diUb ligation, 1 mL cocktail C was added to 10 mg of UbMESNa powder. To this solution was added 10 mg of Ub thiolysine mutant (of each linkage type) and incubated >6 h at 37°C. If LC-MS analysis shows any unreacted Ub thiolysine mutant, a fresh portion of UbMESNa (5 mg) powder was added, followed by an additional incubation for >6 h at 37°C. The resulting diubiquitin conjugate was purified by RP-HPLC (Waters Atlantis® dC_{18} OBD™ preparative RP-HPLC column (19x250 mm, 10 µm) using a protocol that starts with a gradient of 5½ min from 20% to 32% CH_3CN followed by a gradient of 15 min from 32% to 42% CH_3CN (in water containing 0.05% TFA) (*see* **Note 12**). The ligation product elutes from 12-15 min.

For the subsequent desulfurization step, cocktail D containing 6 M Gdn-HCl in 0.2 M sodium phosphate buffer pH 6.5 (*see* **Note 6**), 50 mM 2,2'-azobis(2-amidinopropane) dihydrochloride (**V-50**) (Wacko Chemicals USA), 50 mM Glutathione (GSH) (Aldrich) and 250 mM Tris(2-carboxyethyl)phosphine hydrochloride (TCEP) (ChemImpex) at pH 6.5 was prepared. It is to be noted that the diUb synthesized under native conditions was not desulphurized because the yield was generally lower than that used in denaturing conditions.

To execute radical desulfurization, Cocktail D was first degassed by argon bubbling for 10 min. Then, 10 mL cocktail D was added to 10 mg of the diUb conjugate. After this, 2,2'-Azobis(2-amidinopropane) dihydrochloride (542 mg, final conc= 0.2 M) was added to the mixture. The solution was vortexed for 1 min and incubate for >6 h at 60°C (*see* **Note 13**). After confirming complete desulfurization by LC-MS analysis, the native linked diubiquitin conjugate was purified by RP-HPLC Waters Atlantis® dC_{18} OBD™ preparative RP-HPLC column (19x250 mm, 10 µm) using a protocol that starts with a gradient of 7 min from 5% to 25% CH_3CN followed by a gradient of 20 min from 25% to 45% CH_3CN (in water containing 0.05% TFA). The product elutes from 16-19 min. The overall yields of the Ub-Ub chains vary between 40-70%.

The diUb conjugates were analysed using pre-cast polyacrylamide gels NuPAGE® Novex® 12% Bis-Tris Gels (Invitrogen) run in MES buffer (20x) NuPAGE®: diluted to 1x

using Demi water. The protein marker used was SeeBlue® Plus 2 Prestained Standard 1x (Invitrogen). The sample buffer used contained NuPAGE® LDS Sample Buffer 4x (Invitrogen) and 10% of 14.3 M 2-Mercaptoethanol (Aldrich).

After ligation, the diUb conjugates were analysed by SDS-PAGE gel electrophoresis. For this, 1 mg of diUb conjugate was dissolved in 100 μL DMSO and diluted into 900 μL milliQ water. 5 μL of this sample was added to 10 μL of 3x loading buffer (prepared by diluting 4× NuPAGE® SDS Sample Buffer (900 μL) with 90 μL 2-mercaptoethanol and 210 μL milliQ water). The samples were heated for 10 min at 70°C. Then, 10 μL of each sample was loaded onto a Pre-cast polyacrylamide gels NuPAGE® Novex® 12% Bis-Tris Gel. As a protein marker, 1x SeeBlue ® Plus 2 Prestained Standard and 10 μL of a Ub standard, respectively. The samples were run the gel containing 1x MES buffer at 190V (≈50 min). Finally, the samples were stained with Coomassie Brilliant Blue and destained with H_2O, EtOH, AcOH (50/40/10 v/v/v).

Notes

1. Only use peptide grade NMP. A potential problem with NMP (and DMF) is the presence of amines, which can give rise to partial Fmoc cleavage. To ensure that the NMP is of good quality, we recommend incubating Fmoc-Phe-OMe (5 mg), overnight in 1 mL of NMP and test for Fmoc cleavage by LC-MS analysis.
2. 50 mM Sodium phosphate pH 8.0 is prepared as follows: 284.1 mL of 0.2 M Na_2HPO_4 (Fluka, prepared by dissolving 17.8 g Na_2HPO_4 in 500 mL water) and 15.9 mL of 0.2 M NaH_2PO_4 (Fluka, prepared by dissolving 13.8 g in 500 mL water) were mixed and diluted with 300 mL water. This 0.1 M Sodium phosphate buffer pH 8.0 can then be diluted twice for 50 mM Sodium phosphate buffer pH 8.0.
3. 6 M Gdn·HCl in 0.2 M sodium phosphate buffer pH 7.0 is prepared by dissolving 229.2 g Gdn-HCl in up to 400 mL 0.2 M sodium phosphate buffer pH 7.0. The final pH is adjusted using to 7.0 with 10N NaOH.
4. MPAA does not dissolve readily in water until the pH is adjusted to 8.0. The MPAA stock at pH 8 is prepared as follows: 1.68 g of 4-mercaptophenylacetic acid is added to 7.5 mL water and the pH is adjusted to 8.0 using 10N NaOH. The final volume is around 10.8 mL, corresponding to a 4-mercaptophenylacetic acid concentration of 925 mM.
5. This can also be prepared by dissolving TCEP-HCl (ChemImpex) in milliQ water and adjusting the pH to 7.0 with 10N NaOH followed by 1N NaOH. The solubility of TCEP-HCl in water is >310 g/L (1.08 M); best is to start with a 1.0 M solution since this allows for dilution during the adjustment of the pH.
6. 6 M Gdn.HCl in 0.2 M sodium phosphate pH 6.5 is prepared as follows: 22.9 g of Gdn.HCl is dissolved in 40 mL 0.2 M sodium phosphate buffer pH 8.0 (see ***Note 2***). The pH is adjusted to 6.5 with 1N NaOH.
7. 50 mM NaOAc pH 4.5 is prepared as follows: A 5M NaOAc (Sigma Aldrich) stock is prepared by dissolving 205 g NaOAc in 143 mL acetic acid mixed with 800 mL water and the total volume is adjusted to 1 L with water. The final pH was 4.5. Next, 5 mL of this 5M stock was diluted with 495 mL of water.
8. Besides removing moisture, this also ensures that no traces of acetic acid (or other acids) are present, which can be introduced in trace amounts during the preparation and/or purification of these building blocks.
9. Safety precaution: it is important to cover the rotor baskets with a lid since the diethylether/n-pentane solution is highly volatile.

10. If the material does not dissolve well, the DMSO can be warmed carefully and vortexed. Adding a few drops of TFA is also beneficial, but here it is important to monitor its effect on the pH of the NaOAc buffer used for the cation chromatography.
11. In general, we found the reaction to be complete within 6 h. Best is, to follow the reaction by LC-MS analysis, and once completion is verified, to perform the RP-HPLC directly. Thioesters are labile under basic conditions, but they do show enhanced stability under these conditions when thiols (such as MESNa) are present. If storage is required, we recommend acidifying the reaction (for example by adding 100 mM NaOAc, pH 4.5).
12. It is important to remove any MPAA for the following radical-initiated desulfurization step as MPAA is known to act as a radical scavenger. After preparative HPLC purification of the ligation mixture, the anticipated δ-thiolysine linked diUb conjugates are isolated (partially) as MPAA disulfides. Incubation with TCEP (during the subsequent desulfurization step) gives clean formation of the reduced δ-thiolysine linked diUb conjugates. The amount of MPAA released during this *in situ* reduction has no inhibitory effect on the radical-initiated desulfurization.
13. The **V-50** does not dissolve completely upon addition; this is achieved upon incubation at 60°C. Since N_2-gas is released during the reaction, we recommend to slightly puncture any lid of a plastic reaction vessel.

Supplementary information

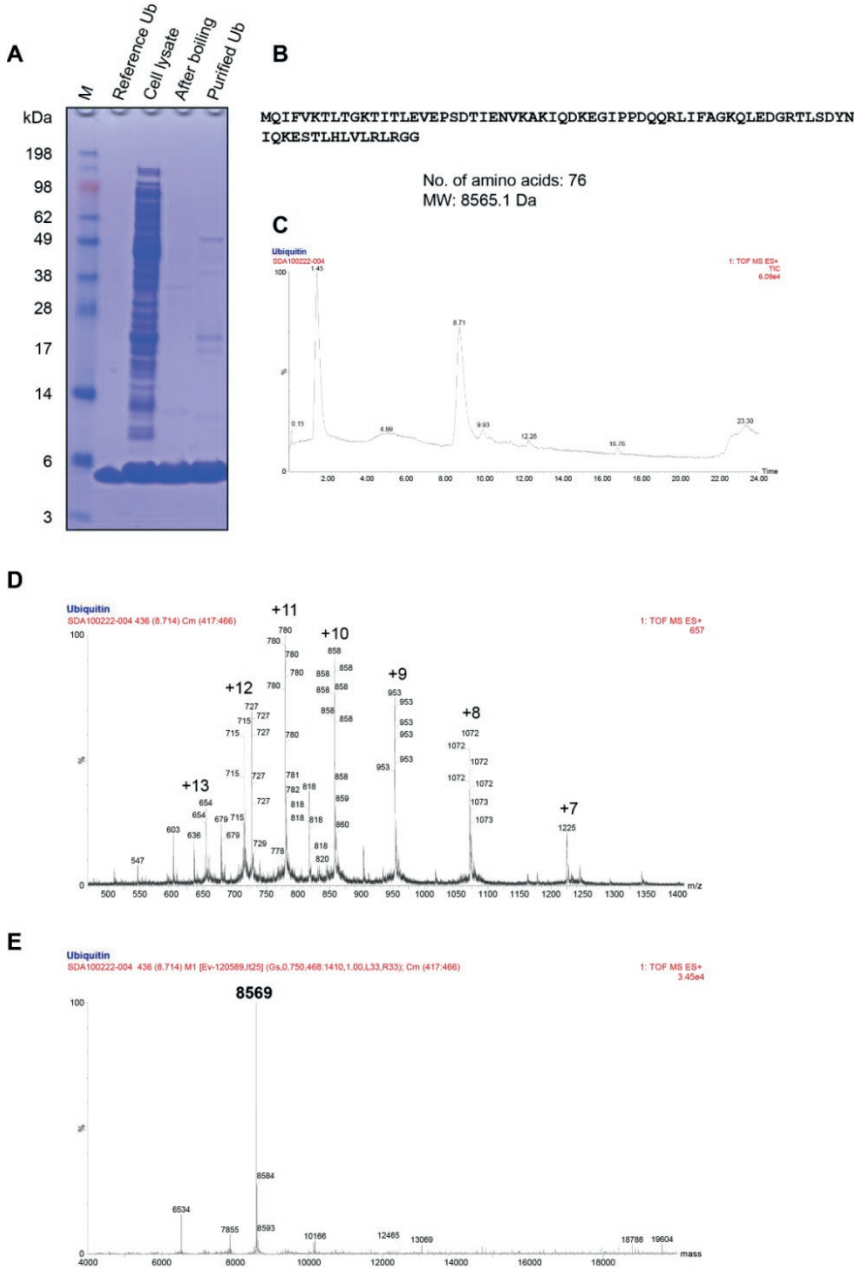


Figure S1: Expression and purification of Ub. ***A:*** *SDS-PAGE analysis of Ub expression in Rosetta BL21 cells and purification by boiling the lysate followed by reversed phase HPLC.* ***B:*** *Sequence of Ub.* ***C:*** *Combined UV chromatogram of Ub purified from bacterial cell lysate.* ***D:*** *Combined Mass spectra of Ub from C.* ***E:*** *Deconvoluted mass of Ub from mass spectra (Expected MW: 8564.8 Da, Observed: 8569 Da).*

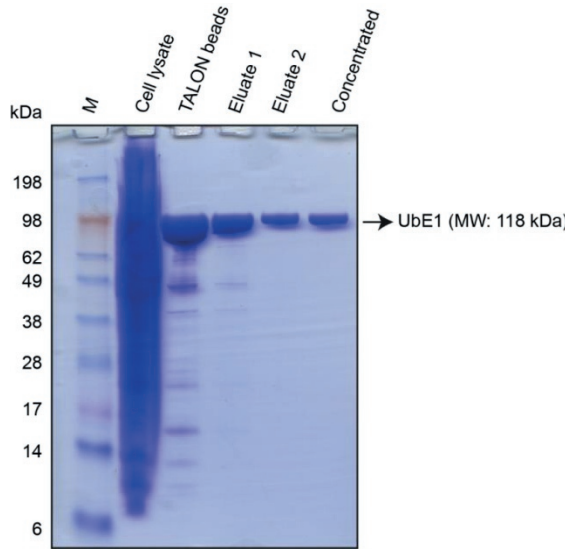


Figure S2: *Expression and purification of human UbE1 enzyme analyzed by SDS-PAGE.*

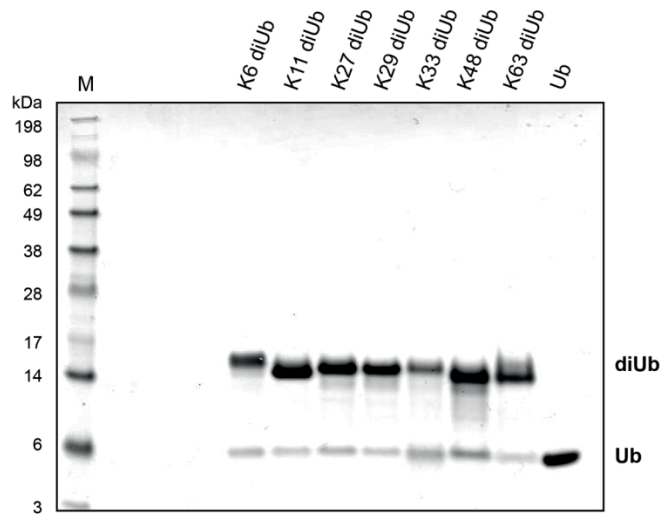


Figure S3: *Isopeptide linked diUbs generated by Native chemical ligation between Ub thioester and Ub K-δ-thiolysine, performed under denaturing conditions. All seven diUbs were prepared, desulfurized and purified using reversed phase HPLC.*

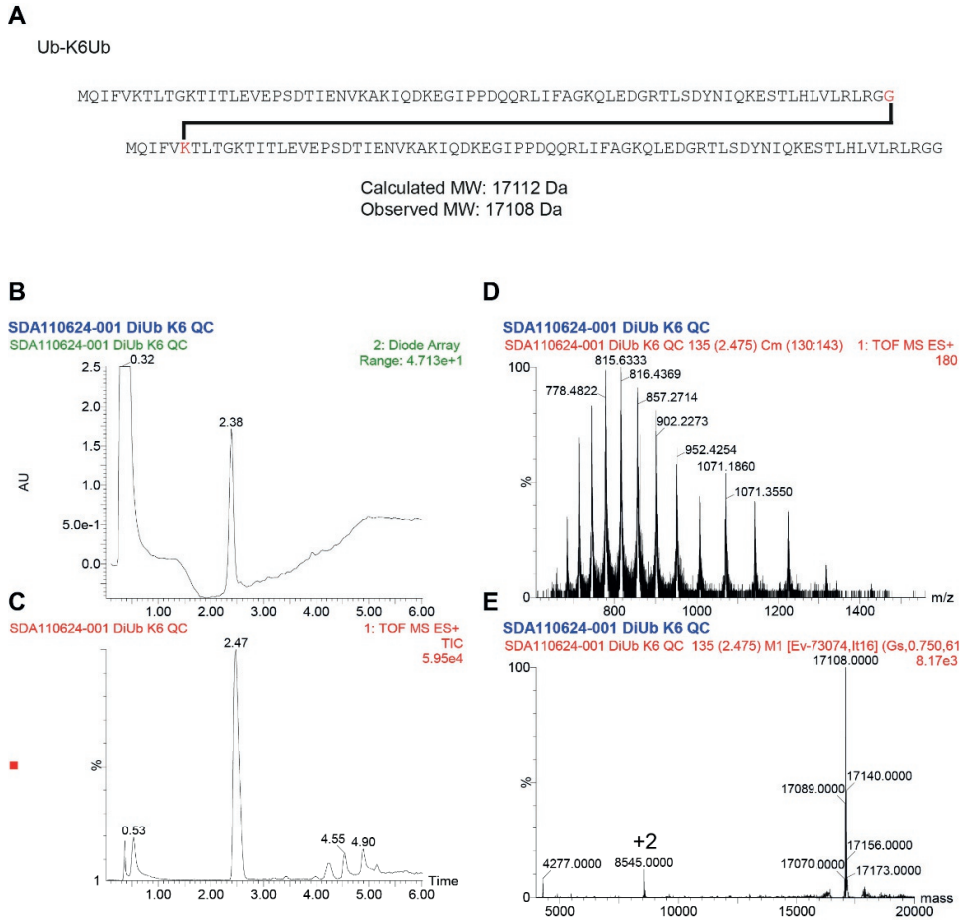


Figure S4: LC-MS analysis of K6diUb sample prepared under denaturing conditions. ***A:*** *Sequence of K6diUb showing the position of isopeptide bond.* ***B:*** *UV chromatogram (λ – 280 nm).* ***C:*** *Mass spectrum.* ***D:*** *Combined mass spectrum of peak at 2.47 min.* ***E:*** *Deconvoluted mass of mass spectra.*

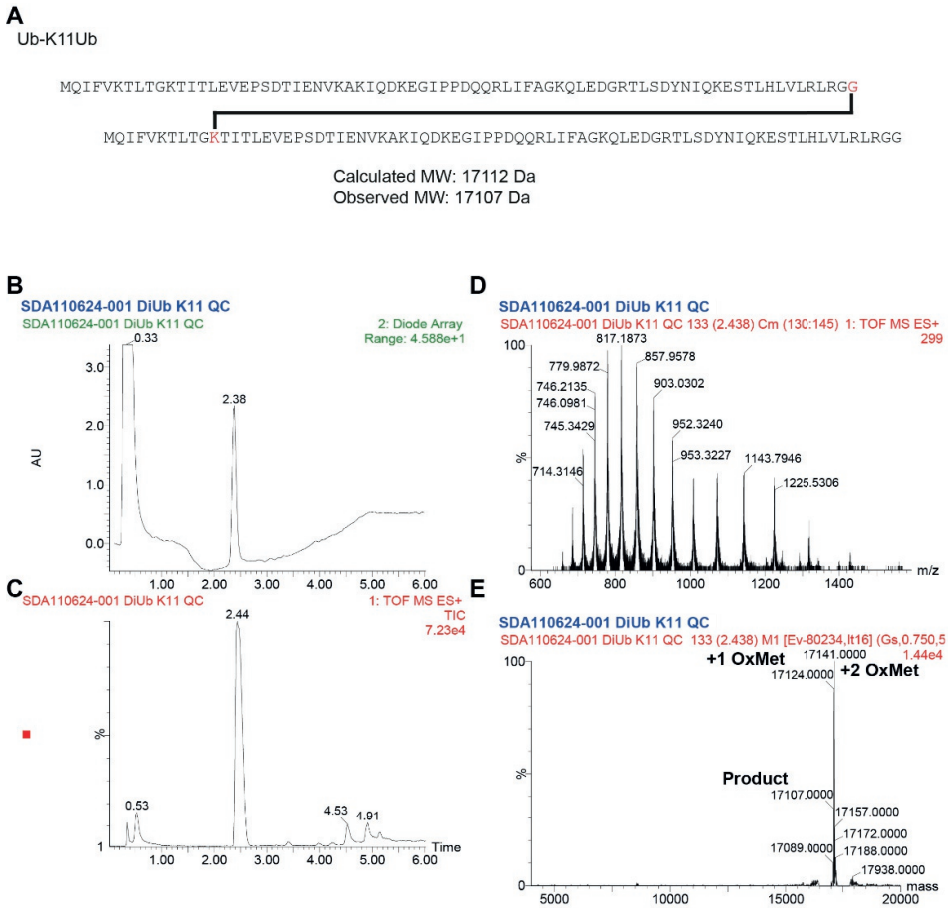


Figure S5: LC-MS analysis of K11diUb sample prepared under denaturing conditions. ***A:*** *Sequence of K11diUb showing the position of isopeptide bond.* ***B:*** *UV chromatogram (λ – 280 nm).* ***C:*** *Mass spectrum.* ***D:*** *Combined mass spectrum of peak at 2.44 min.* ***E:*** *Deconvoluted mass of mass spectra. The two additional masses correspond to oxidized state of the two methionine residues in the diUb molecule.*

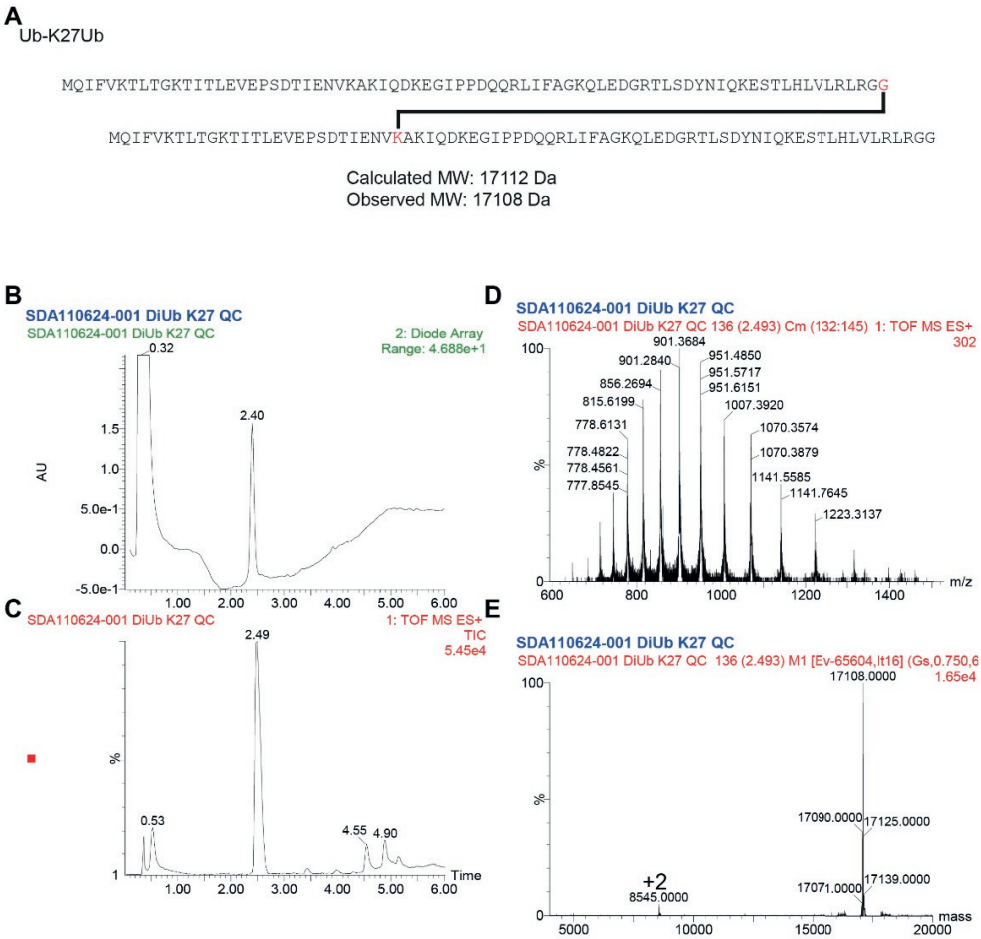


***Figure S6: LC-MS analysis of K27diUb sample prepared under denaturing conditions**. **A:** Sequence of K27diUb showing the position of isopeptide bond. **B:** UV chromatogram (λ – 280 nm). **C:** Mass spectrum. **D:** Combined mass spectrum of peak at 2.49 min. **E:** Deconvoluted mass of mass spectra.*

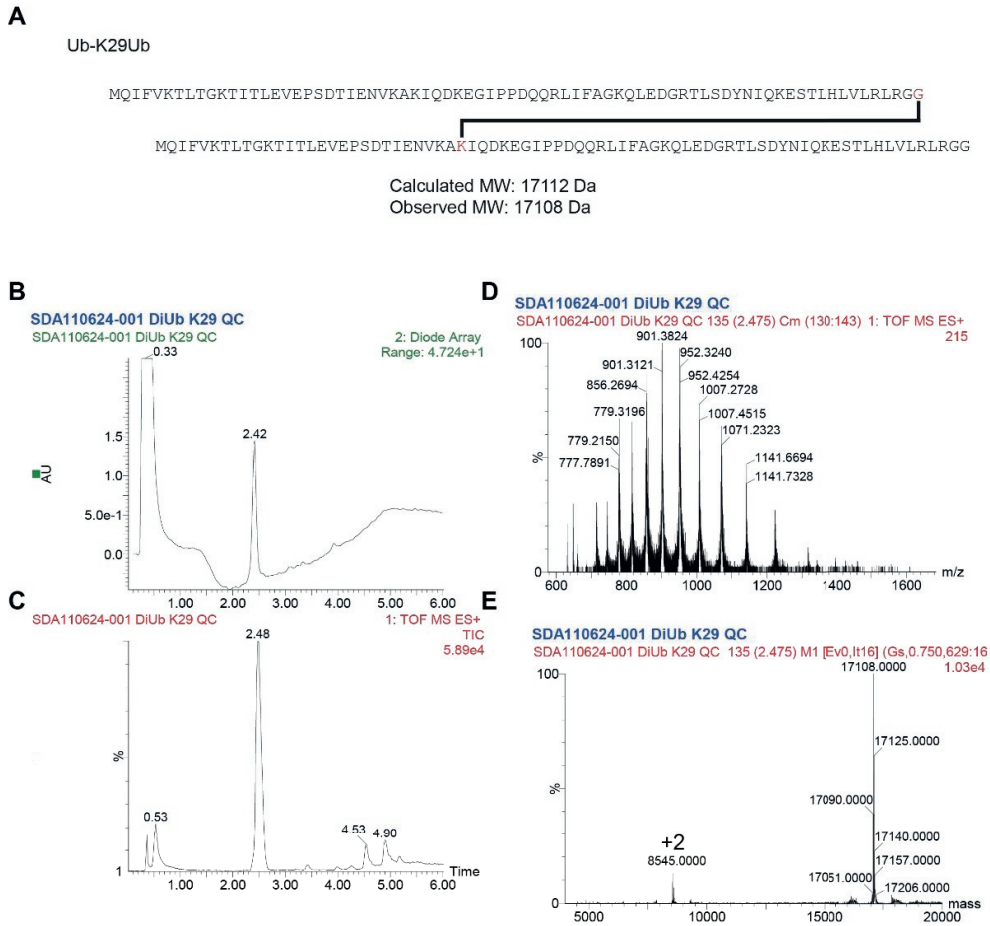


Figure S7: LC-MS analysis of K29diUb sample prepared under denaturing conditions. ***A:*** *Sequence of K29diUb showing the position of isopeptide bond.* ***B:*** *UV chromatogram (λ – 280 nm).* ***C:*** *Mass spectrum.* ***D:*** *Combined mass spectrum of peak at 2.48 min.* ***E:*** *Deconvoluted mass of mass spectra.*

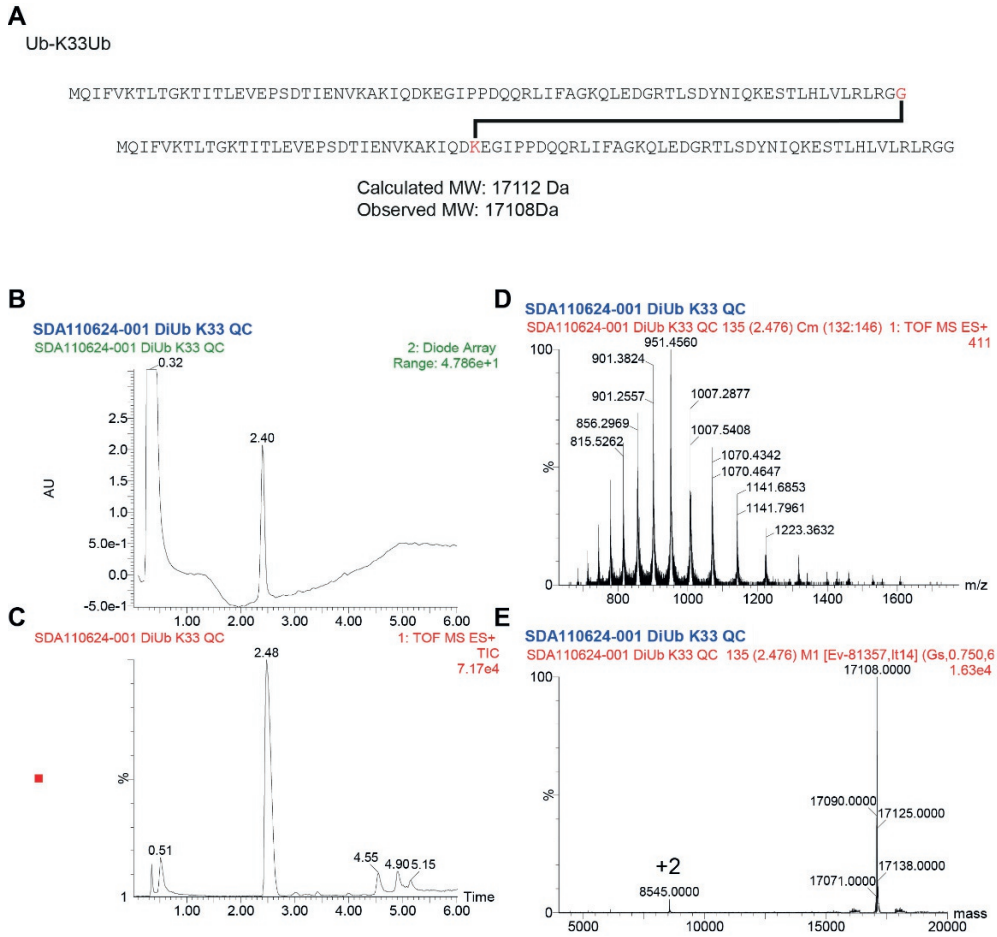


Figure S8: LC-MS analysis of K33diUb sample prepared under denaturing conditions. ***A:*** *Sequence of K33diUb showing the position of isopeptide bond.* ***B:*** *UV chromatogram (λ – 280 nm).* ***C:*** *Mass spectrum.* ***D:*** *Combined mass spectrum of peak at 2.48 min.* ***E:*** *Deconvoluted mass of mass spectra.*

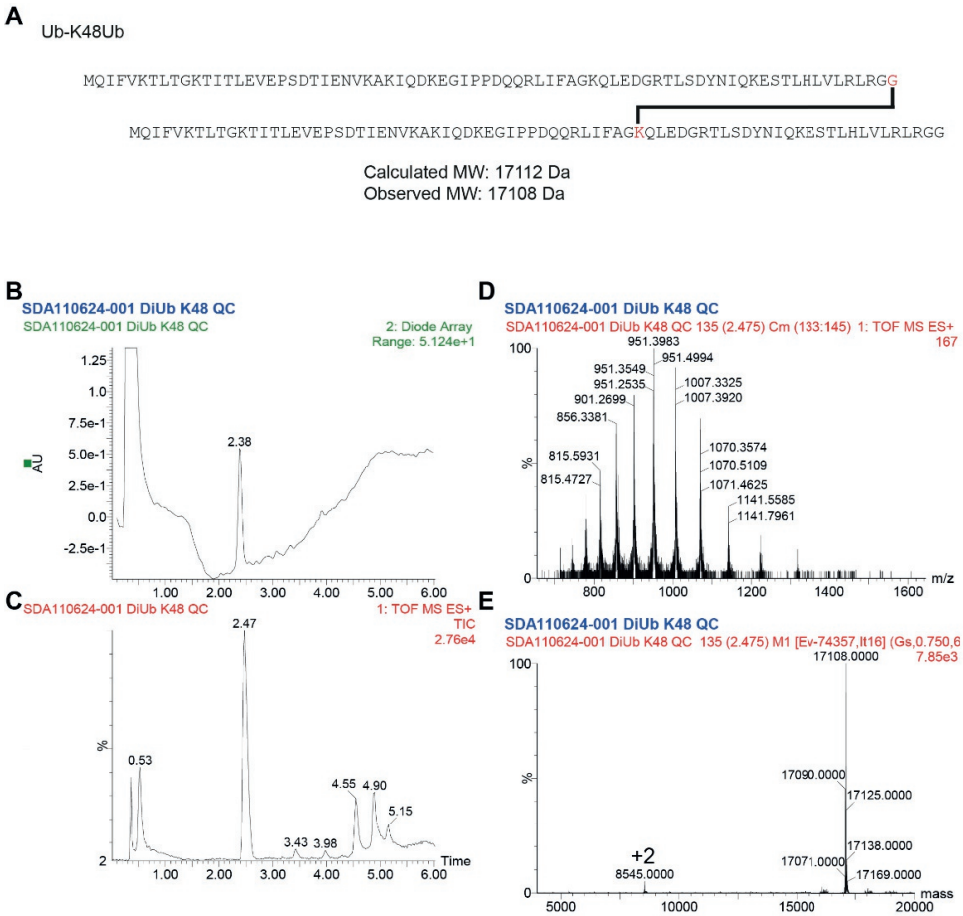


Figure S9: LC-MS analysis of K48diUb sample prepared under denaturing conditions. ***A:*** *Sequence of K48diUb showing the position of isopeptide bond.* ***B:*** *UV chromatogram (λ – 280 nm).* ***C:*** *Mass spectrum.* ***D:*** *Combined mass spectrum of peak at 2.47 min.* ***E:*** *Deconvoluted mass of mass spectra.*

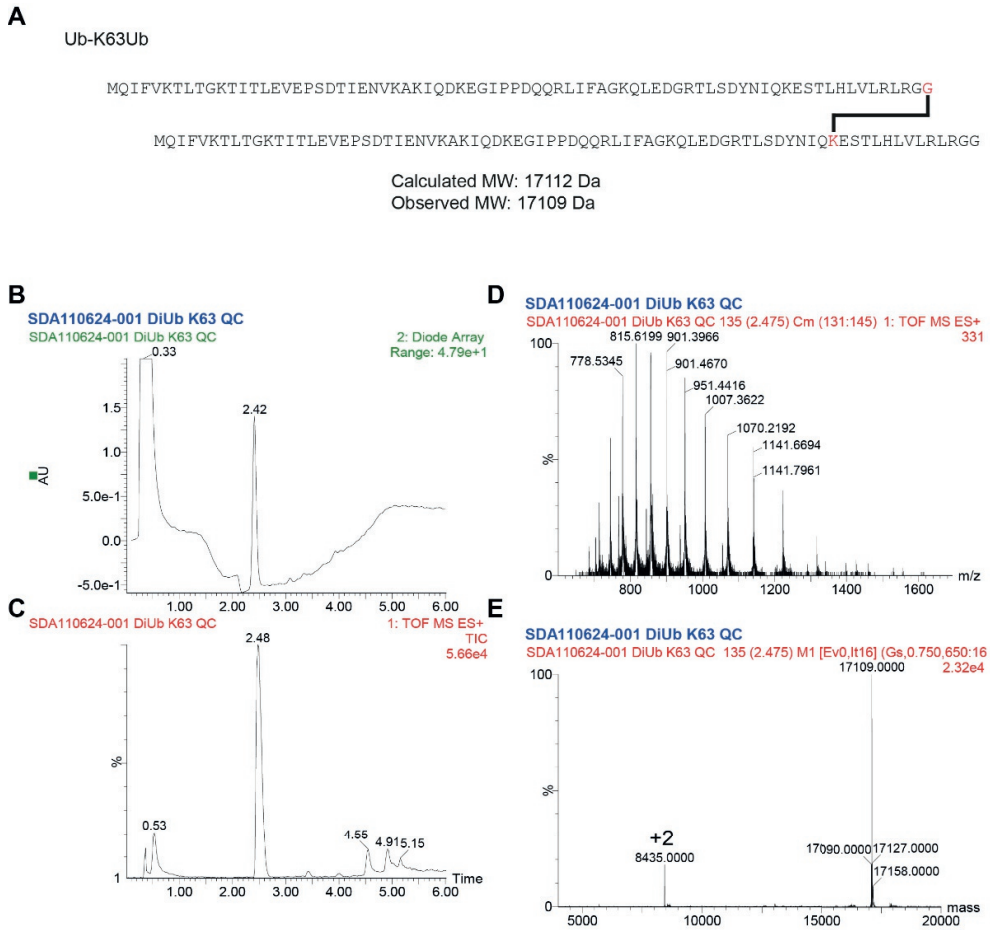


Figure S10: LC-MS analysis of K63diUb sample prepared under denaturing conditions. ***A:*** *Sequence of K63diUb showing the position of isopeptide bond.* ***B:*** *UV chromatogram (λ – 280 nm).* ***C:*** *Mass spectrum.* ***D:*** *Combined mass spectrum of peak at 2.48 min.* ***E:*** *Deconvoluted mass of mass spectra.*

References

1. Deshaies, R.J. and C.A. Joazeiro, *RING domain E3 ubiquitin ligases.* Annu Rev Biochem, 2009. **78**: p. 399-434.
2. Pickart, C.M., *Mechanisms underlying ubiquitination.* Annu Rev Biochem, 2001. **70**: p. 503-33.
3. Scheffner, M., U. Nuber, and J.M. Huibregtse, *Protein ubiquitination involving an E1-E2-E3 enzyme ubiquitin thioester cascade.* Nature, 1995. **373**(6509): p. 81-3.
4. Li, W. and Y. Ye, *Polyubiquitin chains: functions, structures, and mechanisms.* Cell Mol Life Sci, 2008. **65**(15): p. 2397-406.
5. Peng, J., D. Schwartz, J.E. Elias, C.C. Thoreen, D. Cheng, G. Marsischky, J. Roelofs, D. Finley, and S.P. Gygi, *A proteomics approach to understanding protein ubiquitination.* Nat Biotechnol, 2003. **21**(8): p. 921-6.
6. Ohtake, F. and H. Tsuchiya, *The emerging complexity of ubiquitin architecture.* J Biochem, 2017. **161**(2): p. 125-133.
7. Komander, D., M.J. Clague, and S. Urbe, *Breaking the chains: structure and function of the deubiquitinases.* Nat Rev Mol Cell Biol, 2009. **10**(8): p. 550-63.
8. Faggiano, S., C. Alfano, and A. Pastore, *The missing links to link ubiquitin: Methods for the enzymatic production of polyubiquitin chains.* Anal Biochem, 2016. **492**: p. 82-90.
9. Pickart, C.M. and S. Raasi, *Controlled synthesis of polyubiquitin chains.* Methods Enzymol, 2005. **399**: p. 21-36.
10. Bremm, A., S.M. Freund, and D. Komander, *Lys11-linked ubiquitin chains adopt compact conformations and are preferentially hydrolyzed by the deubiquitinase Cezanne.* Nat Struct Mol Biol, 2010. **17**(8): p. 939-47.
11. Dong, K.C., E. Helgason, C. Yu, L. Phu, D.P. Arnott, I. Bosanac, D.M. Compaan, O.W. Huang, A.V. Fedorova, D.S. Kirkpatrick, S.G. Hymowitz, and E.C. Dueber, *Preparation of distinct ubiquitin chain reagents of high purity and yield.* Structure, 2011. **19**(8): p. 1053-63.
12. Hospenthal, M.K., S.M. Freund, and D. Komander, *Assembly, analysis and architecture of atypical ubiquitin chains.* Nat Struct Mol Biol, 2013. **20**(5): p. 555-65.
13. Kristariyanto, Y.A., S.A. Abdul Rehman, D.G. Campbell, N.A. Morrice, C. Johnson, R. Toth, and Y. Kulathu, *K29-selective ubiquitin binding domain reveals structural basis of specificity and heterotypic nature of k29 polyubiquitin.* Mol Cell, 2015. **58**(1): p. 83-94.
14. Kristariyanto, Y.A., S.Y. Choi, S.A. Rehman, M.S. Ritorto, D.G. Campbell, N.A. Morrice, R. Toth, and Y. Kulathu, *Assembly and structure of Lys33-linked polyubiquitin reveals distinct conformations.* Biochem J, 2015. **467**(2): p. 345-52.
15. Michel, M.A., P.R. Elliott, K.N. Swatek, M. Simicek, J.N. Pruneda, J.L. Wagstaff, S.M. Freund, and D. Komander, *Assembly and specific recognition of k29- and k33-linked polyubiquitin.* Mol Cell, 2015. **58**(1): p. 95-109.
16. Virdee, S., Y. Ye, D.P. Nguyen, D. Komander, and J.W. Chin, *Engineered diubiquitin synthesis reveals Lys29-isopeptide specificity of an OTU deubiquitinase.* Nat Chem Biol, 2010. **6**(10): p. 750-7.
17. Dawson, P.E., T.W. Muir, I. Clark-Lewis, and S.B. Kent, *Synthesis of proteins by native chemical ligation.* Science, 1994. **266**(5186): p. 776-9.
18. Ajish Kumar, K.S., M. Haj-Yahya, D. Olschewski, H.A. Lashuel, and A. Brik, *Highly efficient and chemoselective peptide ubiquitylation.* Angew Chem Int Ed Engl, 2009. **48**(43): p. 8090-4.

19. Yang, R., K.K. Pasunooti, F. Li, X.W. Liu, and C.F. Liu, *Dual native chemical ligation at lysine.* J Am Chem Soc, 2009. **131**(38): p. 13592-3.
20. H.Ovaa , F.E.O., *Lysine compounds and their use in site- and chemoselective modification of peptides and proteins*. 2010.
21. El Oualid, F., R. Merkx, R. Ekkebus, D.S. Hameed, J.J. Smit, A. de Jong, H. Hilkmann, T.K. Sixma, and H. Ovaa, *Chemical synthesis of ubiquitin, ubiquitin-based probes, and diubiquitin.* Angew Chem Int Ed Engl, 2010. **49**(52): p. 10149-53.
22. White, P., J.W. Keyte, K. Bailey, and G. Bloomberg, *Expediting the Fmoc solid phase synthesis of long peptides through the application of dimethyloxazolidine dipeptides.* J Pept Sci, 2004. **10**(1): p. 18-26.
23. Merkx, R., G. de Bruin, A. Kruithof, T. van den Bergh, E. Snip, M. Lutz, F. El Oualid, and H. Ovaa, *Scalable synthesis of γ-thiolysine starting from lysine and a side by side comparison with δ-thiolysine in non-enzymatic ubiquitination.* Chemical Science, 2013. **4**(12): p. 4494.
24. Chatterjee, C., R.K. McGinty, J.P. Pellois, and T.W. Muir, *Auxiliary-mediated site-specific peptide ubiquitylation.* Angew Chem Int Ed Engl, 2007. **46**(16): p. 2814-8.
25. Haase, C., H. Rohde, and O. Seitz, *Native chemical ligation at valine.* Angew Chem Int Ed Engl, 2008. **47**(36): p. 6807-10.
26. Wan, Q. and S.J. Danishefsky, *Free-radical-based, specific desulfurization of cysteine: a powerful advance in the synthesis of polypeptides and glycopolypeptides.* Angew Chem Int Ed Engl, 2007. **46**(48): p. 9248-52.
27. Eletr, Z.M. and K.D. Wilkinson, *Regulation of proteolysis by human deubiquitinating enzymes.* Biochim Biophys Acta, 2014. **1843**(1): p. 114-28.
28. Komander, D., *Mechanism, specificity and structure of the deubiquitinases.* Subcell Biochem, 2010. **54**: p. 69-87.
29. Lee, M.J., B.H. Lee, J. Hanna, R.W. King, and D. Finley, *Trimming of ubiquitin chains by proteasome-associated deubiquitinating enzymes.* Mol Cell Proteomics, 2011. **10**(5): p. R110 003871.
30. Clague, M.J., S. Urbe, and D. Komander, *Breaking the chains: deubiquitylating enzyme specificity begets function.* Nat Rev Mol Cell Biol, 2019.
31. D'Arcy, P., X. Wang, and S. Linder, *Deubiquitinase inhibition as a cancer therapeutic strategy.* Pharmacol Ther, 2015. **147**: p. 32-54.
32. Farshi, P., R.R. Deshmukh, J.O. Nwankwo, R.T. Arkwright, B. Cvek, J. Liu, and Q.P. Dou, *Deubiquitinases (DUBs) and DUB inhibitors: a patent review.* Expert Opin Ther Pat, 2015. **25**(10): p. 1191-1208.
33. Pal, A., M.A. Young, and N.J. Donato, *Emerging potential of therapeutic targeting of ubiquitin-specific proteases in the treatment of cancer.* Cancer Res, 2014. **74**(18): p. 4955-66.
34. Flierman, D., G.J. van der Heden van Noort, R. Ekkebus, P.P. Geurink, T.E. Mevissen, M.K. Hospenthal, D. Komander, and H. Ovaa, *Non-hydrolyzable Diubiquitin Probes Reveal Linkage-Specific Reactivity of Deubiquitylating Enzymes Mediated by S2 Pockets.* Cell Chem Biol, 2016. **23**(4): p. 472-82.
35. Faesen, A.C., M.P. Luna-Vargas, P.P. Geurink, M. Clerici, R. Merkx, W.J. van Dijk, D.S. Hameed, F. El Oualid, H. Ovaa, and T.K. Sixma, *The differential modulation of USP activity by internal regulatory domains, interactors and eight ubiquitin chain types.* Chem Biol, 2011. **18**(12): p. 1550-61.
36. Licchesi, J.D., J. Mieszczanek, T.E. Mevissen, T.J. Rutherford, M. Akutsu, S. Virdee, F. El Oualid, J.W. Chin, H. Ovaa, M. Bienz, and D. Komander, *An ankyrin-repeat*

ubiquitin-binding domain determines TRABID's specificity for atypical ubiquitin chains. Nat Struct Mol Biol, 2011. **19**(1): p. 62-71.
37. Kim, R.Q., P.P. Geurink, M.P.C. Mulder, A. Fish, R. Ekkebus, F. El Oualid, W.J. van Dijk, D. van Dalen, H. Ovaa, H. van Ingen, and T.K. Sixma, *Kinetic analysis of multistep USP7 mechanism shows critical role for target protein in activity.* Nat Commun, 2019. **10**(1): p. 231.
38. Erlich, L.A., K.S. Kumar, M. Haj-Yahya, P.E. Dawson, and A. Brik, *N-methylcysteine-mediated total chemical synthesis of ubiquitin thioester.* Org Biomol Chem, 2010. **8**(10): p. 2392-6.

Chapter 3

Diubiquitin-based NMR analysis: interactions between Lys6-linked diUb and UBA domain of UBXN1

Adapted from:
Hameed, D.S., G.B.A. van Tilburg, R. Merkx, D. Flierman, H. Wienk, F. El Oualid, K. Hofmann, R. Boelens, and H. Ovaa, Diubiquitin-Based NMR Analysis: Interactions Between Lys6-Linked diUb and UBA Domain of UBXN1. Front Chem, 2019. 7: 921

Summary

Ubiquitination is a process in which a protein is modified by the covalent attachment of the C-terminal carboxylic acid of ubiquitin (Ub) to the ε-amine of lysine or N-terminal methionine residue of a substrate protein or another Ub molecule. Each of the seven internal lysine residues and the N-terminal methionine residue of Ub can be linked to the C-terminus of another Ub moiety to form 8 distinct Ub linkages and the resulting differences in linkage types elicit different Ub signalling pathways. Cellular responses are triggered when proteins containing ubiquitin-binding domains (UBDs) recognize and bind to specific polyUb linkage types. To get more insight into the differences between polyUb chains, all of the seven lysine-linked di-ubiquitin molecules (diUbs) were prepared and used as a model to study their structural conformations in solution using NMR spectroscopy. We report the synthesis of diUb molecules, fully ^{15}N-labeled on the distal (N-terminal) Ub moiety and revealed their structural orientation with respect to the proximal Ub. As expected, the diUb molecules exist in different conformations in solution, with multiple conformations known to exist for K6-, K48- and K63-linked diUb molecules. These multiple conformations allow structural flexibility in binding with UBDs thereby inducing unique responses. One of the well-known but poorly understood UBD-Ub interaction is the recognition of K6 polyubiquitin by the ubiquitin-associated (UBA) domain of UBXN1 in the BRCA-mediated DNA repair pathway. Using our synthetic ^{15}N-labeled diUbs, we establish here how a C-terminally extended UBA domain of UBXN1 confers specificity to K6 diUb while the non-extended version of the domain does not show any linkage preference. We show that the two distinct conformations of K6 diUb that exist in solution converge into a single conformation upon binding to this extended form of the UBA domain of the UBXN1 protein. It is likely that more of such extended UBA domains exist in nature and can contribute to linkage-specificity in Ub signalling. The isotopically labelled diUb compounds described here and the use of NMR to study their interactions with relevant partner molecules will help accelerate our understanding of Ub signalling pathways.

Introduction

Ubiquitin (Ub) is a small protein of 76 amino acids, involved in the post-translational modification of several proteins in cells [1, 2]. Ub is attached to a target protein in a process called ubiquitination which employs a specific combination of three enzyme classes: Ub activating enzyme E1, Conjugating enzyme E2 and Ub ligase E3 [3]. On the other hand, ubiquitin can be removed from its substrates by enzymes called deubiquitinases (DUBs) [4]. Ub is attached to a target protein as a monomer or as a polymeric chain (polyUb) in which individual Ub molecules are attached via their C-terminal residue to one of the seven lysine residues (K6, K11, K27, K29, K33, K48 and K63) or the N-terminal methionine residue of other Ub molecules [5, 6]. Different types of Ub modifications cause different responses, such as regulation of protein turnover and DNA-repair signalling and are therefore ubiquitination is essential in maintaining cellular homoeostasis. The polyUb chains vary in length, type of linkage (homotypic or branched) and the position of the modified lysine residues in target proteins [7]. Recognition of different polyUb chains by Ub binding domains (UBDs) is essential for stimulation of Ub signalling pathways.

The enzymatic assembly of all but K27-linked homotypical ubiquitin chains can be achieved by using the required combination of ubiquitinating E1-E2-E3 enzymes. [8-11] However, there is lack of control over the length of polyUb chains generated when using enzymatic methods and this often requires either mutating the Ub monomer to halt the chain extension or using extensive purification methods to separate different Ub polymers. In addition, such techniques are known for being less selective and require post-synthesis clean-

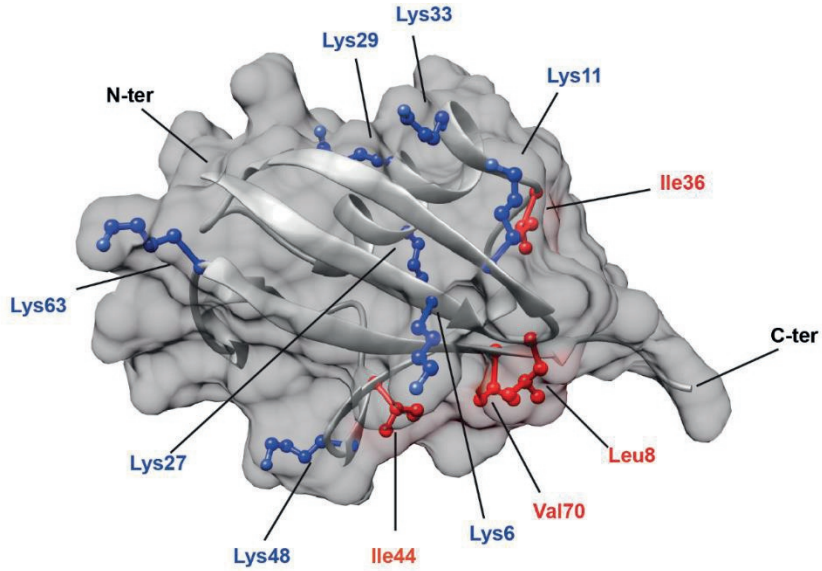


***Figure 1**: Structure of Ub (PDB: 1UBQ) showing the positions of all seven lysine residues (coloured in blue). In addition, hydrophobic residues (coloured in red) known to be involved in protein interactions are also highlighted.*

up of undesired chains using chain-specific DUBs. This results in low yields and long preparation times. To circumvent this, in the past years, we and others have reported the synthesis of ubiquitin chains using chemical tools. [12-15] The use of a thiolysine handle at the sites of ubiquitination and the omission of enzymes resulted in the generation of diUbs of all seven isopeptide linkages [16]. These chains have been used extensively to study the biochemical properties of DUBs [17, 18].

To study the structural behaviour of diUb molecules in solution by nuclear magnetic resonance spectroscopy (NMR), segmental isotope-labelled diUb reagents can be a valuable tool. Such a diUb molecule consists of a labelled Ub moiety linked to an unlabeled Ub moiety at defined positions. Synthesis of labelled diUb molecules has been reported previously relying on expressing recombinant Ub using an evolved tRNA/tRNA-synthetase system, followed by selective deprotection, chemical ligation and purification of diUb molecules [19, 20]. These diUb molecules can be used to study the intermolecular interactions with other proteins involved in the ubiquitin pathway.

It has been reported that Ub chain interactions with other proteins frequently involve a hydrophobic patch containing residues such as Leucine 8, Isoleucines 36 and 44, and Valine 70 on the ubiquitin surface (Figure 1, labelled in red) [21]. This patch is also involved in interactions between the Ub monomers in a diUb molecule or in polyUb chains. However, the position of interacting residues and the strength of the interaction between monomers differ for each Ub linkage [22]. Although structural information on commercially available K48 [23-25] and K63 [26-29] Ub chains and other atypical Ub chains of K6- [10, 30], K11- [31-33], K27- [34], K29- [35] and K33- [9, 20, 36] linkages is available, a comparative study on diUb structural dynamics in solution is necessary to get an idea on the differences in structure of different Ub linkages. Since structure-function relationships are known to be directive in ubiquitin signalling, it is essential to uncover the structural details of diUb

molecules. For obtaining structural details, X-ray crystallography and increasingly also single-particle EM can be used to obtain high-resolution snapshots of protein folding and interactions of diUb molecules with some of their interacting proteins. On the other hand, NMR spectroscopy can provide a more dynamic view on structural transitions due to changes in environmental conditions and allows kinetic analyses of binding and dissociation between proteins and their interacting partners. In this study, we synthesized all seven isopeptide-linked diUbs using native chemical ligation of different proximal lysine-Ubs to a distal ^{15}N-labeled Ub. A comparative study on the interactions between the ^{15}N-labelled distal Ub and the unlabeled proximal Ub for each of the diUb linkages showed different interaction details in good agreement with previously reported data[37, 38] Furthermore, we demonstrate here the usefulness of these tools for gaining structural insights into the selective recognition of a unique Ub-binding domain (UBD) for a diUb linkage.

Each ubiquitin linkage-type leads to a different response in cells, based on their recognition by specific proteins containing a UBD. UBDs provide a structural basis for different responses by recruiting Ub chains and other proteins associated in their respective pathway. For example, the DNA repair pathway is one of the crucial pathways in cells that utilize polyUb signalling and is essential in maintaining genomic integrity during or after cell division. DNA damage can be repaired by several mechanisms [39]. Among them, Non-Homologous End Joining (NHEJ) and Homologous Recombination (HR) are the most prevalent DNA-damage repair pathways. It has been observed that a Ubiquitin ligase called BRCA1 is involved in both of these DNA repair pathways. BRCA1 is an oncogene that is mainly associated with the prevalence of breast cancer [40].

The BRCA-mediated DNA repair pathway involves the recognition of K6 polyubiquitin chains on BRCA1 protein by another protein called UBXN1 [41]. The UBXN1 protein contains a UBD that belongs to the family of ubiquitin-associated domain (UBA) at its N-terminal tail [42]. The UBA domain is one of the earliest types of defined ubiquitin-binding domains described in literature [43]. These domains are short (about 45 amino acids) polypeptide sequences and are frequently observed in the enzymes associated with the ubiquitin machinery. The UBA domains usually consists of three alpha-helix modules which include a highly conserved hydrophobic surface that can bind efficiently with hydrophobic areas of Ub or polyUb chains [44]. The UBA sequences are conserved among proteins and enzymes involved in the proteasome degradation pathway [45] and in DNA repair [46].

Although it has been established that the UBA domain of UBXN1 can specifically recognize a K6 polyUb chain attached to the BRCA1 Ub ligase [42], the mode of interaction between the isolated UBA domain and the K6-Ub chain is largely unknown. Using our synthetic diUbs and biophysical techniques, we established how only an extended version of the UBA domain (UBAext1-52) of the UBXN1 protein binds selectively to K6 diUb. To illustrate the interaction of K6 diUb with UBAext1-52 of the UBXN1 protein, we monitored their titration by NMR and revealed which residues in the distal Ub of the K6 diUb molecule are important for this interaction. Understanding this interaction between the extended UBA domain and K6 Ub chains will help in understanding the interaction preference over other Ub chains.

Materials and methods

Expression of UBE1 enzyme and ^{15}N isotopic labelling of ubiquitin

All chemicals were obtained from Sigma unless stated otherwise. The ubiquitin-activating enzyme (UBA1) was recombinantly expressed with N-terminally fused hexahistidine tag (His6-tag). The enzyme was expressed in BL21 *E.coli* cells by adding 1 mM IPTG when the OD600 reached 0.6, followed by culturing the cells at 18°C overnight.

Cells were then sonicated in a lysis buffer containing 20 mM Tris-HCl, 250 mM NaCl and 5 mM 2-Mercaptoethanol at pH 8. The supernatant was incubated with TALON® metal affinity resin and after two washing steps, the UBA1 was eluted at 250 mM Imidazole concentration in the elution buffer. The imidazole was removed from the buffer using 10 kDa cut-off spin columns (Millipore). The final concentration of the enzyme was measured using a Nanodrop™.

^{15}N-enriched ubiquitin was expressed as an untagged protein using a pET2A expression system in BL21 *E.coli* cells in minimal essential medium. The M9 minimal essential medium contained 50 mM Na_2HPO_4, 50 mM KH_2PO_4, 5 mM Na_2SO_4, 50 mM $^{15}NH_4Cl$, 2 mM $MgSO_4$, 0.01% glycerol, 0.001% glucose and 0.004% lactose (inducer). After expression by autoinduction at 37°C overnight, cells were spun down at 3700 G for 10 minutes and resuspended in Milli-Q™ water containing protease inhibitor cocktail tablets. Then the suspension was heated to 85°C for 30 minutes, cooled down to room temperature and added with 0.3 mg DNase per 50 mL suspension along with 10 mM $MgSO_4$. After heating again at 85°C for 30 minutes, the cell lysate was spun down at 20,000 rcf. The supernatant was purified by cation-exchange chromatography at 4°C using AKTA Unichromat 1500- "PRO" system (15 × 185 mm column packed with Workbeads™ 40 S) with two mobile phases: 50 mM NaOAc, pH 4.5 (solvent A), and 1 M NaCl in 50 mM NaOAc (solvent B), pH 4.5 (Flow-rate 5 mL/min). All fractions were checked on an SDS-PAGE gel. The pure fractions collected from the cation-exchange column were re-purified over a C18 Atlantis preparative reverse-phase HPLC on a Shimadzu Prominence system using two mobile phases: A = 0.05% TFA in water and B = 0.05% TFA in CH_3CN (Column temperature 40°C, flow rate 7.5 mL/min, UV-signal is measured at 230 and 254 nm). Typical ubiquitin yields were 80 mg/L of cell culture.

Preparation of lysine-linked diubiquitin molecules

The ^{15}N-Ub-MESNa thioester was obtained according to a previously reported procedure with >95% yield, which was then purified using RP-HPLC and lyophilized [47]. ^{15}N-Ub-MESNa thioester ligations were performed using the following conditions: 125 mM HEPES-NaOH pH 8; 100 mM MESNa; 10 mM $MgCl_2$; 10 mM ATP and 250 nM UBA1 enzyme at a concentration of 550 μM ^{15}N Ubiquitin. The ^{15}N-Ub-MESNa thioester was then purified using reversed-phase HPLC (RP-HPLC). Ub (K6, K11, K27, K29, K33, K48 and K63) δ-thiolysine derivatives were prepared using chemical synthesis on a solid phase. Diubiquitins were synthesized using a previously reported procedure [13]. Native chemical ligation was performed by adding equal amounts of ^{15}N Ub MESNa thioester and thiolysine-Ub to a final concentration of 50 mg/mL in 6 M Gnd.HCl 0.2 M sodium phosphate buffer pH 8 containing 100 mM MPAA and 50 mM TCEP. After overnight ligation, the product was analyzed by LCMS and then diluted in desulphurization mix to a final concentration of 1 mg/ml protein (Diubiquitin). This mix contains 6 M Gnd.HCl 0.2 M sodium phosphate buffer pH 6.8, 200 mM TCEP, 50 mM reduced Glutathione, and 50 mM radical initiator VA-044 (2,2'-Azobis[2-(2-imidazolin-2-yl)propane]dihydrochloride). After overnight desulphurization, the product was analyzed by LCMS and purified with RP-HPLC.

Preparation of UBA peptides

UBA(1-42) and UBA(ext1-52) peptides were synthesized at 2 μmol scales, coupled with TAMRA on the N-terminus and purified by reversed-phase HPLC. Stock concentrations of TAMRA-UBA peptides were measured using a standard curve of TAMRA-K-G from 0-800 nM in 20 mM Tris pH 7.6 and 150 mM NaCl.

The amino acid sequence of the UBA domain of the UBXN1 protein is as follows:

```
          10         20         30         40         50
MAELTALESL IEMGFPRGRA EKALALTGNQ GIEAAMDWLM EHEDDPDVDE PL
```

Analysis of ubiquitin and diubiquitin molecules

The Ub and diUb molecules were analyzed by 12 % Nu-PAGE SDS gel electrophoresis using MES buffer and Seablue plus 2® as a protein marker. Isolated products with an expected molecular weight (MW) of 17,212 Da were observed as a single band in the gel at around 17 kDa. The MW of the product were also confirmed by LC/MS using a Phenomenex Kinetex C18 (2.1 × 50 mm, 2.6 µm) column (flow rate: 0.8 mL/min; runtime: 6 min; mobile phases: A = 1% CH_3CN, 0.1% formic acid in water and B = 1% water and 0.1% formic acid in CH_3CN; column T = 40°C. Protocol: 0–0.5 min: 5% B; 0.5–4 min: 5–95% B gradient; 4–5.5 min: 95% B). Final yields were measured after freeze-drying the product.

For Circular Dichroism (CD) measurements, a JASCO CD J1000 machine was used (UMC, Utrecht, the Netherlands). Samples were dissolved in DMSO and then diluted in NMR buffer containing 20 mM NaH_2PO_4 pH 6.8 to a final concentration of 4 µM. Measurements were performed at 25°C using wavelengths ranging from 260 nm to 185 nm in a span of 100 mdeg. The scanning speed was 20 nm/min and measurements from 10 experiments were averaged. After CD measurements, the samples were subjected to BCA assay to determine actual concentrations. Based on the observed values of CD measurements and concentration from BCA assay, CD plots were prepared.

NMR measurements

Freeze-dried ubiquitin and diubiquitin samples were dissolved in 5% DMSO (Biosolve) in Milli-Q® water and then redissolved in NMR buffer containing 20 mM $NaPO_4$ pH 6.8 and 10 % D_2O. Then, samples were taken in 15 ml 3.5 kDa Millipore spin filter tubes and spun-washed with three volumes of NMR buffer until DMSO was almost completely removed (LC/MS analysis). Concentrated samples were diluted to 500 µL with NMR buffer and the final concentration was determined using BCA assay using ubiquitin as standard. The pH was carefully measured using a Mettler TOLEDO pH probe.

All NMR studies were carried out on a Bruker 900 MHz spectrometer with a TCI cryoprobe, at 298 K (25°C). [^{1}H, ^{15}N] HSQC-spectra were acquired, processed and calibrated using standard methods. Chemical Shift Perturbations (CSPs) were calculated by comparing the [^{1}H, ^{15}N] HSQC spectra of mono Ub with that of each of the diUb molecules/ The CSP was calculated according to the following formula

$$CSP = \sqrt{(0.2\Delta\delta\mathrm{N})^2 + (\Delta\delta\mathrm{H})^2}$$

where ΔδH and ΔδN are the chemical shift differences for ^{1}H and ^{15}N respectively.
The spectra of K6 diUb indicated two different co-existing conformations. An ‘open conformation’ was assigned based on similarity with the mono-Ub spectrum.

Fluorescence polarization and microscale thermophoresis measurements

Fluorescence polarization (FP) measurements were performed at room temperature preceded by overnight incubation of UBA(ext1-52) domain with diubiquitin at 4°C. Total assay volume was 20 µL in black 384-well plates (low volume, flat bottom, non-binding surface; Corning®; ref 3820). All diubiquitin variants and concentrations were measured in triplicate. The concentration of synthetic TMR-labeled UBA domain was unchanged at 5 nM while diubiquitin was added in six steps of increasing concentrations from 0.78 – 25 µM. A UBA domain-only control (0 µM diubiquitin) was used to normalize measured FP values to

0. For these measurements, native diubiquitins were used and prepared as described previously [13]. DiUbs were additionally purified by gel filtration on a HiLoad 16/600 superdex 75 pg column (GE Healthcare) in 20 mM Tris pH 7.6 and 150 mM NaCl. The measurements were carried out in a FP binding buffer (20 mM Tris pH 7.6, 150 mM NaCl, 0.5 mg/ml BGG, 1% TX-100). Before each measurement, the plates were briefly centrifuged for 1 min at 4°C and 500 G. Read-out was performed on a PHERAstar plate reader (BMG labtech) using a TAMRA filter. Statistical analyses were performed with GraphPad Prism 7 software using non-linear regression analysis (one site binding (hyperbola)).

Microscale thermophoresis (MST) measurements were carried out using the synthetic TAMRA-UBAdomains in FP binding buffer. Concentrations of K6 diUb ranged from 1.53 nM – 50 µM. Samples were incubated for 30 min to allow binding and measured in hydrophobic capillaries on a Monolith NT.115 reader (NanoTemper Technologies, Munich, Germany) using 30% LED and 40% IR-laser power. The analysis was performed with GraphPad Prism 7 software using non-linear regression analysis (log (inhibitor) vs. response (three parameters)).

Results

DiUb synthesis and validation by gel, LCMS

Diubiquitin molecules were synthesized using our previously established native chemical ligation procedure (Figure 2) [13]. Briefly, the different proximal Ub moieties, containing a δ-thiolysine building block instead of a lysine residue, were generated using Fmoc SPPS.

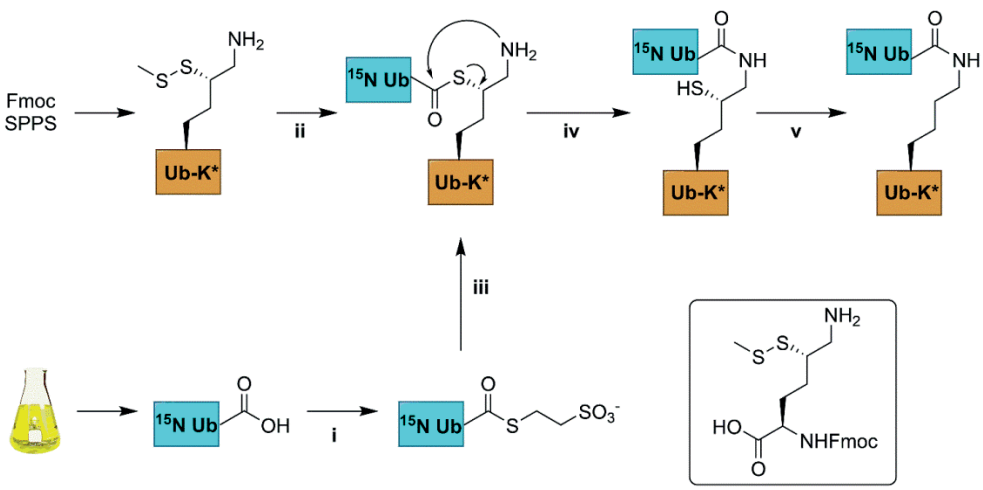


***Figure 2**: Schematic representation of the synthesis of ^{15}N-labelled diUb. ^{15}N-Ub was expressed in a bacterial expression system; thiolysine (inset) containing Ub was synthesized from Fmoc-based SPPS. i) 100 nM UbE1, 100 mM MESNa, pH 8; ii) 50 mM TCEP, 6M Gnd.HCl; iii) Ub-thiolysine after step ii, 100 mM MPAA, 6M Gnd.HCl, pH 8; iv) room temperature, overnight incubation; v) buffer exchange to remove MPAA, 100 mM TCEP, 100 mM VA-044, 6 M Gnd.HCl, pH 7.*

The distal ^{15}N-Ub part was prepared by recombinant bacterial expression in ^{15}N-ammonia enriched M9 minimal medium and converted to ^{15}N-Ub MESNa thioester using UbE1 enzyme and MESNa. The proximal and ^{15}N-distal Ub precursors were ligated using native

chemical ligation conditions. The product was then subjected to chemical desulfurization using TCEP and VA-044 and finally purified by reversed-phase HPLC.

The purified product was dissolved in DMSO and refolded into NMR buffer (20 mM $NaPO_4$ pH 6.8 and 10 % D_2O). ^{15}N-Ub was also purified by HPLC and refolded using the same procedure. To check for proper folding, the products were examined by Circular Dichroism (CD) using commercially available Ub as a control. Based on SDS-PAGE analysis (Figure S1A), the CD spectra (Figure S1B) and LC/MS analysis, the distal ^{15}N labelled diUbs (Figures S14 to S21) are found to be pure and properly refolded.

Comparison of NMR data of monoUb and diUb molecules

By NMR, a 2D [^{1}H.^{15}N] HSQC spectrum was obtained for ^{15}N-Ub (Figure S2). Although most of the signals were identified and assigned according to a previously reported data [48], signals corresponding to Met1, Glu24 and Gly53 backbone amides were missing. The data showed that monoUb is properly folded.

We compared the [^{1}H, ^{15}N] HSQC spectra of each of the different ^{15}N-diUb molecules (hereafter referred to as diUbs) to that of monomeric ^{15}N-Ub to reveal interactions between the distal Ub and proximal Ub moieties. Chemical shift perturbations (CSP) were calculated from ^{1}H and ^{15}N resonance frequency-differences between signals of the same residue in both monoUb and diUb spectra. This was plotted in a graph, illustrating the influence of the attached proximal Ub on residues in the ^{15}N-distal Ub moiety (Figure 3). Previously using a similar approach, the K48 [23, 49, 50] and K63 [29, 51] diUbs have been extensively studied. In our experiments, we also analyzed the NMR spectrum of all other diUb molecules.

CSPs are useful in determining the changes in the local environment of amino acids, which can be attributed to direct or indirect interactions but cannot be differentiated as such. All diUb spectra showed a common CSP behaviour in the C-terminal region of the distal Ub module, where the isopeptide linkage with the proximal Ub module is located. However, the hydrophobic region in Ub including the residues of Leu8, Ile36, Ile44 and Val70 and its surroundings also showed CSPs to a varying degree of magnitude and signal shift directions. In the case of K6 diUb, spectral changes were mostly observed for Leu8, Ile36 and a small region in the second beta-sheet covering residues Thr12, Ile13 and Thr14. K11 diUb showed similar behaviour encompassing residues Thr9, Ile13, Thr14 and Arg42. Here, Lys48, which is in the hydrophobic region surrounding Ile44 residue, was also disturbed. The elusive K27 diUb showed changes for Thr9 and Lys48 nearby the hydrophobic patch that surrounds Leu8 and Ile44 residues respectively. K29 diUb showed disturbances in Leu8, Ile13, Thr14 and Lys48, similar to that of K11 diUb. Intriguingly, the spectra of K27 diUb and K29 diUb show variation likely because the lys29 residue in K29 diUb is more solvent-exposed compared to lys27 in K27 diUb. Similar effects as with K29 diUb were also observed for K33 diUb. K48 diUb, which is the most studied so far, showed CSPs for Val5, Ile13, areas around Ile44 and Val70, encompassing the hydrophobic patch of Ub, suggesting a compact folding as had been observed in X-ray crystal structures of K48 polyUb chains [52]. Finally, K63 diUb shows the least interactions between the distal Ub and proximal Ub, in line with the reported open conformations known for K63 linked Ub chains. Comparing the overall CSPs of each of the diUbs measured in our NMR experiment, we observed that K6 diUb, K11 diUb, K29 diUb and K48 diUb showed more perturbations than K27 diUb, K33 diUb and K63 diUb.

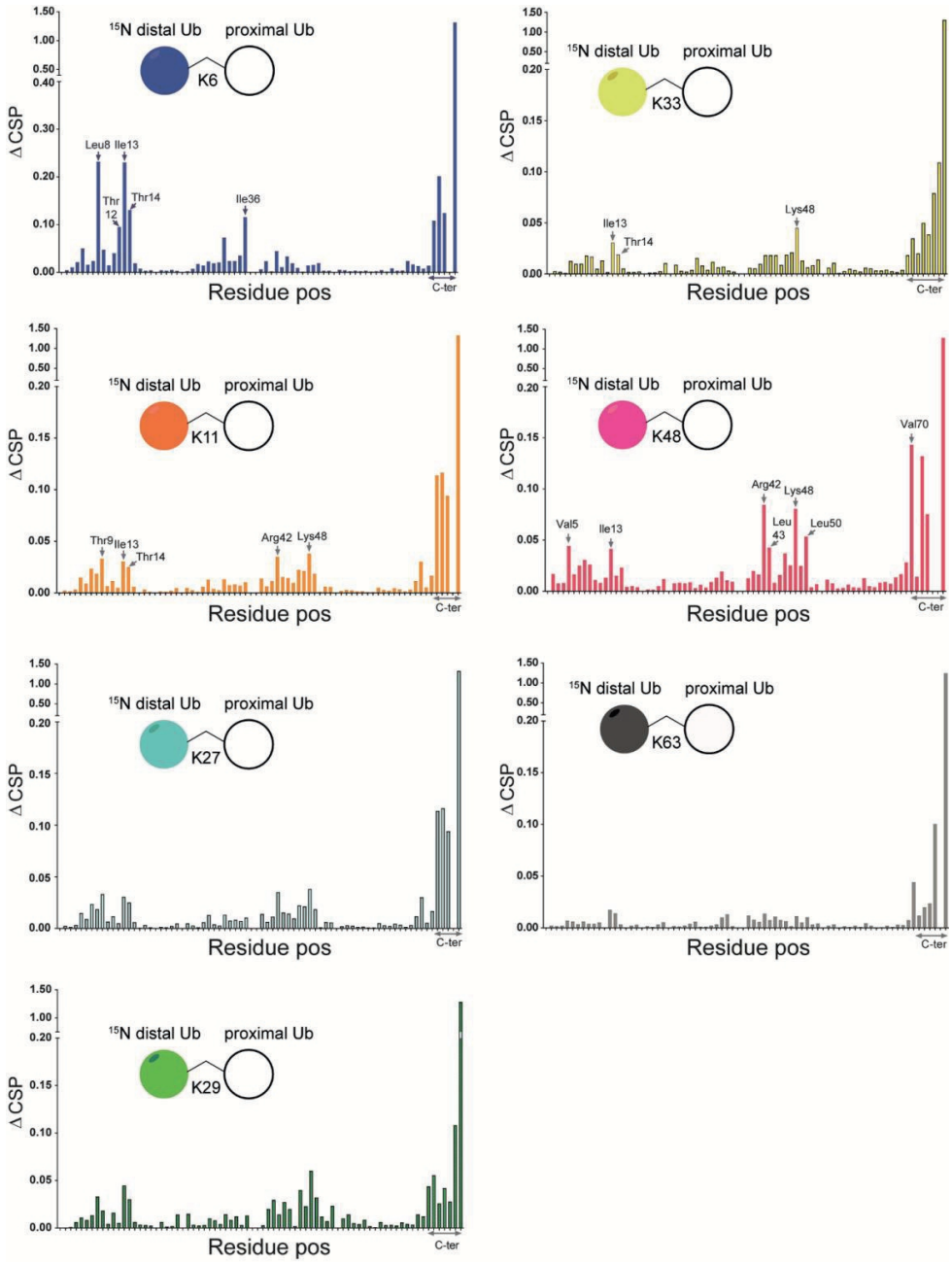


***Figure 3**: CSPs calculated for all isopeptide linked diUbs by comparison of ^{15}N-^{1}H HSQC spectrum of mono-Ub with that of each of the ^{15}N-labelled diUb. Pictorial representations of each of the diUbs are shown (in each panel). In general, the C-terminal residues in all diUbs show CSP due to their covalent bonding with the second unlabeled Ub. However, other residues also show changes, indicating their possible interaction with the unlabeled proximal Ub. The residues that show major CSP besides the C-terminal region are labeled.*

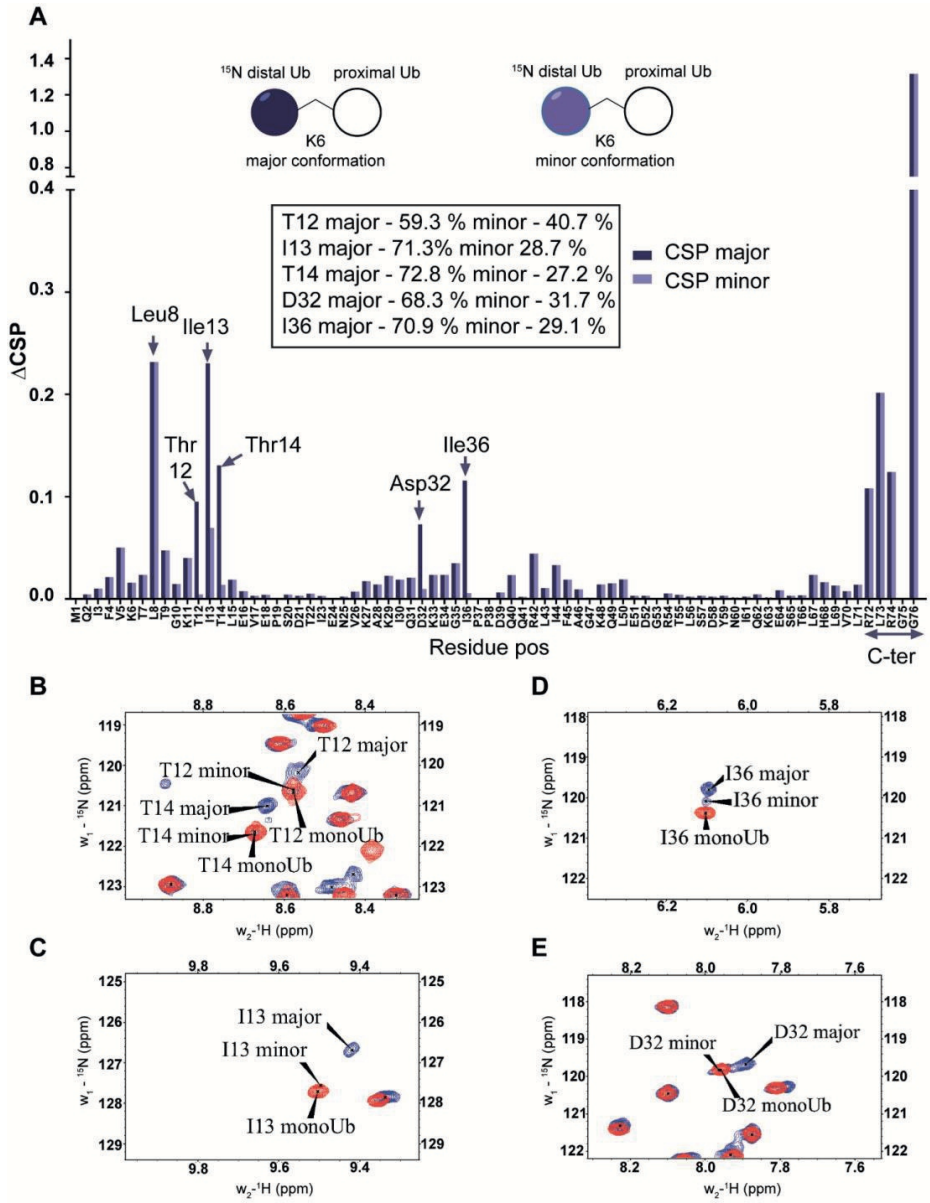


***Figure 4**: **A:** Chemical shift perturbations calculated by comparing the ^{15}N-^{1}H spectrum of mono-Ub and the distally ^{15}N-labelled K6-diUb (structural representation in inset). Although most of the signals are less affected, certain residues like Leu8, Thr12-Thr14, Ile36 and the C-terminal tail from Arg72 to Gly76 are all shifted significantly. This indicates a change in the electronic environment of these residues, which may be attributed to interactions with the unlabeled proximal-Ub. Leu8 and Ile36 show a considerable migration relative to other residues. In addition, signal doubling is observed for Asp32 and Ile36 in K6-diUb. **B-E**: NMR spectral regions showing ^{15}N-^{1}H peaks of Thr12, Ile13, Thr14, Asp32 and Ile36 of K6 diUb (blue) compared with monoUb (red).*

Of particular interest was the K6 diUb spectrum which showed signal-doubling for Thr12, Ile13 and Thr14 and residues Asp32 and Ile36 (Figure 4A-E). After ruling out the presence of impurities in the K6 diUb sample (Figures S1A, S15), we further analyzed this phenomenon. Based on the reported crystal structure for K6 diUb, the region around Asp32 and Ile36 is away from the interface between the two Ub moieties [30]. Our data suggest that there is a second conformation in solution. Assuming that relaxation properties and NMR lineshapes between the two conformations are similar we estimate the major and minor populations in an approximate ratio of 70:30 for K6 diUb (Figure 4). In the major conformation, Leu8, Asp32 and Ile36 could interact with Thr12, Ile13 and Thr14 residues ('loop-in' conformation) which is in agreement with a compact diUb fold. In the minor conformation, there is less effect from Ile36 and therefore less perturbations are seen in Thr12, Ile13 and Thr14 residues ('loop-out' conformation) indicating that this K6 diUb conformation is less compact than the closed one but comparable to K48 diUb.

A novel C-terminally extended UBA domain of the UBXN1 protein binds specifically to K6-linked diubiquitin *in vitro*

K6-linked polyubiquitin chains are known to be involved in BRCA-mediated DNA repair [41]. The BRCA1 protein forms a complex with BARD1 to gain its ubiquitin ligating activity. In addition to ubiquitinating many substrates involved in the DNA repair pathway with K6-linked polyUb chains [53], the BRCA1-BARD1 heterodimer complex can also auto-ubiquitinate itself with K6-linked polyUb chains [42, 54]. In this auto-ubiquitinated state, BRCA1-BARD1 ligase activity is significantly reduced by binding to the protein UBXN1 [42]. UBXN1 contains an N-terminal UBA domain (residues 1-42) that binds to K6-linked polyubiquitin chains conjugated to BRCA1, while the C-terminal sequences of UBXN1 bind the BRCA1/BARD1 heterodimer in a ubiquitin-independent fashion (Wu-Baer et al., 2010). However, the isolated UBA(1-42) domain of UBXN1 did not bind with K6 polyUb chains, while deletion of this section in full length protein did abolish K6 interaction. This implied to us that there might be more residues beyong the UBA domain that are important for the K6-linked ubiquitin interaction [42].

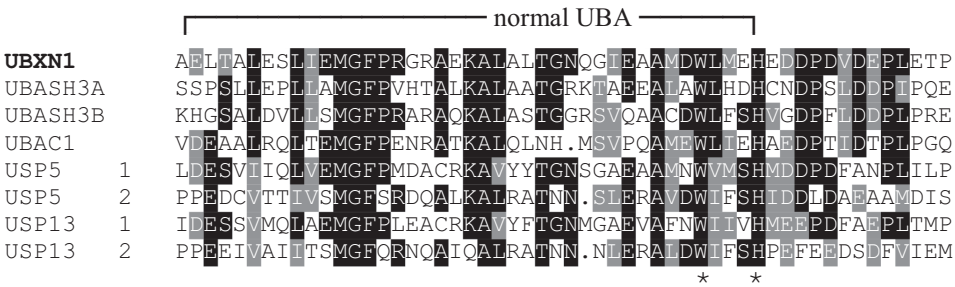


***Table 1**: Comparison of UBA domain sequences from different Ub binding proteins. The C-terminal extension adds about 10 amino acids at the C-terminal end of the conventional UBA domain. Moreover, all extended UBA domains have a totally invariant WxxxH motif within the 3rd helix. While this region is part of the conventional UBA fold, the conservation of this motif is only found in extended UBA-domain-containing members.*

To study this in more detail, we set out to investigate the specificity of the UBXN1 UBA domain for K6 diUb molecules using a Fluorescence Polarization (FP) binding assay in which TAMRA-labeled UBA peptide was added to different concentrations of unlabeled diUbs of

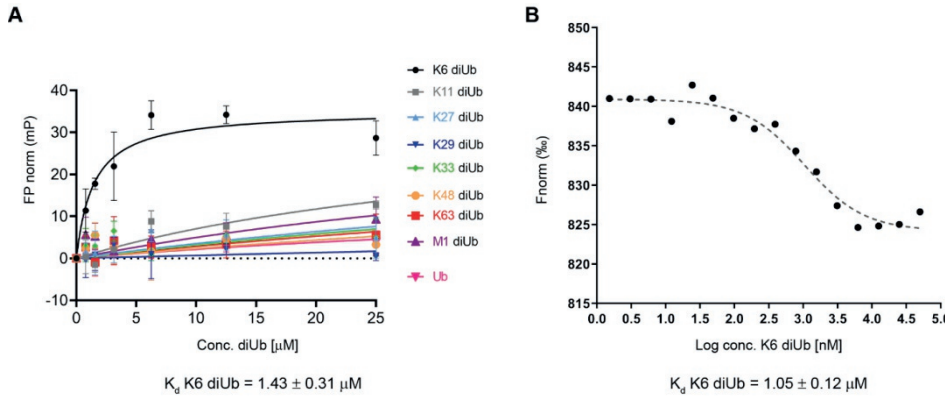


***Figure 5**: **A:** Fluorescence polarization assay using a TAMRA-labeled UBXN1 UBA(ext1-52) domain and different concentrations of all 8 homotypical diUbs and monoUb. **B:** Microscale thermophoresis binding curve of K6 diUb to TAMRA-labeled UBAext1-52 from UBXN1. These experiments show the preference and tight binding of UBA(ext1-52) to K6 diUb.*

all linkage types. Consistent with the findings of Wu-Baer *et al*, we also did not observe binding of K6 diubiquitin with the canonical UBA domain (1-42) of UBXN1 (Figure S10) [42]. On comparing the UBA domains of other proteins, we found that the 10 amino acids following the C-terminus of all conventional UBA domains that we compared showed the existence of a conserved sequence (Table 1). Interestingly when looking at the alignment, a previously unnoticed WxxxH motif was found to be conserved only in the extended versions of the UBA domain and not the shorter ones. To investigate whether this C-terminally extended version of the UBA domain of UBXN1 had any effect on binding to K6 diUb, we repeated the FP binding assay with the UBA (1-52) domain. We observed a tight and linkage specific binding to K6 diubiquitin (Figure 5A). We quantified the linkage specific binding of UBA(ext1-52) to K6 diUb with an approximate K_d of 1.43 ± 0.31 μM which was validated with an orthogonal technique called microscale thermophoresis (MST) (Figure 5B) and found a similar K_d value of 1.05 ± 0.12 μM.

Carefully analyzing the NMR structures of the isolated UBA domains of UBASH3A (pdb: 2CRN), UBASH3B (pdb: 2CPW), UBAC1 (pdb: 2DAI), USP5 UBA2 (pdb: 2DAK) and USP13 (pdb: 2LBC), we found that all three alpha-helices in the conventional UBA domain are structurally conserved whereas the first few residues of the 10 residues extending from the C-terminus starts from the last alpha-helix and then becomes largely unstructured (Figure 6). The C-terminal UBA extension in UBXN1 seemingly adds to K6 diubiquitin specificity and further research is needed to investigate whether this holds true for the other proteins containing this conserved C-terminal UBA extension and thereby establishing a functional role of this conserved motif.

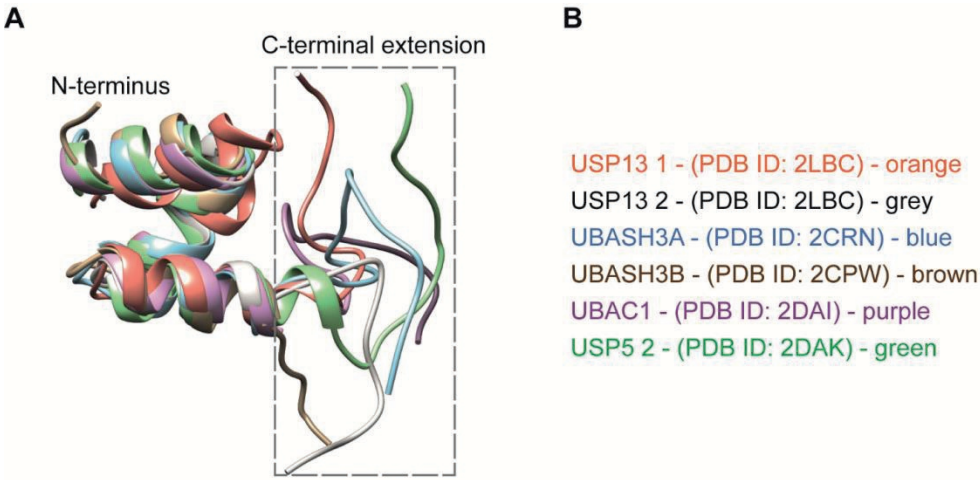


***Figure 6**: **A:** Structural comparisons of extended UBA domains. The C-terminal extension of all the UBA domains mentioned here is found to be disordered. **B:** The UBA-domain containing proteins are colour coded along with their respective PDB IDs.*

NMR of K6 diUb with the UBA (1-52) domain of UBXN1 provides an insight into the mode of interaction

To further study the interaction between the UBA(ext1-52) domain of UBXN1 and K6 diUb, we titrated the UBA(ext1-52) with ^{15}N-K6 diUb and monitored this by NMR. Signals corresponding to Lys 48, Gln49, Leu69, Leu71 and Leu73 disappeared after adding more than 1 equivalent of UBA(ext1-52), suggesting that these sites are in direct interaction with the UBA peptide. For other residues, signal shifts were observed. The CSP results indicated a distinct role of the hydrophobic patch on the distal Ub moiety that encompasses the residues Leu8, Ile44, Ala46 and Val70. Moreover, the residues Val5 to Thr9, Lys11, Ile13 and Thr14, surrounding Leu8 of the distal Ub, were also perturbed (Figure 7A, S11). Interestingly, shifts in Thr12, Ile13 and Thr14 were observed and explained previously as the "loop-in" and "loop-out" conformations for K6 diUb [10].

Some signals that were split in the reference spectrum converged upon the addition of UBA(ext1-52) peptide. For example, Thr12, Ile13 and Thr14 were split in the unbound K6 diUb spectrum, but upon adding increasing concentrations of the UBA(ext1-52) peptide, their signals converged (Figure S12). This indicates that the two different conformations of K6 diUb change into a single conformation upon binding with UBA(ext1-52) peptide. The fact that Ile44 and Leu8 show higher CSP values implying that the K6 diUb molecule is changing preferring the 'loop-out' conformation upon interacting with the UBA peptide. However, residues Asp32 and Ile36 (Figure S13) remained doubled, suggesting that the binding to the UBA(ext1-52) domain has local effects, but does not affect the structure of the entire distal Ub module.

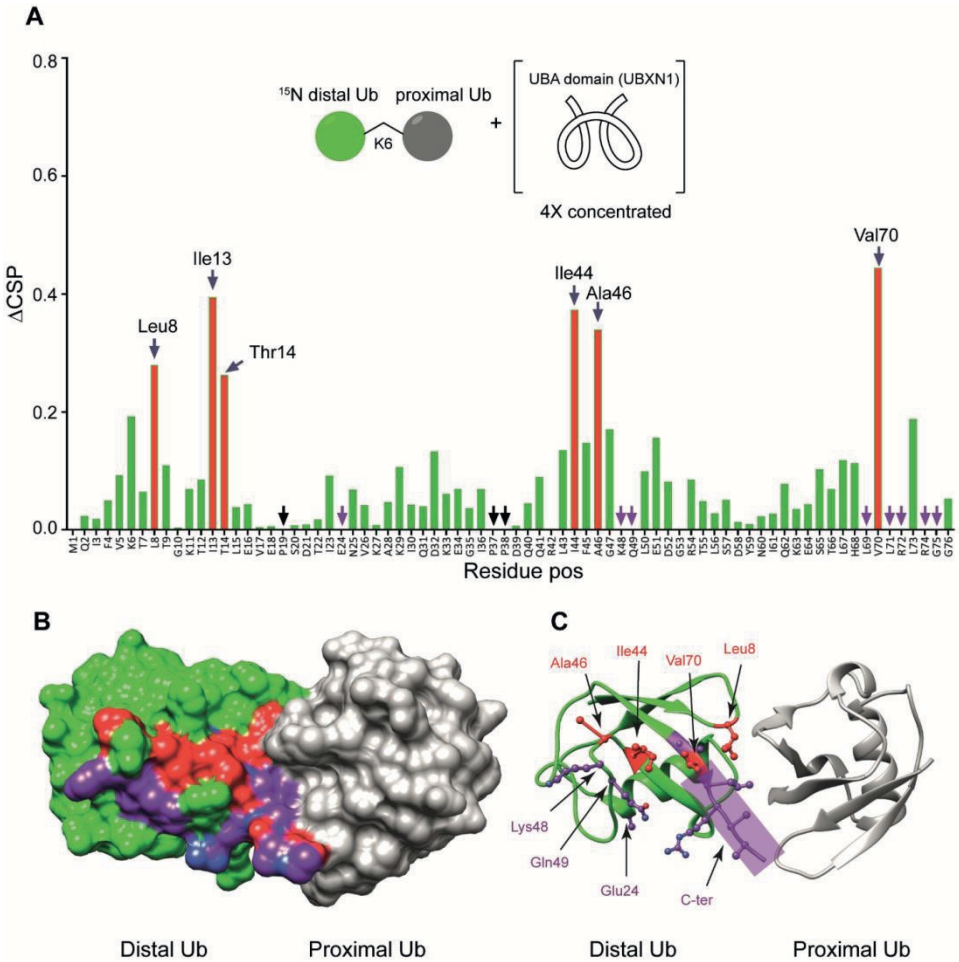


***Figure** 7: **A:** Unlabeled UBAext1-52 domain of UBXN1 was added in different concentrations to ^{15}N-K6 diUb and the CSPs were monitored. At a ratio of 4:1 (UBA(ext1-52) domain:K6 diUb), residues Leu8, Ile44, Ala46 and Val70 (red bars, labelled) shifted more than the rest. Other residues like Tyr 59 remain unchanged. **B:** X-ray crystal structure of a K6 diUb (PDB: 2XEW) showing the residues that were perturbed according to CSP. Residues that shifted more are coloured in red. Residues whose signal disappeared upon addition of UBA(ext1-52) peptide are represented in purple. **C:** The same structure in figure **B** but showing the positions of side chains of the residues that were affected upon UBA(ext1-52) binding. Several perturbed residues are found to be positioned on the surface away from proximal Ub.*

Using the known X-ray crystal structure of K6 diUb, the interacting residues were mapped on the Ub surface (Figure 7B and 7C). It appears that the residues interacting with the extended UBA peptide are positioned away from the proximal Ub moiety. The fact that the Leu8 residue of distal Ub is positioned at the interface between the distal Ub and proximal Ub moieties may suggest a dual role for this residue in interacting with both the proximal Ub and UBA peptide.

Discussion

Structures of all seven isopeptide-linked diUb molecules have been characterized using X-ray crystallography [26, 30, 33, 35, 36, 49, 55]. These crystal structures broadly fall into two categories: compact (K6, K48, K11, K27, K29, K33) and open (M1, K63) conformations [22]. Some Ub chains, however, are known to exist in intermediate forms in solution. For example, K48 chains obtain two different conformations in addition to several intermediate structures [50]. This structural flexibility is essential to facilitate polyUb signalling where K48 polyUb chains contribute to proteasomal degradation [51]. Although they mainly exist in a compact conformation, 10% of K48 Ub chains exist in an open conformation exposing the hydrophobic patches to make these accessible for interactions with proteins such as the UBA domain of hHR23A which leads to the recruitment of K48 poly-ubiquitinated substrates for proteasomal degradation [52]. In another study, the K48 diUb molecule has been found to exist predominantly in an open conformation [49]. It is clear that the existence of multiple conformations of K48 polyUb chains in cells are essential to bind with different proteins and elicit different responses and further research is needed to study the structural dynamics of K48 polyUb chains in cells. Although X-ray data can reveal different conformations of diUb molecules, solution NMR is convenient to study the dynamics between different conformations and interactions with specific binding domains. Moreover, control of the environment in NMR experiments offers freedom to study solution structures at different physiological conditions, pH or temperature. Given the advances in chemical synthesis of Ub and Ub molecules containing thiolysine, we were able to generate distally labelled diUbs and studied the interactions between the two Ub moieties from the perspective of distal Ub. The synthesis of Ub chains by genetic incorporation of protected lysine residues using modified tRNA synthetases followed by selective chemical ligation and deprotection has also enabled generating diUb molecules of all linkages which were then analysed by NMR spectroscopy [37]. Both approaches have demonstrated the advantages of using chemoenzymatic procedures to make diUb molecules to study their structural dynamics related to functionality.

For a better understanding of ubiquitin signalling pathway, it is essential to know how polyUb-specific interacting proteins recognize different polyUb chains. These interacting proteins often contain a specific UBD that can bind to specific polyUb chains, leading to different cellular responses. The best-studied Ub-interaction system is the K48 polyUb chain type and its corresponding interacting protein hHR23a in the proteasomal degradation system.. Recently, it has been shown that hHR23a protein also recognizes K27 Ub chains, thereby implicating it in the DNA repair mechanism [37]. Although K48 chains are readily available for in-vitro studies, K27 chains are impossible to make via biochemical strategies and recombinant enzymes. Hence the chemical synthesis of these chains, such as shown in this study, may develop into a valuable tool in identifying the interacting proteins and establish a mechanism of binding.

DNA repair pathways are essential for the maintenance of the integrity of genomic DNA. The DNA repair pathway requires the efficient action of different protein complexes including the BRCA complex. Ubiquitination also plays an essential role in this pathway by adding different ubiquitin chains onto the proteins involved. For instance, the BRCA/ABRAXIS protein complex can be polyubiquitinated with K6, K48 and K63 polyUb chains by different sets of ubiquitin ligation enzymes and each of these modifications leads to different responses in the cell. Of special interest is the polyubiquitination with K6 chains which leads to recruitment of the DNA polymerase complex to restart DNA synthesis after DNA repair has been accomplished [56]. For K6 polyUb chains, UBXN1 acts as a specific

receptor protein and its UBA domain has been reported to be involved in chain recognition. However, the exact mode of binding has not been shown using any biophysical methods so far. In this study, we showed that to achieve binding to K6-linked ubiquitin, instead of the canonical UBXN1 UBA (1-42) domain, an extended version of the UBXN1 UBA domain, UBA(ext1-52), is needed. For the first time, we gain structural insight into the recognition of this elusive K6-specific ubiquitin-binding domain. Our results suggest that different conformations of K6 chains are locked into one dominant conformation upon binding with the UBXN1 UBA(ext1-52) domain. The additional 10 amino acids long C-terminal extension of the conventional UBA domain is found to be conserved among different proteins and is therefore important to study this in more detail in future experiments.

Conclusion

We have synthesized all isopeptide-linked distally ^{15}N labelled diUb chains using native chemical ligation. This allowed us to study their conformations in solution and the interactions of the distal Ub moiety with the proximal Ub moiety by NMR. We also established that the additional C-terminal residues of the conventional UBA domain of UBXN1 protein are essential in binding specifically with K6 diUb molecule.
Upon comparing different diubiquitins of each linkage, we observed that K48-, K6-, K29- and K11- diUbs were in a relatively closed conformation while K33-, K27- and K63- diUbs were in a more open conformation. The CSPs revealed that K6 diUb exhibits the most closed conformation among all diubiquitins, whereas K63 exhibits the most open conformation. In general, calculating the total CSPs of all residues in each of the diUb spectra, excluding the C-terminal tail encompassing residues 70 to 76, provided a tentative overview on the degree

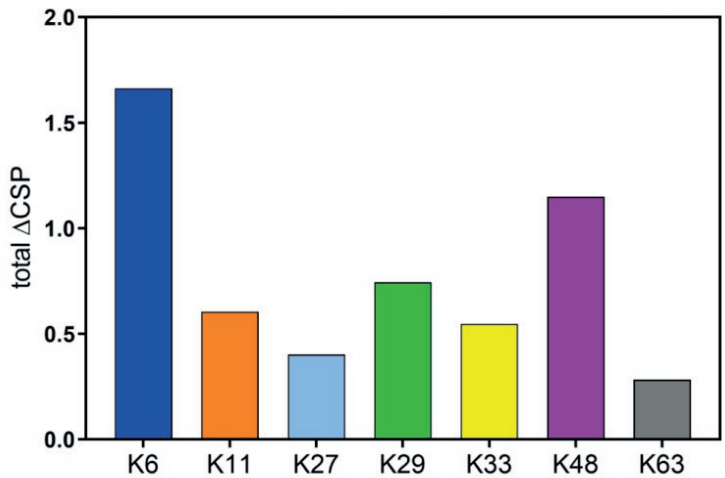


***Figure 8**: Sum of CSPs of residues in distal Ub of all diUbs excluding the C-terminal tail interactions which happen due to the proximity of isopeptide bond, and not exclusively due to the interaction between the interface of the distal and proximal Ub.*

of compactness for each of the diUb molecules (Figure 8). In addition, we found that certain diUbs like K6 diUb, K48 diUb and K63 diUb exist in more than one conformation. For instance, in K6 diUb the residues Val5, Thr12, Ile13, Thr14, Asp32 and Ile36 gave rise to two signals.

Using our synthetic ^{15}N diUbs, we established how only an extended version of the UBA domain (UBAext1-52) of the UBXN1 protein binds selectively to K6 diUb, using NMR titration experiments, revealing the crucial residues in the distal Ub of K6 diUb important for this interaction. With this, we demonstrate the applicability of these ^{15}N labeled diUb chains as tools for gaining structural insights into the selective recognition of a unique UBD for a diUb linkage.

Conflict of Interest

FE and HO declare competing financial interests as shareholder of UbiQ Bio BV.

Author Contributions

D.S.H and R.M. prepared the Ub and diUb reagents for NMR measurements. G.v.T did the FP and MST measurements for UBA(ext1-52) and diUb interactions. H.W. measured the NMR spectra. D.S.H. and H.W. analyzed the NMR data. D.F., F.E.O and K.H. provided valuable suggestions and ideas. R.B. and H.O. supported the work with grants from NWO.

Funding

Work in the Ovaa lab was supported by NWO (VICI grant 724.013.002). NMR experiments were performed at the SONNMRLSF facility, financially supported by an NWO-Groot Grant 175.107.301.10.

Acknowledgements

We would like to thank Henk Hilkmann and Dris el Atmioui for providing synthetic ubiquitin mutants and ubiquitin-binding domains. We would like to thank Dr. Monique Mulder, Dr. Gerbrand J. van der Heden van Noort and Stephan Scherpe for critical reading.

Reference

1. Hochstrasser, M., *Ubiquitin-dependent protein degradation.* Annu Rev Genet, 1996. **30**: p. 405-39.
2. Hershko, A. and A. Ciechanover, *The ubiquitin system.* Annu Rev Biochem, 1998. **67**: p. 425-79.
3. Scheffner, M., U. Nuber, and J.M. Huibregtse, *Protein ubiquitination involving an E1-E2-E3 enzyme ubiquitin thioester cascade.* Nature, 1995. **373**(6509): p. 81-3.
4. Komander, D., M.J. Clague, and S. Urbe, *Breaking the chains: structure and function of the deubiquitinases.* Nat Rev Mol Cell Biol, 2009. **10**(8): p. 550-63.
5. Akutsu, M., I. Dikic, and A. Bremm, *Ubiquitin chain diversity at a glance.* Journal of Cell Science, 2016. **129**(5): p. 875-880.
6. Meierhofer, D., et al., *Quantitative analysis of global ubiquitination in HeLa cells by mass spectrometry.* J Proteome Res, 2008. **7**(10): p. 4566-76.
7. Li, W. and Y. Ye, *Polyubiquitin chains: functions, structures, and mechanisms.* Cell Mol Life Sci, 2008. **65**(15): p. 2397-406.
8. Zhang, M., et al., *Chaperoned ubiquitylation--crystal structures of the CHIP U box E3 ubiquitin ligase and a CHIP-Ubc13-Uev1a complex.* Mol Cell, 2005. **20**(4): p. 525-38.
9. Michel, M.A., et al., *Assembly and specific recognition of k29- and k33-linked polyubiquitin.* Mol Cell, 2015. **58**(1): p. 95-109.
10. Hospenthal, M.K., S.M. Freund, and D. Komander, *Assembly, analysis and architecture of atypical ubiquitin chains.* Nat Struct Mol Biol, 2013. **20**(5): p. 555-65.
11. Faggiano, S., C. Alfano, and A. Pastore, *The missing links to link ubiquitin: Methods for the enzymatic production of polyubiquitin chains.* Anal Biochem, 2016. **492**: p. 82-90.
12. Kumar, K.S., et al., *Total chemical synthesis of di-ubiquitin chains.* Angew Chem Int Ed Engl, 2010. **49**(48): p. 9126-31.
13. El Oualid, F., et al., *Chemical synthesis of ubiquitin, ubiquitin-based probes, and diubiquitin.* Angew Chem Int Ed Engl, 2010. **49**(52): p. 10149-53.
14. van der Heden van Noort, G.J., et al., *Synthesis of Poly-Ubiquitin Chains Using a Bifunctional Ubiquitin Monomer.* Org Lett, 2017. **19**(24): p. 6490-6493.
15. Moyal, T., et al., *Polymerization behavior of a bifunctional ubiquitin monomer as a function of the nucleophile site and folding conditions.* J Am Chem Soc, 2012. **134**(38): p. 16085-92.
16. Merkx, R., et al., *Scalable synthesis of γ-thiolysine starting from lysine and a side by side comparison with δ-thiolysine in non-enzymatic ubiquitination.* Chemical Science, 2013. **4**(12): p. 4494-4498.
17. Licchesi, J.D., et al., *An ankyrin-repeat ubiquitin-binding domain determines TRABID's specificity for atypical ubiquitin chains.* Nat Struct Mol Biol, 2011. **19**(1): p. 62-71.
18. Faesen, A.C., et al., *The differential modulation of USP activity by internal regulatory domains, interactors and eight ubiquitin chain types.* Chem Biol, 2011. **18**(12): p. 1550-61.
19. Castaneda, C., et al., *Nonenzymatic assembly of natural polyubiquitin chains of any linkage composition and isotopic labeling scheme.* J Am Chem Soc, 2011. **133**(44): p. 17855-68.
20. Castaneda, C.A., et al., *Segmental isotopic labeling of ubiquitin chains to unravel monomer-specific molecular behavior.* Angew Chem Int Ed Engl, 2011. **50**(47): p. 11210-4.

21. Sloper-Mould, K.E., et al., *Distinct functional surface regions on ubiquitin.* J Biol Chem, 2001. **276**(32): p. 30483-9.
22. Wang, Y., et al., *PolyUbiquitin chain linkage topology selects the functions from the underlying binding landscape.* PLoS Comput Biol, 2014. **10**(7): p. e1003691.
23. van Dijk, A.D., D. Fushman, and A.M. Bonvin, *Various strategies of using residual dipolar couplings in NMR-driven protein docking: application to Lys48-linked di-ubiquitin and validation against 15N-relaxation data.* Proteins, 2005. **60**(3): p. 367-81.
24. Ryabov, Y. and D. Fushman, *Structural assembly of multidomain proteins and protein complexes guided by the overall rotational diffusion tensor.* J Am Chem Soc, 2007. **129**(25): p. 7894-902.
25. Zhang, N., et al., *Structure of the s5a:k48-linked diubiquitin complex and its interactions with rpn13.* Mol Cell, 2009. **35**(3): p. 280-90.
26. Weeks, S.D., et al., *Crystal structures of Lys-63-linked tri- and di-ubiquitin reveal a highly extended chain architecture.* Proteins, 2009. **77**(4): p. 753-9.
27. He, F., et al., *Myosin VI Contains a Compact Structural Motif that Binds to Ubiquitin Chains.* Cell Rep, 2016. **14**(11): p. 2683-94.
28. Komander, D., et al., *Molecular discrimination of structurally equivalent Lys 63-linked and linear polyubiquitin chains.* EMBO Rep, 2009. **10**(5): p. 466-73.
29. Liu, Z., et al., *Lys63-linked ubiquitin chain adopts multiple conformational states for specific target recognition.* Elife, 2015. **4**.
30. Virdee, S., et al., *Engineered diubiquitin synthesis reveals Lys29-isopeptide specificity of an OTU deubiquitinase.* Nat Chem Biol, 2010. **6**(10): p. 750-7.
31. Matsumoto, M.L., et al., *K11-linked polyubiquitination in cell cycle control revealed by a K11 linkage-specific antibody.* Mol Cell, 2010. **39**(3): p. 477-84.
32. Castaneda, C.A., et al., *Unique structural, dynamical, and functional properties of k11-linked polyubiquitin chains.* Structure, 2013. **21**(7): p. 1168-81.
33. Bremm, A., S.M. Freund, and D. Komander, *Lys11-linked ubiquitin chains adopt compact conformations and are preferentially hydrolyzed by the deubiquitinase Cezanne.* Nat Struct Mol Biol, 2010. **17**(8): p. 939-47.
34. Gao, S., et al., *Monomer/Oligomer Quasi-Racemic Protein Crystallography.* J Am Chem Soc, 2016. **138**(43): p. 14497-14502.
35. Kristariyanto, Y.A., et al., *K29-selective ubiquitin binding domain reveals structural basis of specificity and heterotypic nature of k29 polyubiquitin.* Mol Cell, 2015. **58**(1): p. 83-94.
36. Kristariyanto, Y.A., et al., *Assembly and structure of Lys33-linked polyubiquitin reveals distinct conformations.* Biochem J, 2015. **467**(2): p. 345-52.
37. Castaneda, C.A., et al., *Linkage via K27 Bestows Ubiquitin Chains with Unique Properties among Polyubiquitins.* Structure, 2016. **24**(3): p. 423-36.
38. Castaneda, C.A., et al., *Linkage-specific conformational ensembles of non-canonical polyubiquitin chains.* Phys Chem Chem Phys, 2016. **18**(8): p. 5771-88.
39. Schwertman, P., S. Bekker-Jensen, and N. Mailand, *Regulation of DNA double-strand break repair by ubiquitin and ubiquitin-like modifiers.* Nat Rev Mol Cell Biol, 2016. **17**(6): p. 379-94.
40. Rosen, E.M., et al., *BRCA1 gene in breast cancer.* J Cell Physiol, 2003. **196**(1): p. 19-41.
41. Ohta, T., K. Sato, and W. Wu, *The BRCA1 ubiquitin ligase and homologous recombination repair.* FEBS Lett, 2011. **585**(18): p. 2836-44.

42. Wu-Baer, F., T. Ludwig, and R. Baer, *The UBXN1 protein associates with autoubiquitinated forms of the BRCA1 tumor suppressor and inhibits its enzymatic function.* Mol Cell Biol, 2010. **30**(11): p. 2787-98.
43. Hofmann, K. and P. Bucher, *The UBA domain: a sequence motif present in multiple enzyme classes of the ubiquitination pathway.* Trends Biochem Sci, 1996. **21**(5): p. 172-3.
44. Mueller, T.D. and J. Feigon, *Solution structures of UBA domains reveal a conserved hydrophobic surface for protein-protein interactions.* J Mol Biol, 2002. **319**(5): p. 1243-55.
45. Chen, L., et al., *Ubiquitin-associated (UBA) domains in Rad23 bind ubiquitin and promote inhibition of multi-ubiquitin chain assembly.* EMBO Rep, 2001. **2**(10): p. 933-8.
46. Kozlov, G., et al., *Structural basis of ubiquitin recognition by the ubiquitin-associated (UBA) domain of the ubiquitin ligase EDD.* J Biol Chem, 2007. **282**(49): p. 35787-95.
47. Oualid, F.E., et al., *Synthesis of atypical diubiquitin chains.* Methods Mol Biol, 2012. **832**: p. 597-609.
48. Cornilescu, G., et al., *Validation of protein structure from anisotropic carbonyl chemical shifts in a dilute liquid crystalline phase.* Journal of the American Chemical Society, 1998. **120**(27): p. 6836-6837.
49. Hirano, T., et al., *Conformational dynamics of wild-type Lys-48-linked diubiquitin in solution.* J Biol Chem, 2011. **286**(43): p. 37496-502.
50. Lai, M.Y., et al., *Structural and biochemical studies of the open state of Lys48-linked diubiquitin.* Biochim Biophys Acta, 2012. **1823**(11): p. 2046-56.
51. Jacobson, A.D., et al., *The lysine 48 and lysine 63 ubiquitin conjugates are processed differently by the 26 s proteasome.* J Biol Chem, 2009. **284**(51): p. 35485-94.
52. Varadan, R., et al., *Structural determinants for selective recognition of a Lys48-linked polyubiquitin chain by a UBA domain.* Mol Cell, 2005. **18**(6): p. 687-98.
53. Sato, K., E. Rajendra, and T. Ohta, *The UPS: a promising target for breast cancer treatment.* BMC Biochem, 2008. **9 Suppl 1**: p. S2.
54. Chen, A., et al., *Autoubiquitination of the BRCA1*BARD1 RING ubiquitin ligase.* J Biol Chem, 2002. **277**(24): p. 22085-92.
55. Pan, M., et al., *Quasi-Racemic X-ray Structures of K27-Linked Ubiquitin Chains Prepared by Total Chemical Synthesis.* J Am Chem Soc, 2016. **138**(23): p. 7429-35.
56. Morris, J.R. and E. Solomon, *BRCA1 : BARD1 induces the formation of conjugated ubiquitin structures, dependent on K6 of ubiquitin, in cells during DNA replication and repair.* Hum Mol Genet, 2004. **13**(8): p. 807-17.

Supplementary information

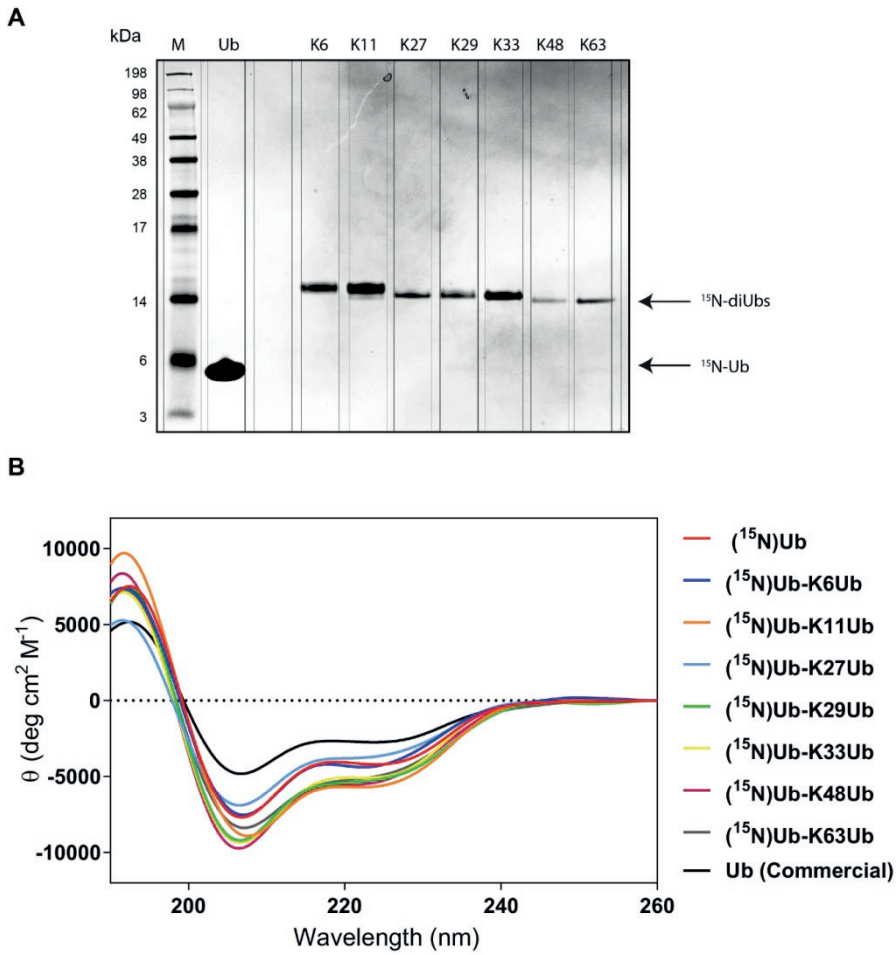


***Figure S1**: **A:** SDS-PAGE analysis of purified NMR samples. ^{15}N-Ub was compared with ^{15}N-diUbs which shows almost no contamination with monoUb samples. **B:** Circular Dichroism spectrum of ^{15}N-Ub and ^{15}N-diUbs compared with expressed Ub from a commercial source (Boston Biochem CAT: U-100H).*

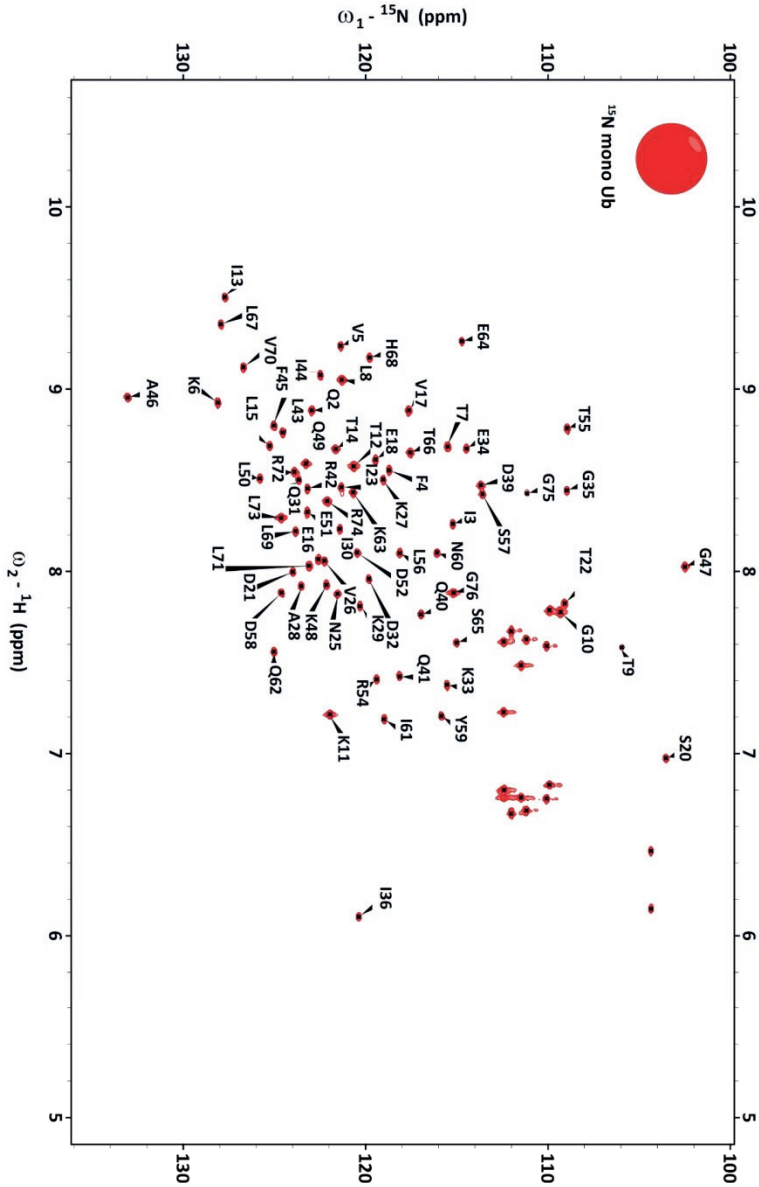


***Figure S2**: **2D NMR spectrum of ^{15}N-Ub**. The NMR (^{1}H-^{15}N HSQC) spectrum of free Ub (red) shows the assignments of main chain ^{1}H-^{15}N cross peaks of almost all the residues.*

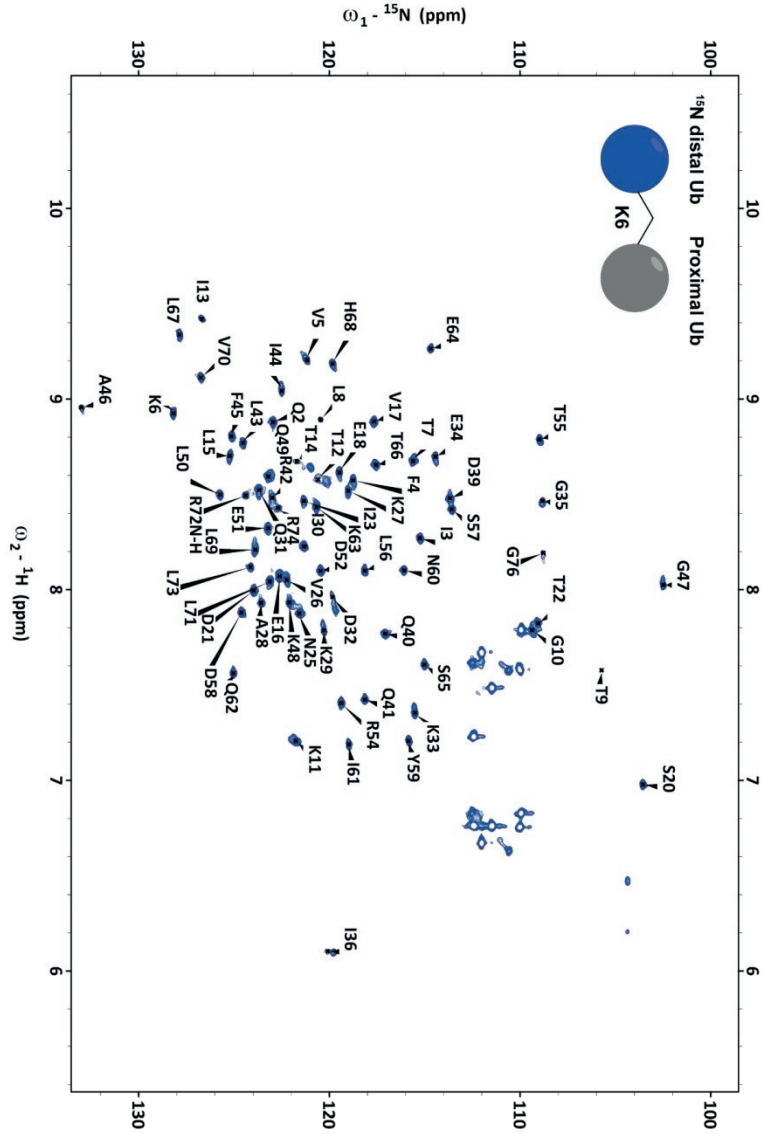


Figure S3: 2D NMR spectrum of ^{15}N-Ub-K6-Ub (K6diUb). *The NMR (^{1}H-^{15}N HSQC) spectrum of ^{15}N-labelled distal Ub (blue) in a K6 diUb molecule shows displacement of some residues as quantified in Figure 3A.*

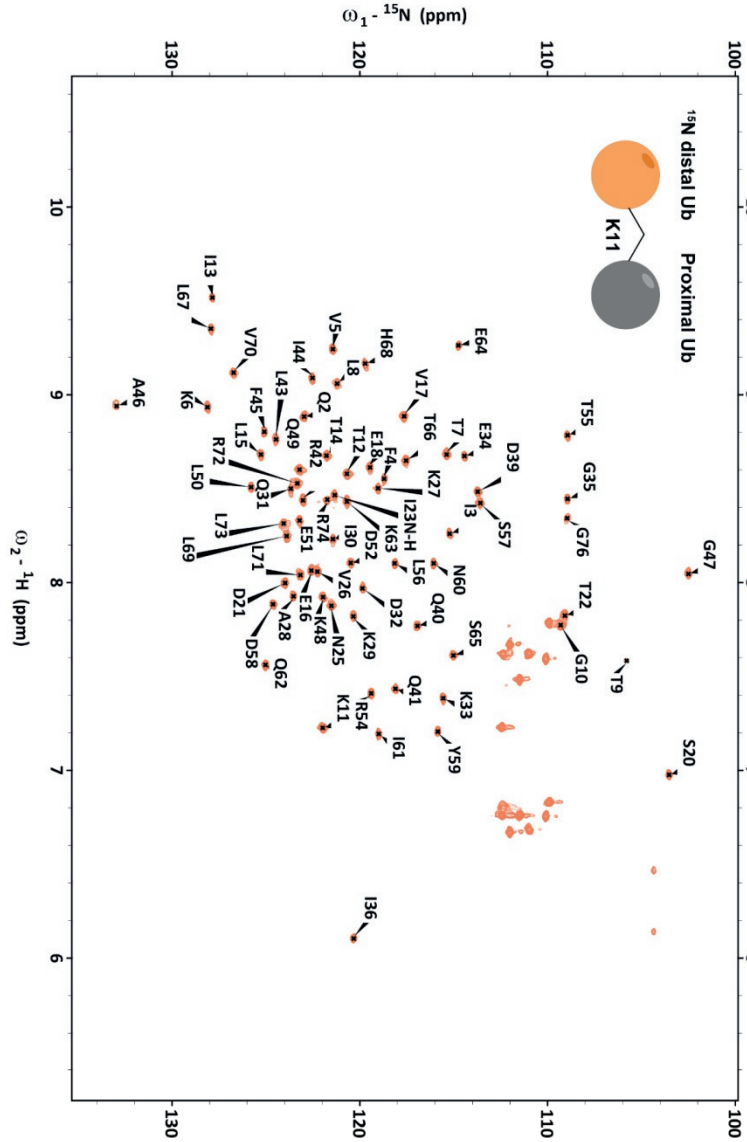


Figure S4: 2D NMR spectrum of ^{15}N-Ub-K11-Ub (K11 diUb). *The NMR (^{1}H-^{15}N HSQC) spectrum of ^{15}N-labelled distal Ub (orange) in a K11 diUb molecule shows displacement of some residues as quantified in Figure 3B.*

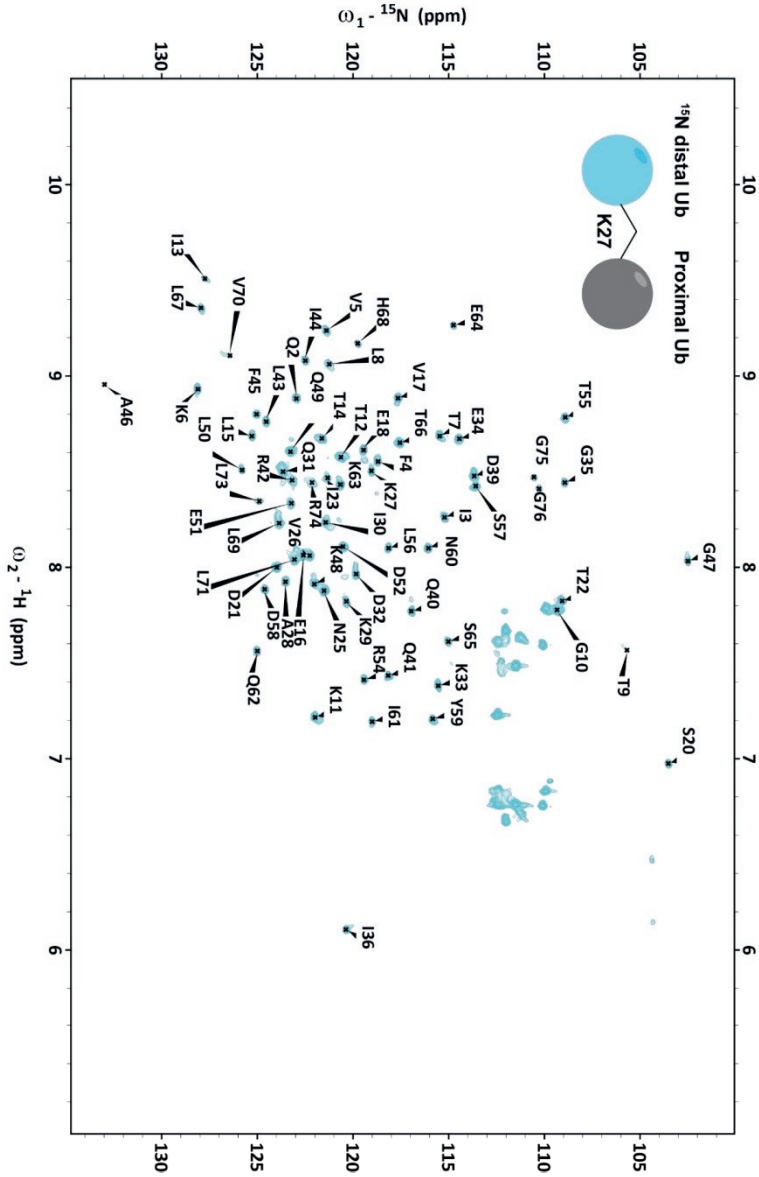


Figure S5: NMR spectrum of ^{15}N-Ub-K27-Ub (K27 diUb). *The NMR (^{1}H-^{15}N HSQC) spectrum of ^{15}N-labelled distal Ub (light blue) in a K27 diUb molecule shows displacement of some residues as quantified in Figure 3C.*

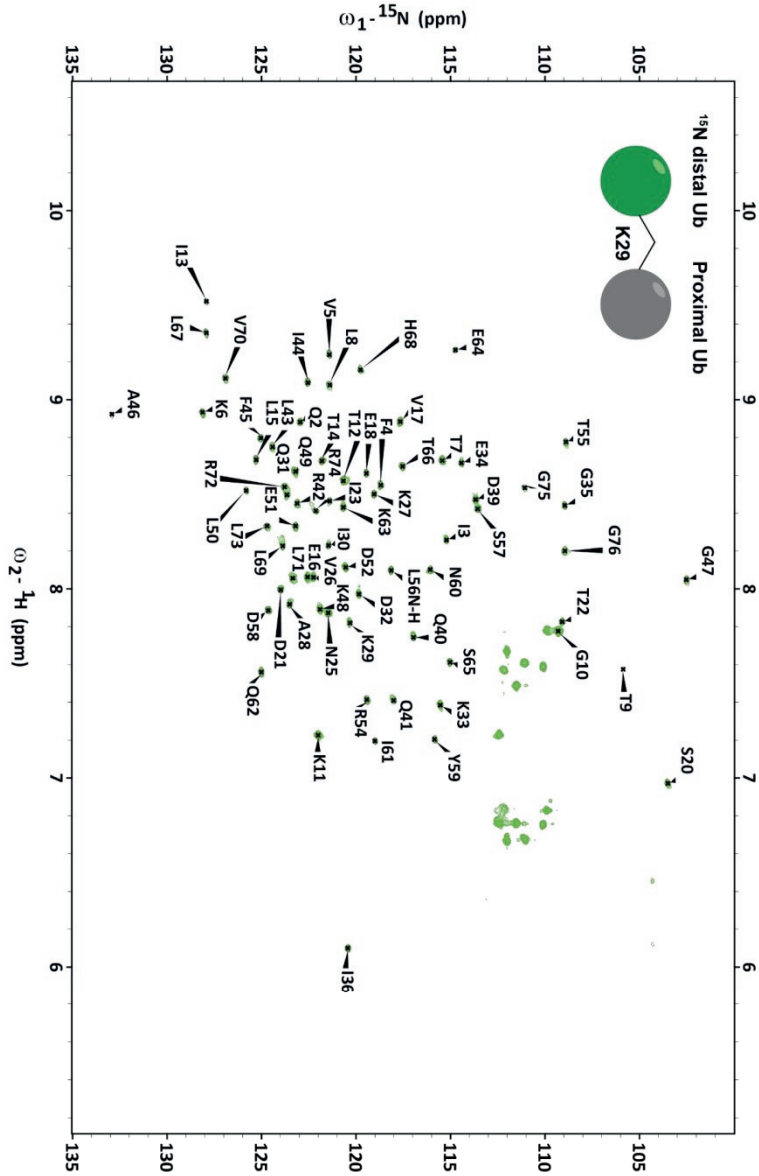


Figure S6: NMR spectrum of ^{15}N-Ub-K29-Ub (K29 diUb). *The NMR (^{1}H-^{15}N HSQC) spectrum of ^{15}N-labelled distal Ub (green) in a K29 diUb molecule shows displacement of some residues as quantified in Figure 3D.*

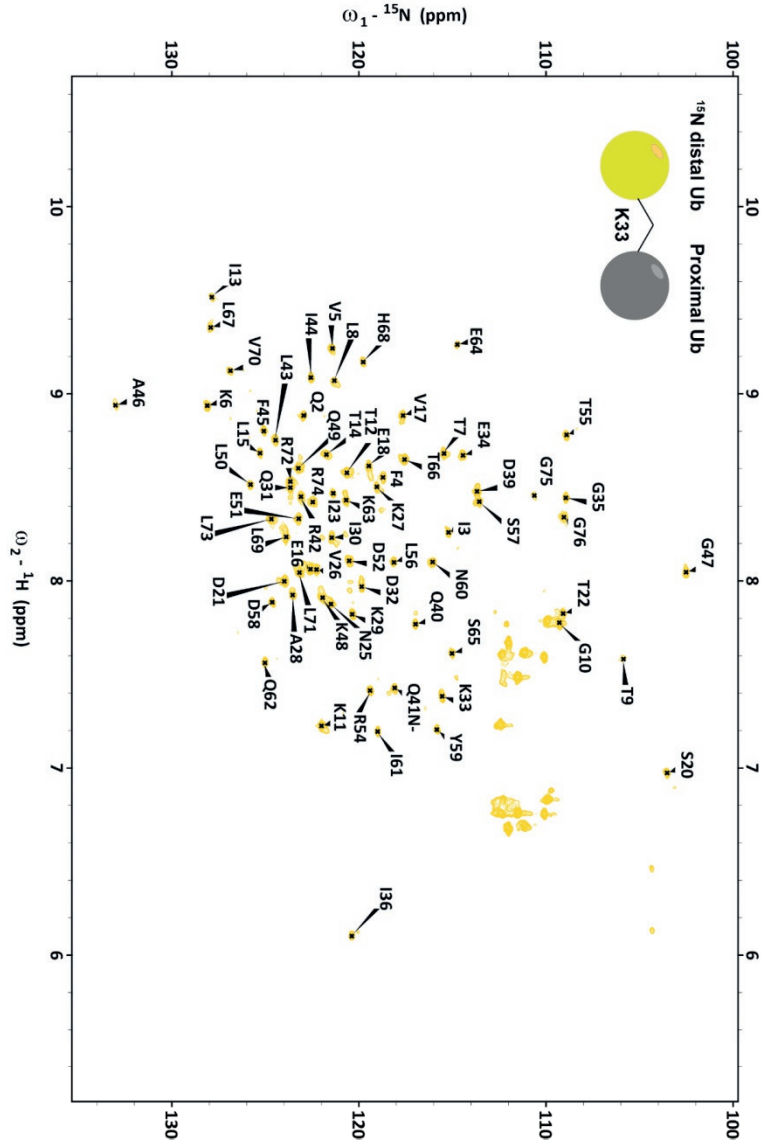


Figure S7: NMR spectrum of ^{15}N-Ub-K33-Ub (K33 diUb). *The NMR (^{1}H-^{15}N HSQC) spectrum of ^{15}N-labelled distal Ub (yellow) in a K33 diUb molecule shows displacement of some residues as quantified in Figure 3E.*

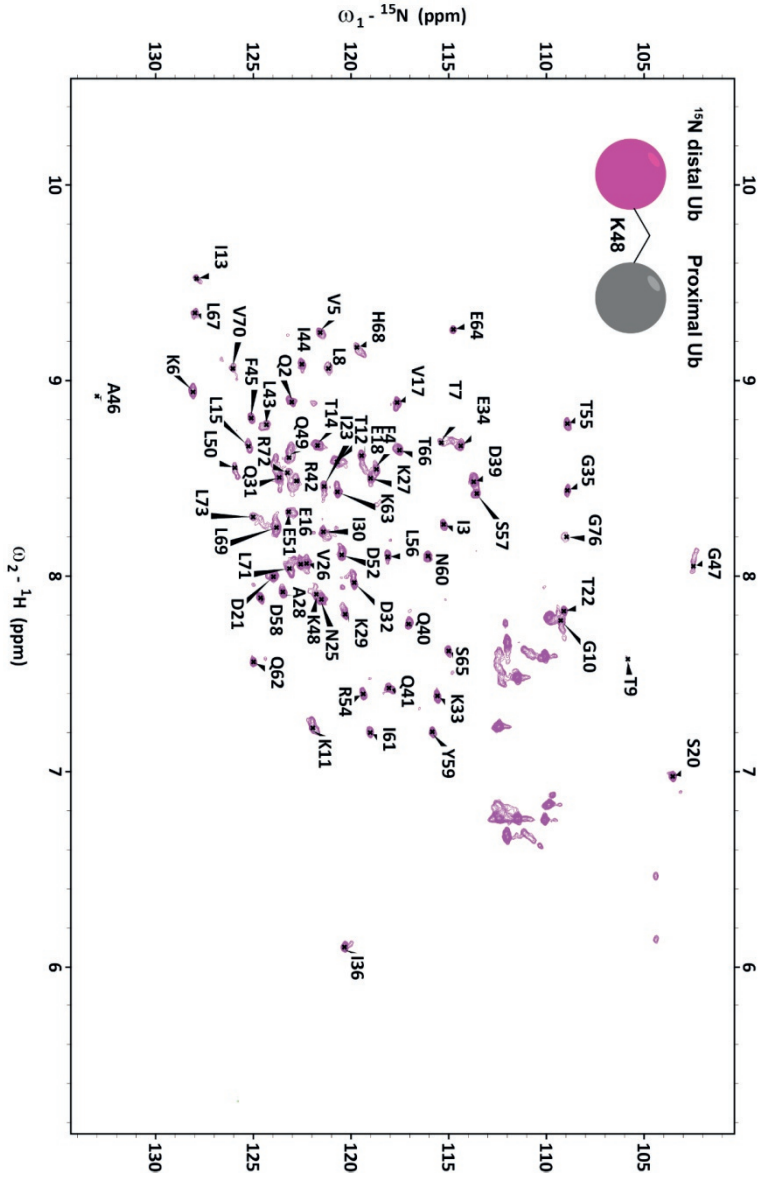


Figure S8: NMR spectrum of ^{15}N-Ub-K48-Ub (K48 diUb). *The NMR (^{1}H-^{15}N HSQC) spectrum of ^{15}N-labelled distal Ub (magenta) in a K48 diUb molecule shows displacement of some residues as quantified in Figure 3F.*

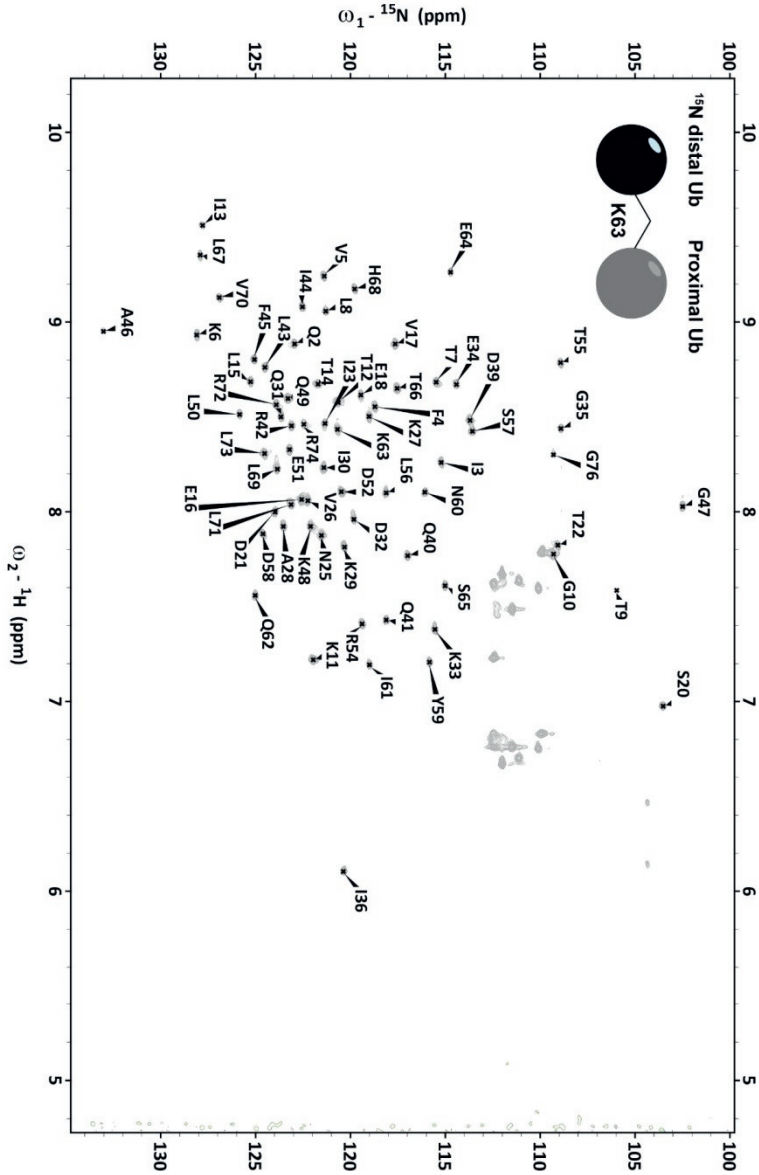


Figure S9: NMR spectrum of ^{15}N-Ub-K63-Ub (K63 diUb). *The NMR (^{1}H-^{15}N HSQC) spectrum of ^{15}N-labelled distal Ub (grey) in a K63 diUb molecule shows displacement of some residues as quantified in Figure 3G.*

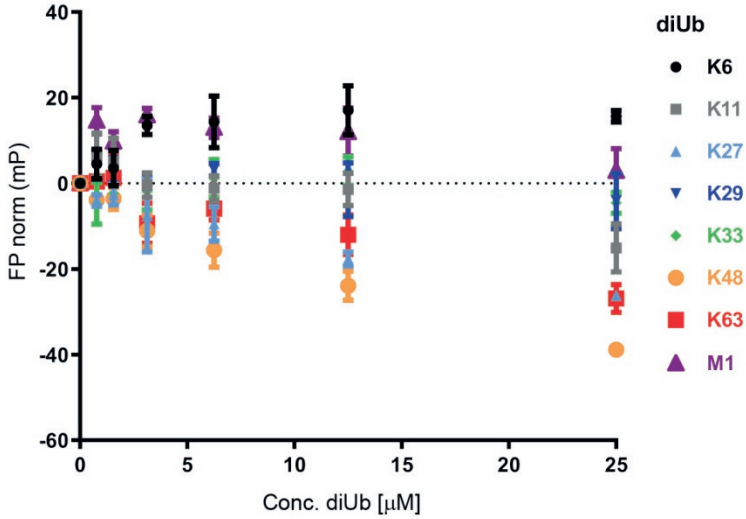


***Figure S10**: Fluorescence polarization assay using TAMRA-labeled UBXN1 UBA (1-42) domain and different concentrations of all 8 homotypical diUbs. There were no interactions of this binding domain with any of the diUbs tested.*

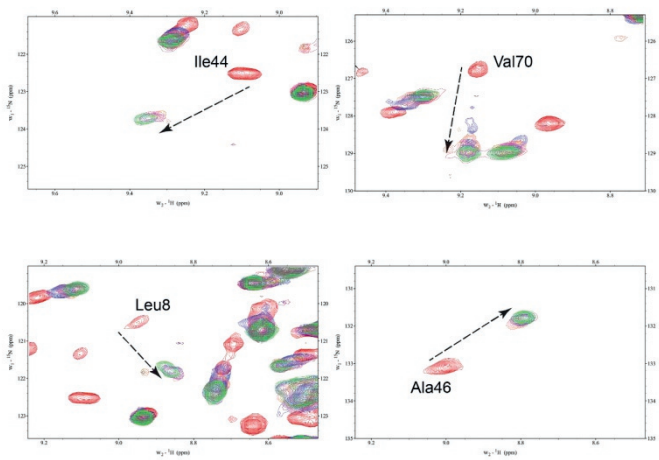


***Figure S11**: NMR spectrum showing key residues of the hydrophobic region in ^{15}N-Ub-K6-Ub (K6 diUb) added with different concentrations of unlabeled UBA(ext1-52) domain of UBXN1. Different colors represent the NMR (^{1}H-^{15}N HSQC) spectrum of ^{15}N-labelled distal Ub in a K6 diUb molecule before (red) and after addition of 108 μM (blue), 135 μM (coral), 175 μM (purple), 270 μM (magenta) and 570 μM (green) of UBA domain.*

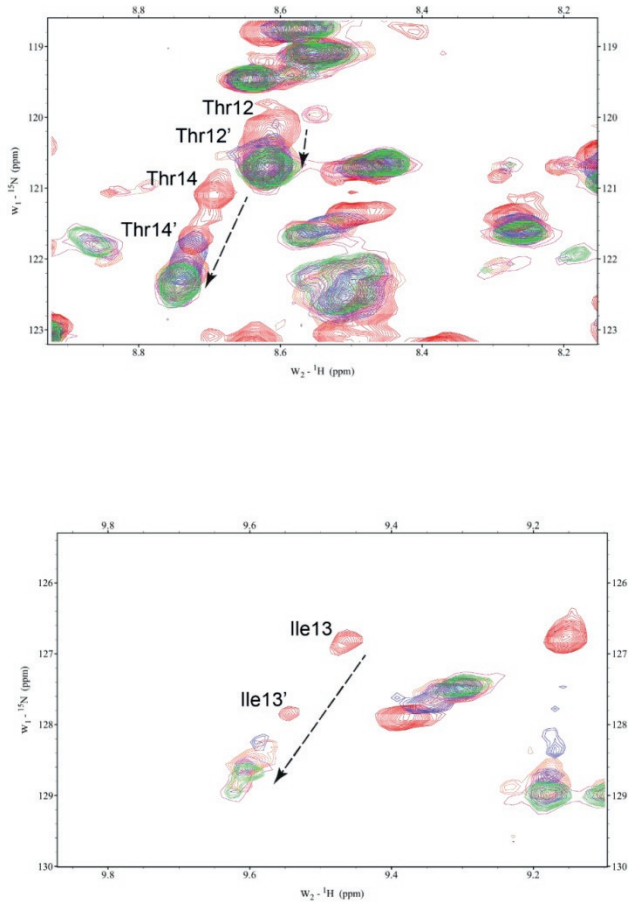


Figure S12: *NMR spectrum showing Thr12, Thr14 (Top) and Ile13 (Bottom) signal shift in ^{15}N-Ub-K6-Ub (K6 diUb) added with different concentrations of unlabeled UBA(ext1-52) domain of UBXN1. Different colors represent the NMR (^{1}H-^{15}N HSQC) spectrum of 15N-labelled distal Ub in a K6 diUb molecule before (red) and after addition of 108 µM (blue), 135 µM (coral), 175 µM (purple), 270 µM (magenta) and 570 µM (green) of UBA domain.*

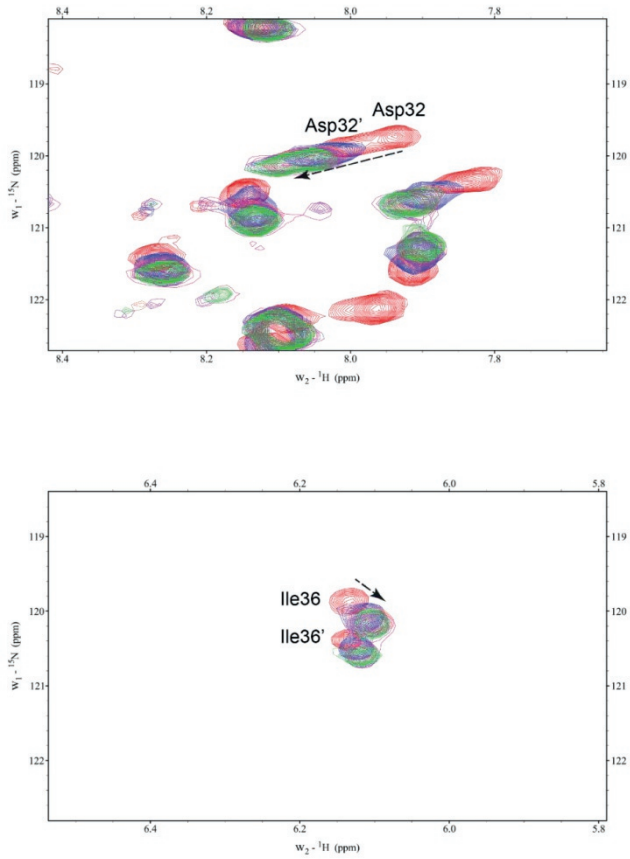


Figure S13*: NMR spectrum showing split signals of Asp32 (Top) and Ile36 (Bottom) in ^{15}N-Ub-K6-Ub (K6 diUb) added with different concentrations of unlabeled UBA(ext1-52) domain of UBXN1. The NMR (^{1}H-^{15}N HSQC) spectrum of 15N-labelled distal Ub in a K6 diUb molecule before (red) and after addition of 108 µM (blue), 135 µM (coral), 175 µM (purple), 270 µM (magenta) and 570 µM (green) of UBA domain.*

^{15}N-Ub

^{15}N-MQIFVKTLTGKTITLEVEPSDTIENVKAKIQDKEGIPPDQQRLIFAGKQLEDGRTLSDYNIQKESTLHLVLRLRGG

Calculated MW: 8670 Da
Observed MW: 8669 Da

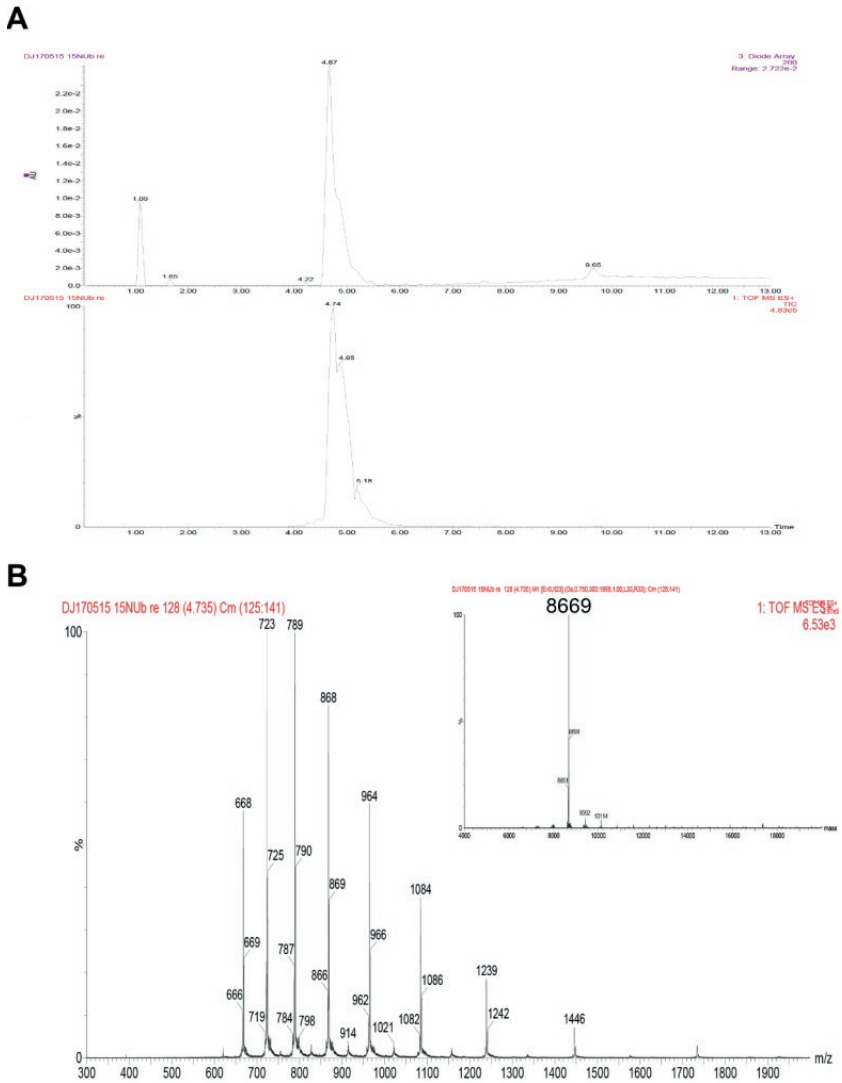


Figure S14: LC-MS analysis of ^{15}N Ub sample*. A. Top: UV chromatogram (λ – 280 nm); Bottom: Mass spectrum. B. Combined mass spectrum of peak at 4.67 min; Inset: Deconvoluted mass of mass spectra.*

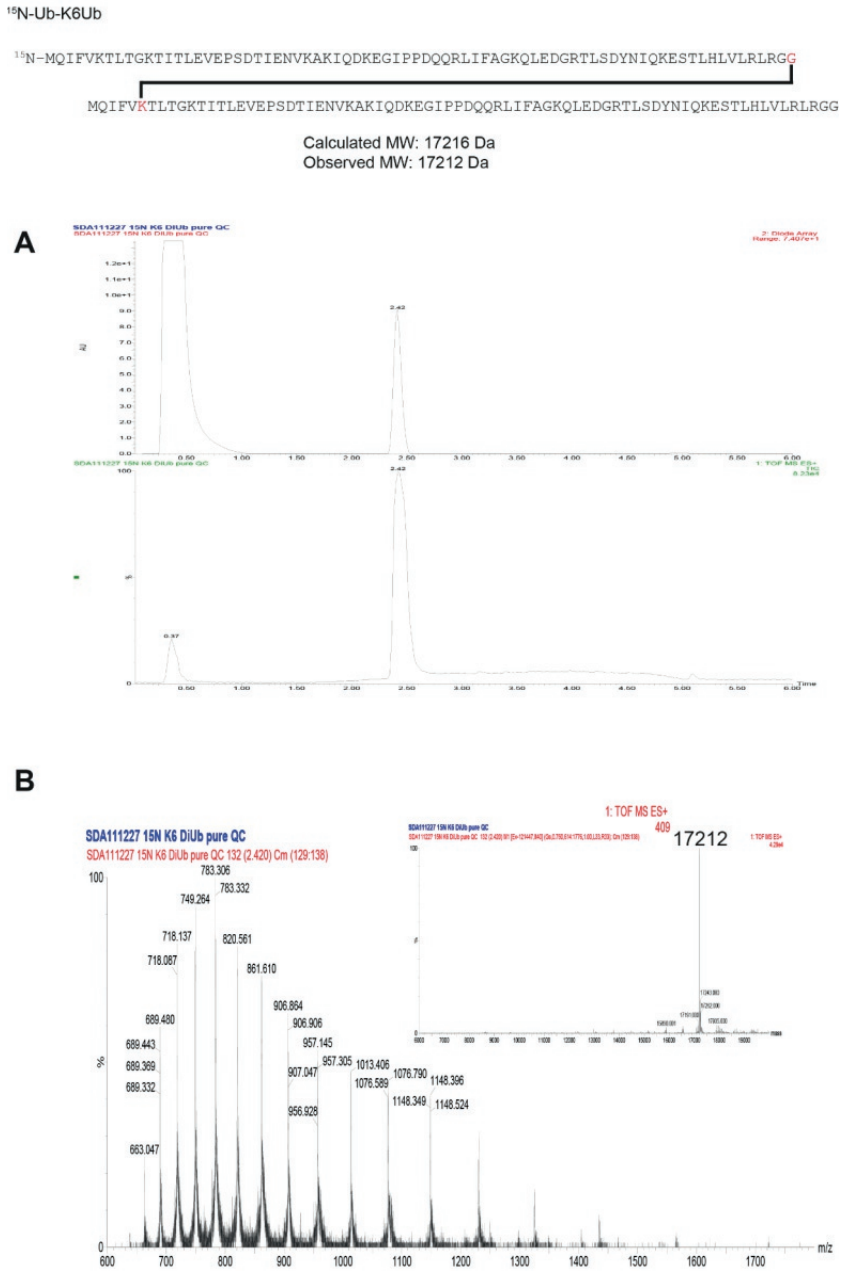


Figure S15: LC-MS analysis of ^{15}N K6 diUb sample. *A. Top: UV chromatogram (λ – 280 nm); Bottom: Mass spectrum. B. Combined mass spectrum of peak at 2.42 min; Inset: Deconvoluted mass of mass spectra.*

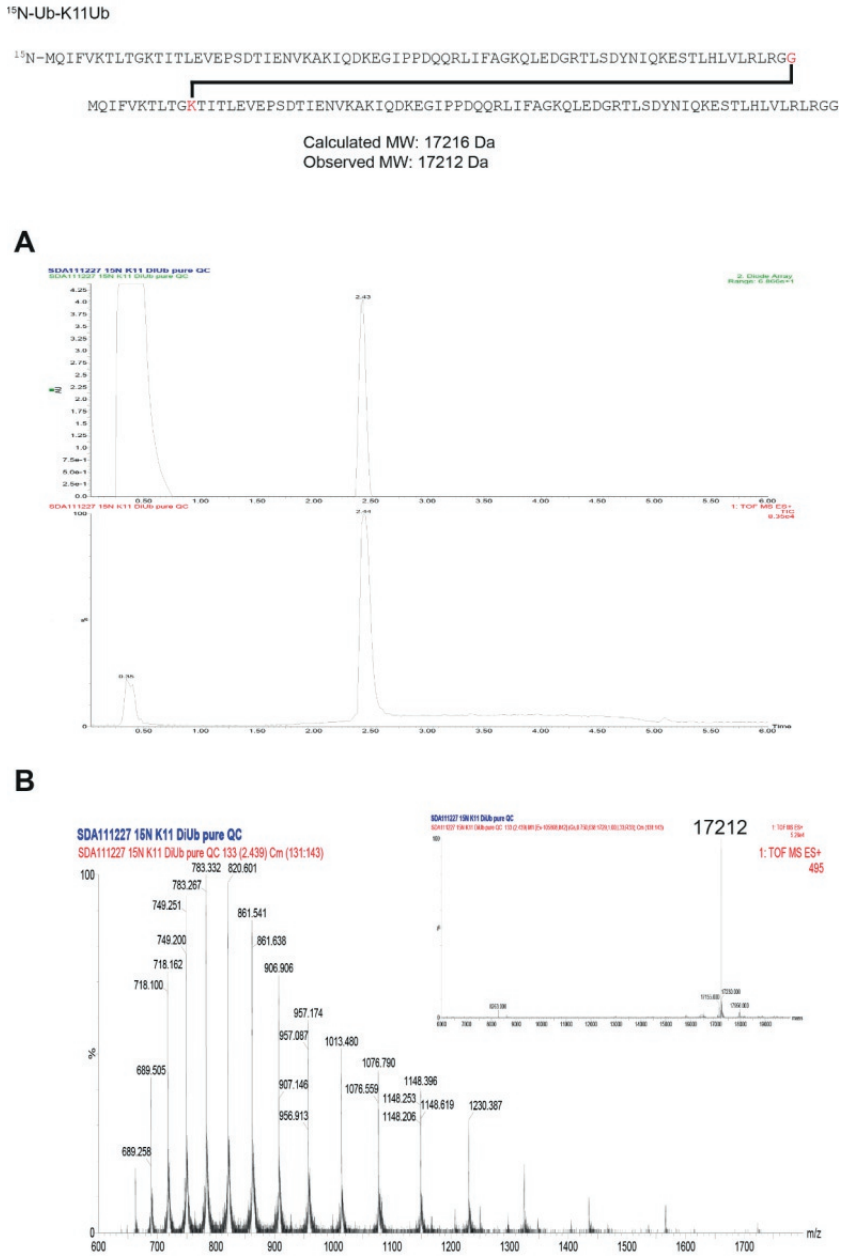


Figure S16: LC-MS analysis of ^{15}N K11 diUb sample*. A. Top: UV chromatogram (λ – 280 nm); Bottom: Mass spectrum. B. Combined mass spectrum of peak at 2.44 min; Inset: Deconvoluted mass of mass spectra.*

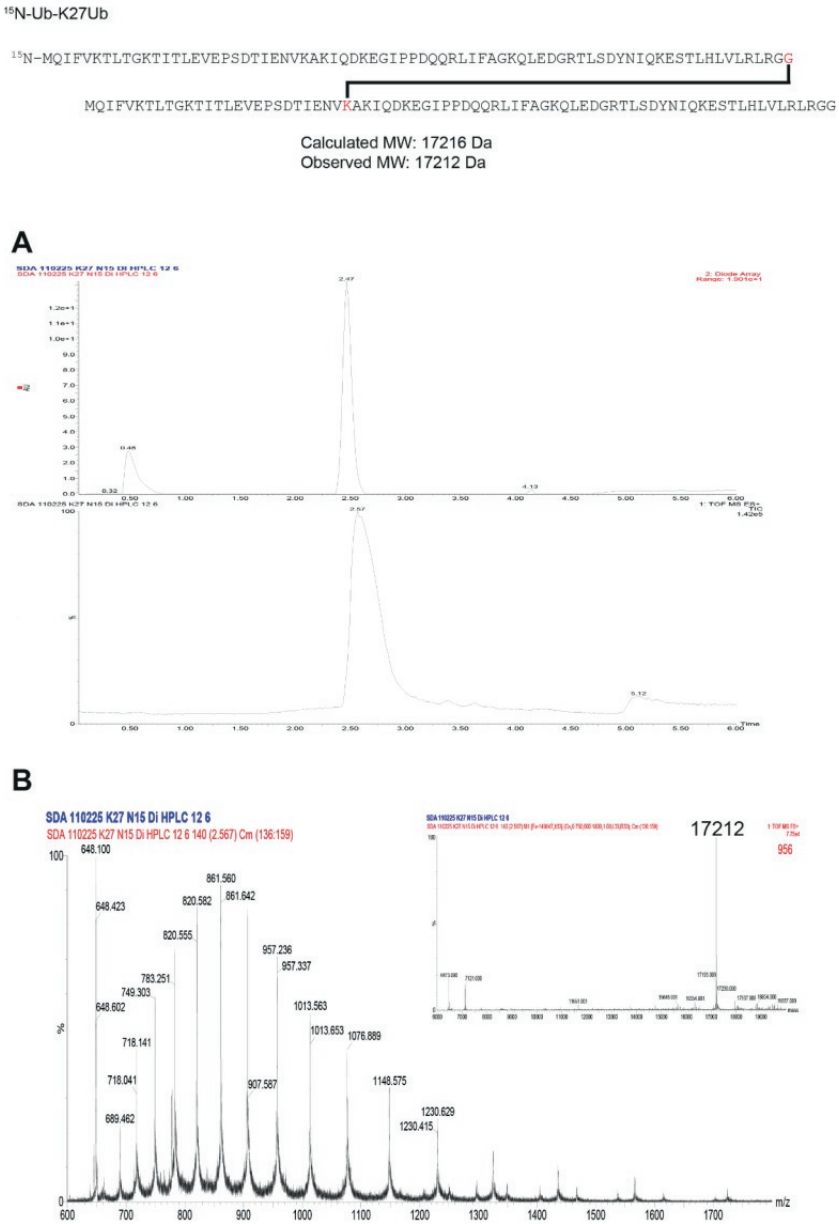


Figure S17: LC-MS analysis of ^{15}N K27 diUb sample*. A. Top: UV chromatogram (λ – 280 nm); Bottom: Mass spectrum. B. Combined mass spectrum of peak at 2.47 min; Inset: Deconvoluted mass of mass spectra.*

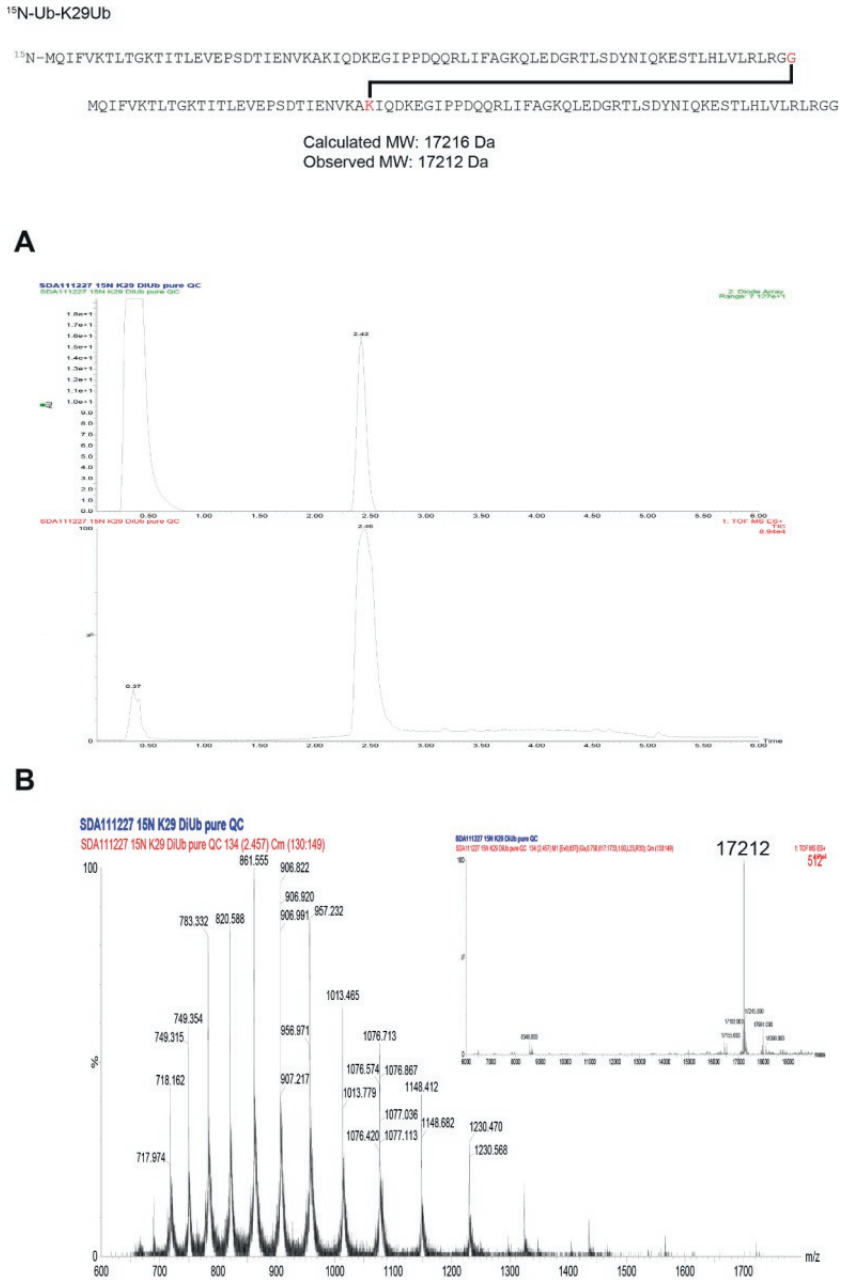


Figure S18: LC-MS analysis of ^{15}N K29 diUb sample*. A. Top: UV chromatogram (λ – 280 nm); Bottom: Mass Spectrum. B. Combined mass spectrum of peak at 2.46 min; Inset: Deconvoluted mass of mass spectra.*

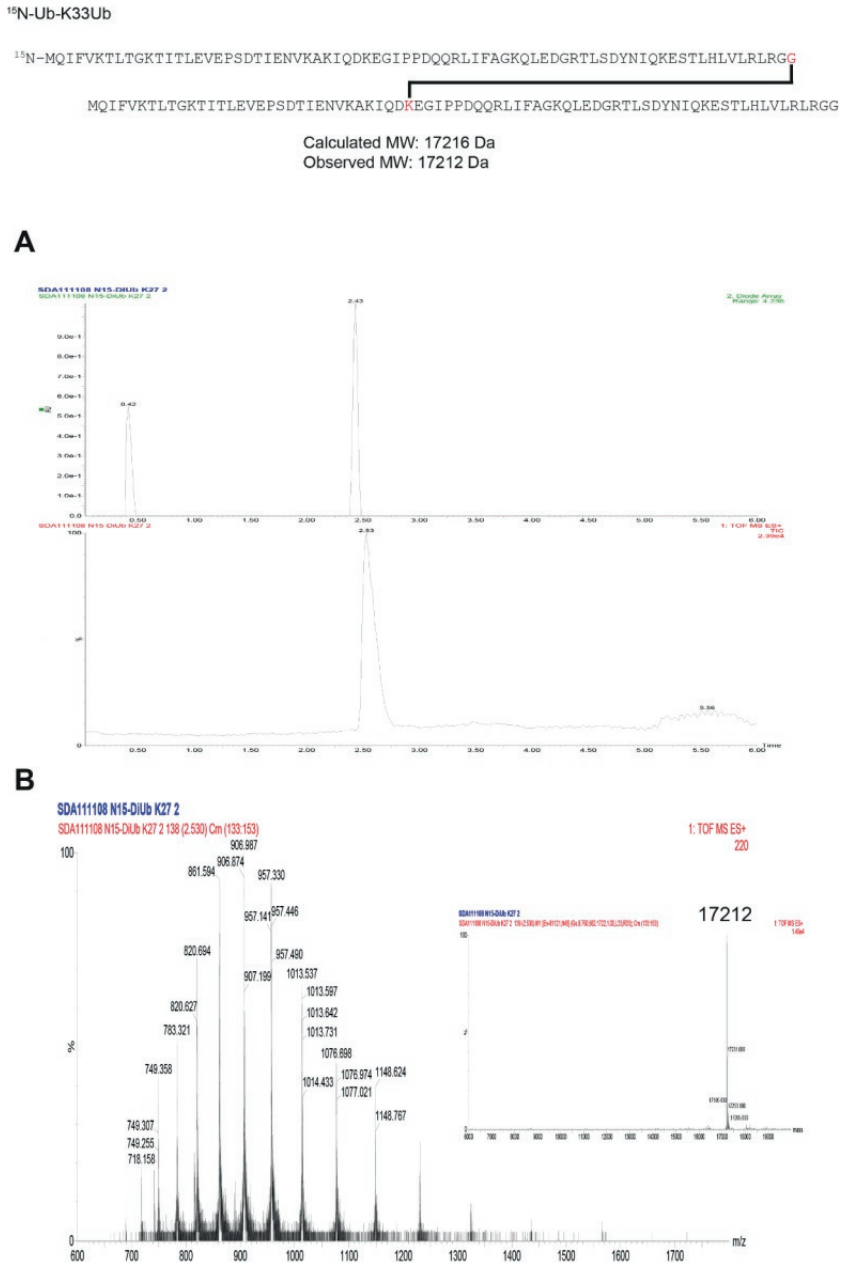


Figure S19: LC-MS analysis of ^{15}N K33 diUb sample. *A. Top: UV chromatogram (λ – 280 nm); Bottom: Mass spectrum. B. Combined mass spectrum of peak at 2.43 min; Inset: Deconvoluted mass of mass spectra.*

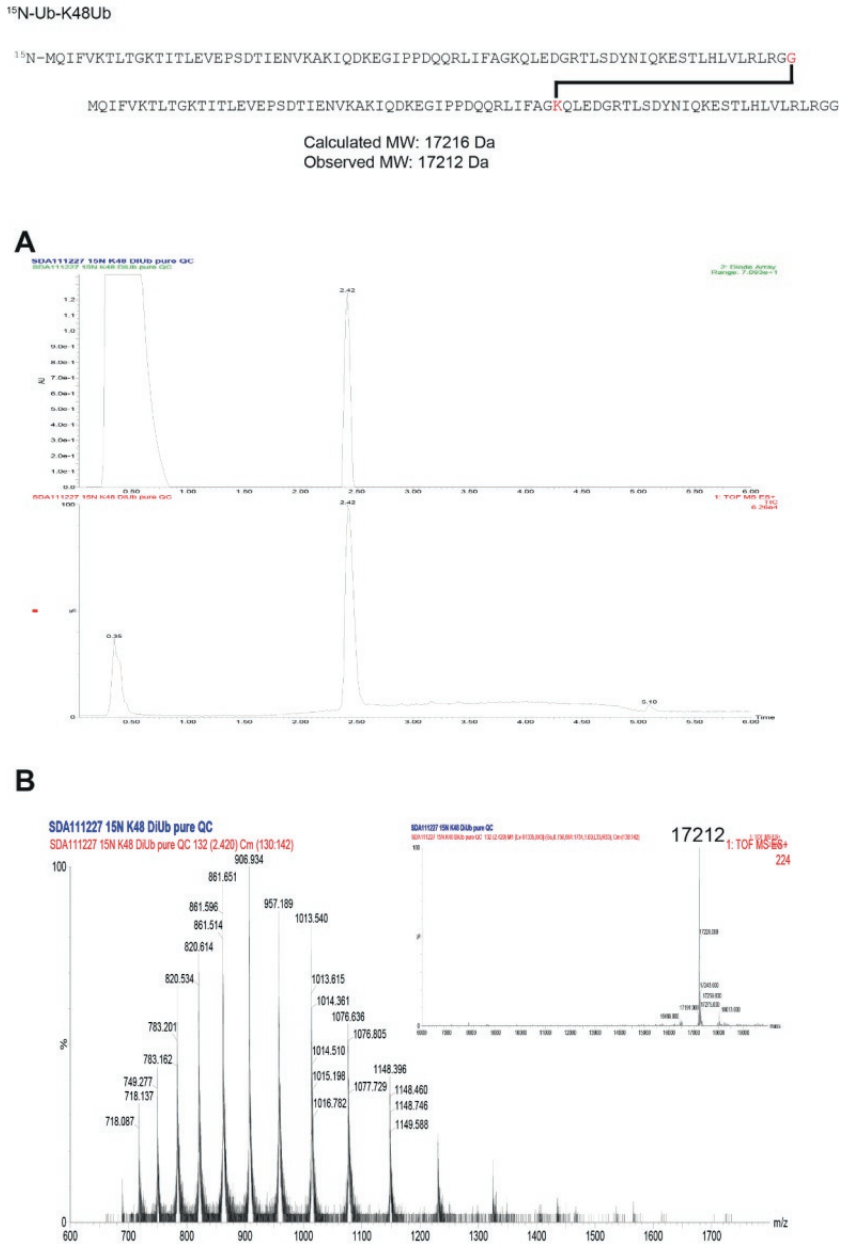


Figure S20: LC-MS analysis of ^{15}N K48 diUb sample*. A. Top: UV chromatogram (λ – 280 nm); Bottom: Mass spectrum. B. Combined mass spectrum of peak at 2.42 min; Inset: Deconvoluted mass of mass spectra.*

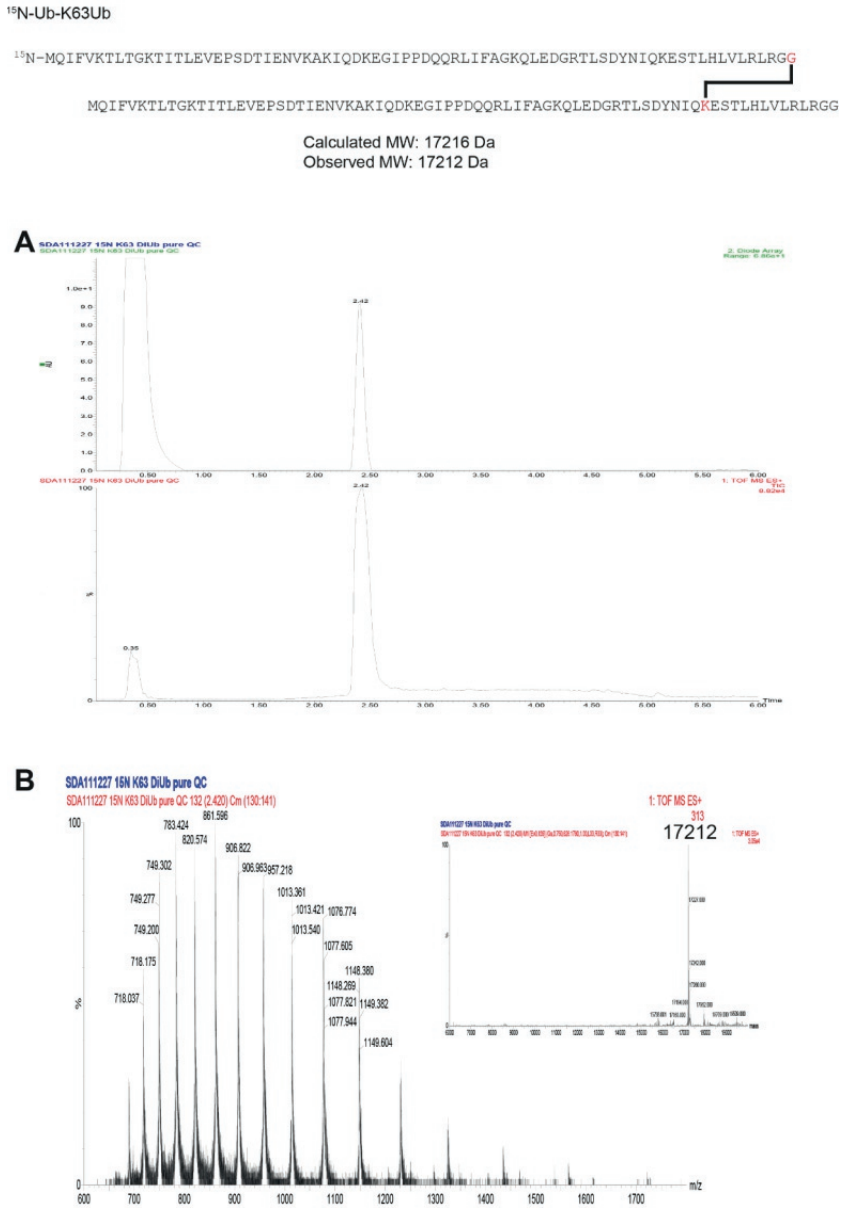


Figure S21: LC-MS analysis of ^{15}N K63 diUb sample. *A. Top: UV chromatogram (λ – 280 nm); Bottom: Mass spectrum. B. Combined mass spectrum of peak at 2.42 min; Inset: Deconvoluted mass of mass spectra.*

Chapter 4

Development of a Ubiquitin based probe for metalloprotease deubiquitinases

Adapted from:
Hameed, D.S., A. Sapmaz, L. Burggraaff, A. Amore, C.J. Slingerland, G.J.P. van Westen, and H. Ovaa, Development of Ubiquitin-Based Probe for Metalloprotease Deubiquitinases. Angew Chem Int Ed Engl, 2019. 58(41): p. 14477-14482.

Summary

The deubiquitinases (DUBs) are a family of enzymes that regulate the ubiquitin signalling cascade by removing ubiquitin from specific proteins in response to distinct signals. The DUBs that belong to the metalloprotease family (metalloDUBs) contain Zn^{2+} in its active site and are an integral part of distinct cellular protein complexes. Little is known about these enzymes due to the lack of specific probes because of the absence of a covalent enzyme-substrate intermediate complex during the deubiquitination process. Here we describe a Ub-based probe that contains a ubiquitin moiety modified at its C-terminus with a Zn^{2+} chelating group based on 8-mercaptoquinoline and that is modified at the N-terminus with a fluorescent tag or a pull-down tag. The probe is validated using Rpn11, a metalloDUB found in the 26S proteasome complex. This probe is able to bind to metalloDUBs and efficiently pulled down overexpressed metalloDUBs from HeLa cell lysate. Such probes may be used to study the mechanism of metalloDUBs in detail. This will allow us to better understand the biochemical processes of protein complexes that contain metalloDUBs.

Introduction

Ubiquitination is an important post-translational modification that plays a key role in many vital cellular events. [1-3] In this process, ubiquitin (Ub) is attached to a substrate protein by the concerted action of an enzyme cascade involving E1, E2 and E3 enzymes and it is removed by an enzyme family known as deubiquitinases (DUBs). [4-6] DUBs are classified into two main families: cysteine proteases and JAMM (JAB1/MPN /MOV34) metalloproteases.

The cysteine protease class of DUBs has a conserved cysteine residue at the active site that acts as a nucleophile [5, 7] and forms a covalent intermediate with the carbonyl group of the scissile amide bond in Ub conjugates. [8-10] This intermediate has been mimicked by several activity-based probes reported by us and others. [11-18]

Unlike cysteine protease DUBs, metalloprotease DUBs (metalloDUBs) do not form a covalent intermediate with their substrate. [1, 2, 19] MetalloDUBs contain a Zn^{2+} ion in their active site that coordinates two histidine residues and an aspartate residue. During deubiquitination by metalloDUBs, a non-covalent intermediate complex is formed between the active site of the enzyme and the scissile isopeptide bond of Ub. [20] This leads to the nucleophilic attack of the amide bond by a water molecule which is also coordinated to the active site Zn^{2+} ion. [21] This mechanism of action, lacking a covalent intermediate between substrate and enzyme, presents a challenge to develop a selective activity-based probe for metalloDUBs. [14, 22] By combining the chemical synthesis of Ub and a small molecule zinc chelator at the C-terminus of Ub, we developed a Ub-based probe that binds and pulls down metalloDUBs from cell lysate.

Results and discussion

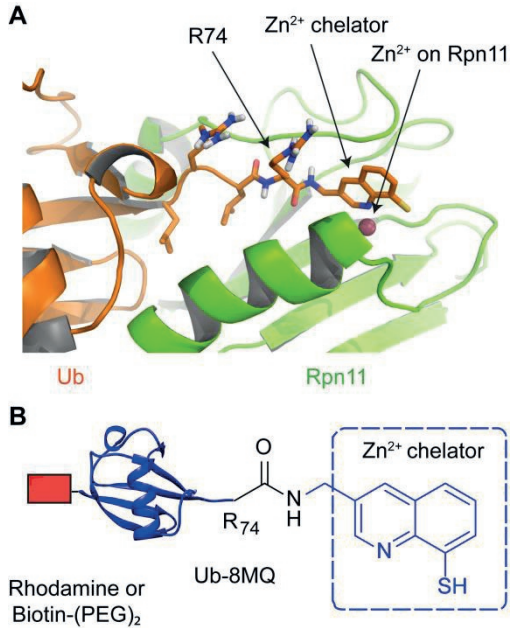
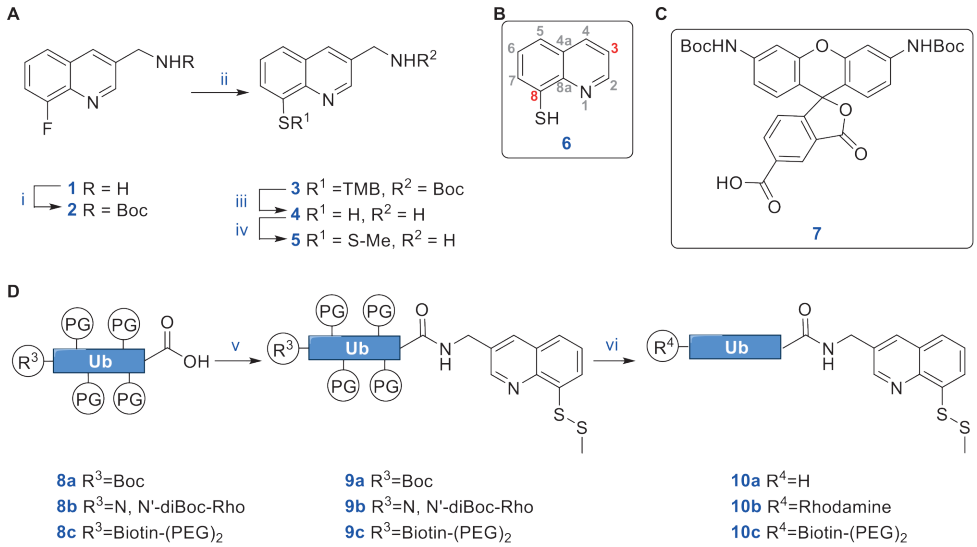


Figure 1: A: *Molecular docking using Prime showing Ub (1-74) coupled to our Zinc chelator at the C-terminus, which coordinated with* Zn^{2+} *on the active site of Rpn11 (PDB: 1UBQ, orange and 4O8X, green).* ***B:*** *The metalloDUB probe consists of an N-terminal dye or a tag, Ub (1-74) and the modified 8-MQ attached at the C-terminus of Arg74 of Ub.*

To develop a generic Ub-based probe, we relied on the information on structural similarity in the catalytic domain of the known metalloDUBs. The X-ray structures of AMSH, Rpn11/Rpn8 complex, and AMSH-LP/Lys63-linked diubiquitin complex reveal a similar active site configuration with a conserved Ub binding motif (Figure S1). [19, 23-25] To validate the inhibition and binding affinity of our Ub-based probe, we used recombinant *S.cerevisae* Rpn11/Rpn8 active enzyme complex which is a part of the 19S proteasome lid (Figure S2). [25] The activity of the recombinant Rpn11/Rpn8 enzyme complex was confirmed using a fluorogenic substrate (Ub-Rho) and a fluorescence polarization (FP) substrate Ub-FP (Ub-TAMRA-K48Ub-peptide). [26, 27] The rates of the enzyme reaction upon incubation with 1 μM of Rpn11/Rpn8 were calculated to be 0.075 $pmol.min^{-1}$ using Ub-Rho substrate and 0.42 $pmol.min^{-1}$ using Ub-TAMRA-K48Ub-peptide substrate (Figure S3, S4).

In order to chelate Zn^{2+} to the active site of metalloDUBs, we first used a hydroxamate moiety, that is known as a general metalloprotease inhibitor, [22, 28, 29] to the C-terminus of Ub. It has also been proposed that Ub containing N-hydroxy isopeptide at the C-terminal glycine may inhibit metalloDUBs. [30] We found that Ub-hydroxamic acid derivatives failed to inhibit Rpn11 (Figure S5). This necessitated a different approach for developing a probe for metalloDUBs.

Many molecules have been reported as zinc chelating agents and among them, 8-mercaptoquinoline (8-MQ) was reported as an efficient chelator. [31, 32] Furthermore, 8-



Scheme 1 A: *i) Di-tert-butyl dicarbonate, DIPEA, CH_3CN, room temperature; ii) TMB-thiol, NaH, THF, 60 °C; iii) TFA, TES, H_2O; iv) MMTS, MeOH.* ***B:*** *Chemical structure of 8-quinolium thiolate (6) and its carbon positions are indicated in numbers.* ***C:*** *N,N'-diBoc protected rhodamine (7) used in Fmoc-SPPS of rhodamine labeled Ub derivatives.* ***D:*** *v) 5, HBTU, HOBT, DIPEA, room temperature (PG- protecting groups); vi) TFA, TIPS, Phenol, H_2O.*

MQ and its derivatives were also reported as a specific inhibitor for metalloDUBs like Rpn11 and AMSH. [32, 33] In addition, it is known that a modification at position 3 (Scheme 1B, **6**) of this molecule will not diminish its inhibitory potential. [34] Hence, an 8-MQ derivative modified with an amino group at position 3 was subsequently synthesized as zinc-binding group (ZBG).

We prepared the 8-MQ derivative **5** (Scheme 1A, Scheme S1) starting from commercially available (8-fluoroquinolin-3-yl) methanamine **1**. After tert-butoxycarbonyl (Boc) protection, the fluorine atom was substituted with trimethoxybenzyl (TMB) thiol and afforded the protected thiol **3**. After acid deprotection of the thiol, compound **4** was obtained. We observed that **4** could dimerize as a disulfide and that this leads to difficulties during purification. Hence, we protected the free thiol as a thio-methyl disulfide **5** which was then purified and used in further peptide-coupling reactions.

In order to precisely accommodate our ZBG on the C-terminus of Ub, we performed molecular docking analysis. For this purpose, we used the known X-ray crystal structure of Rpn11/Rpn8 (PDB: 4O8X) and Ub (PDB: 1UBQ). [25, 35] Among all the models tested, we arrived at optimal binding when our ZBG was attached at the C-terminus of Arg74 of Ub (Figure 1A, S6). Therefore, we designed our metalloDUB probe containing an N-terminally modified Ub (1-74) attached with 3-aminomethyl 8-mercapto quinoline at its C-terminus

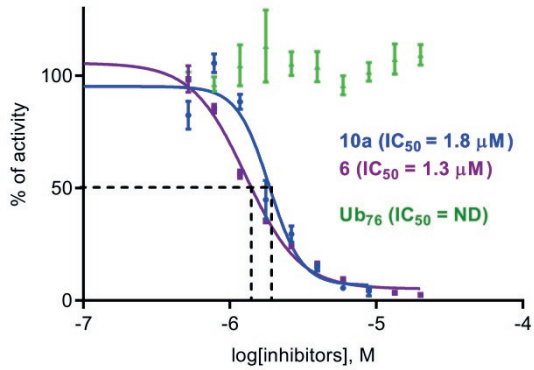


***Figure 2**: Rpn11 inhibition by **6**, **10a** and Ub_{76}. IC_{50} curve of Ub-Rho hydrolysis in a typical fluorogenic assay. In this assay, compound **6** was also taken along, which shows an IC_{50} of about 1.3 μM while **10a** shows an IC_{50} of 2 μM. Full length Ub did not inhibit the enzyme.*

(Figure 1B).

We synthesized fully protected Ub74 containing either protected rhodamine (**7**, Scheme 1C) or Biotin-$(PEG)_2$ or a Boc protecting group at its N-terminus by Fmoc-based SPPS on a 2-chlorotrityl resin. [36-38] After selective C-terminal cleavage using 20% hexafluoroisopropanol (HFIP) in dichloromethane (DCM), we obtained fully protected Ub containing a free C-terminal carboxylate group and either a bis-Boc-rhodamine or Biotin-$(PEG)_2$ or a Boc protecting group on the N-terminus (**8a, 8b, 8c**, Scheme 1C). The amino group of compound **5** was then coupled to the C-terminal carboxylate of Ub74 to yield **9a, 9b** and **9c**. After global deprotection, the final products were purified using reversed-phase HPLC followed by size exclusion chromatography to afford labelled or unlabeled versions of Ub-8MQ reagents **10a, 10b** and **10c**. The disulfide protected Ub-8MQ was reduced using TCEP prior to use and we observed only a slight decrease in the activity of Rpn11/Rpn8 upon the addition of TCEP (Figure S7, S8). Commercially available 8-quinoliniumthiolate (**6**, Scheme 1B) was used as a positive control in our assay.

Inhibition of Rpn11/Rpn8 by **10a** was then tested using both Ub-rhodamine and Ub-fluorescence polarization (Ub-FP) assay reagents as substrates. [25] We observed that both **6** and **10a** were able to inhibit Rpn11/Rpn8 with an IC_{50} of about 2 μM (Figure 2, S9). To discern whether this inhibition is reversible or irreversible, we followed two different approaches. First, we performed a time-course pre-incubation assay using EDTA as a control. EDTA is known to strip Zn^{2+} from many proteins and therefore acts as an irreversible inhibitor. [39] The activity assay showed that inhibition by EDTA increased with longer pre-incubation times. On the other hand, **10a** initially decreased the enzyme activity and then maintained the inhibition irrespective of longer pre-incubation times (Figure S10), suggesting that unlike EDTA, the reagent **10a** reversibly binds by coordinating to the active site of the Rpn11/Rpn8 enzyme.

Secondly, we carried out an activity recovery assay using $ZnSO_4$. After pre-incubating Rpn11/Rpn8 with **6** or **10a**, we added an excess of $ZnSO_4$ to the assay buffer and incubated further. Then, we tested the activity of the enzyme using an FP assay. We observed that the enzyme Rpn11/Rpn8, pre-incubated with **6** and **10a**, completely recovered its activity after adding $ZnSO_4$ to the buffer (Figure S11), implying that the chelating groups in **6** and **10a** bind to Zn^{2+} in a reversible manner.

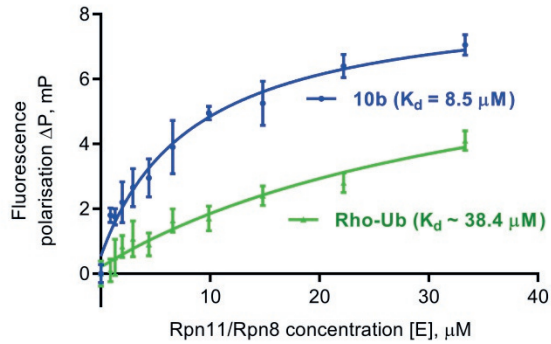


Figure 3: *Fluorescence polarization based binding assay between* ***10b*** *and Rpn11/Rpn8. A typical FP-based binding between Rho-Ub and* ***10b*** *was measured against an unlabelled Rpn11/Rpn8.* ***10b*** *has an almost 5 times higher affinity compared to full length Ub*

In order to establish the binding affinity of **10a** with Rpn11/Rpn8, we used fluorescently labelled derivative **10b** as a fluorescence polarization (FP) probe. [40] We measured the binding of unlabeled Rpn11/Rpn8 using both **10b** and rhodamine-labelled Ub_{76} in a typical

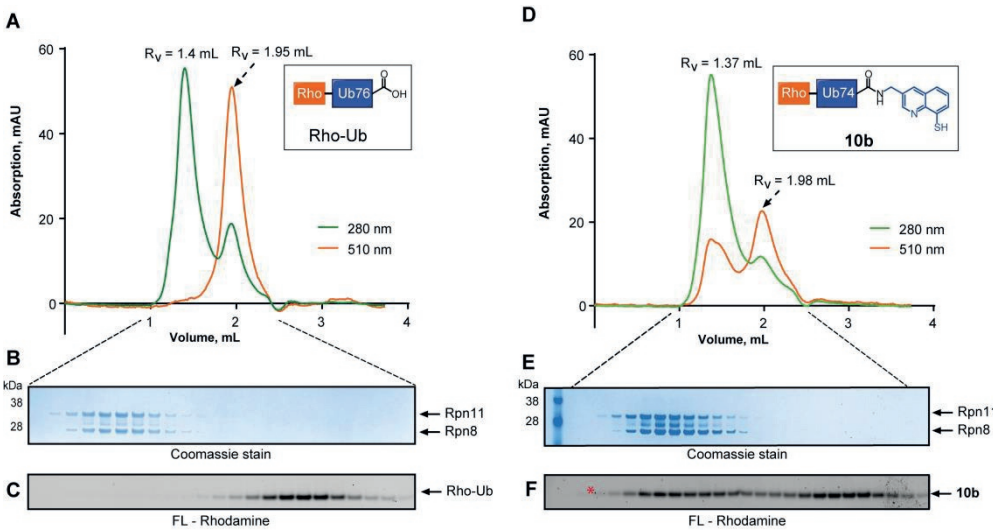


Figure 4: *Co-elution assay.* ***A:*** *Co-elution pattern of RhoUb (inset) with an Rpn11/Rpn8 complex by SEC.* ***B:*** *The fractions from the column in A were used for analysis by SDS-PAGE (coomassie stain).* ***C:*** *The same gel (B) analyzed using fluorescence at the emission wavelength of rhodamine.* ***D:*** *Co-elution pattern of* ***10b*** *(inset) with Rpn11/Rpn8 by SEC.* ***E:.*** *The fractions from the column in D were used in a SDS-PAGE and analyzed by coomassie stain.* ***F:*** *The same gel (E) analyzed using fluorescence at the emission wavelength of rhodamine. The red asterix marks the presence of rhodamine signal from the* ***10b*** *probe in the fractions from D.*

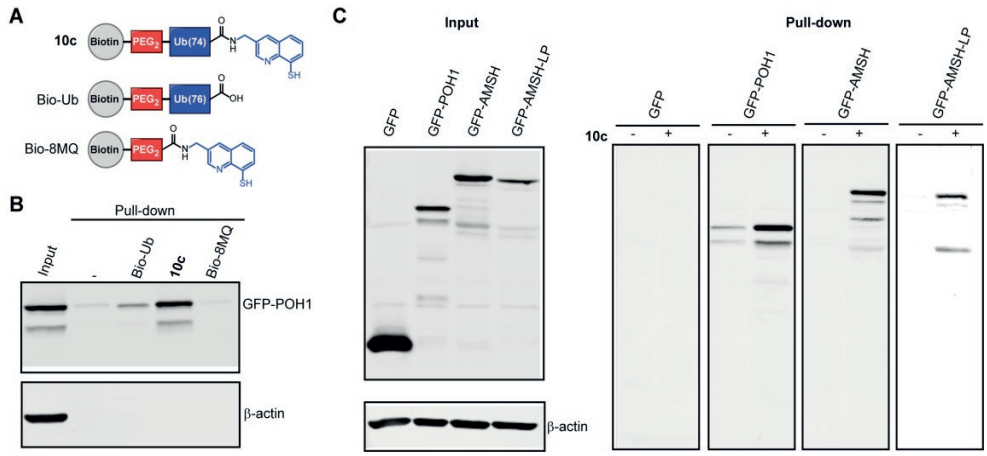


Figure 5: *Pull-down using* ***10c****. **A:** Schematic representation of pull-down reagents used in the assay. **B:** Western Blot analysis of pull-down from cell lysate of HeLa cells overexpressing GFP-POH1.* ***10c*** *efficiently pulled-down GFP-POH1 compared with Bio-Ub or Bio-8MQ alone. **C:** Using* ***10c****, other metalloDUBs like GFP-AMSH and GFP-AMSHLP were also pulled-down from overexpressing HeLa cell lysate.*

FP-binding experiment. In our assays, the reagent **10b** showed a binding affinity of 8.5 μM. On the other hand, full-length Ub binds to Rpn11/Rpn8 with a K_d of 38 μM (Figure 3). This shows that the reagent **10b** can tightly bind to the Rpn11/Rpn8 complex compared to wild-type Ub.

Next, we tested the formation of a stable complex between our probe and Rpn11/Rpn8 in a retention-time shift assay on a size exclusion chromatography (SEC) column. In order to visualize the co-elution of Rpn11/Rpn8 with our probe, we used **10b** and rhodamine-labelled Ub_{76} such that the absorption signal of rhodamine was followed. In addition, the fractions from the SEC column were visualized by SDS-PAGE both by in-gel fluorescence imaging and by Coomassie staining.

Having established the retention times of Rpn11/Rpn8, rhodamine-labelled Ub_{76} and **10b** separately (Figure S12A, S12B and S12C), we incubated Rpn11/Rpn8 with an excess of either rhodamine-labelled Ub_{76} or **10b** and used SEC to determine whether a complex is formed between them. We observed that rhodamine-labelled Ub_{76} does not co-elute with the Rpn11/Rpn8 (Figure 4A). Interestingly, incubating **10b** with Rpn11/Rpn8 resulted in co-elution implying that the Ub74-8MQ forms a tight complex with the enzyme (Figure 4B). This shows that the Ub-8MQ reagent can effectively bind Rpn11/Rpn8.

After determining that Ub-8MQ probe was able to bind efficiently with Rpn11/Rpn8 in our in vitro assays, we examined whether metalloDUBs in cell lysate can be captured by our probe. For this purpose, we synthesized a biotinylated Ub-8MQ probe (**10c**, Scheme 1D) and used biotin-Ub and biotin-8MQ as controls (Figure 5A). Cell lysate prepared from HeLa cells overexpressing GFP-POH1 (human homolog of Rpn11) was incubated with **10c**, along with biotin-Ub and biotin-8MQ and streptavidin beads were used to pull-down GFP-POH1 bound to our probe. As expected, **10c** was able to pull down GFP-POH1 with higher efficiency than biotin-Ub or biotin-8MQ alone (Figure 5B). Even though the IC_{50} values of **10a** and 8MQ are similar (Figure 2), our pull-down experiments show that the Ub handle is indispensable to tightly interact with metalloDUBs.

To determine whether this is true for other known metalloDUBs, we overexpressed GFP-

POH1, GFP-AMSH and GFP-AMSHLP in HeLa cells and carried out a pull-down assay using **10c**. As expected, **10c** was able to pull-down metalloDUBs from cell lysate (Figure 5C). This shows that our probe can also be used to pull-down other metalloDUBs from complex mixtures in human cells.

Conclusion

In conclusion, a zinc chelator was synthesized and coupled to the C-terminal end of Ub to generate a first-generation metalloDUB probe. In our assays, the Ub_{74}-8MQ reagent was able to inhibit the activity of Rpn11/Rpn8 better than full-length Ub alone. In addition, the Ub74-8MQ reagent can form a tight complex with Rpn11/Rpn8. A biotinylated metalloDUB probe was also able to pull-down POH1, AMSH and AMSH-LP from HeLa cell lysates. The metalloprotease DUBs, in general, share similar structural features in the active site of the enzyme and exist as a part of the multi-molecular protein complex. [6] [41-44] Thus, reagents like the one described here may be used as a probe to detect the activity of metalloDUBs and their associated proteins.

Acknowledgements

We would like to thank Henk Hilkmann and Dris el Atmioui for peptide synthesis; Remco Merkx for providing TMB-thiol reagent; Andreas Martin for providing the plasmid for Rpn11/Rpn8 heterodimer expression; Paul Geurink for providing bis-Boc-protected rhodamine, Ub-FP assay reagent and for critical reading of the manuscript. Work in the H.O lab is funded by an NWO (VICI grant 724.013.002) to H.O and an ITN fellowship to A.S.

References

1. Ambroggio, X.I., D.C. Rees, and R.J. Deshaies, *JAMM: a metalloprotease-like zinc site in the proteasome and signalosome.* PLoS Biol, 2004. **2**(1): p. 113-119.
2. Kikuchi, K., et al., *Identification of AMSH-LP containing a Jab1/MPN domain metalloenzyme motif.* Biochem Biophys Res Commun, 2003. **306**(3): p. 637-43.
3. Verma, R., et al., *Role of Rpn11 metalloprotease in deubiquitination and degradation by the 26S proteasome.* Science, 2002. **298**(5593): p. 611-5.
4. Hershko, A. and A. Ciechanover, *The ubiquitin system.* Annu Rev Biochem, 1998. **67**: p. 425-79.
5. Komander, D., *Mechanism, specificity and structure of the deubiquitinases.* Subcell Biochem, 2010. **54**: p. 69-87.
6. Komander, D., M.J. Clague, and S. Urbe, *Breaking the chains: structure and function of the deubiquitinases.* Nat Rev Mol Cell Biol, 2009. **10**(8): p. 550-63.
7. Abdul Rehman, S.A., et al., *MINDY-1 Is a Member of an Evolutionarily Conserved and Structurally Distinct New Family of Deubiquitinating Enzymes.* Mol Cell, 2016. **63**(1): p. 146-55.
8. Hu, M., et al., *Crystal structure of a UBP-family deubiquitinating enzyme in isolation and in complex with ubiquitin aldehyde.* Cell, 2002. **111**(7): p. 1041-54.
9. Kessler, B.M., *Putting proteomics on target: activity-based profiling of ubiquitin and ubiquitin-like processing enzymes.* Expert Rev Proteomics, 2006. **3**(2): p. 213-21.
10. Komander, D. and D. Barford, *Structure of the A20 OTU domain and mechanistic insights into deubiquitination.* Biochem J, 2008. **409**(1): p. 77-85.
11. Hameed, D.S., A. Sapmaz, and H. Ovaa, *How Chemical Synthesis of Ubiquitin Conjugates Helps To Understand Ubiquitin Signal Transduction.* Bioconjug Chem, 2016.
12. Ekkebus, R., et al., *On terminal alkynes that can react with active-site cysteine nucleophiles in proteases.* J Am Chem Soc, 2013. **135**(8): p. 2867-70.
13. Sommer, S., et al., *Covalent inhibition of SUMO and ubiquitin-specific cysteine proteases by an in situ thiol-alkyne addition.* Bioorg Med Chem, 2013. **21**(9): p. 2511-7.
14. Hewings, D.S., et al., *Activity-based probes for the ubiquitin conjugation-deconjugation machinery: new chemistries, new tools, and new insights.* The FEBS Journal, 2017: p. 1555-1576.
15. Gopinath, P., et al., *Chemical and semisynthetic approaches to study and target deubiquitinases.* Chem Soc Rev, 2016. **45**(15): p. 4171-98.
16. Borodovsky, A., et al., *Chemistry-based functional proteomics reveals novel members of the deubiquitinating enzyme family.* Chem Biol, 2002. **9**(10): p. 1149-59.
17. Lam, Y.A., et al., *Editing of ubiquitin conjugates by an isopeptidase in the 26S proteasome.* Nature, 1997. **385**(6618): p. 737-40.
18. Meledin, R., et al., *Activity-Based Probes Developed by Applying a Sequential Dehydroalanine Formation Strategy to Expressed Proteins Reveal a Potential alpha-Globin-Modulating Deubiquitinase.* Angew Chem Int Ed Engl, 2018. **57**(20): p. 5645-5649.
19. Davies, C.W., et al., *Structural and thermodynamic comparison of the catalytic domain of AMSH and AMSH-LP: nearly identical fold but different stability.* J Mol Biol, 2011. **413**(2): p. 416-29.
20. Clague, M.J., et al., *Deubiquitylases from genes to organism.* Physiol Rev, 2013. **93**(3): p. 1289-315.

21. Tran, H.J., et al., *Structure of the Jab1/MPN domain and its implications for proteasome function.* Biochemistry, 2003. **42**(39): p. 11460-5.
22. Saghatelian, A., et al., *Activity-based probes for the proteomic profiling of metalloproteases.* Proc Natl Acad Sci U S A, 2004. **101**(27): p. 10000-5.
23. Pathare, G.R., et al., *Crystal structure of the proteasomal deubiquitylation module Rpn8-Rpn11.* Proc Natl Acad Sci U S A, 2014. **111**(8): p. 2984-9.
24. Sato, Y., et al., *Structural basis for specific cleavage of Lys 63-linked polyubiquitin chains.* Nature, 2008. **455**(7211): p. 358-62.
25. Worden, E.J., C. Padovani, and A. Martin, *Structure of the Rpn11-Rpn8 dimer reveals mechanisms of substrate deubiquitination during proteasomal degradation.* Nat Struct Mol Biol, 2014. **21**(3): p. 220-7.
26. Hassiepen, U., et al., *A sensitive fluorescence intensity assay for deubiquitinating proteases using ubiquitin-rhodamine110-glycine as substrate.* Anal Biochem, 2007. **371**(2): p. 201-7.
27. Geurink, P.P., et al., *A general chemical ligation approach towards isopeptide-linked ubiquitin and ubiquitin-like assay reagents.* Chembiochem, 2012. **13**(2): p. 293-7.
28. Morell, M., et al., *Coupling protein engineering with probe design to inhibit and image matrix metalloproteinases with controlled specificity.* J Am Chem Soc, 2013. **135**(24): p. 9139-48.
29. Sieber, S.A., et al., *Proteomic profiling of metalloprotease activities with cocktails of active-site probes.* Nat Chem Biol, 2006. **2**(5): p. 274-81.
30. Maity, S.K., S. Ohayon, and A. Brik, *Synthesis of N-Hydroxy Isopeptide Containing Proteins.* Org Lett, 2015. **17**(14): p. 3438-41.
31. Kawai, K. and N. Nagata, *Metal-ligand interactions: an analysis of zinc binding groups using the Protein Data Bank.* Eur J Med Chem, 2012. **51**: p. 271-6.
32. Perez, C., et al., *Discovery of an Inhibitor of the Proteasome Subunit Rpn11.* J Med Chem, 2017.
33. Li, J., et al., *Capzimin is a potent and specific inhibitor of proteasome isopeptidase Rpn11.* Nat Chem Biol, 2017. **13**(5): p. 486-493.
34. Zhou, H., Parlati, F., Roufflet, M., Emberley, E., Deshaies, R., Cohen, S., WO/2012/158435, *COMPOSITIONS AND METHODS FOR JAMM PROTEIN INHIBITION*. 2012.
35. Vijay-Kumar, S., C.E. Bugg, and W.J. Cook, *Structure of ubiquitin refined at 1.8 A resolution.* J Mol Biol, 1987. **194**(3): p. 531-44.
36. El Oualid, F., et al., *Chemical synthesis of ubiquitin, ubiquitin-based probes, and diubiquitin.* Angew Chem Int Ed Engl, 2010. **49**(52): p. 10149-53.
37. Shanmugham, A., et al., *Nonhydrolyzable ubiquitin-isopeptide isosteres as deubiquitinating enzyme probes.* J Am Chem Soc, 2010. **132**(26): p. 8834-5.
38. Geurink, P.P., et al., *Development of Diubiquitin-Based FRET Probes To Quantify Ubiquitin Linkage Specificity of Deubiquitinating Enzymes.* Chembiochem, 2016. **17**(9): p. 816-20.
39. Nyborg, J.K. and O.B. Peersen, *That zincing feeling: the effects of EDTA on the behaviour of zinc-binding transcriptional regulators.* Biochem J, 2004. **381**(Pt 3): p. e3-4.
40. Buchli, R., et al., *Real-time measurement of in vitro peptide binding to soluble HLA-A*0201 by fluorescence polarization.* Biochemistry, 2004. **43**(46): p. 14852-63.
41. Cooper, E.M., et al., *K63-specific deubiquitination by two JAMM/MPN+ complexes: BRISC-associated Brcc36 and proteasomal Poh1.* EMBO J, 2009. **28**(6): p. 621-31.

42. Cope, G.A., et al., *Role of predicted metalloprotease motif of Jab1/Csn5 in cleavage of Nedd8 from Cul1.* Science, 2002. **298**(5593): p. 608-11.
43. McCullough, J., et al., *Activation of the endosome-associated ubiquitin isopeptidase AMSH by STAM, a component of the multivesicular body-sorting machinery.* Curr Biol, 2006. **16**(2): p. 160-5.
44. Yao, T. and R.E. Cohen, *A cryptic protease couples deubiquitination and degradation by the proteasome.* Nature, 2002. **419**(6905): p. 403-7.

Supplementary figures

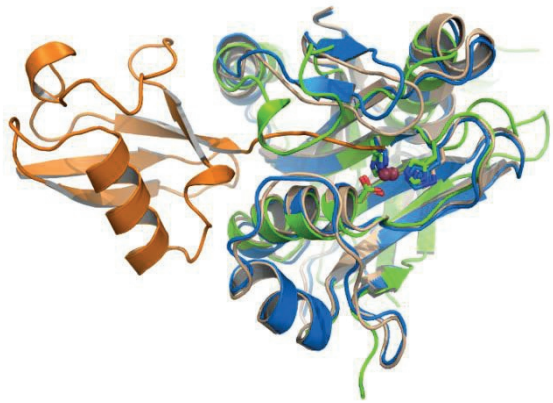


***Figure S1**: X-ray structures showing the catalytic domain of AMSH in complex with Ub (Blue for AMSH and orange for Ub, PDB: 2ZNV), overlaid on the catalytic domains of AMSH-LP (Brown, PDB: 3RZU) and Rpn11 (Green, PDB:4O8X). The active site containing two histidine residues and the aspartate residue is shown in a stick representation while the Zn^{2+} is shown in dark pink colour. The C-terminus of Ub is accommodated into a groove that extends into the active-site residues and the Zn^{2+} ion.*



***Figure S2**: Coomassie-stained image of the SDS-PAGE gel containing the eluted fractions of Rpn11/Rpn8 heterodimer complex from size-exclusion chromatography. Rpn11/Rpn8 heterodimer was expressed into BL21 E.coli cells and eluted from the cell lysate using TALON Metal Affinity Resin™. The heterodimer complex of Rpn11/Rpn8 was purified by size-exclusion chromatography on a HiLoad 16/60 Superdex 200 pg column (GE Life Sciences). Pure fractions were pooled, concentrated and stored at -80 ºC for future use.*

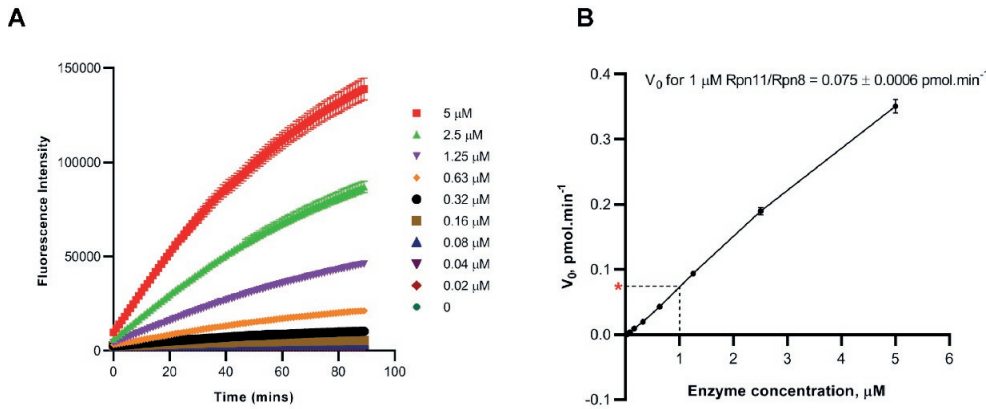


***Figure S3**: **A**: The activity of the purified Rpn11/rpn8 enzyme complex was measured using the rate of hydrolysis of Ub-Rho assay reagent. Rpn11/Rpn8 heterodimer complex was taken at different concentrations ranging from 5 μM down to 0.01 μM and used against 2 μM of Ub-Rho substrate. **B:** An enzyme concentration vs initial enzyme-velocity plot showing an almost linear correlation. The red asterisk (*) shows the value of V_0 for 1 μM of Rpn11/Rpn8 used in the assay.*

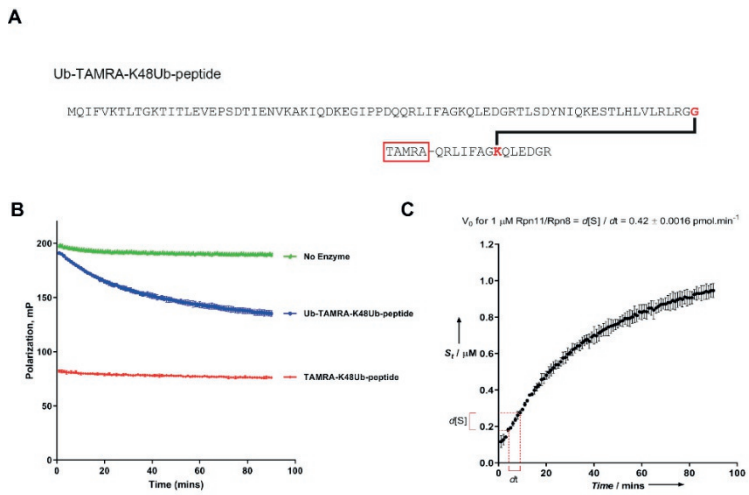


***Figure S4: A:** Sequence of the FP assay reagent that was chosen based on Rpn11/Rpn8 preference towards K48 linked diUbs [1]. The FP assay reagent contains full-length Ub ligated with a TAMRA-labelled peptide containing residues 41-54 of Ub. **B:** The hydrolysis of Ub- FP assay reagent by Rpn11/Rpn8, measured using a TAMRA-based fluorescence polarization assay. Upon hydrolysis by Rpn11, the TAMRA-labeled peptide is released, and the fluorescence polarization was measured on the Y-axis against time on the X-axis. [2] **C:** The rate of hydrolysis of the FP assay reagent in Figure S4B were calculated. The rate of consumption of the substrate was plotted on Y-axis against time on X-axis. The initial rate of enzyme activity (V_0) was calculated from the slope of the linear part of the curve, shown in red.*

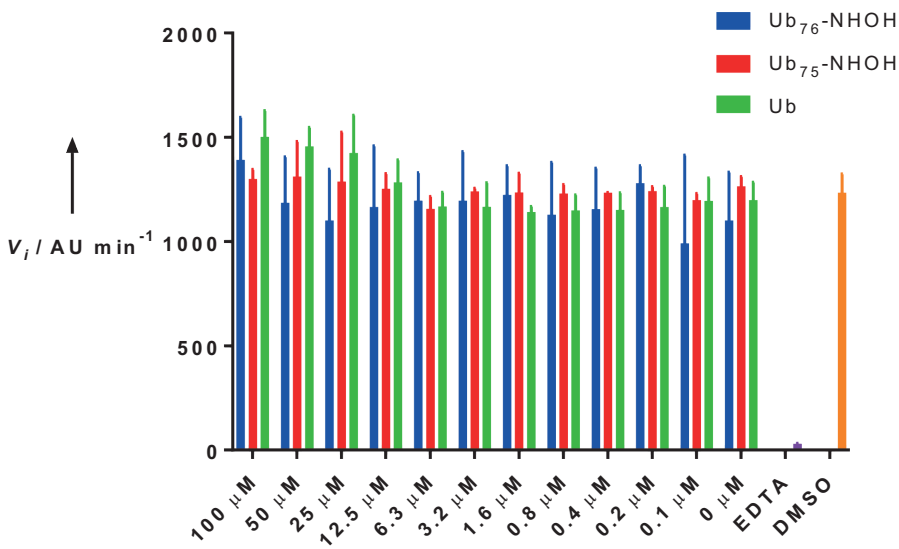


***Figure S5**: Two different lengths of ubiquitin-hydroxamate were used at different concentrations in a Ub-Rho assay to test for inhibition of Rpn11/Rpn8. Full-length Ub was used as a control. Ub_{76}, Ub_{75}-NHOH and Ub_{76}-NHOH did not inhibit the Rpn11/Rpn8 enzyme even at the highest concentrations used here.*

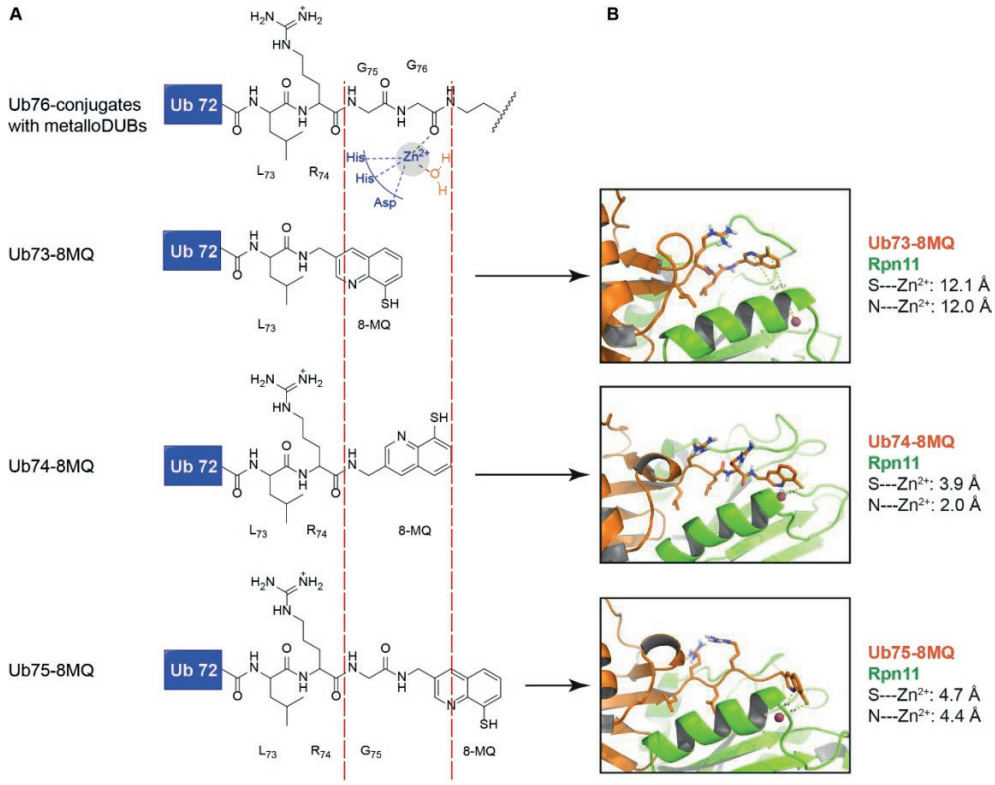


Figure S6: A: *Design of Ub74-8MQ. Comparing Ub76 with Zn^{2+} of metalloDUB, Ub73-8MQ falls short of a length, while Ub75-8MQ is longer. Ub74-8MQ provides the exact length that matches with Ub76.* ***B:*** *Molecular docking using Rpn11 (green, PDB: 4O8X) and different lengths of Ub-8MQ (orange, based on 1UBQ and 8MQ). Distance calculations from Zn^{2+} to the coordinating elements namely the Sulphur and Nitrogen of 8MQ shows that Ub74-8MQ is much closely positioned for coordinating with Zn^{2+} on the active site of Rpn11.*

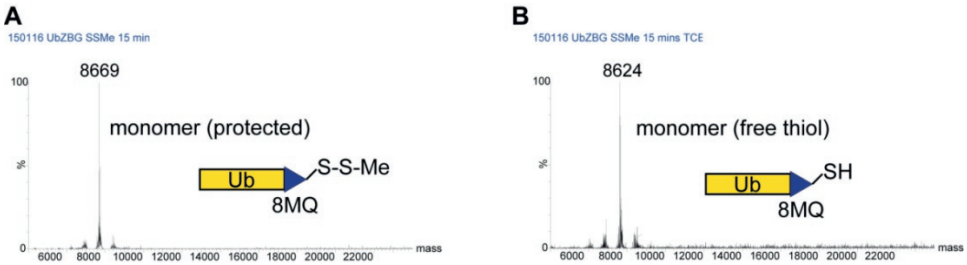


Figure S7: A: *Deconvoluted mass spectrum data for* ***10a*** *(Ub_{74}-8MQ) protected as a disulfide of methyl thiol. ESI-Mass [M+H] for protected* ***10a*** *- Expected: 8666 / Found: 8669.* ***B:*** *Deconvoluted mass spectrum data for* ***10a*** *after the addition of 25 mM TCEP for 15 minutes at RT. ESI-Mass [M+H] for reduced* ***10a*** *- Expected: 8622 / Found: 8624.*

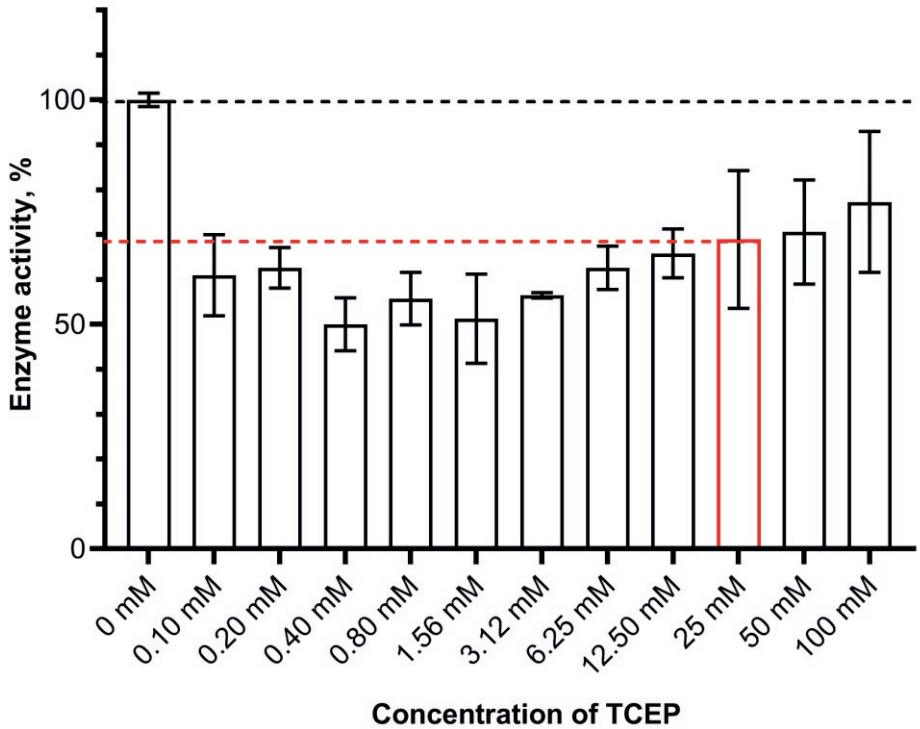


Figure S8*: The influence of TCEP on Rpn11/Rpn8 activity at different concentrations was measured using Ub-rho assay. Although there is a general reduction in the enzyme activity by approximately 30%, the enzyme was active even at the concentrations of 100 mM TCEP. For practical purposes, we used 25 mM TCEP in our assay buffers in order to reduce* ***10a, 10b and 10c****.*

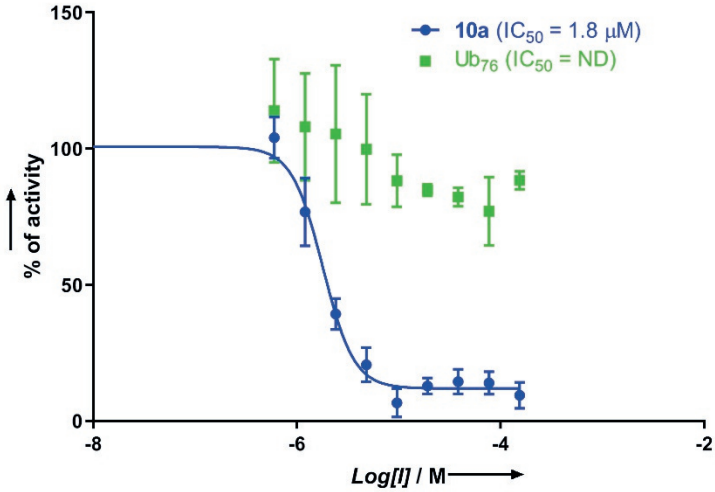


***Figure S9**: The Ub-FP assay reagent (Figure S4) was used in an FP assay and the IC_{50} values of **10a** on Rpn11/Rpn8 were calculated. The IC_{50} values were comparable to the results in the Ub-Rho assay (Figure 2).*

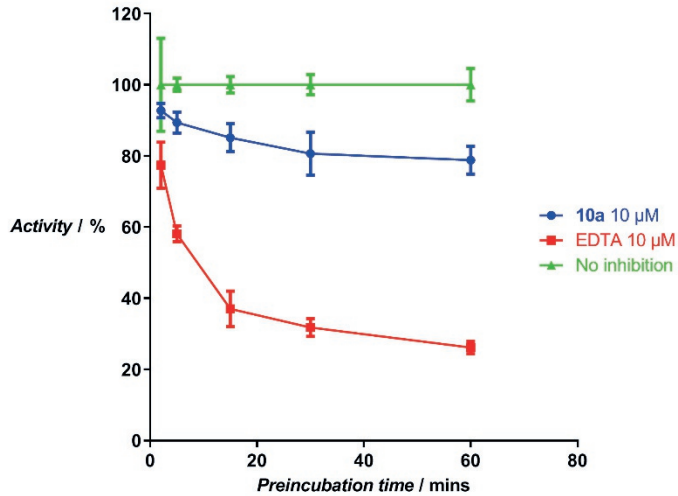


***Figure S10**: In this assay, Rpn11/Rpn8 and **10a** or EDTA were pre-incubated at different time durations before adding Ub-rhodamine substrate. EDTA progressively increased the inhibition of Rpn11/Rpn8 on increasing the incubation time while **10a** showed no such correlation, although a minimal decrease was initially observed. Normalized enzyme activity was shown in the Y-axis and different pre-incubation time is plotted in the X-axis.*

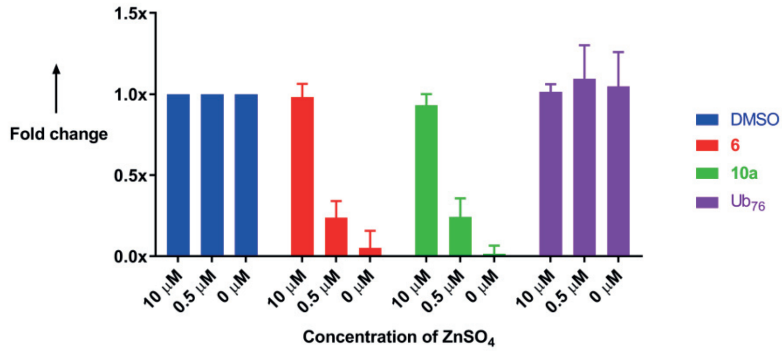


Figure S11*: Rpn11/Rpn8 was pre-incubated with either 5 μM 8-MQ, 10 μM* ***10a*** *or 10 μM* Ub_{76} *for 30 minutes at RT. Later, 10 μM, 0.5 μM or 0 μM* $ZnSO_4$ *was added to the FP assay buffer for 15 minutes and then the activity of the enzyme was measured using K48 FP reagent. The initial velocity of the enzyme for different inhibitors was normalized to DMSO control samples. Rpn11/Rpn8 was able to recover its activity after incubating with higher concentrations of* $ZnSO_4$.

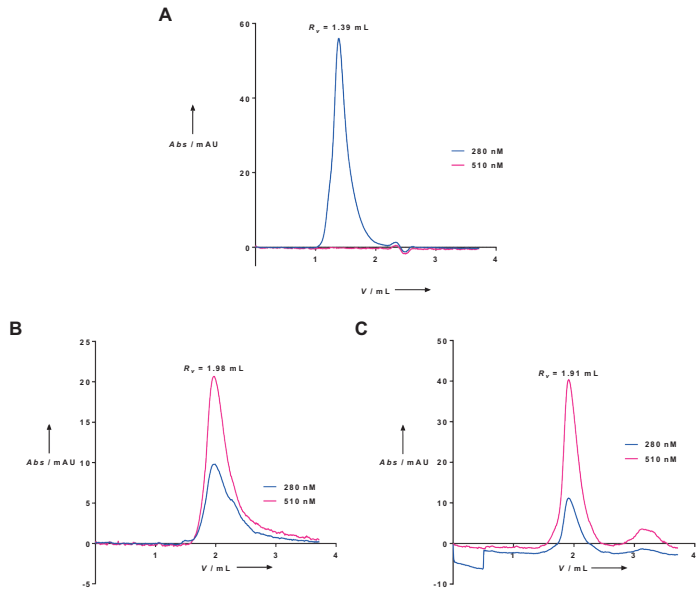
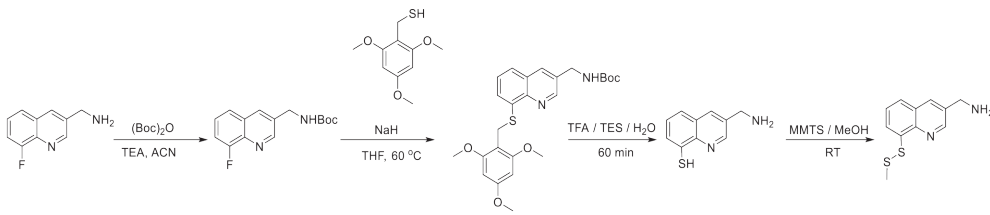


Figure S12: A: *1 μM of Rpn11/Rpn8 was loaded on S75/200 column and the absorbance at 280 nm and 510 nm was measured. The retention time for Rpn11/Rpn8 was about 1.39 mL.* ***B:*** *8 μM of* ***10b*** *was loaded on S75/200 column and the absorbance at 280 nm and 510 nm was measured. The retention time for* ***10b*** *was about 1.98 mL.* ***C:*** *8 μM of RhoUb was loaded on S75/200 column and the absorbance at 280 nm and 510 nm was measured. The retention time for RhoUb was about 1.91 mL.*

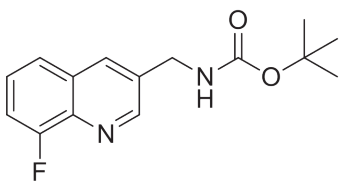
Synthesis scheme of 8-mercapto quinolone 3 methylamine

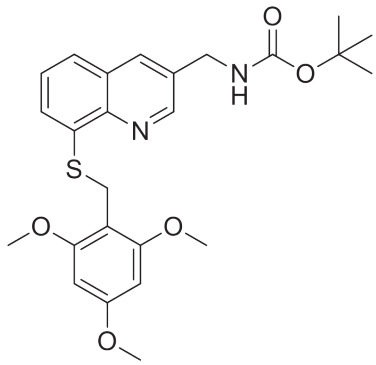
General: All commercial materials (Aldrich, Fluka, Novabiochem) were used without further purification. All solvents were reagent grade or HPLC grade. DCM and THF were passed through a column of alumina. Unless stated otherwise, reactions were performed under inert atmospheres. NMR spectra (1H and 13C) were recorded with a Bruker Avance 300 spectrometer, referenced to TMS or residual solvent. LC-MS analysis was performed with a system containing a Waters 2795 separation module (Alliance HT), Waters 2996 Photodiode Array Detector (190–750 nm), Waters Alltima C18 (2.1 x 100 mm) or Phenomenex Kinetex XB-C18 (2.1 x 50 mm) reversed-phase column and a MicromassLCT-TOF mass spectrometer. Samples were run at 0.40 mL min x 1(Waters C18) or 0.80 mL min x 1 (Kinetex C18) with the use of a gradient of two mobile phases: A) aq. formic acid (0.1 %), and B) formic acid in CH_3CN (0.1 %). Data processing was performed with the aid of Waters MassLynx 4.1 software (deconvolution with Maxent1 function). Preparative HPLC was performed with a Shimadzu LC-20AD/T instrument fitted with a C18 Vydac column (Grace Davison Discovery Sciences) with the use of gradient elution [mobile phases: A) aq. TFA (0.05 %) and B) TFA in CH_3CN (0.05 %)].



Scheme S1: Synthesis of the zinc chelating molecule (8-(methyldisulfaneyl)quinolin-3-yl)methanamine

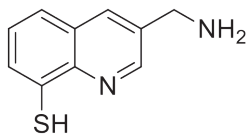
Synthesis of tert-butyl ((8-fluoroquinolin-3-yl)methyl) carbamate (2). Commercially available (8-fluoroquinolin-3-yl)methanamine (**1**, 465 mg, 2.84 mmol) was dissolved in acetonitrile (25 mL). To this, a solution of TEA (2 eq, 5.68 mmol, 756.5 µL) was added drop wise. Then, a solution of di-*tert* butyl dicarbonate (1.75 eq, 4.97 mmol, 1.08 g) in acetonitrile (25 mL) was added. and the resulting mixture was allowed to stir at room temperature for 16 h. The reaction mixture was evaporated to dryness and purified by flash column chromatography (33% → 50% EtOAc/Heptane) to give the desired product **2** as a yellow solid (639 mg, 2.3 mmol, 81%). **^{1}H NMR** (300 MHz, $CDCl_3$) δ 1.44 (s, 9H), 4.49 (d, J = 5.9 Hz, 2H), 5.24 (br s, 1H, NH), 7.28-7.39 (m, 1H), 7.44 (td, J = 7.9, 5.2 Hz, 1H), 7.55 (app d, J = 8.1 Hz, 1H), 8.04 (s, 1H), 8.87 (d, J = 1.7 Hz, 1H) ppm; 13C NMR (75 MHz, $CDCl_3$) δ 28.5, 42.5, 80.2, 113.4 (d, J (C,F) = 18.9 Hz), 123.4 (d, J (C,F) = 4.7 Hz), 126.8 (d, J (C,F) = 8.1 Hz), 129.6 (d, J (C,F) = 2.2 Hz), 133.2, 133.8, 137.8 (d, J (C,F) = 12.0 Hz), 158.8 (d, J (C,F) = 1.6 Hz), 156.0, 158.1 (d, J (C,F) = 256.9 Hz) ppm.





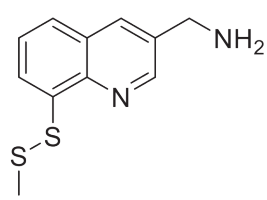
Synthesis of tert-butyl ((8-((2,4,6-trimethoxybenzyl)thio)quinolin-3-yl)methyl)carbamate (3).

To a solution of (2,4,6-trimethoxyphenyl)methanethiol (3 eq, 1.26 g, 5.91 mmol) in dry THF (10 mL) was added NaH (3eq, 236.4 mg, 5.91 mmol) portion wise. To this, a solution of compound **2** (545 mg, 1.97 mmol) in dry THF (10 mL) was added. The resulting mixture was refluxed overnight. After this time, water was added to quench the reaction and the mixture was extracted with EtOAc (3 x 30 mL). The combined organic layers were dried over Na_2SO_4 and concentrated under reduced pressure. The mixture was purified by column chromatography (33% EtOAc/Toluene) to give the desired product 3 as a yellow oil (155 mg, 0.33 mmol, 16.7%). **^{1}H NMR** (300 MHz, $CDCl_3$) δ 1.45 (s, 9H), 2.35 (s, 1H), 3.76 (s, 6H), 3.81 (s, 3H), 4.32 (s, 2H), 4.47 (d, J = 5.9 Hz, 2H), 4.99 (br s, 1H, NH), 6.12 (s, 2H), 7.12-7.28 (m, 1H), 7.41-7.59 (m, 2H), 7.64 (dd, J = 6.9, 1.7 Hz, 1H), 7.97 (d, J = 2.0 Hz, 1H), 8.81 (d, J = 2.2 Hz, 1H) ppm.



Synthesis of 3-(aminomethyl)quinoline-8-thiol (4).

A 3 mL solution of TFA:TES:H_2O, 95:2.5:2.5 (v/v/v) was added to Compound **3** (135 mg, 0.28 mmol) and left stirring at room temperature for 1 hour. After this, the reaction mixture was co-evaporated with DCM (3 x 30 mL) and freeze dried (CH_3CN/H_2O/AcOH, 65/25/10, v/v/v). The desired compound **4** was obtained pure as a yellow oil (50.8 mg, 0.266 mmol, 95%). **^{1}H NMR** (300 MHz, CD_3OD) δ 4.43 (s, 2H), 7.52 (dd, J = 8.2, 7.5 Hz, 1H), 7.81 (dd, J = 8.3, 1.2 Hz, 1H), 7.90 (dd, J = 7.5, 1.2 Hz, 1H), 8.46 (d, J = 2.3 Hz, 1H), 9.03 (d, J = 2.3 Hz, 1H) ppm.



Synthesis of (8-(methyldisulfaneyl)quinolin-3-yl)methanamine (5).

Compound **4** (50.8 mg, 0.266 mmol) dimerized as a disulfide over time and hence the free thiol was protected. Before protecting the thiol, **4** was reduced by adding 1 eq. of ethane-thiol in methanol and left stirring at RT for 3 hours. After total reduction of thiol, 4 eq. S-Methyl methanethiosulfonate (MMTS) was added as a solution to this mixture. The protection of free thiol was followed by LCMS. After complete conversion, the mixture was evaporated and purified over reversed-phase HPLC to yield the desired compound **5** (81%). **^{1}H NMR** (300 MHz, CD_3OD) δ 2.47 (s, 3H), 4.39 (s, 2H), 7.72 (dd, *J* = 8.2, 7.7 Hz, 1H), 7.82 (dd, *J* = 8.3, 1.2 Hz, 1H), 8.22 (dd, *J* = 7.45, 1.2 Hz, 1H), 8.43 (d, *J* = 2.2 Hz, 1H), 8.91 (d, *J* = 2.2 Hz, 1H) ppm. **^{13}C ^{1}H NMR** (75 MHz, $CDCl_3$) δ 151.02, 151.00, 138.79, 138.11, 129.60, 129.23, 128.73, 126.89, 126.69, 49.30, 42.13, 22.53.

Enzyme expression, purification and activity assay

Expression and purification of Rpn11–Rpn8 heterodimers.

A pETDuet-1 vector containing the MPN domains of Rpn11 and Rpn8, a kindly gift from Dr. Andreas Martin, was transformed into BL21 *E.coli* strain. Protocol for expression and purification was described in a previous study.[1] BL21 cells containing Rpn11-Rpn8 expression plasmid were grown in 2xYT medium was supplemented with 150 μM $ZnCl_2$ at 37 ºC until reaches to OD_{600} of about 0.6-0.8. Protein expression was induced with 1mM IPTG and the cells were grown overnight at 18 ºC. Cells were then harvested by centrifugation and lysed with lysis buffer (60 mM HEPES, pH 8.0, 100 mM NaCl, 100 mM KCl, 10% glycerol, 20 mM imidazole, 2 mg/mL lysozyme (Sigma-Aldrich), DNAse I (Roche), and EDTA-free protease inhibitors cocktail tablets (Roche). Further lysis was done by sonication at an amplitude of 60 for 2 min (15 sec pulse-on time and 45 sec pulse-off time) and the cell lysate was clarified by ultracentrifugation at 21,000g for 30 minutes. Soluble cell lysate fraction was incubated with Talon Metal Affinity Resin™ (Clontech) and washed with lysis buffer. Rpn11/Rpn8 heterodimers were eluted with the buffer containing 60 mM HEPES, pH 7.6, 100 mM NaCl, 100 mM KCl, 10% glycerol, and 250 mM imidazole. Eluted proteins were then purified by size-exclusion chromatography on a HiLoad 16/60 Superdex 200 pg column (GE Life Sciences) and then concentrated with a 3K MWCO Amicon Ultra spin filter (Millipore). Purified protein was aliquoted into a small volume and stored at -80 ºC.

Enzyme activity assay:

Ubiquitin-rhodamine assay. The DUB mediated hydrolysis of Ub-rho yields free rhodamine and Ub. The rhodamine signal is measured in a fluorescence intensity assay using a buffer containing 50 mM HEPES, 100 mM NaCl, 100 mM KCl, 1mg/ml CHAPS, 0.1 mM DTT and 0.5 mg/ml BGG at pH 8 and at room temperature. The enzyme (10μL/well) and the substrates (10μL/well) were added to a 384-well Corning™ low volume flat-bottom plates. Fluorescence intensity was monitored at an excitation wavelength of 487 nm and an emission wavelength of 535 nm using EnVision Multilabel Reader, BMG PHERAstar® FSX or BMG CLARIOstar® plate reader. In order to calculate the rate of the enzyme reaction, different concentrations of Rpn11/Rpn8 was added to 2 μM of Ub-rhodamine substrate. The concentration of the hydrolysed product (rhodamine-glycine) was calculated from the fluorescence signal of the free rhodamine-glycine dye after adding 20 nM UCHL3 which ensured the complete hydrolysis of 2 μM of Ub-rhodamine substrate. For general enzyme reactions, the enzyme stock was diluted into the assay buffer at a final concentration of 1 μM. The Ub-rhodamine substrate was prepared synthetically according to the previously reported procedure.[3] The substrate dissolved in DMSO was diluted out in water and later in the assay buffer to a final concentration of 2 μM. The different inhibitor reagents were also prepared as a DMSO stock and diluted out in water and then into the buffer.

Ubiquitin-peptide-TAMRA assay. The DUB-assisted cleavage of Ubiquitin-peptide-TAMRA was followed by fluorescence polarization (FP) in buffer containing 50 mM HEPES, 100 mM NaCl, 100 mM KCl, 1mg/ml CHAPS, 0.1 mM DTT and 0.5 mg/ml BGG at pH 8 and at room temperature. The enzyme (10μL/well) and the substrates (10μL/well) were added to a 384-well Corning™ low volume flat-bottom plates. FP was monitored at 0º and at 90º relative to the polarization of the incident beam at an excitation wavelength of 540

nm and an emission wavelength of 590 nm using BMG PHERAstar® FSX or BMG CLARIOstar® plate reader. Ubiquitin-peptide of different lysine linkages were synthesized according to the procedure described previously. [2] Ubiquitin-TAMRA-K48Ub-peptide (Ub-FP) was used as a substrate in all the FP assays used in this manuscript. The rate of the enzyme activity was calculated by using 1 μM of Rpn11/Rpn8 and 2 μM of the FP assay reagent. Inhibitor reagents were prepared in DMSO as described before. The initial velocity of the enzyme activity was measured as a unit of substrate consumed in the initial part of measurements where the signal is linear. [2]

Computational methodology

The Rpn11/ubiquitin protein complex was constituted using Rpn11 from the Rpn11/Rpn8 complex (PDB: 4O8X) [1] and ubiquitin (PDB: 1UBQ) [4]. Both Rpn11 and ubiquitin were superposed to the structure of AMSH-LP DUB domain in complex with Lys63-linked ubiquitin (PDB: 2ZNV) [5]. The resulting superposed Rpn11/ubiquitin complex was optimized by refining Rpn11 loop-residues 71-84 with Prime [6], followed by molecular dynamic relaxation of the complex. The 8MQ chelator was docked into apo Rpn11 using a constraint for interaction with the Rpn11 pocket zinc atom. The derived 8MQ pose was manually linked to Arg74 from ubiquitin, removing residues 75-76, to construct Ub74. Rpn11 in complex with Ub74 was optimized using molecular dynamics (100 ns) [7]. Other ubiquitin/8MQ chelators were constructed by replacing ubiquitin C-terminus residues with 8MQ manually, followed by optimization using molecular dynamics.

IC_{50} assays

All assay reagents were prepared in the buffer mentioned in the fluorogenic assays described before. For dissolving the inhibitors, the compounds or Ub variants were prepared in DMSO as a stock solution. Then they were dissolved in MQ water and then into one of the fluorogenic assay buffers which contains 25 mM TCEP in order to reduce the protected thiol of the zinc chelating group. Serial dilutions of the inhibitors were prepared in the buffer. After 30 minutes of incubation, the substrate (Ub-rho or UbFP assay reagent) was added centrifuged for 30 secs at 1000 rpm. They are then immediately measured in a plate-reader over a period of up to 90 minutes at RT.

FP binding assay

In a typical FP assay, polarized light at the excitation wavelength is used to excite the fluorogenic molecule. Depending upon the tumbling nature of the molecule, the emitted wavelength is depolarized. This tumbling depends on the binding of the fluorogenic and non-fluorogenic components of the reaction. In our assays, we used rhodamine-labelled Ub-based probes against unlabeled Rpn11/Rpn8 heterodimer. The rho-Ub variants were prepared in DMSO as a stock solution. This was then added to MQ water and then into FP buffer (2μM final concentration) containing 25 mM TCEP to reduce the protected thiol of the zinc chelating group. To this, Rpn11/Rpn8 was added in different concentrations and incubated for 30 minutes at RT. The fluorescence polarization was then measured in a BMG PHERAstar® FSX using end-point measurement and the data was used in GraphPad Prism™ to calculate the binding coefficient.

Enzyme-activity recovery assay

For this assay, 4 μM of the Rpn11/Rpn8 enzyme was pre-incubated with **6** or **10a** at 5 μM and 10 μM respectively for 30 minutes at RT in an FP assay buffer containing 25 mM TCEP to reduce the protected thiol of the zinc chelating group. After this pre-incubation, 10 μM of $ZnSO_4$ was added to the assay buffer containing the enzyme and inhibitor and pre-incubated for another 15 minutes at RT. Later, Ub-K48(TAMRA-peptide) substrate was added and FP was measured over time.

Time-based inhibition assay

In this assay, EDTA, **6**, **10a** and Ub76 were pre-incubated with Rpn11/Rpn8 for different time intervals in an assay buffer containing 25 mM TCEP to reduce the protected thiol of the zinc chelating group. After pre-incubation, the Ub-Rho substrate was added, and the activity of the enzyme was measured in a BMG PHERAstar® FSX for 90 minutes at RT. A graph was plotted with pre-incubation time on the X-axis and rate of the enzyme catalysis on the Y-axis.

Co-elution assay

In this assay, **10b** or Rho-Ub was incubated with Rpn11/Rpn8 in a ratio of 8:1 in a buffer containing 60 mM HEPES, pH 7.6, 100 mM NaCl, 100 mM KCl and 25 mM TCEP. We then used a micro AKTA™ system using native buffer conditions and used an S75/200 column in order to resolve between bound and unbound Rpn11/Rpn8 with **10b**. The eluted fractions were run on a precast 12% NuPAGE Bis-Tris gels on a Novex NuPAGE SDS-PAGE Gel System containing MES buffer. Fluorescence scan was measured on a ProXPRESS 2D Proteomic imaging system (Perkin–Elmer) with a resolution of 100 μm and exposure time of 15 s, with filter settings ($\lambda_{ex}/\lambda_{em}$) 490/540 nm (Rho).

Pull-down assay

HeLa cells were transfected with GFP-POH1, GFP-AMSH, GFP-AMSH-LP and empty GFP vector. After 24 hours, cells were lysed using lysis buffer containing 25 mM HEPES.NaOH (pH 7.4), 50 mM NaCl, 100 mM KCl, NP40 5 mM TCEP and EDTA-free protease inhibitor cocktail (Roche Cat#:5056489001). After centrifugation, the clear lysate was added with **10c** along with other controls like Biotin-8MQ and Biotin-Ub and incubated for 1 hr at RT. Later, Streptavidin beads were added to the lysate and incubated at 4 C for 2 hours. Streptavidin beads were washed with wash buffer cointaning 25 mM HEPES.NaOH (pH 7.4), 50 mM NaCl, 100 mM KCl, NP40 5 mM TCEP. the beads were added with SDS-loading dye containing 10mM DTT. The samples were loaded onto a 10% SDS-PAGE and transferred to nitrocellulose membrane. Antibodies against GFP were used to check for pull-down of GFP-tagged metalloDUBs.

Synthesis of Ub variants

Solid-phase peptide synthesis of Ub

The synthesis of ubiquitin by solid-phase peptide synthesis was carried out according to the previously reported protocol. [3] Ubiquitin (1-74) and Ub (w.t.) were synthesized by solid-phase peptide synthesis on TentaGel Trt R resin. In the case of Rhodamine labelled Ub variants, Rhodamine was coupled on-resin to the N-terminal end of Ub variant by standard chemical coupling. For coupling compound **5** (Scheme **1**) to the C-terminal end of Ub (1-74), the Ub variant was cleaved from resin in a fully-protected version using 20% HFIP in DCM.

After co-evaporating HFIP under reduced pressure, the protected Ub variant was obtained as a colourless oil. In the case of full-length Ub, TFA cleavage mix containing TFA: H_2O: TiPS: Phenol (92.5/2.5/2.5/2.5 v/v/v/v) was used to fully deprotect Ub. The final compound was precipitated in the dry ice cold ether:pentane (3:1) mix and later on lyophilized to yield crude powder which was then purified over reversed-phase HPLC.

Synthesis of Ub_{76}-NHOH and Ub_{75}-NHOH

Ubiquitin was synthesized in a linear fashion in the same way as described before. Fmoc-hydroxylamine was coupled to chlorotrityl-chloride resin using PyBOP and DiPEA. After checking the loading of resin, the rest of the peptides based on the sequence of Ub (1-75) or Ub (1-76) were synthesized using SPPS. After global deprotection, the final product was obtained as Ub_{76}-NHOH and Ub_{75}-NHOH as confirmed by LCMS analysis. (**Figure S21 and S22**)

Synthesis of Ub-8MQ-SMe (10a)

Ub (1-74) was synthesized on a TentaGel Trt R resin. After cleaving the protected peptide from the resin by treating the resin with 20% HFIP in DCM, the C-terminus of Ub74 was coupled in solution to compound **5** using 4 eq each of HOBT and HBTU and 8 eq of DiPEA, in order to minimize racemization problems associated with coupling to side-chain containing amino acids. [8, 9] The reaction mix was left overnight and checked by LCMS for the full conversion into the product. After confirming the formation of the product, the final compound was subjected to global deprotection using TFA cleavage mix mentioned before, precipitated in the dry ice cold ether: pentane, and finally lyophilized as a powder.

Synthesis of Rho-Ub-8MQ-SMe (10b)

Rhodamine was attached to the N-terminal of linearly synthesized ubiquitin on resin using standard coupling conditions containing 4 eq PyBOP, 4 eq Rhodamine diBoc and 8 eq DiPEA. After this, the protected ubiquitin was cleaved off the resin using 20% HFIP in DCM and co-evaporated. [10] Compound **5** was attached to the C-terminal end using the procedure mentioned before.

Synthesis of Bio-$(PEG)_2$-Ub-8MQ-SMe (10c)

First, Fmoc-$(PEG)_2$ was attached to the N-terminal of linearly synthesized ubiquitin on resin using standard coupling conditions containing 4 eq PyBOP, 4 eq Biotin and 8 eq DiPEA. The Fmoc is then cleaved using 20% piperidine in NMP. Next, Biotin was coupled on the N-terminus of $(PEG)_2$-Ub on the resin. After this, the protected ubiquitin was cleaved off the resin using 20% HFIP in DCM and co-evaporated. [10] Compound **5** was attached to the C-terminal end using the procedure mentioned before.

Synthesis of Biotin-$(PEG)_2$-8MQ

Biotin-$(PEG)_2$ was initially prepared by coupling Fmoc-(PEG)2 on Chloro-trityl chloride resin with a loading of 0.4 g/Mol. Fmoc was removed using 20% piperidine in NMP. Biotin was then coupled on the N-terminus of $(PEG)_2$ using 4 eq PyBOP, 4 eq Biotin and 8 eq DiPEA, overnight. The resulting Biotin-(PEG)2 was cleaved from the resin using TFA cleavage mix mentioned in the standard procedure. Compound **5** was attached to the C-terminal end using the procedure mentioned before. The product was then purified using reverse-phase HPLC to obtain Biotin-$(PEG)_2$-8MQ.

Preparation of sample for HPLC purification

All Ub variants were first dissolved in DMSO. This solution was slowly added to MQ water containing 0.05% TFA and filtered through a GfxO/0.45µm GHP membrane Acrodisc® Premium 25mm syringe filter. The sample was then injected onto a Waters XBridge™ Prep C18 Column (30 x 150 mm, 5µm OBD™) at a flow rate of 37.5 ml/min. The protein was purified with the gradient outlined in the table below using aq. 0.05% TFA (Solvent A) and acetonitrile containing 0.05% TFA (Solvent B) as eluents.

Time (in mins)	Solvent B (%)
0 ⇨ 5	5
5 ⇨ 7	5 ⇨ 25
7 ⇨ 22	25 ⇨ 55
22 ⇨ 24	55 ⇨ 95
24 ⇨ 27	95
27 ⇨ 27.5	95 ⇨ 5
27.5 ⇨ 30	5

The retention time for the ubiquitin variants was approximately 10 minutes. All fractions containing the protein were confirmed by checking the mass using a LC-MS R_t 2.8 min; Phenomenex Kinetex™ XB-C18 100A (50 x 2 x 10 mm, 2.6 µm); solvents - MQ water with 0.1% formic acid (Solvent A) and acetonitrile containing 0.1% formic acid (Solvent B), flow rate = 0.5 mL/min, run time = 6 min, column T = 45°C. Gradient: 5% ⇨ 95% B over 3.5 min. All samples containing pure protein were pooled together and lyophilized.

Analysis of purified ubiquitin variants

The ubiquitin variants were dissolved in DMSO to a concentration of 10 mg/mL. 0.5 µL of this sample was resuspended in 100 µL MQ water. This was then used in LCMS analysis using LCT Premiere™ mass spectroscopy analysis.

The LC-MS analysis of the purified reagents

All purified proteins were confirmed by checking the mass using LC-MS. Phenomenex Kinetex™ C18 (100A, 100 x 21 mm, 2.6 µm); solvents – aq. 0.1% formic acid (Solvent A) and acetonitrile containing 0.1% formic acid (Solvent B), flow rate = 0.4 mL/min, runtime = 13 min, column T = 45°C. Gradient: 5% ⇨ 95% B over 7.6 min.

1. Zinc chelating molecule (5)

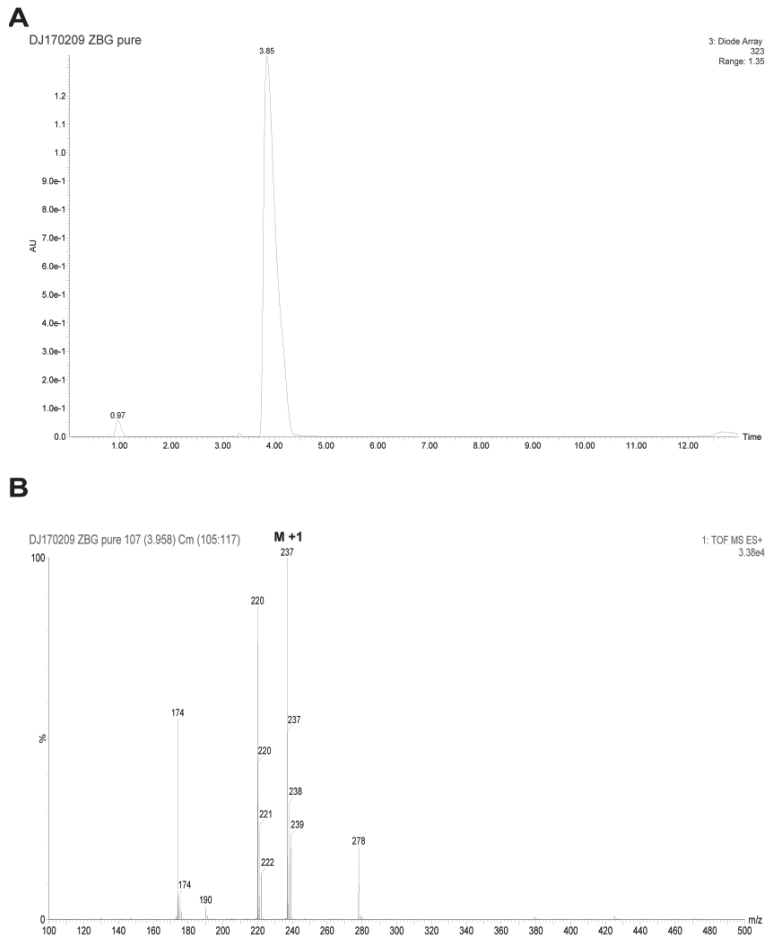


Figure S13: *Analytical data for the synthesized zinc chelator (Compound* ***5****).* ***A:*** *UV chromatogram (λ - 323 nm) using LC-MS;* ***B:*** *Spectrum of the peak at 3.85 min; ESI-Mass [M+H] Expected: 237.35 / Found: 237.*

2. Ub-8MQ (10a, reduced)

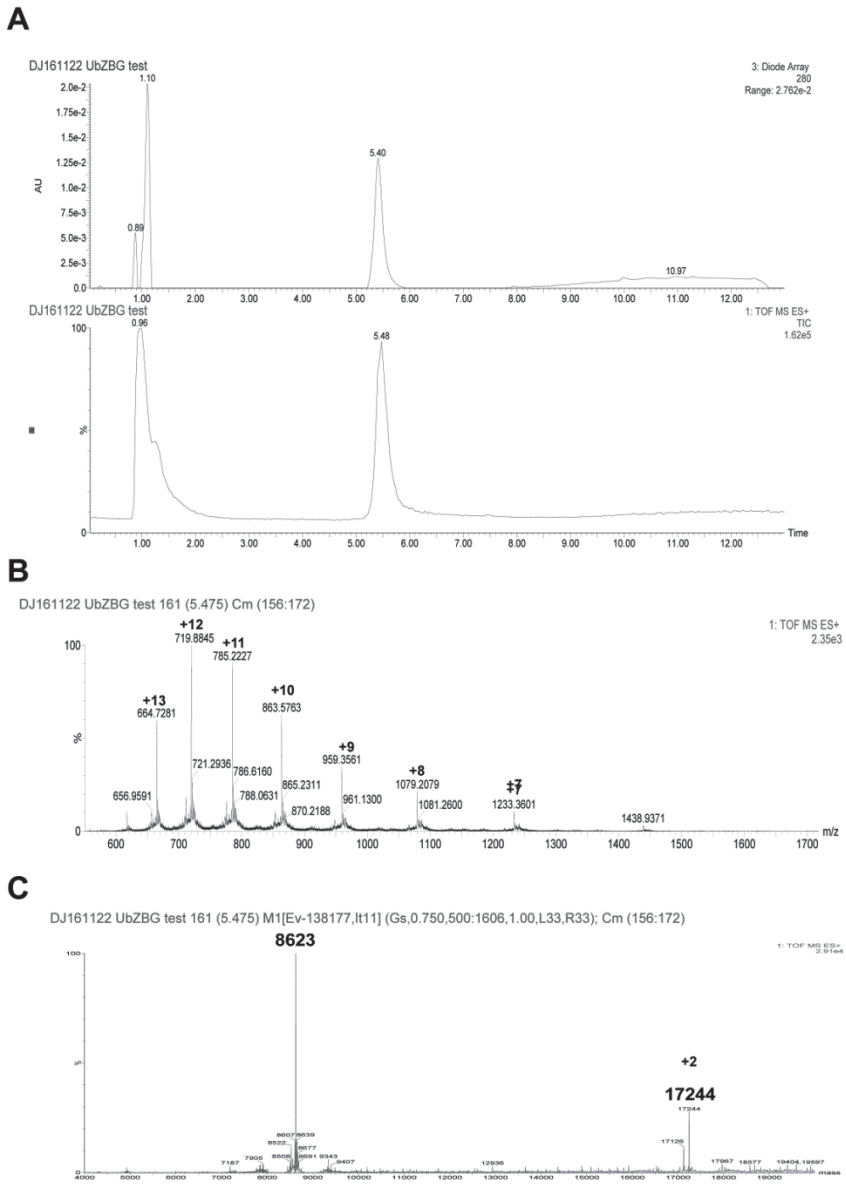


Figure S14: *Ub-8MQ.* ***A:*** *Top: UV chromatogram (λ - 280 nm); Bottom: combined mass spectrum using LC-MS;* ***B:*** *Spectrum of the peak at 5.40 min;* ***C:*** *Deconvoluted mass of peak spectra. ESI-Mass [M+H] Expected: 8622.9 / Found:* ***M+1H*** *= 8623;* ***M+2H*** *= 17244.*

3. Ub-8MQ-SMe (10a)

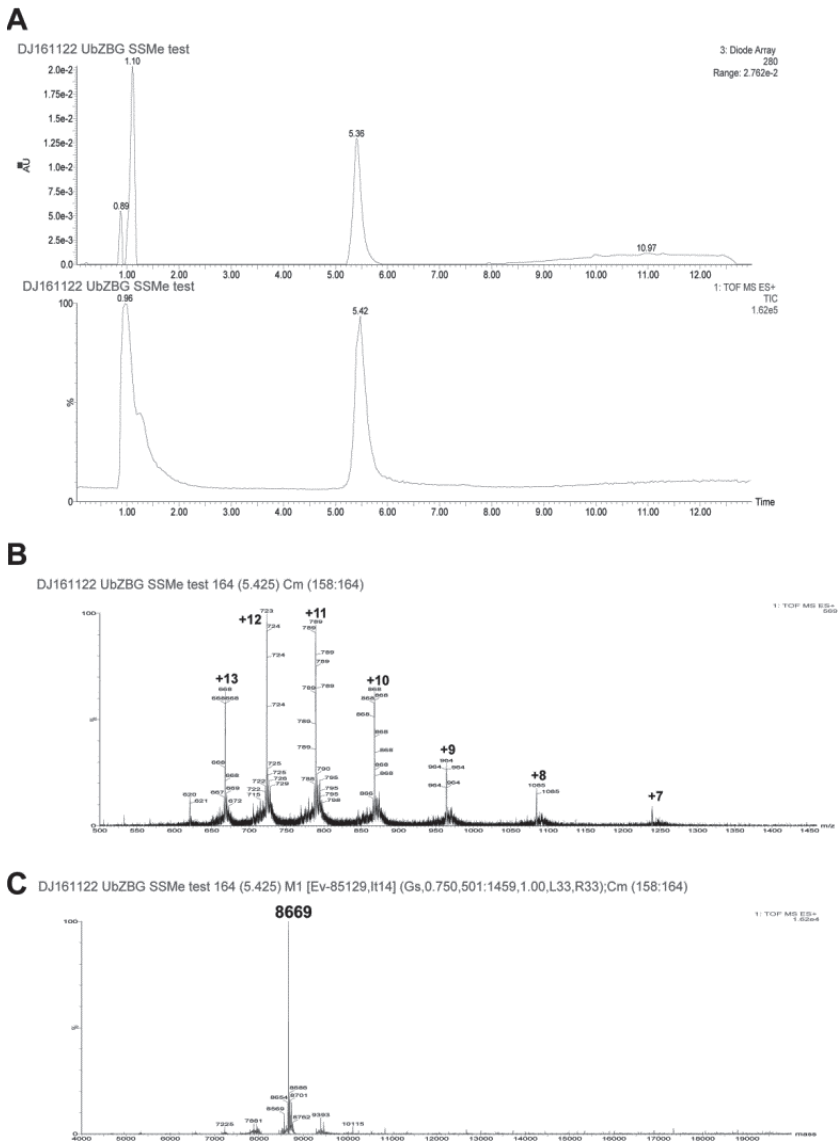


Figure S15:*Ub-8MQ-SMe (**9a**). **A:** Top: UV chromatogram (λ - 280 nm); Bottom: combined mass spectrum using LC-MS; **B:** Spectrum of the peak at 5.36 min; **C:** Deconvoluted mass of peak spectra. ESI-Mass [M+H] Expected: 8667.9 / Found: 8669.*

4. RhoUb-8MQ-SMe (10b)

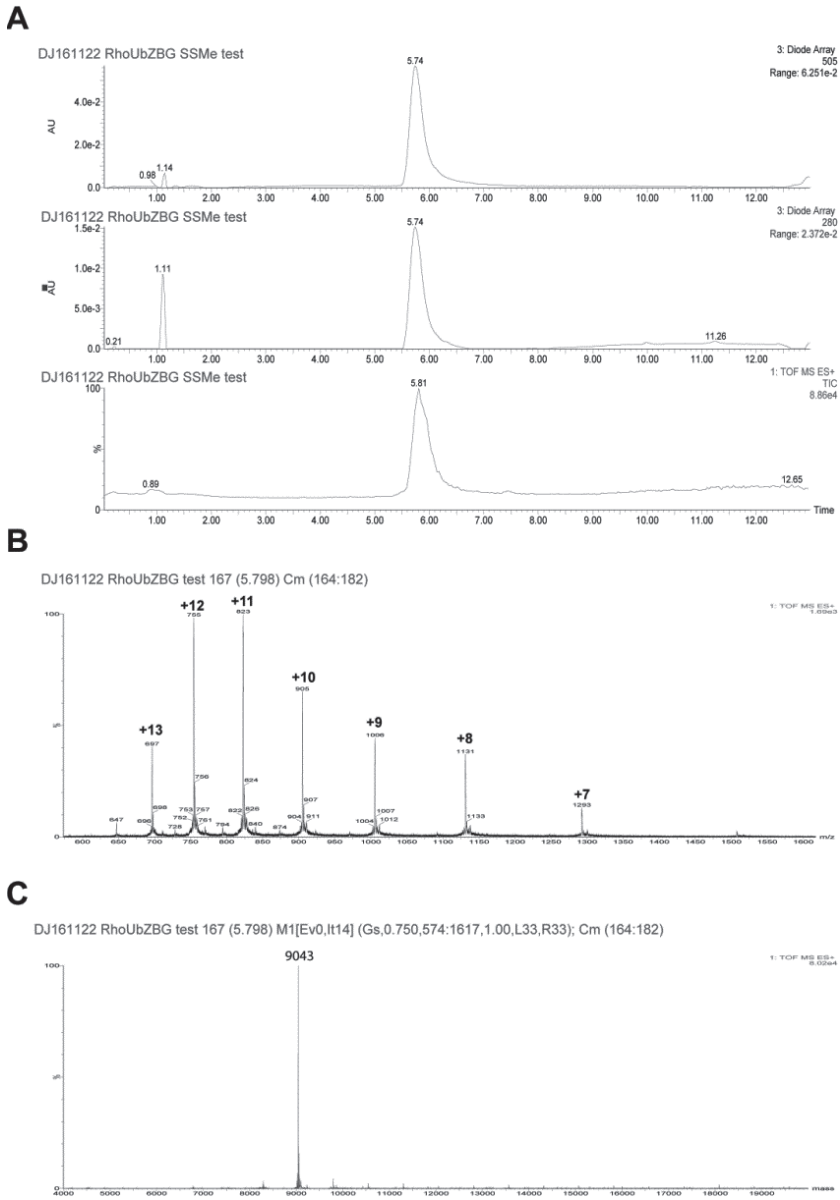


Figure S16: *RhoUb-8MQ-SMe (**9b**). **A:** Top: UV chromatogram (λ - 505 nm); Middle: UV chromatogram (λ - 280 nm); Bottom: combined mass spectrum using LC-MS; **B:** Spectrum of the peak at 5.74 min; **C:** Deconvoluted mass of peak spectra. ESI-Mass [M+H] Expected: 9042.9 / Found: 9043.*

5. RhoUb

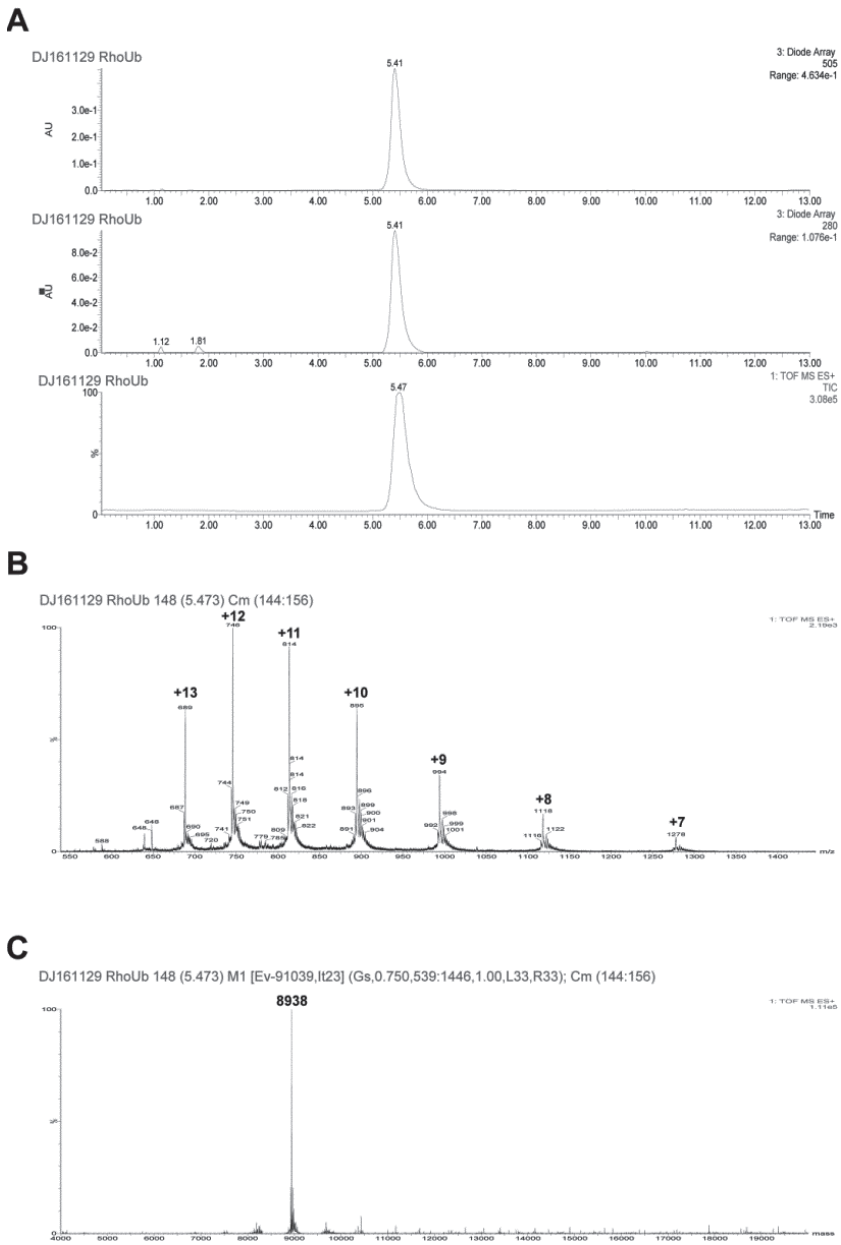


Figure S17: *RhoUb.* ***A:*** *Top: UV chromatogram (λ - 505 nm); Middle: UV chromatogram (λ - 280 nm); Bottom: combined mass spectrum using LC-MS;* ***B:*** *Spectrum of the peak at 5.41 min;* ***C:*** *Deconvoluted mass of peak spectra. ESI-Mass [M+H] Expected: 8938.9 / Found: 8938.*

6. Biotin-(PEG)$_2$-Ub8MQ-SMe (10c)

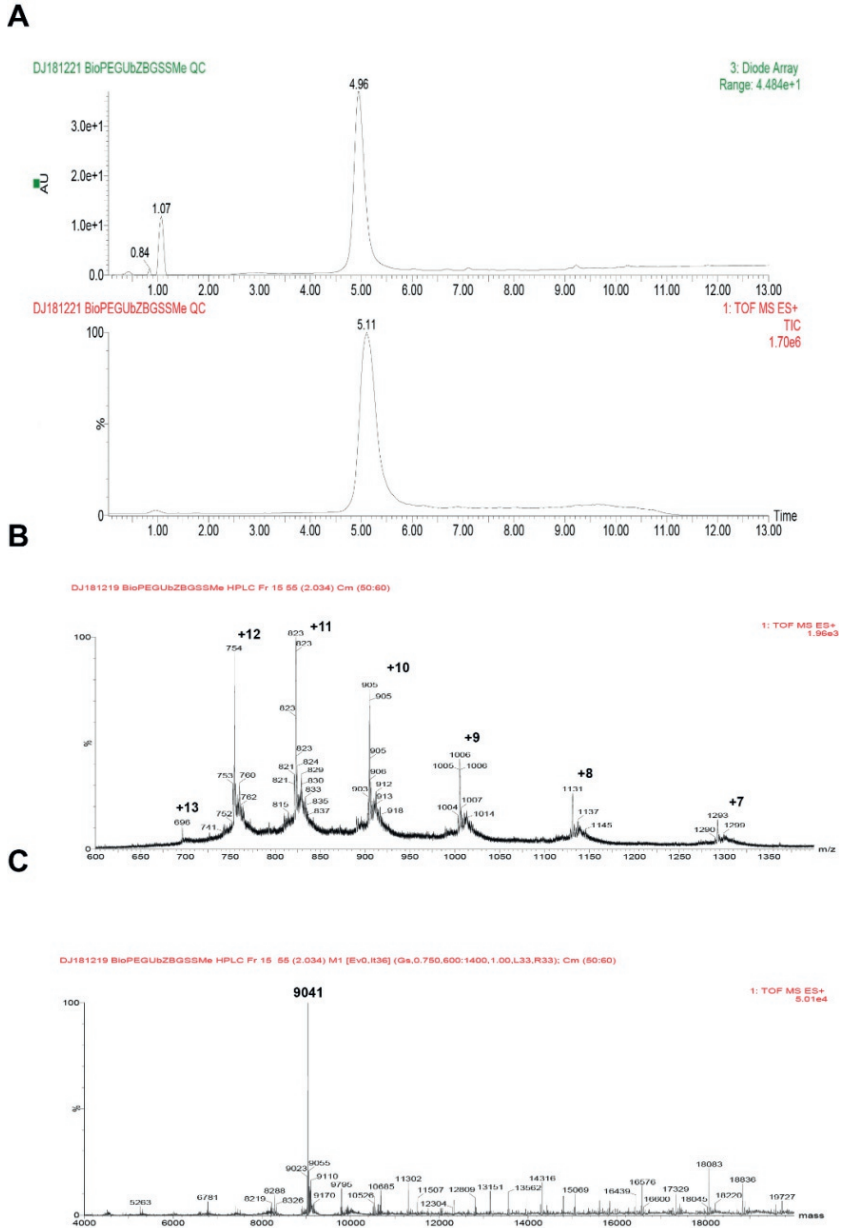


Figure S18: *Biotin-(PEG)$_2$-Ub-8MQ-SMe.* ***A:*** *Top: UV chromatogram (λ - 280 nm); Bottom: combined mass spectrum using LC-MS;* ***B:*** *Spectrum of the peak at 5.11 min;* ***C:*** *Deconvoluted mass of peak spectra. ESI-Mass [M+H] Expected: 9042.2 / Found: 9041.*

7. Biotin-(PEG)$_2$-8MQ-SMe

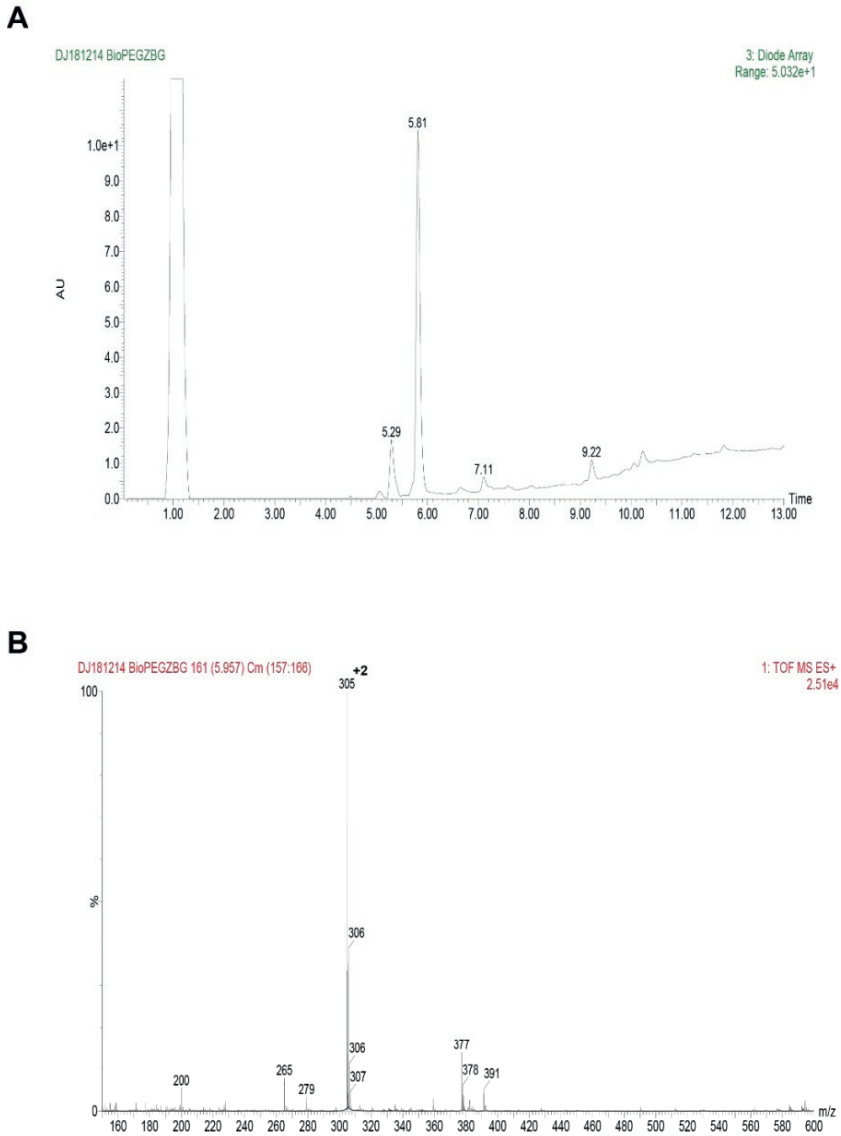


Figure S19: *Biotin-(PEG)$_2$- 8MQ-SMe.* ***A:*** *UV chromatogram (λ - 280 nm);* ***B:*** *Spectrum of the peak at 5.81 min; ESI-Mass [M+2H] Expected: 305.7 / Found: 305.*

8. Biotin-(PEG)$_2$-Ub

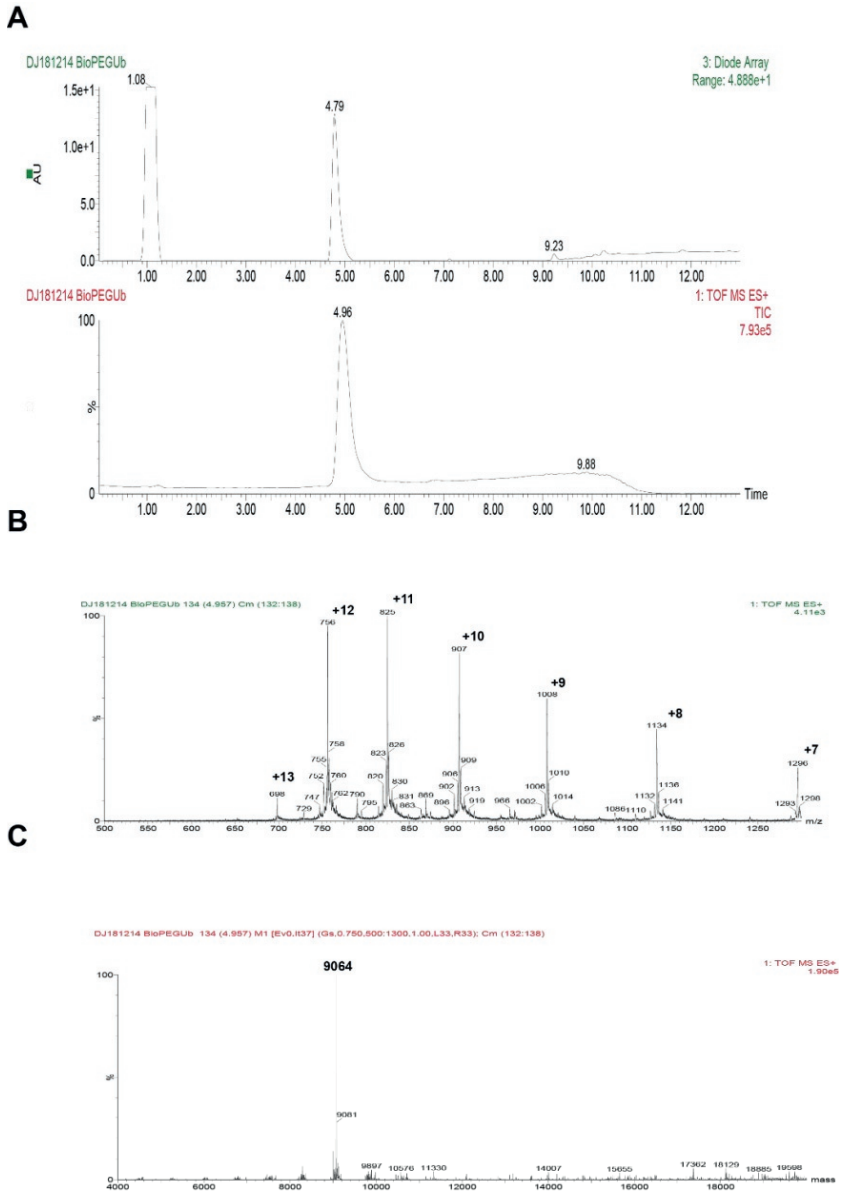


Figure S20: *Biotin-(PEG)$_2$-Ub.* ***A:*** *Top: UV chromatogram (λ - 280 nm); Bottom: combined mass spectrum using LC-MS;* ***B:*** *Spectrum of the peak at 4.96 min;* ***C:*** *Deconvoluted mass of peak spectra. ESI-Mass [M+H] Expected: 9065.6 / Found: 9064.*

9. Ub_{76}-NHOH

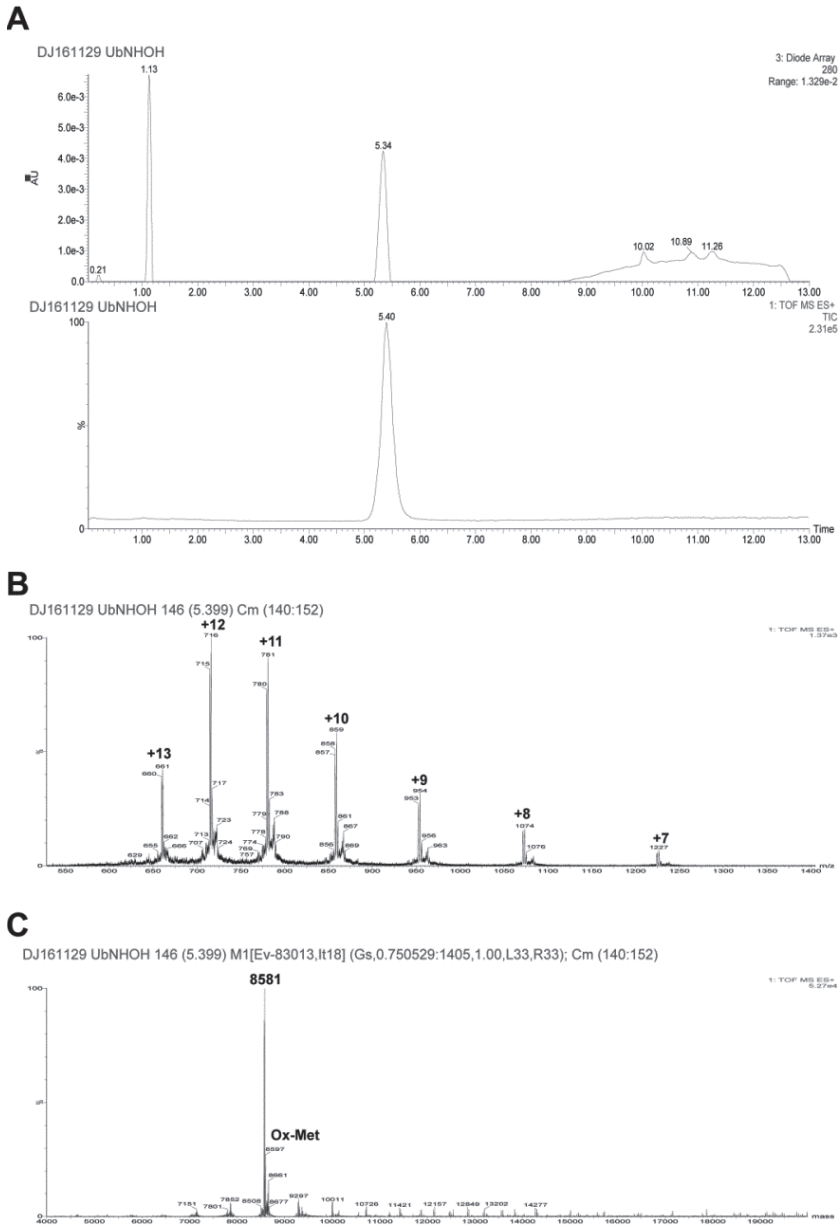


Figure S21: *Ub_{76}NHOH.* ***A:*** *Top: UV chromatogram (λ - 280 nm); Bottom: combined mass spectrum using LC-MS;* ***B:*** *Spectrum of the peak at 5.34 min;* ***C:*** *Deconvoluted mass of peak spectra. ESI-Mass [M+H] Expected: 8579.9 / Found: 8581; Oxidized-Methionine Ub_{76}NHOH mass: 8597.*

10. Ub_{75}-NHOH

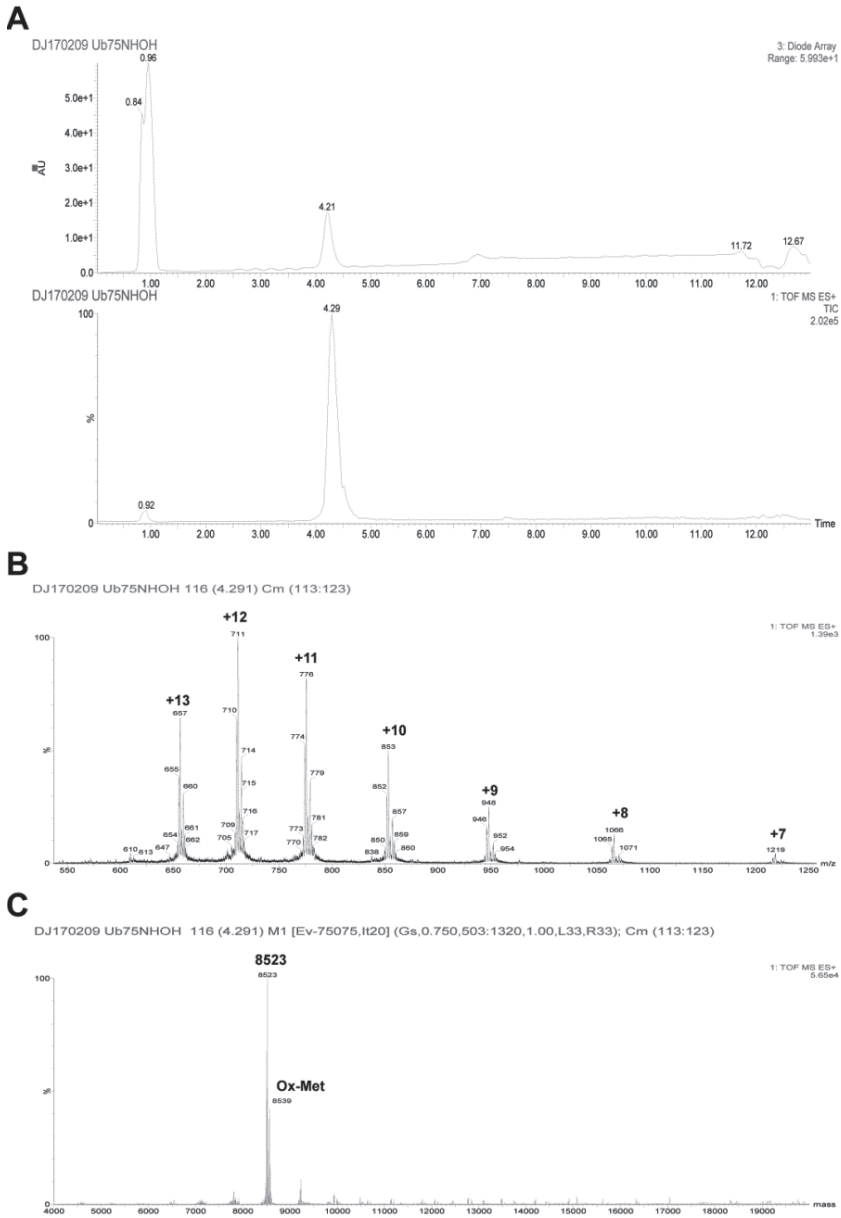


Figure S22: *Ub_{75}NHOH.* ***A:*** *Top: UV chromatogram (λ - 280 nm); Bottom: combined mass spectrum using LC-MS;* ***B:*** *Spectrum of the peak at 5.34 min;* ***C:*** *Deconvoluted mass of peak spectra. ESI-Mass [M+H] Expected: 8521.9 / Found: 8523; Oxidized-Methionine Ub_{75}NHOH mass: 8539.*

Supplementary References

1. Worden, E.J., C. Padovani, and A. Martin, *Structure of the Rpn11-Rpn8 dimer reveals mechanisms of substrate deubiquitination during proteasomal degradation.* Nat Struct Mol Biol, 2014. **21**(3): p. 220-7.
2. Geurink, P.P., et al., *A general chemical ligation approach towards isopeptide-linked ubiquitin and ubiquitin-like assay reagents.* Chembiochem, 2012. **13**(2): p. 293-7.
3. El Oualid, F., et al., *Chemical synthesis of ubiquitin, ubiquitin-based probes, and diubiquitin.* Angew Chem Int Ed Engl, 2010. **49**(52): p. 10149-53.
4. Vijay-Kumar, S., C.E. Bugg, and W.J. Cook, *Structure of ubiquitin refined at 1.8 A resolution.* J Mol Biol, 1987. **194**(3): p. 531-44.
5. Sato, Y., et al., *Structural basis for specific cleavage of Lys 63-linked polyubiquitin chains.* Nature, 2008. **455**(7211): p. 358-62.
6. *Schrödinger Release 2017-4: Prime, Schrödinger, LLC, New York, NY, 2017*.
7. *Schrödinger Release 2017-4: Desmond Molecular Dynamics System, D. E. Shaw Research, New York, NY, 2017. Maestro-Desmond Interoperability Tools, Schrödinger, New York, NY, 2017.*
8. Knorr, R., et al., *New coupling reagents in peptide chemistry.* Tetrahedron Letters, 1989. **30**(15): p. 1927-1930.
9. Xiao, N., Z.X. Jiang, and Y.B. Yu, *Enantioselective synthesis of (2R, 3S)- and (2S, 3R)-4,4,4-trifluoro-N-Fmoc-O-tert-butyl-threonine and their racemization-free incorporation into oligopeptides via solid-phase synthesis.* Biopolymers, 2007. **88**(6): p. 781-96.
10. Geurink, P.P., et al., *Development of Diubiquitin-Based FRET Probes To Quantify Ubiquitin Linkage Specificity of Deubiquitinating Enzymes.* Chembiochem, 2016. **17**(9): p. 816-20.

Chapter 5

Enhanced delivery of synthetic labelled ubiquitin into live cells by using next-generation Ub-TAT conjugates

Adapted from:
Hameed, D.S., A. Sapmaz, L. Gjonaj, R. Merkx, and H. Ovaa, *Enhanced Delivery of Synthetic Labelled Ubiquitin into Live Cells by Using Next-Generation Ub-TAT Conjugates*. Chembiochem, 2018. 19(24): p. 2553-2557.

Summary

Proteins and macromolecules can be delivered into live cells by non-invasive techniques using cell-penetrating peptides. These peptides are easily synthesized using solid phase peptide synthesis and can be conjugated onto cargo molecules to mediate cellular delivery. We designed a TAT-based cell-penetrating ubiquitin (Ub) reagent by conjugating a dimeric disulfide-linked TAT to the C-terminus of a rhodamine-labelled Ub (RhoUb) molecule. This reagent efficiently enters the cell by endocytosis and escapes from endosomes into the cytoplasm. Once inside the cytoplasm, the delivery vehicle is proteolytically removed by endogenous deubiquitinases (DUBs) upon which the intrinsic ubiquitination machinery is able incorporate RhoUb into ubiquitin conjugates. Our approach enables the controlled delivery of labeled or mutant Ub molecules into the cells, increasing our options for studying the ubiquitin system.

Introduction

Ubiquitination plays an essential role in cellular protein homeostasis through regulation of protein degradation, and other key signal transduction functions. [1, 2] The 76 amino acid protein ubiquitin (Ub) modifies a targeted protein by forming covalent Ub conjugates. Its C-terminus is attached to a lysine residue or N-terminus in a target protein by the concerted action of ubiquitinating enzymes namely E1 (Ub-activating enzyme), E2 (Ub-conjugating enzyme) and E3 (Ub-ligase).[3] The process can be reversed by deubiquitinases (DUBs).[4] Ub can also form polymeric chains (PolyUb) by attaching one Ub with the N-terminal methionine or one of the seven lysine side chains to another Ub.[5] Although the ubiquitination has been extensively studied using various synthetic *in-vitro* tools,[6] there is an increasing need for tools *in vivo* to study ubiquitin conjugation in live cells.[7, 8] Therefore, the generation of methods that deliver Ub into live cells is key to further our understanding of ubiquitination in cells in real-time.

A wealth of literature describes the delivery of macromolecules into cells mediated by cell-penetrating peptides (CPPs).[9-12] A widely used CPP is the TAT peptide derived from Trans-Activator of Transcription protein of HIV-1 (TAT).[13, 14] This polycationic peptide consists of a series of lysine and arginine residues which promotes endocytosis.[15] Although TAT peptide enter cells together with its cargo molecules through the endocytic route, the escape from endosomes is essential to deliver cargo molecules into the cytoplasm and subsequently to their final destination where their functions are studied. The TAT peptides can deliver proteins into cells by simple co-incubation, but it does not guarantee efficiency in terms of collective delivery.[16] However, TAT peptide fused with proteins (TAT-fusion proteins, TFPs) provided efficient delivery into cells escaping from endosomes.[17, 18] But the endosomal escape of these TFPs was significantly impaired because of the monomeric nature of the TAT peptide fusion.[19-22] Hence, improved techniques are needed to deliver proteins that can efficiently escape from the endosomes.[23] It has been previously shown that attaching a monomeric TAT at the N-terminus of Ub resulted in endosomal entrapment of the TAT-Ub fusion protein.[24] To overcome this, Inomata *et al* has used a chemical-mediated direct translocation of a C-terminally fused Ub-TAT to deliver labelled-Ub into live cells.[25] The Ub-TAT fusion was recombinantly expressed and labelled with a dye. In order to achieve efficient delivery, a chemical mediator called 1-pyrene butyrate, along with a very high concentration of Ub-TAT fusion, was needed for direct translocation into the cytoplasm. This technique clearly indicates the potential of intracellular Ub

delivery. Recently, a disulfide-modified TAT dimer was reported to promote enhanced endosomal escape into the cytosol with no noticeable toxicity. [26, 27] Hence, we hypothesized that a Ub-TAT fusion with a dimeric disulfide-linked TAT at the C-terminus could have an enhanced endosomal escaping property to facilitate a spontaneous and efficient Ub delivery into the cytoplasm of live cells.

Our design takes advantage of Solid Phase Peptide Synthesis (SPPS) and the use of a disulfide-modified dimeric C-TAT peptide conjugated to the C-terminus of a synthetic Ub molecule. [26] We synthesized Ub with a rhodamine (Rho) tag on the N-terminus to follow the distribution using the fluorescent signal in cells. After being delivered inside the cell and escaping from the endosome, the C-TAT peptide was cleaved from RhoUb by endogenous DUBs, which allowed RhoUb to be incorporated into the ubiquitin chains by the Ub system.

Results and discussion

RhoUb and C-TAT peptide (CKRKKRRQRRRG) precursors were synthesized by Fmoc-based solid phase peptide synthesis (Fmoc-SPPS).[28] The RhoUb-C-TAT (**1**) reagent and the C-TAT peptide were generated on a Rink amide resin in a linear fashion resulting in the amidation of the C-terminus that renders the peptides resistance to exopeptidase-degradation. We then synthesized a dimeric disulfide-linked C-TAT reagent, RhoUb-di-C-TAT (**2**) using **1** and the C-TAT peptide (Figure 1, S1). The cleavage site for DUBs is located between the Gly-Gly motif at the C-terminal end of RhoUb and the N-terminal end of the (di)-C-TAT peptide sequence (Figure 2A). The reagents **1** and **2** were refolded under non-reducing conditions before addition to cells.

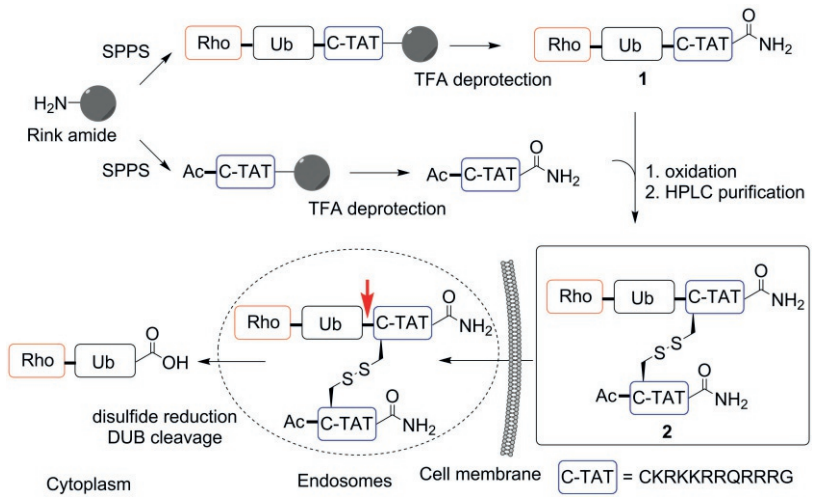


Figure 1: *Synthesis of penetrating Rhodamine-Ub conjugates. Using Fmoc-SPPS, both the Rho-Ub-C-TAT (**1**) and C-TAT peptides were synthesized. Under oxidative conditions in PBS buffer containing 5 % DMSO, RhoUb-di-C-TAT (**2**) was generated and purified by HPLC. After **2** enters the cell by endocytosis and escapes from endosomes, DUBs cleave di-C-TAT from **2** (cleavage site is denoted by the red arrowhead) yielding RhoUb which can form Ub conjugates.*

To investigate the cleavage of C-TAT fusions from RhoUb by endogenous DUBs, we performed an *in-vitro* DUB assay using cell lysate. It is known that lysate from HeLa cells contains active DUBs which were profiled using various Ub-based probes. [29] Therefore we incubated **1** and **2** with fresh HeLa cell lysate for 30 minutes at 37 °C and analysed the reaction using non-reducing SDS-PAGE (Figure 2B). We observed that the C-TAT peptide at the C-terminal end of RhoUb was cleaved from both **1** and **2** very efficiently, suggesting that free RhoUb can be released after endosomal escape into the cytoplasm to become accessible to the endogenous ubiquitin machinery.

To test the delivery of **1** and **2** into human HeLa cells, we used confocal microscopy and monitored the cellular distribution of these compounds along with the processed RhoUb derivatives. Compounds **1** and **2** were dissolved in DMSO and then refolded in PBS. HeLa cells were then incubated with compounds **1** and **2** in PBS for 5 minutes at room temperature. We avoided the use of DMEM (Dulbecco's Modified Eagle's Medium) since this medium caused disulfide reduction due to the presence of cysteine (Figure S2). The cells were then thoroughly washed with DMEM in order to reduce and remove excess of reagents from extracellular space, after which cells were fixed at different time points and studied by confocal microscopy. We showed that both **1** and **2**, but not RhoUb, were delivered inside cells after 5 minutes of incubation, implying that the reagents were cell penetrating and actively taken up by the cells due to the presence of the C-TAT fusion (Figure S3).

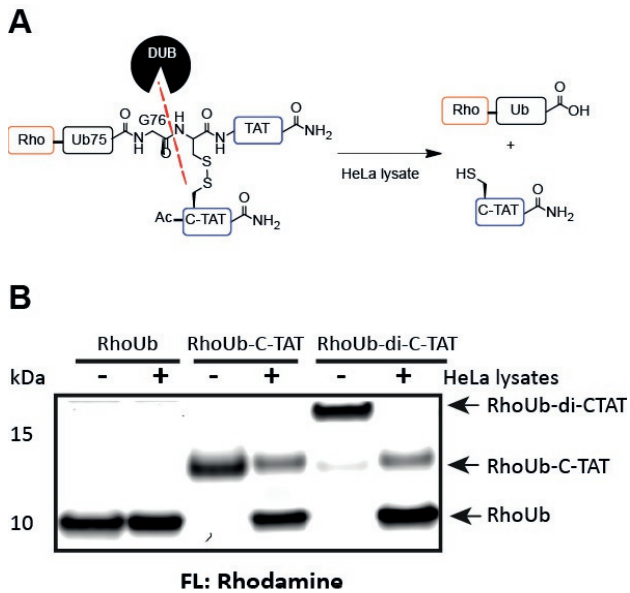


Figure 2: ***A:*** *Schematic representation of DUB cleavage of RhoUb-di-C-TAT. DUBs from HeLa cell lysate cleave the peptide bond between Gly76 of RhoUb and the cysteine residue of the di-C-TAT sequence.* ***B:*** *Fluorescence scan of SDS-PAGE showing hydrolysis of C-TAT peptides from RhoUb-C-TAT conjugates before (-) and after (+) the addition of HeLa cell lysates.*

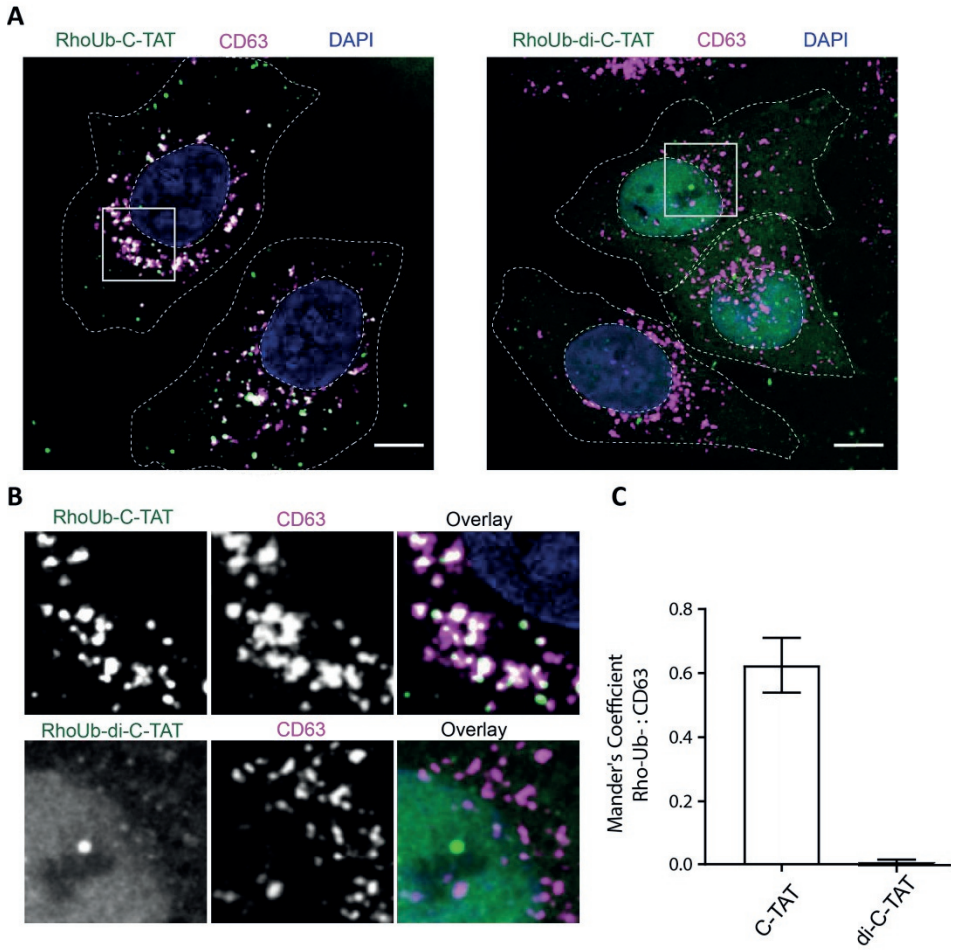


Figure 3: A: *Fluorescence micrographs of HeLa cells after addition of RhoUb-cell penetrating reagents (green). Cells were incubated for 5 minutes in PBS containing different penetrating reagents and then fixed after 8 hours, stained with the anti-CD63 antibody (magenta), and DAPI (blue), and imaged by confocal microscopy. Cell boundaries and nuclei are demarcated with dashed lines. Scale bars: 10 um.* ***B:*** *Zoom-ins of boxed regions in (A) are shown as an overlay of RhoUb-CPP with late endosomal marker CD63.* ***C:*** *Quantification of colocalization of the different RhoUb-penetrating reagents with the late endosomal marker CD63 is shown in the graph. See also Supplementary Figure 3.*

Having established that C-TAT-conjugated RhoUb reagents can be effectively taken up by the cells, we then determined whether these reagents can escape from endosomes. We introduced **1** and **2** to cells and cultured them for another 8 hours. After fixation, the cells were analyzed by confocal microscopy.

RhoUb-di-C-TAT (**2**) escaped efficiently from endosomes while RhoUb-C-TAT (**1**) almost exclusively remained in the endosomes. The RhoUb processed from **2** was predominantly localized in the nucleus as expected where it is conjugated onto histones.

[30] Thus the RhoUb derived from **2** behaved similarly to endogenous Ub. On the other hand, a majority of compound **1** was found only in vesicles that are positive for the late endosomal marker CD63. This implies that RhoUb-C-TAT was trapped in endosomes with no endosomal escape. (Figure 3A and B, Figure S4).

To know whether the RhoUb derived from **2** was recognized by the intrinsic Ub machinery, HeLa cells were first incubated with **1** or **2** and left for 4 hours. The cells were then exposed to MG132 which blocks proteasomal degradation of polyUb substrates resulting in the accumulation of higher order polyUb conjugates. [31] Cell lysate was prepared, and proteins were separated using SDS-PAGE followed by fluorescence scanning and blotting for the β-actin loading control.[32] We observed signals for higher molecular weight proteins only in cells incubated with compound **2**. We also observed an

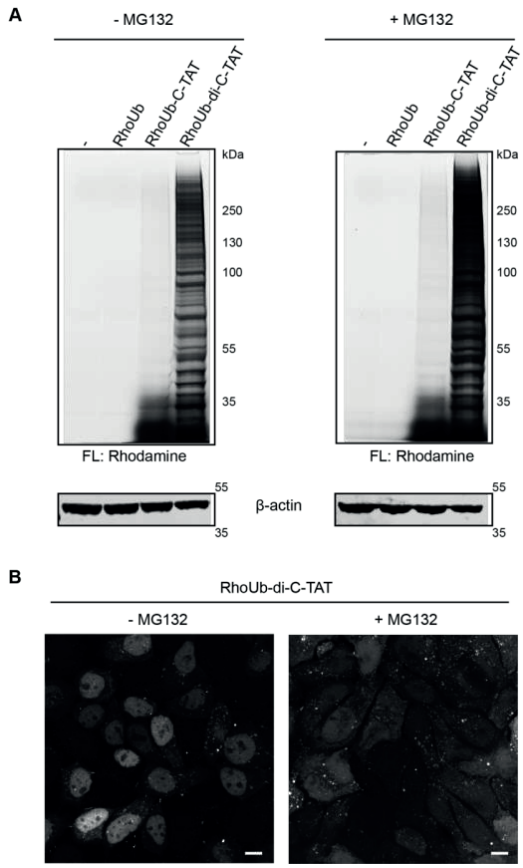


Figure 4: A: *Incorporation of RhoUb in polyUb chains and higher order Ub conjugates in HeLa cells incubated with different RhoUb-penetrating reagents in the absence or presence of MG132 proteasome inhibitor. The rhodamine signal was measured using a fluorescence scanner. β-actin was used as a loading control.* ***B:*** *Representative fluorescence images of HeLa cells showing relocalization of RhoUb from nucleus into the cytoplasm upon treatment with 25 μM of MG132 proteosome inhibitor. Scale bars: 10 um*

increase in RhoUb signal for MG132 treated cells compared to non-treated cells (Figure 4A). This shows that the RhoUb processed from RhoUb-di-C-TAT reagent was dynamically re-conjugated by the ubiquitin pathway in response to MG132. Taken together, these results showed that di-C-TAT fusion compound **2** was delivered to the cytoplasm via endosomal escape and efficiently incorporated by the endogenous ubiquitin machinery.

To show the dynamics of RhoUb with respect to its nuclear and cytosolic distribution, we studied the influence of MG132 on HeLa cells treated with RhoUb-di-C-TAT. Under normal conditions, the nuclear localization is evident after the delivery of RhoUb-di-C-TAT into cells (Figure 4B, left). However, subjecting the cells to the proteasome inhibitor MG132 perturbs this pattern causing re-localization of RhoUb from nucleus to the cytoplasm (Figure 4B, right), in accordance with previous report. [30]

Conclusions

In summary, we show that the RhoUb-di-C-TAT fusion was able to efficiently enter cells by endocytosis, escape from the endosomes into the cytoplasm and processed by endogenous DUBs to generate conjugatable RhoUb which was utilized by the intrinsic ubiquitination machinery. Thus, the presence of the C-TAT disulfide fusion proved essential for its endosomal escape.

Delivery of synthetic Ub in live cells enables studies of the ubiquitination pathway in real time. [33, 34] Here we report the design and synthesis of a simple and efficient cell penetrating Ub reagent that was spontaneously delivered inside live cells. Recently, Gui *et al* reported the use of a cell-permeable cyclic poly-Arginine-based peptide conjugated to Ub-based probes that allow DUB profiling in live cells.[35] The technique that we presented here was used in incorporating RhoUb into the intrinsic Ub machinery and may be further extended towards the delivery of Ub mutants, hydrolytically stable Ub conjugates and probes or other ubiquitin-like derivatives allowing studies of the ubiquitin system in cells in real time. [36, 37]

Acknowledgements

We would like to thank Dris el Atmioui and Cami Talavera Ormeno for peptide synthesis; We also thank A.M.A van der Laan and L. Voortman of LUMC for microscopy facility support microscopy facility support. We would like to thank Dr. Gerbrand J. van der Heden van Noort and Dr. Koraljka Husnjak for critical reading. Work in the Ovaa lab was supported by NWO (VICI grant 724.013.002)

References

1. Komander, D., M.J. Clague, and S. Urbe, *Breaking the chains: structure and function of the deubiquitinases.* Nat Rev Mol Cell Biol, 2009. **10**(8): p. 550-63.
2. Ciechanover, A., *The unravelling of the ubiquitin system.* Nat Rev Mol Cell Biol, 2015. **16**(5): p. 322-4.
3. Hameed, D.S., A. Sapmaz, and H. Ovaa, *How Chemical Synthesis of Ubiquitin Conjugates Helps To Understand Ubiquitin Signal Transduction.* Bioconjug Chem, 2017. **28**(3): p. 805-815.
4. Kessler, B.M., *Putting proteomics on target: activity-based profiling of ubiquitin and ubiquitin-like processing enzymes.* Expert Rev Proteomics, 2006. **3**(2): p. 213-21.
5. Akutsu, M., I. Dikic, and A. Bremm, *Ubiquitin chain diversity at a glance.* J Cell Sci, 2016. **129**(5): p. 875-80.
6. van Tilburg, G.B., A.F. Elhebieshy, and H. Ovaa, *Synthetic and semi-synthetic strategies to study ubiquitin signaling.* Curr Opin Struct Biol, 2016. **38**: p. 92-101.
7. Matilainen, O., S. Jha, and C.I. Holmberg, *Fluorescent Tools for In Vivo Studies on the Ubiquitin-Proteasome System.* Methods Mol Biol, 2016. **1449**: p. 215-22.
8. Wagner, S.A., et al., *A proteome-wide, quantitative survey of in vivo ubiquitylation sites reveals widespread regulatory roles.* Mol Cell Proteomics, 2011. **10**(10): p. M111 013284.
9. Farkhani, S.M., et al., *Cell penetrating peptides: efficient vectors for delivery of nanoparticles, nanocarriers, therapeutic and diagnostic molecules.* Peptides, 2014. **57**: p. 78-94.
10. Bechara, C. and S. Sagan, *Cell-penetrating peptides: 20 years later, where do we stand?* FEBS Lett, 2013. **587**(12): p. 1693-702.
11. Copolovici, D.M., et al., *Cell-penetrating peptides: design, synthesis, and applications.* ACS Nano, 2014. **8**(3): p. 1972-94.
12. Di Pisa, M., G. Chassaing, and J.M. Swiecicki, *When cationic cell-penetrating peptides meet hydrocarbons to enhance in-cell cargo delivery.* J Pept Sci, 2015. **21**(5): p. 356-69.
13. Schwartz, J.J. and S. Zhang, *Peptide-mediated cellular delivery.* Curr Opin Mol Ther, 2000. **2**(2): p. 162-7.
14. Torchilin, V.P., *Tat peptide-mediated intracellular delivery of pharmaceutical nanocarriers.* Adv Drug Deliv Rev, 2008. **60**(4-5): p. 548-58.
15. Rudolph, C., et al., *Oligomers of the arginine-rich motif of the HIV-1 TAT protein are capable of transferring plasmid DNA into cells.* J Biol Chem, 2003. **278**(13): p. 11411-8.
16. Varkouhi, A.K., et al., *Endosomal escape pathways for delivery of biologicals.* J Control Release, 2011. **151**(3): p. 220-8.
17. Burns, K.E. and J.B. Delehanty, *Cellular delivery of doxorubicin mediated by disulfide reduction of a peptide-dendrimer bioconjugate.* Int J Pharm, 2018. **545**(1-2): p. 64-73.
18. Nischan, N., et al., *Covalent attachment of cyclic TAT peptides to GFP results in protein delivery into live cells with immediate bioavailability.* Angew Chem Int Ed Engl, 2015. **54**(6): p. 1950-3.
19. Richard, J.P., et al., *Cell-penetrating peptides. A reevaluation of the mechanism of cellular uptake.* J Biol Chem, 2003. **278**(1): p. 585-90.

20. LeCher, J.C., S.J. Nowak, and J.L. McMurry, *Breaking in and busting out: cell-penetrating peptides and the endosomal escape problem.* Biomol Concepts, 2017. **8**(3-4): p. 131-141.
21. Caron, N.J., S.P. Quenneville, and J.P. Tremblay, *Endosome disruption enhances the functional nuclear delivery of Tat-fusion proteins.* Biochem Biophys Res Commun, 2004. **319**(1): p. 12-20.
22. Gump, J.M. and S.F. Dowdy, *TAT transduction: the molecular mechanism and therapeutic prospects.* Trends Mol Med, 2007. **13**(10): p. 443-8.
23. Lonn, P., et al., *Enhancing Endosomal Escape for Intracellular Delivery of Macromolecular Biologic Therapeutics.* Sci Rep, 2016. **6**: p. 32301.
24. Loison, F., et al., *A ubiquitin-based assay for the cytosolic uptake of protein transduction domains.* Mol Ther, 2005. **11**(2): p. 205-14.
25. Inomata, K., et al., *High-resolution multi-dimensional NMR spectroscopy of proteins in human cells.* Nature, 2009. **458**(7234): p. 106-9.
26. Erazo-Oliveras, A., et al., *Protein delivery into live cells by incubation with an endosomolytic agent.* Nat Methods, 2014. **11**(8): p. 861-7.
27. Pescina, S., et al., *Cell penetrating peptides in ocular drug delivery: State of the art.* J Control Release, 2018. **284**: p. 84-102.
28. El Oualid, F., et al., *Chemical synthesis of ubiquitin, ubiquitin-based probes, and diubiquitin.* Angew Chem Int Ed Engl, 2010. **49**(52): p. 10149-53.
29. Leestemaker, Y., A. de Jong, and H. Ovaa, *Profiling the Activity of Deubiquitinating Enzymes Using Chemically Synthesized Ubiquitin-Based Probes.* Methods Mol Biol, 2017. **1491**: p. 113-130.
30. Dantuma, N.P., et al., *A dynamic ubiquitin equilibrium couples proteasomal activity to chromatin remodeling.* J Cell Biol, 2006. **173**(1): p. 19-26.
31. Mimnaugh, E.G., et al., *Rapid deubiquitination of nucleosomal histones in human tumor cells caused by proteasome inhibitors and stress response inducers: effects on replication, transcription, translation, and the cellular stress response.* Biochemistry, 1997. **36**(47): p. 14418-29.
32. Meierhofer, D., et al., *Quantitative analysis of global ubiquitination in HeLa cells by mass spectrometry.* J Proteome Res, 2008. **7**(10): p. 4566-76.
33. Husnjak, K. and I. Dikic, *Ubiquitin-binding proteins: decoders of ubiquitin-mediated cellular functions.* Annu Rev Biochem, 2012. **81**: p. 291-322.
34. Peng, J., et al., *A proteomics approach to understanding protein ubiquitination.* Nat Biotechnol, 2003. **21**(8): p. 921-6.
35. Gui, W., et al., *Cell-Permeable Activity-Based Ubiquitin Probes Enable Intracellular Profiling of Human Deubiquitinases.* J Am Chem Soc, 2018. **140**(39): p. 12424-12433.
36. Bondalapati, S., et al., *Chemical synthesis of phosphorylated ubiquitin and diubiquitin exposes positional sensitivities of e1-e2 enzymes and deubiquitinases.* Chemistry, 2015. **21**(20): p. 7360-4.
37. Liu, Q., et al., *A General Approach Towards Triazole-Linked Adenosine Diphosphate Ribosylated Peptides and Proteins.* Angew Chem Int Ed Engl, 2018. **57**(6): p. 1659-1662.

Supplementary figures

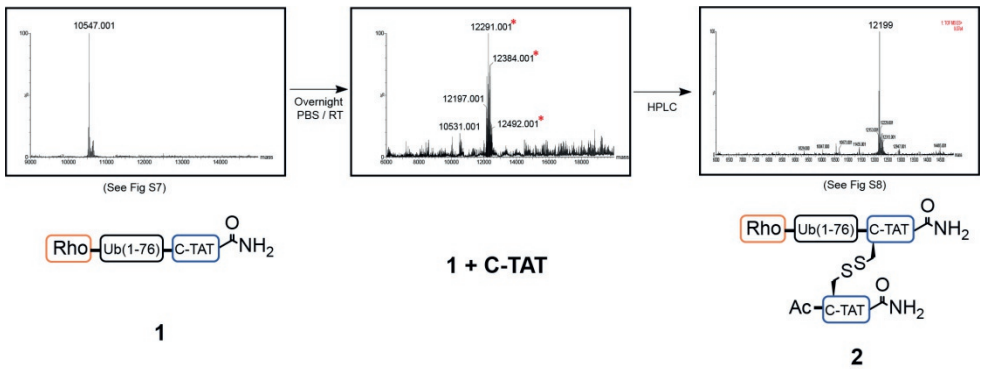


Figure S1: Oxidation of 1 and C-TAT peptide to form 2. *RhoUb-C-TAT (**1**, MW: 10,547 Da), dissolved in DMSO, was added to C-TAT peptide dissolved in aerated PBS and left overnight at RT. The reaction was followed by LC/MS with measurements taken after overnight incubation showing the formation of RhoUb-di-C-TAT (**2**, MW: 12,199 Da). LC/MS of purified **2** is shown in figure S8. Star (*) indicates TFA salt adducts of **2**, which can be a consequence of TFA deprotection of the C-TAT peptide, commonly observed for synthetic peptides containing a high number of cationic residues in their sequence.*

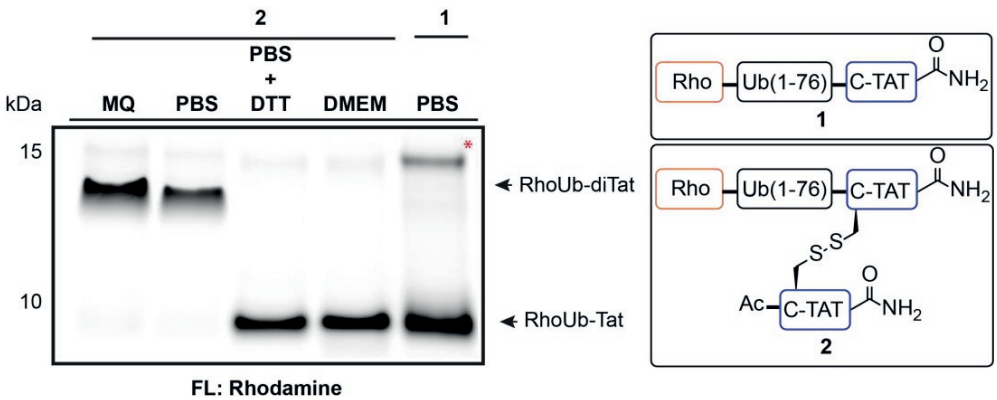


Figure S2: Effect of DMEM in the stability of RhoUb-di-C-TAT. *RhoUb-di-C-TAT (2) was incubated in DMEM medium and in PBS containing 5 mM DTT for 30 minutes at RT and then analyzed by non-reducing SDS-PAGE. RhoUb-C-TAT (1) in PBS and 2 in MQ water were taken as controls. Star (*) indicates an SDS-PAGE gel artefact band. Samples were resolved in a 12 % SDS-PAGE gel. The Rho signal from the gel was analyzed with a Typhoon FLA 9500.*

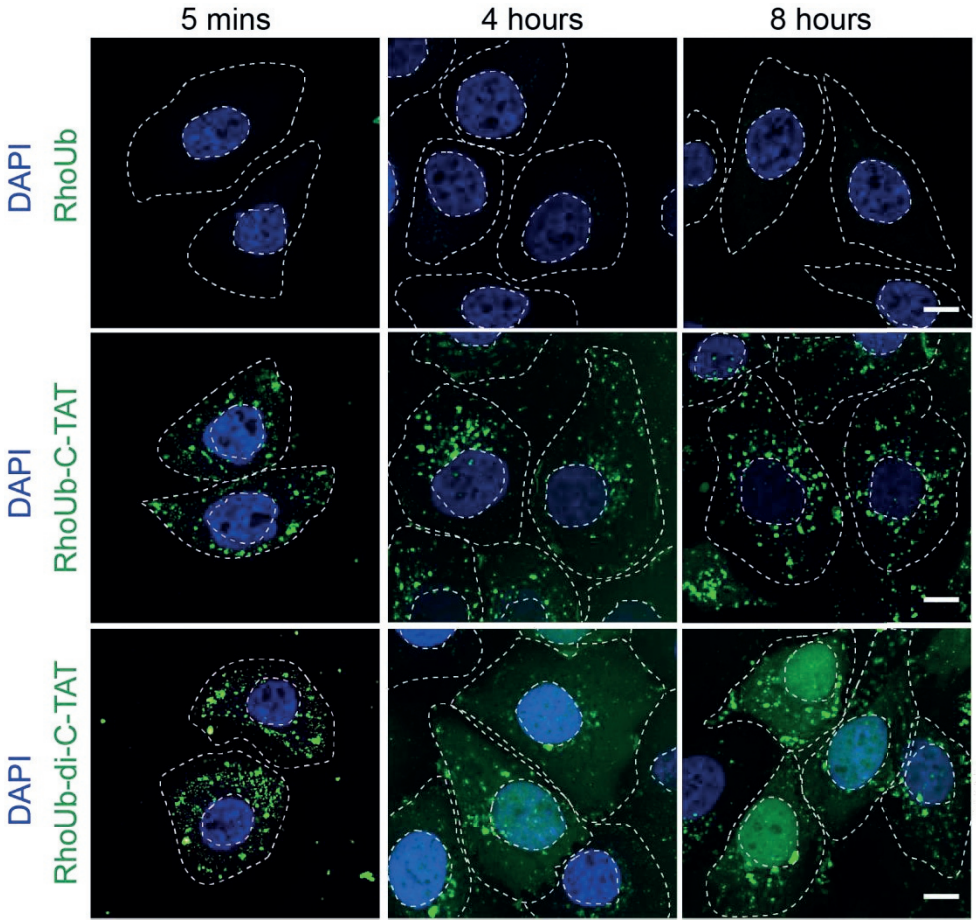


Figure S3: Delivery of RhoUb-CPP over time.
Confocal images of different RhoUb-CPP (green) treated HeLa cells. HeLa cells were incubated with RhoUb, RhoUb-C-TAT or RhoUb-di-C-TAT for various time intervals. Nuclear and cell boundaries are depicted in dashed lines. DAPI (blue) is a nuclear counterstain. Scale Bars: 10 μm.

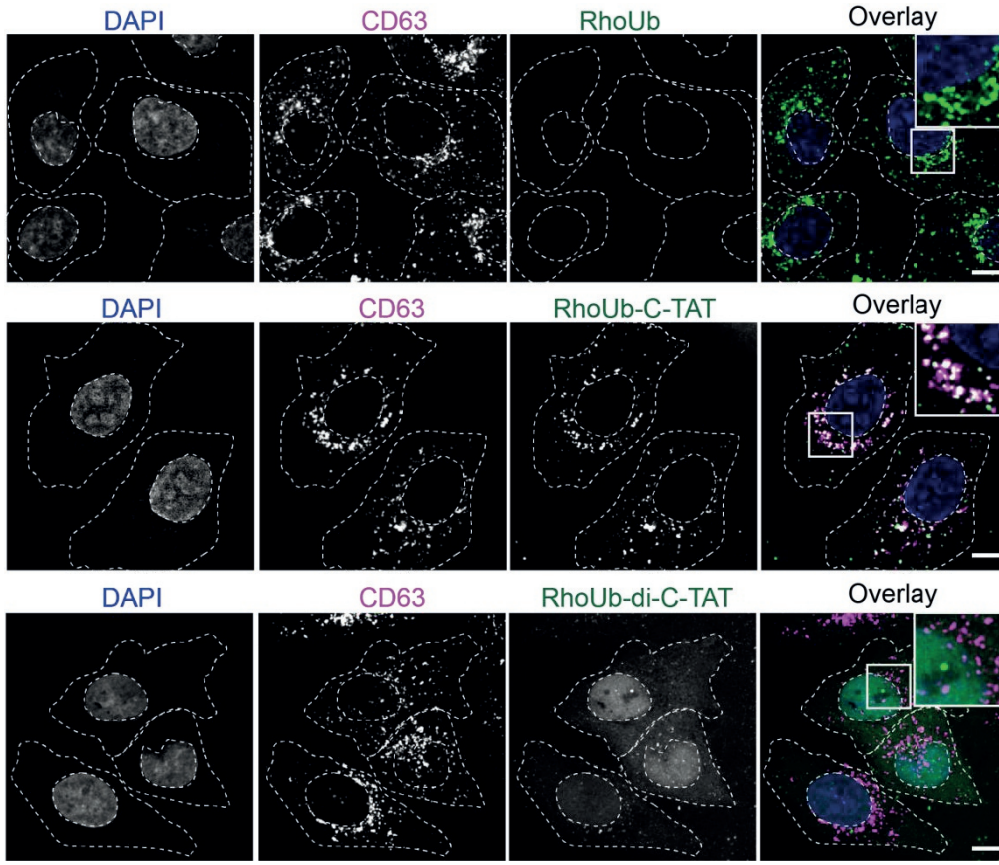


Figure S4: Cellular localization of different RhoUb-CPP reagents.
Confocal images of RhoUb-CPPs treated HeLa cells. Cells were incubated for 8 hours. Fixed cells were stained with a late endosomal marker, CD63, and nuclear stain, DAPI. Nuclear and cell boundaries are depicted in dashed lines. Scale bars: 10 μm. See also Figure 3 for zoom-ins and quantification.

Experimental section

Synthesis of C-TAT, RhoUb, Compounds 1 and 2

General: All commercial materials (Aldrich, Fluka, Novabiochem) were used without further purification. All solvents were reagent grade or HPLC grade. LC/MS analysis was performed with a system containing a Waters 2795 separation module (Alliance HT), Waters 2996 Photodiode Array Detector (190–750 nm), Phenomenex Kinetex XB-C18 (2.1 x 50 mm) reversed phase column and a MicromassLCT-TOF mass spectrometer. Samples were run at 0.80 mL min x 1 (Kinetex C18) with the use of a gradient of two mobile phases: A) aq. formic acid (0.1 %), and B) formic acid in CH_3CN (0.1 %). Data processing was performed with the aid of Waters MassLynx 4.1 software (deconvolution with Maxent1 function). Preparative HPLC was performed with a Shimadzu LC-20AD/T instrument fitted

with a Waters XBridge™ Prep C18 Column (10 x 150 mm, 5µm OBD™) with the use of gradient elution [mobile phases: A) aq. FA (0.1 %) and B) FA in CH_3CN(0.1 %)].

Fmoc SPPS strategy:
SPPS was performed on a Syro II MultiSyntech Automated Peptide synthesizer using standard 9-fluorenylmethoxycarbonyl (Fmoc) based solid phase peptide chemistry at 25 µmol scales.[1] All amino acids were used in excess and dipeptides were used in positions that were determined earlier.[1] The TAT peptide containing Cysteine residue (referred as C-TAT) and Ub(1-76)-Cys-TAT (RhoUb-C-TAT) were synthesized by SPPS on H-Rink amide Chemmatrix® resin (Sigma-Aldrich) so that the C-terminal end was protected as amide. DiBoc-Rhodamine was coupled on-resin to the N-terminal end of Ub or Ub (1-76)-C-TAT compound by standard chemical coupling conditions. [2]

Work-up
The resin was dried after washing with diethyl ether under high vacuum conditions overnight. Due to the presence of Cys-tBu in the peptide sequence, we used a deprotection mix consisting of TFA/H_2O/dioxa-1, 8-octane-dithiol/iPr_3SiH 92.5/2.5/2.5/2.5 v/v/v/v and treated the resin with this mix for 3 hours at RT. The deprotected peptides were filtered and collected in ice-cold diethyl-ether/n-pentane 3:1 v/v mix. The resulting precipitate was then washed 3x with diethyl-ether and dried completely in air. The pellet was then dissolved in a mixture of H_2O/CH_3CN/HOAc (65/25/10 v/v/v) and lyophilized.

Purification of the C-TAT peptide

Due to the presence of a series of lysine and arginine residues in the TAT sequence, the synthesized C-TAT peptide was highly hydrophilic. This made purification by reversed phase HPLC more difficult as the peptide was not retained by the column. In addition, we observed at least four species of TFA-salt adducts of our C-TAT peptide (Figure S6) due to the use of TFA-mix to deprotect the peptide from SPPS. However, the purity of the synthesized C-TAT peptide was good enough to be used in the formation of compound **2** (Figure S6). Hence the C-TAT peptide was used directly after being obtained from SPPS. The C-TAT peptide was stored under an inert atmosphere as a lyophilized powder at -20 ºC for future use.

Synthesis of compound 2

PBS was aerated in air for 15 minutes before being used for inter-molecular disulfide formations of the TAT peptides. Compound **1** (MW: 10,547 Da) was dissolved in DMSO at a concentration of 10 mg/mL. TAT peptide (MW: 1,625 Da) was dissolved in aerated PBS at a concentration of 4 mM. Compound **1** was added to this mix and left overnight at RT. The reaction was followed by LC/MS and the reaction was stopped after more than 90% of the desired product **2** (MW: 12,199 Da) was formed (Figure S1). The reaction was stopped by acidifying the reaction mix by adding a few drops of 10 % Formic acid.

Purification of RhoUb-C-TAT and RhoUb-di-C-TAT by reverse phase HPLC

RhoUb-C-TAT was first dissolved in DMSO. This solution was slowly added to MQ water containing 1% Formic acid and filtered through a GfxO/0.45 µm GHP membrane Acrodisc® Premium 25mm syringe filter. In the case of RhoUb-di-C-TAT, the reaction mix was first acidified adding a few drops of 10% formic acid. Later on, the reaction mix was diluted 10 times in MQ water. In both the cases, the sample was then injected onto a Waters XBridge™

Prep C18 Column (10 x 150 mm, 5µm OBD™) at a flow rate of 10 ml/min using a preparative HPLC system mentioned in the general experimental section. The protein was purified with the gradient outlined in the following table using aq. 0.1% FA (Solvent A) and acetonitrile containing 0.1% FA (Solvent B) as eluents.

Time (in mins)	Solvent B (%)
0 ⇨ 5	5
5 ⇨ 7	5 ⇨ 25
7 ⇨ 22	25 ⇨ 55
22 ⇨ 24	55 ⇨ 95
24 ⇨ 27	95
27 ⇨ 27.5	95 ⇨ 5
27.5 ⇨ 30	5

The retention time for the RhoUb-C-TAT was 10 minutes in the preparative HPLC. In the case of RhoUb-di-C-TAT, the C-TAT peptide first eluted along with the injection peak, followed by RhoUb-di-C-TAT that eluted at 12 minutes. All fractions containing the protein were confirmed by checking the mass using a LC/MS R_t 3 min; Phenomenex Kinetex™ XB-C18 100A (50 x 2 x 10 mm, 2.6 µm); solvents - MQ water with 0.1% formic acid (Solvent A) and acetonitrile containing 0.1% formic acid (Solvent B), flow rate = 0.5 mL/min, run time = 6 min, column T = 45°C. Gradient: 5% ⇨ 95% B over 3.5 min. All samples containing pure protein were pooled together and lyophilized.

LC/MS analysis of the purified reagents

All purified proteins were confirmed by checking the mass using LC/MS. Phenomenex Kinetex™ C18 (100A, 100 x 21 mm, 2.6 µm); solvents – aq. 0.1% formic acid (Solvent A) and acetonitrile containing 0.1% formic acid (Solvent B), flow rate = 0.4 mL/min, runtime = 13 min, column T = 45°C. Gradient: 5% ⇨ 95% B over 7.6 min. For C-TAT peptide analysis, the program used has the following parameters: flow rate = 0.5 mL/min, run time = 6 min, column T = 45°C. Gradient: 5% ⇨ 95% B over 3.5 min.

Cell culture

Human HeLa cells were cultured in DMEM (Gibco) supplemented with 7.5 % fetal calf serum (FCS, Greiner). Cells were cultured at 37°C and 5 % CO_2.

Delivery of Ubiquitin-cell penetrating conjugates in cells

40 x 10^5 Human HeLa cells were seeded into 24 well plates and grown at 37 °C and 5% CO_2 overnight. Compounds **1** and **2** were first dissolved in DMSO at a concentration of 1 mM. This DMSO stock was diluted into sterile PBS solution at a final concentration of 5 µM. Different RhoUb-CPP in PBS were added to cells prepared one day before. Cells were incubated with RhoUb-CPP reagents for 5 minutes before being washed 2 times with DMEM. After this, cells were left to recover over the duration of the experiment. Cells were prepared for confocal microscopy analysis as indicated below.

Confocal microscopy

For fluorescence confocal microscopy of fixed samples, cells were seeded into 24 well plates containing 13 mm slide, fixed with 3.7 % formaldehyde (acid-free, Merck Millipore) in PBS for 20 min and washed three times with PBS. Fixed cells were permeabilized with 0.1% TritonX-100 (T8787, Sigma-Aldrich) in PBS for 10 min and washed quickly twice with PBS.

After permeabilization, cells were blocked with 5% (w/v) milk powder (skim milk powder, LP0031, Oxiod) in PBS for 30 min and stained using mouse anti-CD63 antibody (NKI-C3) [3] diluted (1:100) in blocking buffer for 1 hr at room temperature. Following washes in PBS (3 x 5 min), cells were incubated in appropriate secondary anti-rabbit/mouse/rat Alexa-dye coupled antibodies (Invitrogen) diluted (1:300) in blocking buffer for 30 min. After washing (3 times 5 min), cells were mounted using ProLong Gold antifade Mounting medium with DAPI (Life Technologies, Cat# P36941). Samples were imaged using Leica SP8 microscopes equipped with appropriate solid-state lasers.
For all confocal imaging, HCX PL 63x 1.32 oil objectives and HyD detectors were used. Digital zoom ranging from 1.5x-3x was employed as applicable. Z-stacks were imaged with a z-step size of 0.5 μm and visualized as max z-projections.

Ubiquitination assay

Human HeLa cells were grown up to 70-80% confluency. The DMEM medium was removed and cells were washed with PBS. RhoUb-C-TAT and RhoUb-di-C-TAT were dissolved in PBS and added to the cells and left incubating at RT for 5 minutes. After this, the excess of RhoUb-CPPs was removed and the cells were washed twice with DMEM medium before left to incubate in DMEM for the duration of the experiment. MG132 was added to cells after 4 hours. Cells were collected after 6 hours or 8 hours in total and then lysed with lysis buffer. The samples were run by SDS-PAGE and the fluorescence signal was analyzed by Typhoon FLA 9500.

SDS-PAGE and western blotting

Samples were separated by 4 – 12 % SDS-PAGE (NuPAGE Bis-Tris gel, ThermoFisher Scientific). Fluorescence scan was made in a Typhoon FLA 9500 (GE Healthcare LifeSciences) using filters set at 473 nm (excitation wavelength) and 532 nm (emission wavelength). Proteins were transferred to a nitrocellulose membrane (Protan BA85, 0.45 μm, GE Healthcare) at 300 mA for 2.5 h. The membranes were blocked in 5 % milk (skim milk powder, LP0031, Oxiod) in 1x PBS (P1379, Sigma-Aldrich), incubated with a primary antibody diluted in 5 % milk in 0.1 % PBS-Tween 20 (PBST) for 1 h, washed three times for 10 min in 0.1 % PBST, incubated with the secondary antibody diluted in 5 % milk in 0.1 % PBST for 30 min and washed three times again in 0.1 % PBST. β-actin antibody (Sigma-Aldrich, Cat# A5441) was used as a loading control in a 1:10000 dilution for Western blot. IRDye 680LT goat anti-mouse IgG (H+L) (926-68020, Li-COR) were used as a secondary antibody. The signal was detected using direct imaging by the Odyssey Classic imager (Li-Cor).

Quality analysis of purified reagents

1. RhoUb

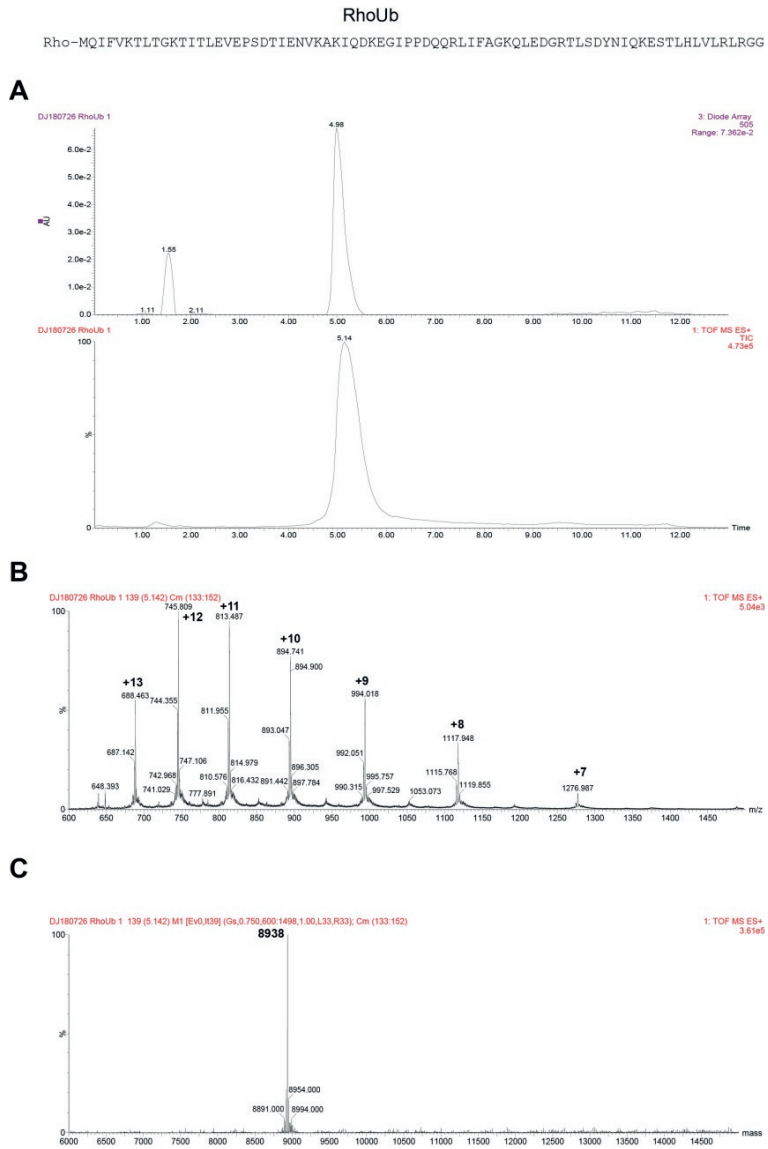


Figure S5: *RhoUb.* ***A:*** *Top: UV chromatogram (λ - 505 nm); Bottom: combined mass spectrum using LC/MS;* ***B:*** *Spectrum of the peak at 4.98 min;* ***C:*** *Deconvoluted mass of peak spectra. ESI-Mass [M+H] Calculated: 8940 / Found: 8938.*

2. C-TAT peptide

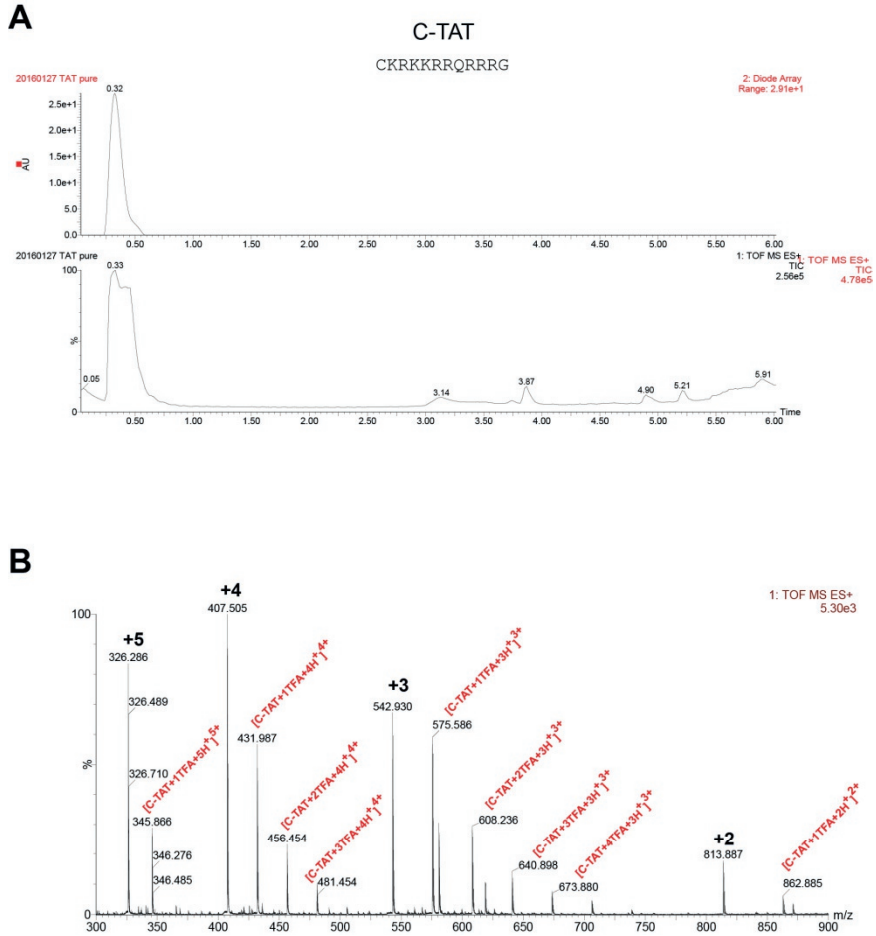


Figure S6: *C-TAT peptide.* ***A:*** *Top: UV chromatogram (λ - 280 nm); Bottom: combined mass spectrum using LC/MS;* ***B:*** *Spectrum of the peak at 1.78 min; ESI-Mass [M+H] Calculated: 1625 / Found:* $[\mathbf{M+4H}]^{4+}$ *= 407.33;* $[\mathbf{M+2H}]^{2+}$ *= 811.04. In addition, 1 to 4 TFA adducts of the C-TAT peptides were also observed as a consequence of using TFA in the peptide-deprotection mix.*

3. RhoUb-C-TAT

RhoUb-C-TAT

Rho-MQIFVKTLTGKTITLEVEPSDTIENVKAKIQDKEGIPPDQQRLIFAGKQLEDGRTLSDYNIQKESTLHLVLRLRGGCKRKKRRQRRRG

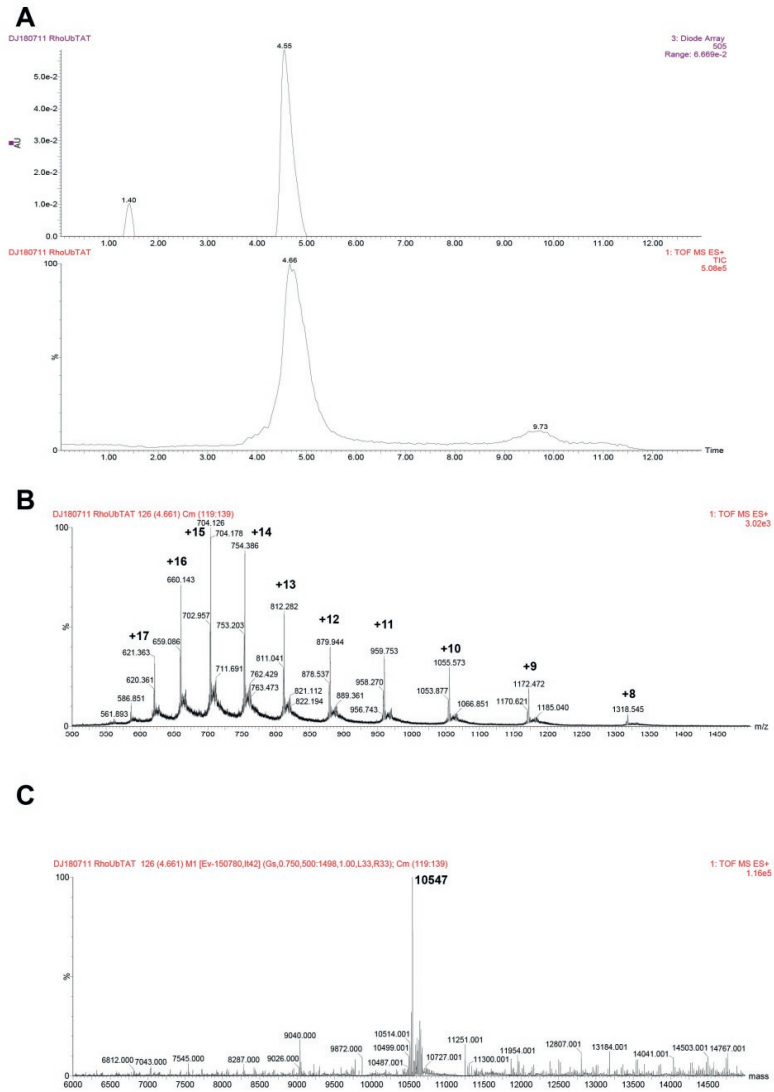


Figure S7: *RhoUb-C-TAT* ***A:*** *Top: UV chromatogram (λ – 505 nm); Bottom: combined mass spectrum using LC/MS;* ***B:*** *Spectrum of the peak at 4.55 min;* ***C:*** *Deconvoluted mass of peak spectra. ESI-Mass [M+H] Calculated: 10546 / Found: 10547.*

4. RhoUb-di-C-TAT

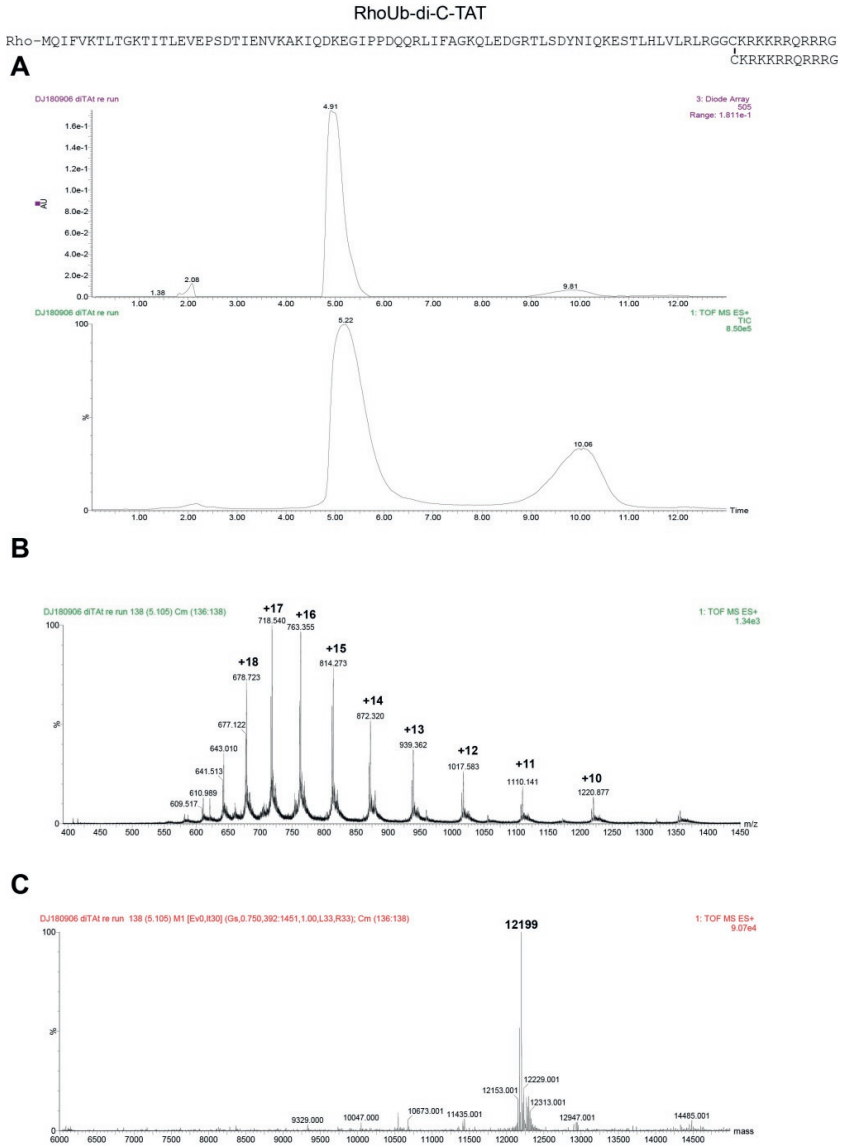


Figure S8: *RhoUb-di-C-TAT.* ***A:*** *Top: UV chromatogram (λ - 505 nm); Bottom: combined mass spectrum using LC/MS;* ***B:*** *Spectrum of the peak at 4.62 min;* ***C;*** *Deconvoluted mass of peak spectra. ESI-Mass [M+H] Calculated: 12204 / Found: 12199.*

Supplementary References

1. El Oualid, F., R. Merkx, R. Ekkebus, D.S. Hameed, J.J. Smit, A. de Jong, H. Hilkmann, T.K. Sixma, and H. Ovaa, *Chemical synthesis of ubiquitin, ubiquitin-based probes, and diubiquitin.* Angew Chem Int Ed Engl, 2010. **49**(52): p. 10149-53.
2. Geurink, P.P., B.D. van Tol, D. van Dalen, P.J. Brundel, T.E. Mevissen, J.N. Pruneda, P.R. Elliott, G.B. van Tilburg, D. Komander, and H. Ovaa, *Development of Diubiquitin-Based FRET Probes To Quantify Ubiquitin Linkage Specificity of Deubiquitinating Enzymes.* Chembiochem, 2016. **17**(9): p. 816-20.
3. Vennegoor, C. and P. Rumke, *Circulating melanoma-associated antigen detected by monoclonal antibody NKI/C-3.* Cancer Immunol Immunother, 1986. **23**(2): p. 93-100.

Chapter 6

A Ub-derived cyclic peptide inhibits UCHL5 associated with the 26S proteasome

Manuscript in preparation
D.S.Hameed, Leestemaker.Y., Sahtoe.D., Flierman.D., Sixma.T., Ovaa.H.

Summary

UCHL5 (UCH37 in humans) is one of the proteasome-associated deubiquitinase (DUB) enzymes that facilitate trimming of poly-ubiquitin (PolyUb) chains, an important regulatory mechanism in the proteasomal degradation pathway. Polyubiquitinated proteins that are deemed for degradation may escape from the proteasome when polyUb chains are cropped from the target protein before they are being translocated into the core particle of the 26S proteasome. Although UCHL5 is known to deubiquitinate substrates, its influence on 26S proteasome activity is poorly understood. Inhibition of UCHL5 is known to induce apoptosis in specific types of cancer. So far, there are no selective inhibitors identified for UCHL5. Here, we describe a peptide derived from Ub, that can bind and inhibit UCHL5. From the reported structure of UCHL5 bound to Ub-PRG probe, a β-sheet containing peptide derived from Ub was identified, synthesized, cyclized and validated against recombinant UCHL5. We report that this stable peptide derived from Ub can impart binding and inhibition of UCHL5 that is associated with the 26S proteasome.

Introduction

Ubiquitination is an important post-translational modification involved in various cellular metabolic processes. [1, 2] These processes are tightly regulated by a set of ubiquitinating enzymes involving the Ub-activating E1 enzymes, the E2 conjugating enzymes and an E3-ligases. [3] Substrates can be modified either with a single Ub or multiple Ub moieties or polyUb chains connected via different internal lysine residues or the N-terminal methionine residue of Ub. [4] The substrates can be deubiquitinated by enzymes called deubiquitinases (DUBs). [5]

One of the most important post-translational Ub modifications of substrates is the K48-linked polyubiquitin modification. [6] This is a key signal for protein degradation by the proteasome. [7] The 26S proteasomes in mammals contain many different subunits that work in conjunction with each other to facilitate effective protein degradation. [8] The degraded proteins are then converted to short peptides and amino acids that are recycled while a small portion of polypeptides is presented to the immune system by MHC Class I molecules. [9]

Proteasome activity is tightly regulated to prevent problems associated with unwarranted protein degradation. [10] Among the regulatory proteins associated with the proteasome are the deubiquitinases (DUBs). [11] So far, two DUBs have been identified that are tightly associated with the 26S proteasome complex: UCHL5 (UCH37 in humans) and USP14 (Ubp6 in humans), while Rpn11 (POH1 in humans) is an integral part of the 19S proteasome lid. [11, 12] UCHL5 and USP14 are cysteine-proteases, while Rpn11 is a JAMM/MPN+ metalloprotease. [13]

Although the structure of the 26S proteasome has been studied for years, the exact mechanism of action of the proteasomal DUBs is still under debate. [8] Evidence has pointed out that Rpn11, which is located at the base of the lid complex in close proximity to the 20S core complex, removes the polyUb chain *en-bloc* from substrate proteins while the substrate protein is concomitantly forced into the core complex for degradation. [14, 15] It has been proposed that USP14 functions as a chain-trimming DUB that removes Ub monomers from polyUb chains before the substrate is degraded by the proteasome. [16] However, much less is known about the mechanism of action of UCHL5 mainly due to the lack of good inhibitors.

Recently, the structure of UCHL5 in complex with the regulatory proteins Rpn13 and INO80G respectively has been reported. [17, 18] Based on the structural data, a model has been proposed that explains how the activity of UCHL5 is regulated by these two proteins.

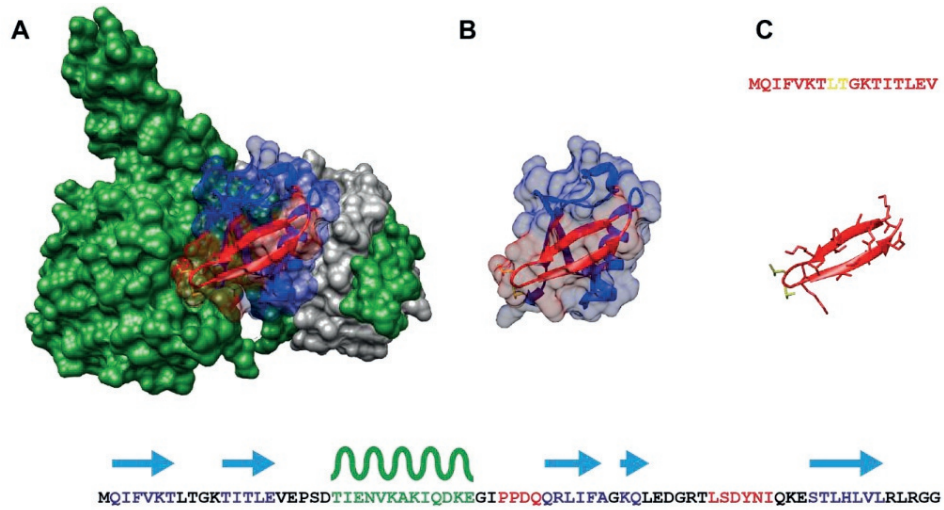


Figure 1*: Structure of Ub binding to UCHL5/Rpn13.* ***A:*** *X-ray structure of UCHL5 (in green) bound to Ub-PRG (in blue) and Rpn13 (grey) (PDB: 4UEL). Location of the binding pocket for Lue8 and Thr9 of Ub is represented in orange and the first* β*-sheet of Ub is shown in red.* ***B:*** *Isolated structure of Ub showing the orientation of the first β-sheet (in red). The sequence of Ub showing different secondary structures is shown below.* ***C:*** *Structure of the β-sheet peptide of Ub encompassing residues 1 to 17 in which the important residues, namely Leu8 and Thr9, are highlighted in yellow. D: Sequence of full-length Ub showing residues that comprises the β-sheet (blue arrows) and the α-helix (green curves). Residues that constitute the connecting loops are highlighted in red.*

The deubiquitination efficiency of UCHL5 increases when it is associated with the DEUBAD domain of Rpn13. It was shown that Rpn13 augments deubiquitination of UCHL5 by providing additional recognition of ubiquitin, thereby bringing the C-terminus of Ub close to the active site of UCHL5. On the other hand, in association with full-length INO80G located inside the nucleus, the deubiquitination activity of UCHL5 is completely abolished. This is caused by the binding of INO80G to UCHL5 which in turn interferes with the binding of Ub to UCHL5. [17, 18]

In the X-ray crystal structure of Ub-UCHL5/Rpn13 (PDB: 4UEL), it can be seen that the covalent Ub-based probe called Ub-PRG [19] binds to UCHL5 in complex with Rpn13 through a hydrophobic patch consisting of residues Leucine 8, Threonine 9, and Isoleucine 44 of Ub in addition to the C-terminal tail of Ub (Figure 1A). [17] Specific residues in the N-terminus of Ub are in direct contact to a hydrophobic pocket in UCHL5 consisting of residues Phe218 and Leu38. The residues of Ub involved in this interaction include Lue8 and Thr9, Phe5 and Ile13 that are present in the first β-sheet of Ub. Therefore, we postulated that this particular β-sheet of Ub comprising of residues 1 to 17, could be used as a discrete binding motif for UCHL5/Rpn13 thereby functioning as an inhibitor of UCHL5.

Chemical synthesis of Ub has been reported by us and others using different strategies yielding multi-milligram quantities of synthetic ubiquitin. [20] We used the same strategy to synthesize the Ub-peptide consisting of residues 1 to 17 and refolded them to form the β-sheet. To trap the peptide in a more stable β-sheet conformation, we also cyclized the peptide directly after synthesis by SPPS. Both the linear version and cyclic version of this peptide

were checked for the β-sheet folding using circular dichroism (CD) measurements. The peptides were then tested against UCHL5/Rpn13 using enzyme-activity assays in a plate reader format, that revealed inhibition of UCHL5. Finally, we tested this peptide on the proteasome with functionally associated UCHL5 and USP14 where we used a Ub-based covalent probe (Ub-PRG) as a competitor to this peptide and observed that this peptide is an inhibitor of UCHL5 and not of USP14. We also confirmed that these peptides did not interfere with the activity of Rpn11, the metalloprotease DUB found in the lid of the 26S proteasome. This shows that both the linear and the cyclic versions of the peptide inhibits UCHL5 selectively within the context of the 26S proteasome activity.

Synthesis of linear and cyclic Ub-peptides

The synthesis of peptides by Fmoc-based solid phase peptide synthesis was carried out according to a previously reported procedure. [20] The cyclic and the terminally-protected linear version of ubiquitin peptides (1-17) were synthesized on TentaGel-TrtR resin and Rink-amide resin respectively. The Ub (1-17) peptide that was to be cyclized was synthesized on a Trt-resin with a free N-terminal methionine residue. The fully protected peptide was cleaved from the resin using 20% HFIP in DCM to afford the peptide with a free carboxy terminal group. After co-evaporating HFIP with DCM under reduced pressure, the protected Ub (1-17) peptide was obtained as a colourless oil. Cyclization of this peptide was carried out by adding 1.2 eq PyBOP and 1.2 eq DiPEA to the peptide dissolved in DMF at a concentration of 0.5 mg/ml. Completion of the reaction was followed by LC/MS analysis (Figure S1). After evaporating DMF under vacuum, TFA cleavage mix containing TFA: H_2O: TiPS: Phenol (92.5/2.5/2.5/2.5 v/v/v/v) was used to fully deprotect the final peptide. The peptide was then precipitated with dry-ice cooled ether:pentane (3:1) mix, followed by centrifugation and lyophilized to yield crude peptide that was then purified by reversed-phase HPLC. In the case of linear protected Ub (1-17) peptide containing an N-terminal acetyl group and a C-terminal amide group, the peptide was synthesized on a Rink amide resin with the N-terminal methionine residue protected with an acetyl group. Upon TFA cleavage using the TFA cleavage mix, the peptide was precipitated and lyophilized and purified using reversed phase HPLC.

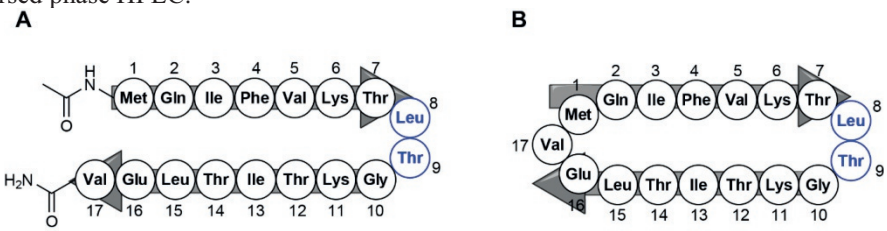


Figure 2*: Illustration of the linear end-protected peptide (**A**) and the cyclic peptide (**B**) based on Ub sequence from residues 1 to 17. The* β*-strand is represented by the arrow. Leu8 and Thr9 residues are the key residues of interaction with UCHL5 in this sequence (highlighted in blue.).*

Results

The structure of UCHL5 in complex with Ubiquitin and Rpn13 had been reported. [17, 18] This structure shows the binding pocket for residues 1 to 17 of Ub. Therefore, a peptide containing residues 1 to 17 of Ub was synthesized using Fmoc-SPPS. Since the structural stability of this β-sheet was not known, we synthesized both terminally-protected

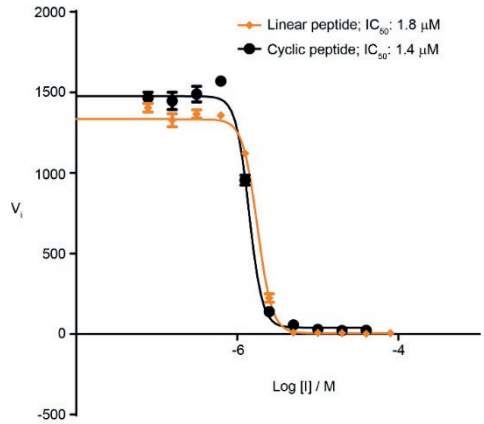


Figure 3: IC_{50} curves of Ub β-sheet peptide*. Both linear and cyclic version of the peptides were tested for inhibition of UCHL5 activity in a standard plate-reader assay using Ub-Rho as a substrate. Both the peptides inhibited the enzyme in a similar fashion.*

linear peptide and a cyclized peptide (Figure 2). In order to check for their folding, peptides were analysed using circular dichroism, which revealed a β-sheet conformation in both the cases (Figure S2).

First, we tested whether our peptides were able to inhibit UCHL5 activity using a standard Ub-rhodamine substrate in a plate-reader assay. As expected, both the linear and cyclic peptides were able to inhibit the activity of UCHL5. The linear peptide inhibited UCHL5 with an IC_{50} of 1.78 µM while the cyclic version inhibited at an IC_{50} of 1.4 µM (Figure 3).

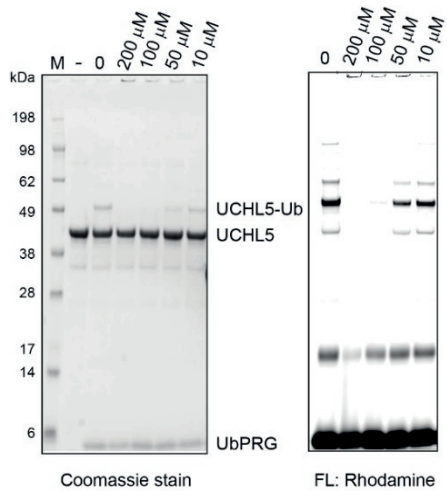


Figure 4: SDS-PAGE analysis of UCHL5 labelling using Rho-Ub-PRG in the presence of cyclic Ub β-sheet peptide*. **Left**: Coomassie stain showing inhibition of UCHL5 labelling by cyclic peptide at concentrations higher than 50 µM. **Right**: Fluorescence scan of the same gel showing disappearance of Rho-UbPRG-UCHL5 signal at higher concentrations of Ub peptide.*

For comparison, a known 19S DUB inhibitor called b-AP15, that has been reported to inhibit both UCHL5 and USP14, has an IC_{50} value of 16 μM. [21] This suggests that these peptide inhibitors are 10-fold more potent in inhibiting UCHL5 alone. Next, we tested whether our peptide can compete with Ub-PRG labelling of UCHL5. Ub-PRG acts by binding covalently to the active site cysteine with the alkyne group at its C-terminus. We incubated UCHL5 with different concentrations of the cyclic peptide Ub (1-17) for 30 minutes at RT. Rho-Ub-PRG was then added to this sample and incubated for 5 minutes. The samples were run on SDS-PAGE and labelling of UCHL5 was measured using a fluorescence scanner. The results show that the peptide was able to completely inhibit Ub-PRG labelling of UCHL5 at a concentration of 100 μM. (Figure 4).

Since our cyclic peptide was able to prevent binding of Ub-probe with UCHL5, we verified whether it is specific for UCHL5. UCHL5 is mainly associated with proteasome activity, along with USP14, another cysteine protease DUB associated with the proteasome. We verified whether our cyclic peptide can inhibit UCHL5 selectively over USP14 in the 26S proteasome. Isolation and purification of the proteasome in complex with UCHL5 and USP14 were carried out as reported previously. [22] (Figure 5A).

We incubated 5 μM of the cyclic peptide with 0.5 μg purified 26S proteasome for 30 minutes at 37 °C. Then, Rho-Ub-PRG was added to this sample for 15 minutes at 37 °C and analyzed on a denaturing SDS-PAGE gel. Visualization under a fluorescence scanner showed that the cyclic peptide was able to inhibit labelling of UCHL5 by Rho-Ub-PRG but not of USP14 (Figure 5B). On the other hand, 5 μM of IU1, a USP14 specific inhibitor was unable to inhibit UCHL5 (Figure 5C). This shows that our peptide inhibitor can inhibit UCHL5 in a specific manner in the context of the 26S proteasome.

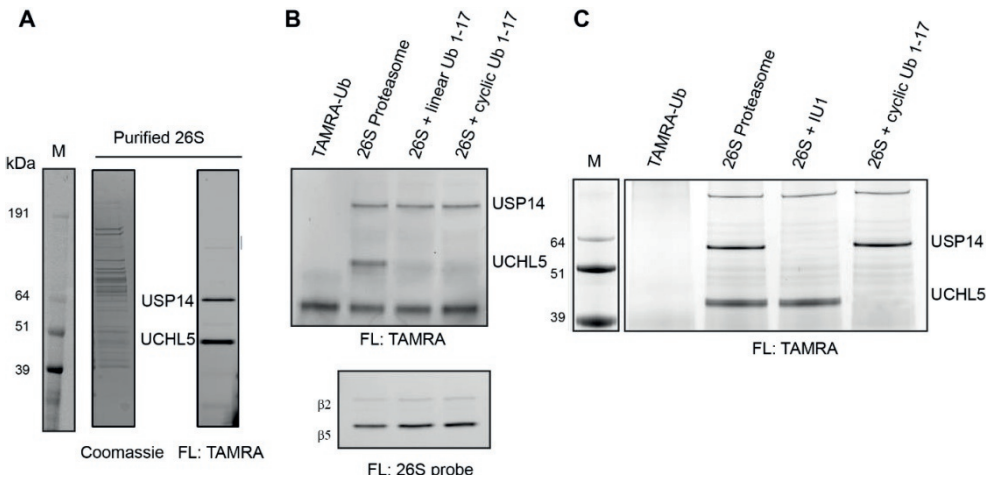


Figure 5: Inhibition of UCHL5 associated with the 26S proteasome. A: *The purified 26S proteasome (0.5 μg) is shown in Coomassie stain on the left. TAMRA-Ub-PRG labelling of the two cysteine-protease DUBs UCHL5 and USP14 is shown in the fluorescence scan on the right.* ***B:*** *Both the linear and cyclic Ub β-sheet peptide inhibits UCHL5 labelling by TAMRA-Ub-PRG but showing no change in USP14 labelling; the peptides did not affect the 26S protease activity as shown below.* ***C:*** *Selective inhibition of USP14 using IU1 and UCHL5 using cyclic Ub β-sheet peptide.*

In order to check whether our peptide can interfere with the activity of Rpn11, we checked its inhibition in a standard Ub-FP assay. Rpn11/Rpn8 heterodimer was expressed and purified using bacterial expression as described. [15] Using a Ub-FP substrate containing Ub linked by an isopeptide bond to a TAMRA-labelled Ub peptide, comprising residues 41to 54 of Ub, was used in a fluorescence polarization assay. [23] We observed that the cyclic peptide was unable to inhibit Rpn11/Rpn8 activity, suggesting that the peptide is specific to UCHL5 among other DUBs in the proteasome complex (Figure S3).

Discussions

The Ub interaction with UCHL5/Rpn13 has been studied using X-ray crystallography. [17, 18] These studies revealed the mode of binding of Ub to the surface of UCHL5. We used this information to design a linear and a cyclic beta-sheet peptide based on residues 1-17 of Ub. This provided competitive binding with UCHL5, as revealed with competitive labelling using a Ub-PRG probe. These peptides inhibited UCHL5/Rpn13 with an IC_{50} in the range of 1.4 μM to 1.8 μM, which is similar to the IC_{50} of the known UCHL5 inhibitor, b-AP15. [24] In addition, using Rho-Ub-PRG labelling of UCHL5, we show how the peptide competes with Ub binding by inhibiting labelling of UCHL5 with a Rho-Ub-PRG probe.

All of the known proteasomal DUBs have been implicated in the regulation of proteasomal degradation, upstream to its protease activity. Two of the DUBs namely UCHL5 and USP14 are strongly associated with chain trimming activity, which prevents degradation of polyUb-substrate. On the other hand, the metalloDUB Rpn11, positioned between the lid and the core complex is involved in the removal of Ub chains from the substrate when it is translocated into the core complex. This prevents the spontaneous degradation of Ub. Although specific inhibitors are known for USP14 and Rpn11, the lack of inhibitors for UCHL5 has hampered studies on substrate processing. The specificity of our peptide to UCHL5 in the context of the proteasome will help to study the role of each of the three DUBs in the activity of the 26S proteasome.

Conclusion

Studies on proteasome inhibition are indispensable for both fundamental and therapeutic research. It is essential that this process is studied in detail for further understanding of proteasomal function and the development of better pharmacological agents that can be used to treat diseases including cancer. So far, bortezomib has been used in the treatment of cancer including multiple myeloma and mantle cell lymphoma. It functions by blocking proteolytic activities in the core particle. However, several enzymes act upstream of the proteasome that tightly regulates its function. Such enzymes can also be targeted to enhance or inhibit proteasome activity, potentially leading to alternative therapy for specific types of cancers. [25, 26]

Among such enzymes are the deubiquitinases that function as regulators of Ub-dependent proteasomal degradation. UCHL5 and USP14 are two cysteine-protease class of DUBs that essentially trim polyUb chains before the substrate is being processed by the proteasome core particle. On the other hand, Rpn11 which is a metalloprotease DUB, is part of the proteasome and facilitates the removal of polyUb en-bloc from the substrate before it is degraded by the core particle.

Inhibition of UCHL5 and USP14 is known to increase the activity of the proteasome. [21] Although specific inhibitors of USP14 exist, UCHL5-specific inhibition has been pursued for a long time. [11] We now report the design and synthesis of a small Ub-derived peptide that can inhibit UCHL5 associated with the proteasome. Our design is based on a known Ub-binding site and the resulting peptide was synthesized and validated against a UCHL5/Rpn13

heterodimeric complex. Peptide-based inhibitors that can retain their secondary structure in a cellular environment and that simultaneously resist exopeptidase cleavage potentially can be used for therapeutic purposes in treating diseases such as cancer.

References

1. Ciechanover, A., *The unravelling of the ubiquitin system.* Nat Rev Mol Cell Biol, 2015. **16**(5): p. 322-4.
2. Komander, D., M.J. Clague, and S. Urbe, *Breaking the chains: structure and function of the deubiquitinases.* Nat Rev Mol Cell Biol, 2009. **10**(8): p. 550-63.
3. Hochstrasser, M., *Ubiquitin-dependent protein degradation.* Annu Rev Genet, 1996. **30**: p. 405-39.
4. Yau, R. and M. Rape, *The increasing complexity of the ubiquitin code.* Nat Cell Biol, 2016. **18**(6): p. 579-86.
5. Hershko, A. and A. Ciechanover, *The ubiquitin system.* Annu Rev Biochem, 1998. **67**: p. 425-79.
6. Xu, P., et al., *Quantitative proteomics reveals the function of unconventional ubiquitin chains in proteasomal degradation.* Cell, 2009. **137**(1): p. 133-45.
7. Chau, V., et al., *A multiubiquitin chain is confined to specific lysine in a targeted short-lived protein.* Science, 1989. **243**(4898): p. 1576-83.
8. Collins, G.A. and A.L. Goldberg, *The Logic of the 26S Proteasome.* Cell, 2017. **169**(5): p. 792-806.
9. Grant, E.P., et al., *Rate of antigen degradation by the ubiquitin-proteasome pathway influences MHC class I presentation.* J Immunol, 1995. **155**(8): p. 3750-8.
10. Mani, A. and E.P. Gelmann, *The ubiquitin-proteasome pathway and its role in cancer.* J Clin Oncol, 2005. **23**(21): p. 4776-89.
11. de Poot, S.A.H., G. Tian, and D. Finley, *Meddling with Fate: The Proteasomal Deubiquitinating Enzymes.* J Mol Biol, 2017. **429**(22): p. 3525-3545.
12. Lee, M.J., et al., *Trimming of ubiquitin chains by proteasome-associated deubiquitinating enzymes.* Mol Cell Proteomics, 2011. **10**(5): p. R110 003871.
13. Selvaraju, K., et al., *Inhibition of proteasome deubiquitinase activity: a strategy to overcome resistance to conventional proteasome inhibitors?* Drug Resist Updat, 2015. **21-22**: p. 20-9.
14. Lander, G.C., et al., *Complete subunit architecture of the proteasome regulatory particle.* Nature, 2012. **482**(7384): p. 186-91.
15. Worden, E.J., C. Padovani, and A. Martin, *Structure of the Rpn11-Rpn8 dimer reveals mechanisms of substrate deubiquitination during proteasomal degradation.* Nat Struct Mol Biol, 2014. **21**(3): p. 220-7.
16. Kim, H.T. and A.L. Goldberg, *The deubiquitinating enzyme Usp14 allosterically inhibits multiple proteasomal activities and ubiquitin-independent proteolysis.* J Biol Chem, 2017. **292**(23): p. 9830-9839.
17. Sahtoe, D.D., et al., *Mechanism of UCH-L5 activation and inhibition by DEUBAD domains in RPN13 and INO80G.* Mol Cell, 2015. **57**(5): p. 887-900.
18. Vander Linden, R.T., et al., *Structural basis for the activation and inhibition of the UCH37 deubiquitylase.* Mol Cell, 2015. **57**(5): p. 901-911.
19. Ekkebus, R., et al., *On terminal alkynes that can react with active-site cysteine nucleophiles in proteases.* J Am Chem Soc, 2013. **135**(8): p. 2867-70.
20. El Oualid, F., et al., *Chemical synthesis of ubiquitin, ubiquitin-based probes, and diubiquitin.* Angew Chem Int Ed Engl, 2010. **49**(52): p. 10149-53.
21. Wang, X., et al., *The 19S Deubiquitinase inhibitor b-AP15 is enriched in cells and elicits rapid commitment to cell death.* Mol Pharmacol, 2014. **85**(6): p. 932-45.
22. Wang, X., et al., *Mass spectrometric characterization of the affinity-purified human 26S proteasome complex.* Biochemistry, 2007. **46**(11): p. 3553-65.

23. Geurink, P.P., et al., *A general chemical ligation approach towards isopeptide-linked ubiquitin and ubiquitin-like assay reagents.* Chembiochem, 2012. **13**(2): p. 293-7.
24. D'Arcy, P., et al., *Inhibition of proteasome deubiquitinating activity as a new cancer therapy.* Nat Med, 2011. **17**(12): p. 1636-40.
25. D'Arcy, P. and S. Linder, *Proteasome deubiquitinases as novel targets for cancer therapy.* Int J Biochem Cell Biol, 2012. **44**(11): p. 1729-38.
26. Tian, Z., et al., *A novel small molecule inhibitor of deubiquitylating enzyme USP14 and UCHL5 induces apoptosis in multiple myeloma and overcomes bortezomib resistance.* Blood, 2014. **123**(5): p. 706-16.

Supplementary information:

General methods:

All commercial materials (Aldrich, Fluka, Novabiochem) were used without further purification. All solvents were reagent grade or HPLC grade. LC/MS analysis was performed with a system containing a Waters 2795 separation module (Alliance HT), Waters 2996 Photodiode Array Detector (190–750 nm), Phenomenex Kinetex XB-C18 (2.1 x 50 mm) reversed phase column and a MicromassLCT-TOF mass spectrometer. Samples were run at 0.80 mL min (Kinetex C18) with the use of a gradient of two mobile phases: A) aq. formic acid (0.1 %), and B) formic acid in CH_3CN (0.1 %). Data processing was performed using Waters MassLynx 4.1 software (deconvolution with Maxent1 function). Preparative HPLC was performed on a Waters XBridge™ Prep C18 Column (30 x 150 mm, 5µm OBD™) at a flow rate of 37.5 mL/min using aq. 0.05% TFA (Solvent A) and acetonitrile containing 0.05% TFA (Solvent B) as eluents. The gradient used for purification of peptides was from 25% B to 95% B over 18 minutes. All samples containing pure peptide were pooled together and lyophilized.

Fmoc-SPPS of peptides:

SPPS was performed on a Syro II MultiSyntech Automated Peptide synthesizer using standard 9-fluorenylmethoxycarbonyl (Fmoc) based solid phase peptide chemistry at 25 µmol scales. All amino acids were used in excess and coupling mix containing PyBOP and DIPEA were used accordingly. Linear Ub (1-17) peptide was synthesized on H-Rink amide Chemmatrix® resin (Sigma-Aldrich), and the N-terminus of this peptide was capped with acetyl group using acetic anhydride. After synthesis, the peptide was completely deprotected using TFA cleavage mix (TFA: H_2O: TiPS: Phenol (92.5/2.5/2.5/2.5 v/v/v/v)). The cyclic peptide of Ub (1-17) was synthesized on TentaGel Trt R resin with a free N-terminus. Immediately after synthesis, the cyclic peptide was cleaved from the resin using HFIP in DCM (20% v/v) so that the side chains remain protected while the N- and C-terminus are freed. Cyclization was done using 1.2 equiv. PyBOP, 1.4 equiv. DIPEA in DMF at a peptide concentration of 0.5 mg/mL, overnight at Room Temperature. After cyclization, the peptide was completely deprotected using the same TFA cleavage mix used for linear peptide. Following deprotection, the peptide was precipitated in the dry-ice cold ether:pentane (v:v 1:1), dried and lyophilized. The lyophilized peptides were then dissolved in aqueous DMSO (5%) and purified using preparative RP-HPLC.

Circular Dichroism (CD) measurements:

For Circular Dichroism (CD) measurements, a JASCO CD J1000 machine was used (UMC, Utrecht, the Netherlands). Samples were diluted in 20 mM TrisHCl, 20 mM NaCl pH 7.4, to a final concentration of 4 µM. Measurements were performed at 25 °C using wavelengths ranging from 260 nM to 185 nM in a span of 100 mdeg. The scanning speed was 20 nM/min and measurements from 10 experiments were accumulated. Based on the observed values of CD measurements and concentration used in measurements, CD plots were drawn.

IC_{50} assay of linear and cyclic peptides:

The DUB mediated hydrolysis of Ub-rho yields free rhodamine and Ub. The rhodamine signal is measured in a fluorescence intensity assay using a buffer containing 25 mM HEPES pH 7.5, 150 mM NaCl, 5 mM DTT, 0.05% Tween-20 and 0.1 mg/ml BGG at pH 8 and at room temperature [1]. The enzyme and the substrates were added to a 384-well Corning™ low volume flat bottom plates. Fluorescence intensity was monitored at an excitation wavelength of 487 nm and an emission wavelength of 535 nm using BMG CLARIOstar® plate reader. The enzyme stock was diluted into the assay buffer at a final concentration of 1 nM. The Ub-rhodamine substrate was prepared synthetically according to the previously reported procedure [2]. The substrate dissolved in DMSO was diluted out in the water and later in the assay buffer to a final concentration of 100 nM. For dissolving the peptides, samples were prepared in DMSO as a 5 mM stock solution. Then they were dissolved in MQ water and then into one of the fluorogenic assay buffers. Serial dilution of the peptides was prepared in the assay buffer. After 30 minutes of incubation, the substrate (Ub-Rho or UbFP assay reagent) was added. They are then immediately measured in a plate-reader over a period of up to 90 minutes at RT.

Covalent Ub-probe labelling of UCHL5:

Recombinant UCHL5/Rpn13 was taken at a concentration of 1 μM in a labelling buffer containing 25 mM HEPES pH 7.5, 150 mM NaCl and 5 mM DTT. To this, cyclic peptide Ub (1-17) at different concentrations ranging from 200 μM to 10 μM was added and incubated for 30 minutes at RT. After this, 2 μM of Rho-Ub-PRG probe was added and incubated for 5 minutes at RT. The samples were run on an SDS-PAGE agarose gel using MES buffer. The gel was scanned for fluorescence of Rhodamine in a Typhoon FLA 9500 (GE Healthcare Lifesciences) using filters set at 473 nm (excitation wavelength) and 532 nm (emission wavelength). Coomassie staining was carried out using InstantBlue™ Protein Stain (Sigma-Aldrich).

26S Proteasome purification:

The 26S proteasome was purified from mammalian cells using a previously reported procedure [3]. HTBH-Rpn11-HEK293T cells were treated with 5 mM of the indicated compounds for 16 hours after which cells were washed and collected by scraping in lysis buffer (100 mM NaCl, 50 mM sodium phosphate, 10% glycerol, 5 mM ATP, 1 mM DTT, 5 mM $MgCl_2$, 13 protease inhibitor (Roche), 13 phosphatase inhibitor (Roche), and 0.5% NP-40 (pH 7.5)). After a centrifugation step (21,100 g for 15 minutes) HTBH-tagged Rpn11-containing 26S proteasomes were isolated from the lysate by overnight incubation at 4°C with streptavidin beads. After 3 washes with wash buffer (50 mM Tris-HCl (pH 7.5)), 10% glycerol, 1 mM ATP), 26S proteasomes were cleaved from the beads by treatment with 1% TEV enzyme (protein expressed and purified in-house by the NKI protein facility) for 1 hour at 30°C in wash buffer. Protein concentration was determined using NanoDrop. For proteomic analysis, proteasome isolation was performed four separate times for each condition. HEK293T cells stably expressing HTBH-tagged Rpn11 were kindly provided by Lan Huang (University of California, Irvine).

Supplementary figures:

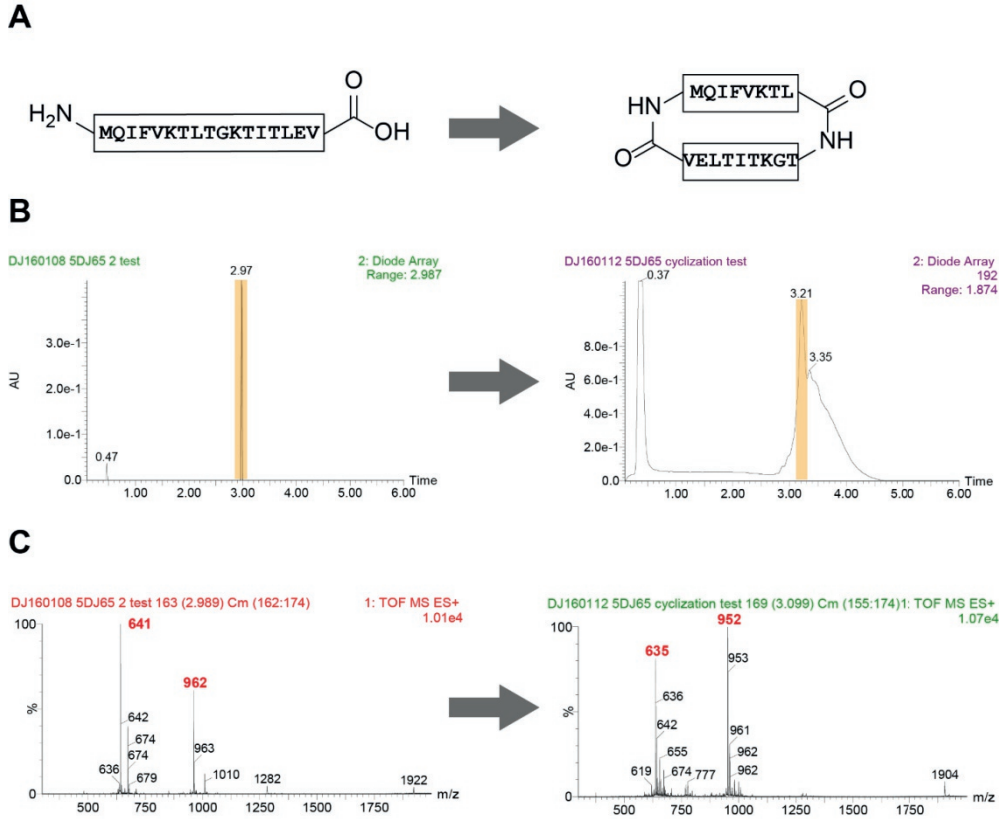


Figure S1: Cyclization of Ub (1-17) peptide. ***A***: *Schematic illustration of cyclization procedure where the N- and the C-terminus of the peptide is conjugated together using peptide coupling procedure.* ***B***: *UV chromatogram from the LC/MS measurement of the peptide before (left) and after (right) cyclization procedure.* ***C***: *Mass spectrometric signals of Ub (1-17) peptide before (left) and after(right) the completion of cyclization.*

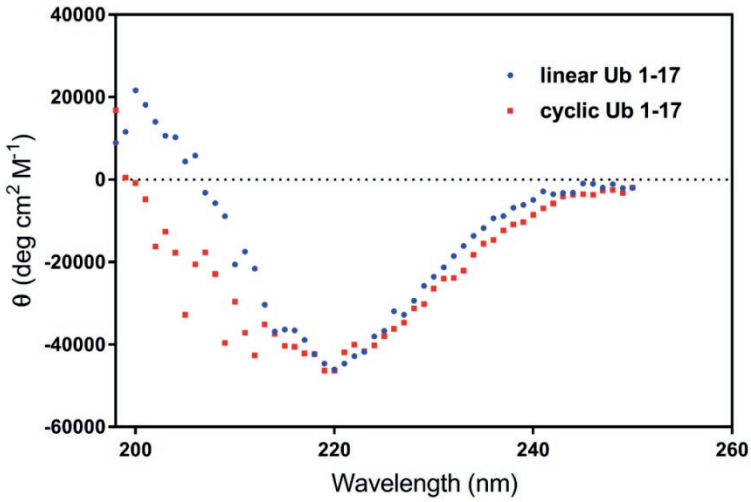


Figure S2: Circular Dichroism spectrum of both the linear and the cyclic Ub (1-17) *peptide. The pattern is similar to what is generally observed for a β-sheet peptide.*

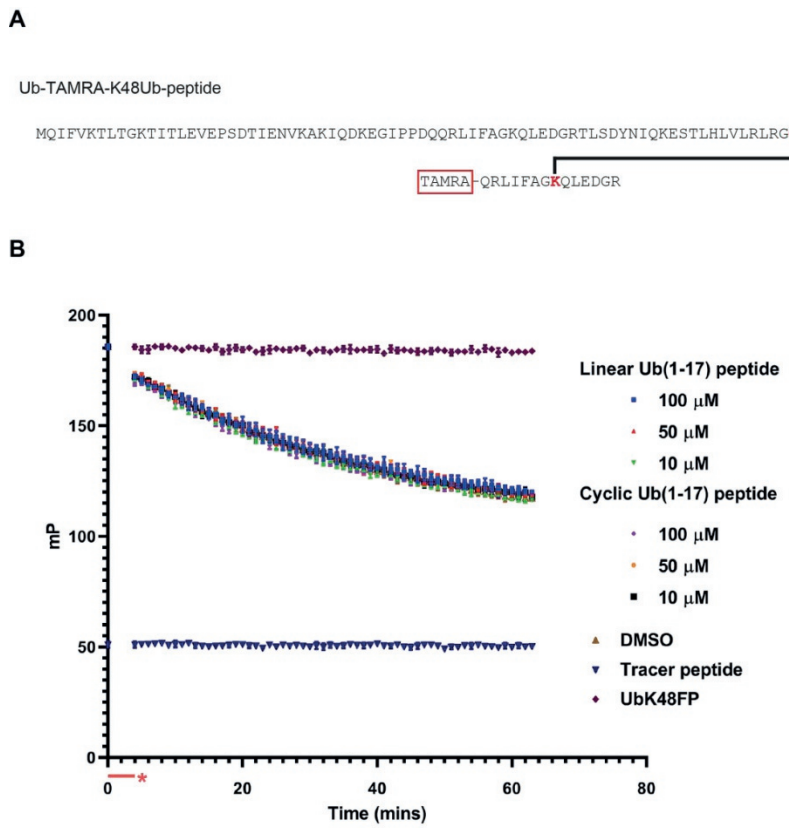


***Figure S3**: **A**: Sequence of U-TAMRA-K48Ub-peptide (UbK48FP) substrate used in Rpn11 enzyme activity assay. **B**: Fluorescence polarization data of Rpn11/Rpn8 activity in the presence of different concentrations of both linear and cyclic Ub (1-17) peptide. UbK48FP reagent was used as a substrate and TAMRA-K48(Ub) peptide was used as tracer peptide. The first four minutes were not measured due to the time taken from adding substrates to measuring the plate.*

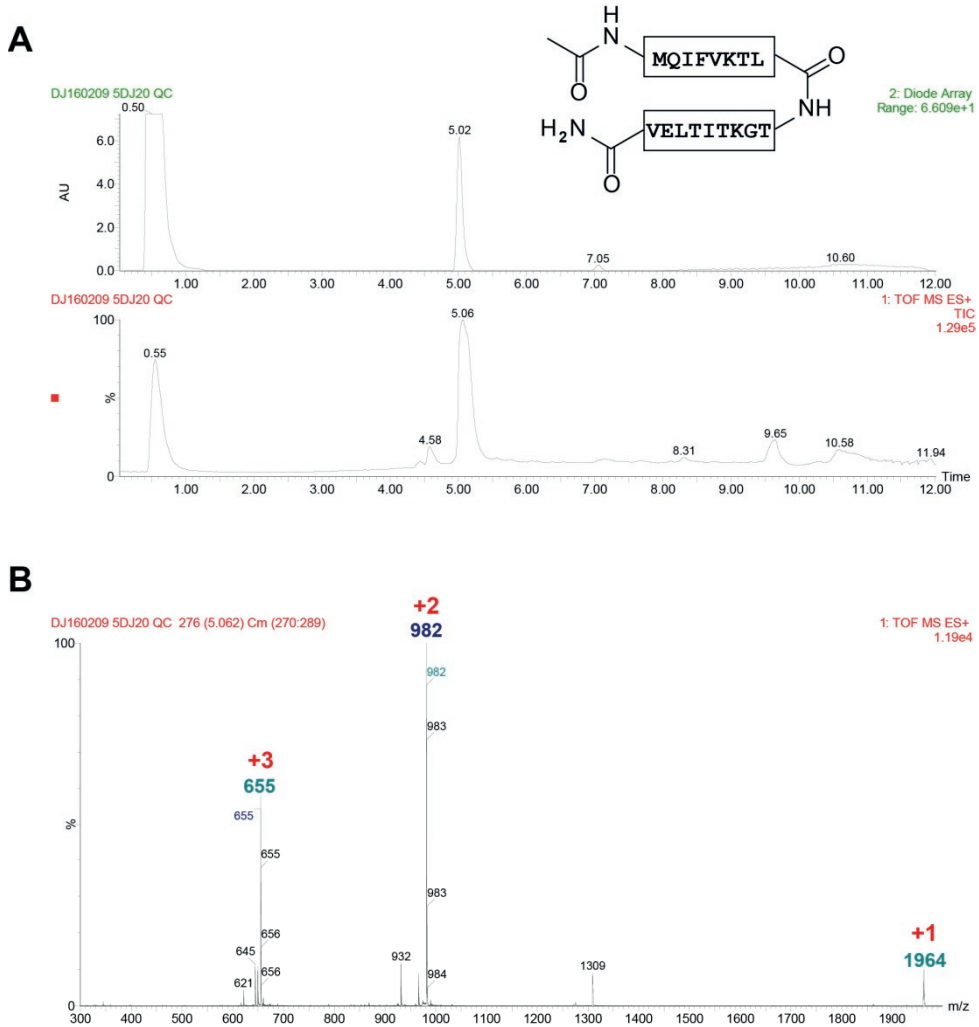


Figure S4: *LC-MS analysis of linear Ub (1-17) peptide.* ***A:*** *Top: UV chromatogram; Bottom: Combined Mass spectrum; Inset: illustration of linear peptide.* ***B:*** *Combined mass spectrum of UV peak at 5.02 min. Calculated mass: 1963.4 Da. Observed mass: 1964(M+1), 982 (M+2) and 655 (M+3).*

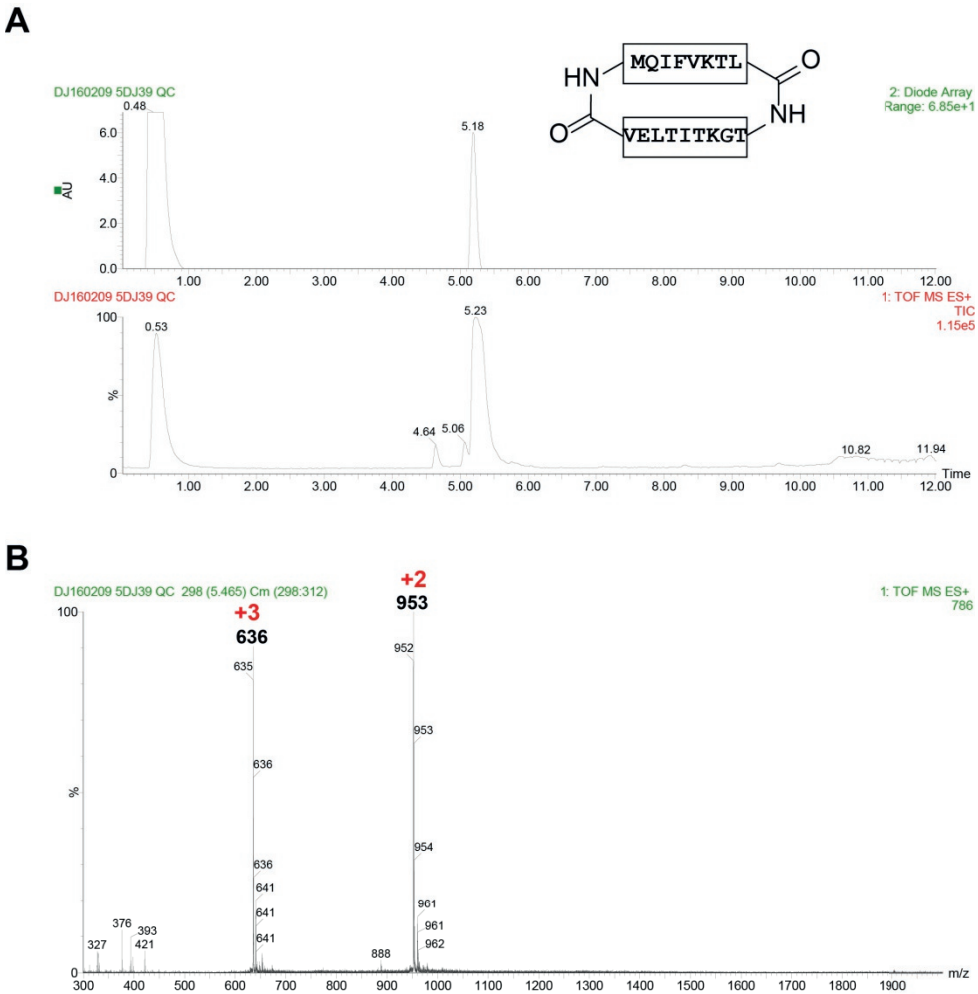


Figure S5: *LC-MS analysis of cyclic Ub (1-17) peptide.* ***A:*** *Top: UV chromatogram; Bottom: Combined Mass spectrum; Inset: illustration of cyclic peptide.* ***B:*** *Combined mass spectrum of UV peak at 5.18 min. Calculated mass: 1922.4 Da. Observed mass: 953 (M+2) and 636 (M+3).*

Supplementary references:

1. Sahtoe, D.D., et al., *Mechanism of UCH-L5 activation and inhibition by DEUBAD domains in RPN13 and INO80G.* Mol Cell, 2015. **57**(5): p. 887-900.
2. El Oualid, F., et al., *Chemical synthesis of ubiquitin, ubiquitin-based probes, and diubiquitin.* Angew Chem Int Ed Engl, 2010. **49**(52): p. 10149-53.
3. Wang, X., et al., *Mass spectrometric characterization of the affinity-purified human 26S proteasome complex.* Biochemistry, 2007. **46**(11): p. 3553-65.

Chapter 7

Summary and outlook

Hameed, D.S., Ovaa, H.

The scope of this thesis concerns the synthesis of novel tools based on ubiquitin (Ub) using Fmoc-based solid-phase peptide synthesis (SPPS) to study Ub signalling pathways. The chemical synthesis of large polypeptides and proteins has relied on combining fragments of peptide sequences using chemical ligation techniques [1]. These ligation techniques depend on the sequence of the polypeptide or protein and the ability of the final product to refold post-synthesis. The thiol group found in cysteine residues is frequently used as a chemical ligation handle [2]. For polypeptides and proteins that lack a cysteine residue in their sequence, cysteine can be introduced to replace an alanine residue to allow ligation to another peptide segment, followed by desulphurization to reinstate alanine. Ligation procedures have been refined over the years to improve ligation yield and efficiency. However, the intermediate purifications of peptide fragments make this approach less favourable for generating many polypeptides in a fully automated procedure and in parallel. This can be avoided by synthesizing polypeptides in a conceivably linear fashion. This approach has been helpful in the chemical synthesis of Ub [3]. Since Ub lacks a cysteine residue in its sequence, the most convenient approach is to synthesize it in a linear fashion. Furthermore, the short sequence of 76 amino acids and the excellent refolding capacity of Ub gives the edge to synthesize Ub in a linear fashion with a relatively short duration and high yields. This also helps us in making virtually any mutant Ub with both natural and unnatural amino acids at any position of our choice. SPSS also allows the introduction of fluorescent dyes, crosslinkers and other chemical handles conveniently at will.

In **Chapter 1**, I provide an overview of the various Ub conjugates, assay reagents and probes that have been generated using Fmoc-based SPPS [4]. The Ovaa lab has established an automatic procedure to synthesize full-length Ub by SPPS in parallel. This allows easy N-terminal modification of Ub with dyes such as rhodamine or tetramethylrhodamine (TAMRA), while the C-terminal carboxylate of Ub can also be easily modified to create, for example, activity-based probes (ABPs) or fluorogenic assay substrates. The internal residues of Ub can also be mutated at will (Figure 1). For example, the synthesis of a mutant Ub containing a ligation handle such as a protected δ- or γ-thiolysine residue at the location of a lysine residue has enabled the synthesis of Ub dimers of different linkage topologies. The resulting diubiquitin (diUb) molecules have allowed studies of the substrate specificity of deubiquitinases (DUBs) to better understand their biochemical properties [5]. Moreover, assay reagents containing Ub conjugated to synthetic fluorescently-labelled peptides containing enzyme-specific sequences have also been generated using thiolysine-mediated chemical Ub conjugation which has allowed studies of DUBs kinetics [6]. Modification of the C-terminus of Ub with an active-site cysteine-reactive element has enabled the synthesis of activity-based Ub probes specific for DUBs. The use of SPPS has also facilitated the incorporation of photo-crosslinkers in the sequence of Ub at positions deemed to interact with Ub interacting proteins. Such Ub reagents were generated and incorporated into polyUb chains that were generated enzymatically and the resulting polyUb chains containing photo-crosslinkers were used to trap linkage-specific interacting proteins in the Ub-proteasome system [7]. The procedure to synthesize Ub variants of virtually any sequence has accelerated the study of Ub biology in cells. The same procedure has also been applied to synthesize many Ub-like (Ubl) proteins in a linear fashion using Fmoc-SPPS.

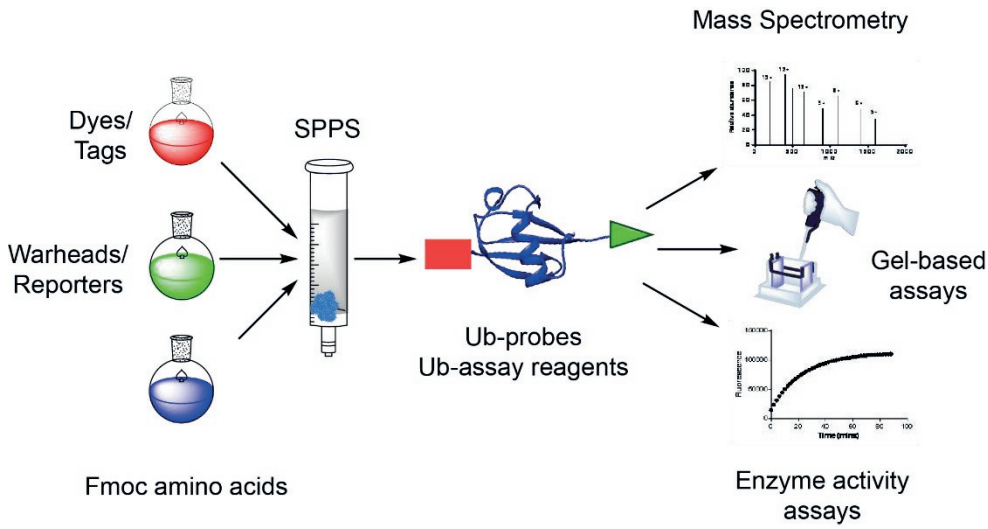


Figure 1: Overview of Fmoc-based SPPS of Ub conjugates. *Synthetic Ub can be generated in a linear fashion using SPPS. Modification of the C-terminus, N-terminus or internal residues of Ub is made possible during or after synthesis. Such reagents are used to study Ub biology.*

Synthesis of ubiquitin dimers linked by an isopeptide bond using enzymatic procedures is often difficult due to two main reasons: first, lack of knowledge of enzymes or enzyme combinations that can generate these specific linkages efficiently *in-vitro*; and secondly, the lack of control of the enzymatic reaction to make conjugates of well-defined lengths without the generation of undesired linkage types as a by-product of these enzymatic reactions [8-10]. In order to address these issues, an alternative procedure was developed to make Ub chains by chemical synthesis of Ub molecules using a native chemical ligation technique. In **Chapter 2**, I explain how the synthesis of a Ub molecule containing a native chemical ligation handle called δ-thiolysine at positions of lysine residues has enabled the synthesis of diubiquitins (diUbs) of specific linkages via chemical ligation [3, 11]. The Ub module whose C-terminal glycine residue participates in the isopeptide bond is called the distal Ub whereas the lysine-contributing Ub moiety is called the proximal Ub. I utilized together with my colleagues the biochemical activation of wild type Ub by Ub activating (E1) enzyme and isolated stable (distal) Ub-thioesters. Using SPPS, the proximal Ub containing δ-thiolysine at specific lysine sites was synthesized and conjugated to the activated Ub-thioesters to make isopeptide linked diubiquitins. After radical-mediated desulfurization, these diUbs were isolated and purified in high yields. These conjugates have allowed studies of the specificity of USP and OTU families of deubiquitinating enzymes [5, 12]. This procedure to make diUb topoisomers has also laid the groundwork for the synthesis of isopeptide-linked dimers of SUMO conjugates [13].

The ability to make Ub dimers of different lysine linkages has opened the possibility to study their structural properties. Different Ub chains are known to be involved in eliciting distinct cellular responses through binding ubiquitin-specific proteins [14]. The recognition of different Ub topoisomers by linkage-specific Ub receptor proteins proceeds through interactions with ubiquitin-binding domains (UBDs) [15]. The mechanism of interaction of UBDs and Ub chains can be studied using various biophysical techniques. Among them, NMR has been instrumental in providing insight into the solution-dynamics and Ub-UBD

interactions. In **Chapter 3**, I describe the generation of Ub dimers where only the distal Ub module is isotopically labelled with ^{15}N atoms. I used these diUbs in NMR experiments to provide information on the binding of the distal Ub moiety with respect to the proximal Ub moiety in different isopeptide-linked diUb molecules. I expressed ^{15}N-isotopically labelled Ub in E. Coli and a ^{15}N-Ub-thioester was then generated enzymatically. Similar to the procedure reported in Chapter 2, I made all seven isopeptide-linked diUbs but this time ^{15}N-distally labelled. Upon measuring the ^{1}H-^{15}N HSQC spectra of these reagents by NMR, I observed that the interactions between the two Ub modules in a diUb molecule are different for each lysine linkage-type. Next to obtaining information on the structural orientation of Ub modules in a diUb molecule, I also studied how the UBD UBXN1 interacts specifically with K6 diUb. UBDs function by interacting with Ub and Ub chains thereby forming the basis for ubiquitin signalling in cells [16]. One of the UBDs is the UBA domain that is found in many ubiquitin-interacting enzymes. These UBA domains are about 45 amino acids long containing three alpha-helices in their structure. A UBA domain found in the UBXN1 protein is specific for K6 diUb chains and UBXN1 is involved in DNA damage repair. Even though this domain was found to interact with K6 polyUb chains, [17] I now show with my colleagues how only the C-terminally extended version of the UBA domain of UBXN1 interacts with K6 diUb chains. Using a fluorescence polarization binding assay and microscale thermophoresis it was found by Gabrielle van Tilburg that this extended domain is needed for K6 specificity. I investigated this interaction further by NMR using a distally labelled K6 diUb molecule in solution. Moreover, studies using bioinformatics revealed that this C-terminal extension was conserved among commonly appearing UBA domains (data from Kay Hoffman, University of Cologne). This opens the possibility that the C-terminal extensions of UBA domains contain sequences that contribute to Ub-linkage selectivity, which remains to be investigated. Thus, I demonstrated the potential of using labelled diUb molecules in studying the interactions of Ub chains with UBDs.

In this study, I conveniently labelled distal Ub elements in Ub chains and studied their interactions with proximal Ub moieties and the specific interaction of distally labelled K6 di Ub with an extended UBD found in UBXN1. Since the proximal Ub that was used in the native chemical ligation technique contains a thiolysine residue, it is difficult to express it in bacteria. However, using an evolved $tRNA^{CUA}$/tRNA synthetase pair, this may potentially be achieved (Figure 2) [18]. An evolved $tRNA^{CUA}$/tRNA synthetase pair can be developed to efficiently incorporate δ- or γ- thiolysine in Ub in a bacterial expression. By using this technique, it is possible to express ^{15}N-labelled proximal Ub which can then be used to make proximally ^{15}N-labelled diUb molecules of all lysine-linkage types. This way, a complete diUb toolkit containing segmentally isotope-labelled ^{15}N-diUb molecules can be synthesized and used in NMR experiments to study the solution-dynamics of diUbs and their mode of interaction with specific UBDs.

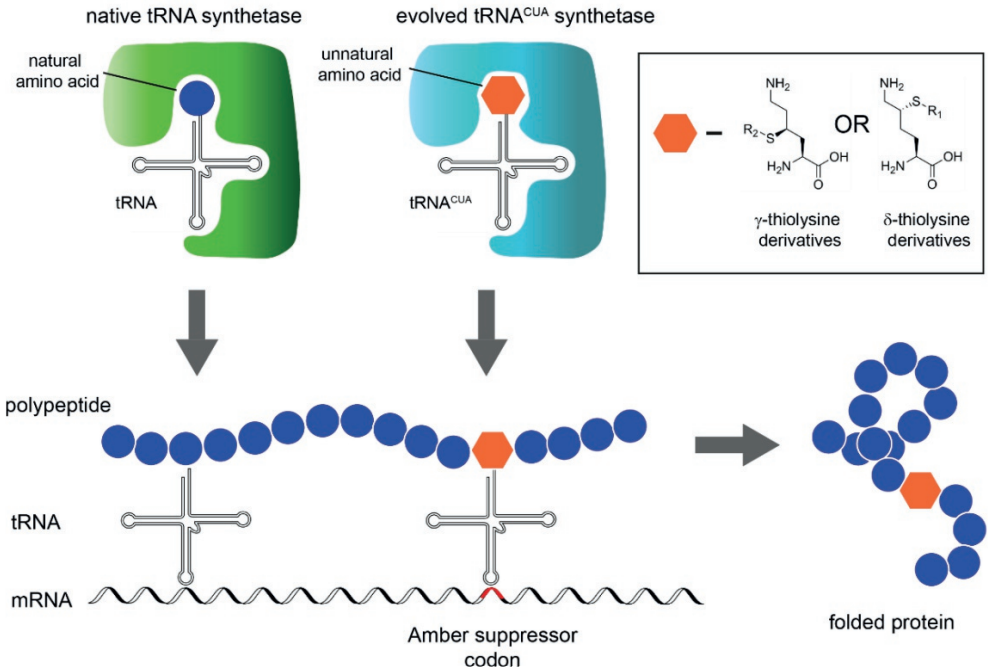


Figure 2: Incorporation of thiolysine derivatives into Ub or another protein by using an evolved tRNA^{CUA}/tRNA synthetase pair. *The tRNA^{CUA} recognizes a stop codon and incorporates the unnatural amino acid in that position, which can be translated into a folded protein and purified from the bacterial lysate. [19]. By evolving an efficient tRNA^{CUA}/tRNA synthetase pair, a γ- or δ-thiolysine (Inset) containing a protected thiol (R_1 and R_2) can be used as the unnatural amino acid and incorporated into full-length Ub in positions of lysine residues. This provides a convenient method to isotopically label the proximal Ub of a diUb molecule for studying them in NMR experiments.*

The feasibility of Ub synthesis using SPPS has opened the possibility to make Ub-based ABPs against enzymes involved in ubiquitination or deubiquitination. Among the different families of DUBs, the cysteine-protease DUBs have been extensively studied so far mainly because of the availability of Ub-probes and assay reagents [20, 21]. A Ub probe mimics upon reaction the covalent enzyme-substrate intermediate formed between the active site cysteine residue of the enzyme and the carbonyl group of the isopeptide bond at the C-terminus of Ub. However, these covalent intermediates are absent in catalysis by the metalloprotease family of DUBs (metalloDUBs) because these enzymes use Zn^{2+} that is chelated by two histidine residues and an aspartate residue in the active site of the enzyme. It is, therefore, a challenge to generate Ub-based ABPs for metalloDUBs [22]. In **Chapter 4**, I report the synthesis of a chelating Ub-based activity probe that targets metalloDUBs [23]. For this purpose, a chemically synthesized zinc-binding group (ZBG) was conjugated with the C-terminus of a truncated synthetic Ub obtained by SPPS. A metalloDUB called Rpn11 was used to validate our Ub-ZBG probe because of its vital role in the 26S proteasome [24, 25]. First, the mode of interaction in an Rpn11/Rpn8-Ub complex was analyzed and molecular docking was used to design the Ub-ZBG probe. Based on this information, Ub (1-74) was synthesized and conjugated with 8-mercaptoquinoline (8MQ), a Zn^{2+} chelating

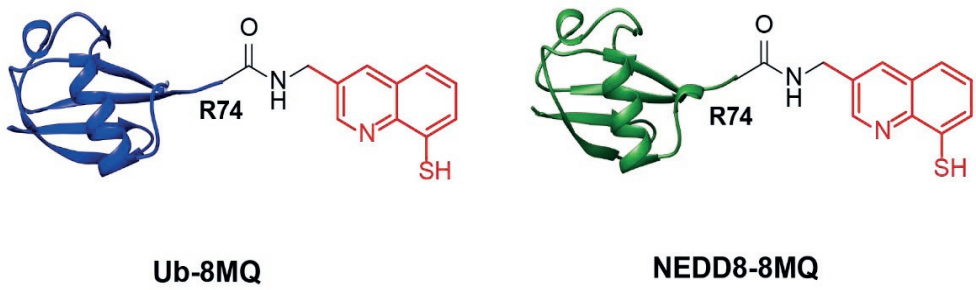


Figure 3: *Comparison of the structure of Ub-8MQ reagent that was validated against Rpn11/Rpn8 complex and a similar reagent made with NEDD8 that can be used to study the metalloprotease called CSN5 of the COP9 signalosome complex in cells.*

moiety, at the C-terminus of Arg74 of Ub [26]. Furthermore, Ub-8MQ was also labelled with a fluorescent dye or a biotin tag on the N-terminus, which facilitated studying their interaction with Rpn11/Rpn8 heterodimer complex and carrying out pull-down experiments of over-expressed metalloDUBs from cell lysate.

This technique can be easily expanded to the synthesis of probes that target metalloproteases specific for ubiquitin-like proteins (Ubl). One of the interesting Ubl-metalloproteases is the CSN5, a metalloprotease in the COP9 signalosome complex that de-NEDDylates Cullin proteins [27]. Since NEDD8 and Ub are similar in size, they can be synthesized in a similar fashion (Figure 3) [28]. This technique can be further extended to other Ub-like proteins like SUMO and ISG15, potentially leading to the discovery of putative metalloproteases.

So far, I described Ub reagents or probes that can be used mainly for *in-vitro* experiments. However, studying the ubiquitin machinery *in-vivo* is essential to understand the ubiquitin signalling pathway in the greatest detail. Such studies require the delivery of synthetic Ub reagents and conjugates into live cells so that the ubiquitination or deubiquitination machinery can be studied in cells and preferably in real-time [29]. One of the widely used biophysical techniques to deliver Ub into live cells is electroporation. For example, this technique was used to deliver Ub-dehydroalanine probes into mammalian cells to study the E1-E2-E3 enzyme cascade [30]. One of the drawbacks of electroporation is the harsh nature of this technique [31]. Therefore, I investigated other less-invasive methods to deliver synthetic Ub into live cells. In **Chapter 5**, I explain how I made a Ub molecule containing a synthetic cell-penetrating delivery vehicle [32]. The TAT peptide derived from the HIV virus has been extensively used to deliver large proteins into live cells by simple co-incubation [33]. However, the uptake efficiency is generally low and therefore TAT-fusion proteins (TFPs) were developed to circumvent this issue. TFPs containing a single copy of the TAT peptide are generally trapped at the endosomal uptake step without further delivery into the cytoplasm unless used at elevated concentrations which generally leads to cell lysis. However, surprisingly a dimeric disulfide-linked TAT peptide was reported to be able to escape from endosomes into the cytoplasm of cells [34] and this proved indeed the case in my hands. Based on this, a cell-permeable Ub conjugate was designed and synthesized using Fmoc-SPPS by making a dimeric disulfide-linked TAT fusion peptide at the C-terminus of a rhodamine-labelled Ub molecule. This delivery reagent efficiently traversed the cell membrane via the endosomal pathway and escaped from the endosomes into the cytoplasm

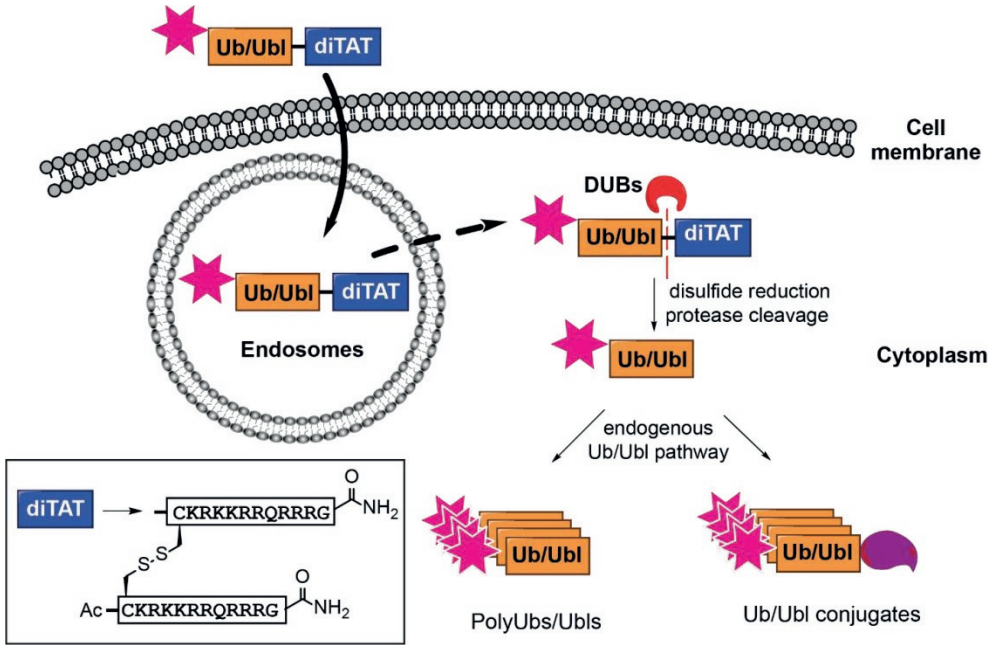


Figure 4: *The mechanism of delivery of labelled synthetic Ub or Ubl by using a dimeric disulfide-linked TAT peptide conjugated at the C-terminus of Ub. This reagent enters cells via the endosomal pathway and escapes from endosomes due to the dimeric nature of the TAT peptide used here. The delivery vehicle is then cleaved by cytosolic DUBs or Ubl-specific proteases. Once freed from the TAT peptide, the synthetic Ub or Ubl can be conveniently incorporated into the endogenous Ub or Ubl pathways.*

(Figure 4). Once in the cytoplasm, the dimeric disulfide-linked TAT peptide was reduced and removed from the C-terminus of rhodamine-Ub by the action of endogenous DUBs. Furthermore, these rhodamine-Ub reagents were incorporated into the intrinsic Ub machinery effectively. This study shows the potential to deliver virtually any synthetic Ub or Ubl reagent mildly into live cells.

Direct structural interactions between a Ub protein and DUBs are essential for deubiquitination. This interaction has been utilized to make Ub-based ABPs for DUBs and the X-ray crystal structures of different covalently trapped DUB-Ub complex have been determined [35]. One very interesting DUB that is associated with the 26S proteasome is the UCHL5 enzyme. An X-ray crystal structure of Ub-UCHL5 has been determined by trapping a UCHL5/Rpn13 complex with a Ub-PRG probe [36, 37]. From this structure, the residues Leu8 and Thr9 at the N-terminus of the Ub molecule were found to directly interact with a hydrophobic pocket in UCHL5. Therefore, a peptide sequence in Ub containing residues from 1 to 17 (that evidently includes the Leu8 and Thr9 residues) can potentially be used as an inhibitor of UCHL5 activity. **Chapter 6** deals with the synthesis of a stable cyclic β sheet peptide containing residues 1 to 17 of Ub, which was validated using the UCHL5/Rpn13 complex. I observed that this peptide inhibits UCHL5/Rpn13 both in isolation and in complex with the 26S proteasome. Moreover, the activity of the 26S proteasome was found to be increased upon inhibiting UCHL5, likely since UCHL5 has been implicated in Ub-chain

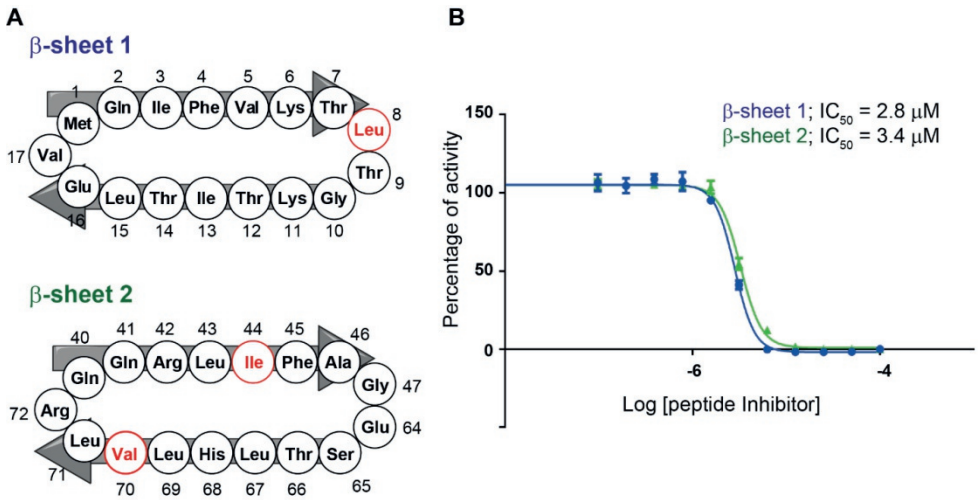


Figure 5: A: *Sequences of two β-sheet containing peptides derived from the Ub sequence. β-sheet peptide 1 contains residues 1 to 17 of Ub while β-sheet peptide 2 contains residues 40 to 47 and 64 to 72 of Ub which are combined and cyclized.* ***B:*** *IC_{50} values of both the β-sheet peptides show similar values when tested against UCHL5/Rpn13.*

trimming activity prior to substrate degradation by the 26S proteasome [38]. This inherent function of UCHL5 is hypothesized to save the substrate protein from being degraded by the 26S proteasome. Therefore, inhibition of UCHL5 with this cyclic peptide inhibitor renders substrate proteins potentially more prone to degradation. Further experiments enhance the properties of this UCHL5 inhibitor are ongoing. The use of SPPS offers more options to mutate the peptide with natural or unnatural amino acids and make them more selective to UCHL5.

Ubiquitin is known to contain four beta-sheets in its structure. This forms the core of the hydrophobic patch encompassing the residues of Leu8, Ile36, Ile44 and Val70. The UCHL5 inhibiting peptide contains the Leu8 residue. Other β-sheet peptides of Ub containing residues such as Ile36, Ile44 and Val70 can also be synthesized as a stable beta-sheet peptide inhibitor for DUBs. One such a peptide containing residues 40-47 and 64 to 72 of Ub were combined and cyclized. I observed that this peptide also inhibited UCHL5 with a similar IC_{50} value (Figure 5). The inhibitory potential of such Ub-derived β-sheet containing peptides can form the basis for future DUB inhibitors active in cells. Recent advances in generating large cyclic peptide libraries containing unnatural aminoacids have opened new possibilities in the discovery of highly efficient peptide inhibitors. One such method called RaPID screening uses modified ribozymes capable of incorporating unnatural aminoacids into peptide sequence generating a highly diverse peptide library, thereby increasing the chances of finding high affinity peptide inhibitors for DUBs [39]. Such a library can be developed using a Ub-derived peptide sequence as the basis and potentially identify better peptide inhibitors for UCHL5.

To summarize the thesis, I have investigated how the chemical synthesis of Ub conjugates and peptides based on Ub can be used to study and modulate the ubiquitination system both *in-vitro* and in live cells. With an expanding set of reagents to study the Ub system, it will become easier to develop future drugs that act on this system for therapeutic purposes.

References

1. Jaradat, D.M.M., *Thirteen decades of peptide synthesis: key developments in solid phase peptide synthesis and amide bond formation utilized in peptide ligation.* Amino Acids, 2018. **50**(1): p. 39-68.
2. Dawson, P.E., T.W. Muir, I. Clark-Lewis, and S.B. Kent, *Synthesis of proteins by native chemical ligation.* Science, 1994. **266**(5186): p. 776-9.
3. El Oualid, F., R. Merkx, R. Ekkebus, D.S. Hameed, J.J. Smit, A. de Jong, H. Hilkmann, T.K. Sixma, and H. Ovaa, *Chemical synthesis of ubiquitin, ubiquitin-based probes, and diubiquitin.* Angew Chem Int Ed Engl, 2010. **49**(52): p. 10149-53.
4. Hameed, D.S., A. Sapmaz, and H. Ovaa, *How Chemical Synthesis of Ubiquitin Conjugates Helps To Understand Ubiquitin Signal Transduction.* Bioconjug Chem, 2017. **28**(3): p. 805-815.
5. Faesen, A.C., M.P. Luna-Vargas, P.P. Geurink, M. Clerici, R. Merkx, W.J. van Dijk, D.S. Hameed, F. El Oualid, H. Ovaa, and T.K. Sixma, *The differential modulation of USP activity by internal regulatory domains, interactors and eight ubiquitin chain types.* Chem Biol, 2011. **18**(12): p. 1550-61.
6. Geurink, P.P., F. El Oualid, A. Jonker, D.S. Hameed, and H. Ovaa, *A general chemical ligation approach towards isopeptide-linked ubiquitin and ubiquitin-like assay reagents.* Chembiochem, 2012. **13**(2): p. 293-7.
7. Chojnacki, M., W. Mansour, D.S. Hameed, R.K. Singh, F. El Oualid, R. Rosenzweig, M.A. Nakasone, Z. Yu, F. Glaser, L.E. Kay, D. Fushman, H. Ovaa, and M.H. Glickman, *Polyubiquitin-Photoactivatable Crosslinking Reagents for Mapping Ubiquitin Interactome Identify Rpn1 as a Proteasome Ubiquitin-Associating Subunit.* Cell Chem Biol, 2017. **24**(4): p. 443-457 e6.
8. Michel, M.A., P.R. Elliott, K.N. Swatek, M. Simicek, J.N. Pruneda, J.L. Wagstaff, S.M. Freund, and D. Komander, *Assembly and specific recognition of k29- and k33-linked polyubiquitin.* Mol Cell, 2015. **58**(1): p. 95-109.
9. Hospenthal, M.K., S.M. Freund, and D. Komander, *Assembly, analysis and architecture of atypical ubiquitin chains.* Nat Struct Mol Biol, 2013. **20**(5): p. 555-65.
10. Faggiano, S., C. Alfano, and A. Pastore, *The missing links to link ubiquitin: Methods for the enzymatic production of polyubiquitin chains.* Anal Biochem, 2016. **492**: p. 82-90.
11. Oualid, F.E., D.S. Hameed, D.E. Atmioui, H. Hilkmann, and H. Ovaa, *Synthesis of atypical diubiquitin chains.* Methods Mol Biol, 2012. **832**: p. 597-609.
12. Mevissen, T.E., M.K. Hospenthal, P.P. Geurink, P.R. Elliott, M. Akutsu, N. Arnaudo, R. Ekkebus, Y. Kulathu, T. Wauer, F. El Oualid, S.M. Freund, H. Ovaa, and D. Komander, *OTU deubiquitinases reveal mechanisms of linkage specificity and enable ubiquitin chain restriction analysis.* Cell, 2013. **154**(1): p. 169-84.
13. Mulder, M.P.C., R. Merkx, K.F. Witting, D.S. Hameed, D. El Atmioui, L. Lelieveld, F. Liebelt, J. Neefjes, I. Berlin, A.C.O. Vertegaal, and H. Ovaa, *Total Chemical Synthesis of SUMO and SUMO-Based Probes for Profiling the Activity of SUMO-Specific Proteases.* Angew Chem Int Ed Engl, 2018. **57**(29): p. 8958-8962.
14. Fushman, D. and K.D. Wilkinson, *Structure and recognition of polyubiquitin chains of different lengths and linkage.* F1000 Biol Rep, 2011. **3**: p. 26.
15. Randles, L. and K.J. Walters, *Ubiquitin and its binding domains.* Front Biosci (Landmark Ed), 2012. **17**: p. 2140-57.
16. Komander, D. and M. Rape, *The ubiquitin code.* Annu Rev Biochem, 2012. **81**: p. 203-29.

17. Wu-Baer, F., T. Ludwig, and R. Baer, *The UBXN1 protein associates with autoubiquitinated forms of the BRCA1 tumor suppressor and inhibits its enzymatic function.* Mol Cell Biol, 2010. **30**(11): p. 2787-98.
18. Virdee, S., P.B. Kapadnis, T. Elliott, K. Lang, J. Madrzak, D.P. Nguyen, L. Riechmann, and J.W. Chin, *Traceless and site-specific ubiquitination of recombinant proteins.* J Am Chem Soc, 2011. **133**(28): p. 10708-11.
19. Wals, K. and H. Ovaa, *Unnatural amino acid incorporation in E. coli: current and future applications in the design of therapeutic proteins.* Front Chem, 2014. **2**: p. 15.
20. Leestemaker, Y., A. de Jong, and H. Ovaa, *Profiling the Activity of Deubiquitinating Enzymes Using Chemically Synthesized Ubiquitin-Based Probes.* Methods Mol Biol, 2017. **1491**: p. 113-130.
21. Hewings, D.S., J.A. Flygare, M. Bogyo, and I.E. Wertz, *Activity-based probes for the ubiquitin conjugation-deconjugation machinery: new chemistries, new tools, and new insights.* FEBS J, 2017. **284**(10): p. 1555-1576.
22. Shrestha, R.K., J.A. Ronau, C.W. Davies, R.G. Guenette, E.R. Strieter, L.N. Paul, and C. Das, *Insights into the mechanism of deubiquitination by JAMM deubiquitinases from cocrystal structures of the enzyme with the substrate and product.* Biochemistry, 2014. **53**(19): p. 3199-217.
23. Hameed, D.S., A. Sapmaz, L. Burggraaff, A. Amore, C.J. Slingerland, G.J.P. van Westen, and H. Ovaa, *Development of a Ubiquitin based probe for metalloprotease deubiquitinases.* Angew Chem Int Ed Engl, 2019.
24. Worden, E.J., C. Padovani, and A. Martin, *Structure of the Rpn11-Rpn8 dimer reveals mechanisms of substrate deubiquitination during proteasomal degradation.* Nat Struct Mol Biol, 2014. **21**(3): p. 220-7.
25. Pathare, G.R., I. Nagy, P. Sledz, D.J. Anderson, H.J. Zhou, E. Pardon, J. Steyaert, F. Forster, A. Bracher, and W. Baumeister, *Crystal structure of the proteasomal deubiquitylation module Rpn8-Rpn11.* Proc Natl Acad Sci U S A, 2014. **111**(8): p. 2984-9.
26. Perez, C., J. Li, F. Parlati, M. Rouffet, Y. Ma, A.L. Mackinnon, T.F. Chou, R.J. Deshaies, and S.M. Cohen, *Discovery of an Inhibitor of the Proteasome Subunit Rpn11.* J Med Chem, 2017. **60**(4): p. 1343-1361.
27. Echalier, A., Y. Pan, M. Birol, N. Tavernier, L. Pintard, F. Hoh, C. Ebel, N. Galophe, F.X. Claret, and C. Dumas, *Insights into the regulation of the human COP9 signalosome catalytic subunit, CSN5/Jab1.* Proc Natl Acad Sci U S A, 2013. **110**(4): p. 1273-8.
28. Ekkebus, R., S.I. van Kasteren, Y. Kulathu, A. Scholten, I. Berlin, P.P. Geurink, A. de Jong, S. Goerdayal, J. Neefjes, A.J. Heck, D. Komander, and H. Ovaa, *On terminal alkynes that can react with active-site cysteine nucleophiles in proteases.* J Am Chem Soc, 2013. **135**(8): p. 2867-70.
29. Matilainen, O., S. Jha, and C.I. Holmberg, *Fluorescent Tools for In Vivo Studies on the Ubiquitin-Proteasome System.* Methods Mol Biol, 2016. **1449**: p. 215-22.
30. Mulder, M.P., K. Witting, I. Berlin, J.N. Pruneda, K.P. Wu, J.G. Chang, R. Merkx, J. Bialas, M. Groettrup, A.C. Vertegaal, B.A. Schulman, D. Komander, J. Neefjes, F. El Oualid, and H. Ovaa, *A cascading activity-based probe sequentially targets E1-E2-E3 ubiquitin enzymes.* Nat Chem Biol, 2016. **12**(7): p. 523-30.
31. van Wijk, S.J., S. Fulda, I. Dikic, and M. Heilemann, *Visualizing ubiquitination in mammalian cells.* EMBO Rep, 2019. **20**(2).
32. Hameed, D.S., A. Sapmaz, L. Gjonaj, R. Merkx, and H. Ovaa, *Enhanced Delivery of Synthetic Labelled Ubiquitin into Live Cells by Using Next-Generation Ub-TAT Conjugates.* Chembiochem, 2018. **19**(24): p. 2553-2557.

33. Fawell, S., J. Seery, Y. Daikh, C. Moore, L.L. Chen, B. Pepinsky, and J. Barsoum, *Tat-mediated delivery of heterologous proteins into cells.* Proc Natl Acad Sci U S A, 1994. **91**(2): p. 664-8.
34. Erazo-Oliveras, A., K. Najjar, L. Dayani, T.Y. Wang, G.A. Johnson, and J.P. Pellois, *Protein delivery into live cells by incubation with an endosomolytic agent.* Nat Methods, 2014. **11**(8): p. 861-7.
35. van Tilburg, G.B., A.F. Elhebieshy, and H. Ovaa, *Synthetic and semi-synthetic strategies to study ubiquitin signaling.* Curr Opin Struct Biol, 2016. **38**: p. 92-101.
36. Vander Linden, R.T., C.W. Hemmis, B. Schmitt, A. Ndoja, F.G. Whitby, H. Robinson, R.E. Cohen, T. Yao, and C.P. Hill, *Structural basis for the activation and inhibition of the UCH37 deubiquitylase.* Mol Cell, 2015. **57**(5): p. 901-911.
37. Sahtoe, D.D., W.J. van Dijk, F. El Oualid, R. Ekkebus, H. Ovaa, and T.K. Sixma, *Mechanism of UCH-L5 activation and inhibition by DEUBAD domains in RPN13 and INO80G.* Mol Cell, 2015. **57**(5): p. 887-900.
38. Lee, M.J., B.H. Lee, J. Hanna, R.W. King, and D. Finley, *Trimming of ubiquitin chains by proteasome-associated deubiquitinating enzymes.* Mol Cell Proteomics, 2011. **10**(5): p. R110 003871.
39. Passioura, T. and H. Suga, *A RaPID way to discover nonstandard macrocyclic peptide modulators of drug targets.* Chem Commun (Camb), 2017. **53**(12): p. 1931-1940.

Nederlandse Samenvatting

Het doel van dit onderzoek is het bestuderen van de Ub-signaalroute door middel van het synthetiseren van nieuwe bouwstenen gebaseerd op het eiwit ubiquitin (Ub).

Sinds zijn ontdekking is het Ub eiwit uitgebreid bestudeerd en daaruit is gebleken dat het eiwit essentieel is voor verschillende processen in de cel. Naast het binden aan eiwitten voor afbraak in de cel is Ub ook betrokken bij deeltjestransport, het repareren van beschadigd DNA en verschillende andere processen. Tezamen vormen zij een complexe route, de zgn. ubiquitinroute.

Omdat er een groot aantal eiwitten betrokken is in deze hele route is het belangrijk om een uitgebreide set bouwstenen te ontwikkelen zodat de biologie van deze eiwitten in de cel bestudeerd kan worden. Zulke bouwstenen helpen ons de principes van de Ub-signaalroute te begrijpen maar ook om mogelijk therapeutische doelen in de Ub-route te identificeren omdat zij een belangrijke rol spelen bij ziekten. Het aanpassen van de enzymen die betrokken zijn bij de Ub-transductie heeft ook een belangrijke rol bij de behandeling van verschillende ziekten, waaronder kanker.

In het verleden werden grote polypeptiden gesynthetiseerd door korte peptidefragmenten te koppelen met behulp van diverse chemische bindingstechnieken. De techniek is afhankelijk van de volgorde van de polypeptiden en van de mogelijkheid om het peptide na de synthese te kunnen vouwen. Polypeptiden kunnen worden geproduceerd in kleine stukjes en daarna samengevoegd tot de volledige lengte van een eiwit. Deze methode is de afgelopen jaren verfijnd met als resultaat een grotere efficiency en een hogere opbrengst. Echter de benodigde tussentijdse zuiveringen van de peptidefragmenten maakt deze methode minder geschikt om grotere gevarieerde polypeptiden geautomatiseerd te synthetiseren. Dit kan voorkomen worden door het polypeptide in een keer te synthetiseren. Dat heeft tevens als voordeel dat het de mogelijkheid biedt om op bijna elke plek in het peptide een niet natuurlijk aminozuur in te bouwen.

Deze techniek is erg nuttig gebleken bij de chemische synthese van Ub, mede omdat het eiwit slechts 76 aminozuren bevat en erg goed vouwt na de synthese. Dit geeft dus de mogelijkheid om het eiwit in een keer te synthetiseren met een hoge opbrengst. Daarnaast is het ook mogelijk om bijna elke praktische variant van Ub te maken met zowel natuurlijke als onnatuurlijk aminozuren. Ook kunnen er makkelijk verschillende fluorescerende kleurstoffen of andere componenten aan het begin en aan het eind van Ub gekoppeld worden.

Met deze methode zijn verschillende sets chemisch aangepaste Ub-bouwstenen en Ub-testreagentia gemaakt die werken op een specifieke groep van enzymen. Echter zijn er nog steeds relevante routes die niet volledig begrepen worden vanwege het ontbreken van de juiste bouwstenen. Dit komt voornamelijk door uitdagingen in het ontwerp en het maken van de juiste bouwstenen en reagentia. In dit proefschrift ben ik die uitdaging aangegaan.

De hier gesynthetiseerde reagentia kunnen worden gebruikt om enzymen in de deubiquitination-route te onderzoeken, de relatie tussen functie en structuur van Ub-ketens te bestuderen, een unieke groep enzymen te onderzoeken, Ub-reagentia in levende cellen in te brengen en zelfs voor de selectieve remming van een enzym. Al deze bouwstenen kunnen ingezet worden om fundamentele vragen in de Ub- biologie te beantwoorden. Een eerste stap hiertoe is gezet in dit proefschrift.

List of publications

1. **Hameed, D.S.**, G.B.A. van Tilburg, R. Merkx, D. Flierman, H. Wienk, F. El Oualid, K. Hofmann, R. Boelens, and H. Ovaa, *Diubiquitin-Based NMR Analysis: Interactions Between Lys6-Linked diUb and UBA Domain of UBXN1.* Front Chem, 2019. **7**: 921.

2. **Hameed, D.S**., A. Sapmaz, L. Burggraaff, A. Amore, C.J. Slingerland, G.J.P. van Westen, and H. Ovaa, *Development of Ubiquitin-Based Probe for Metalloprotease Deubiquitinases.* Angew Chem Int Ed Engl, 2019. **58**(41): p. 14477-14482.

3. Mulder, M.P.C., R. Merkx, K.F. Witting, **D.S. Hameed**, D. El Atmioui, L. Lelieveld, F. Liebelt, J. Neefjes, I. Berlin, A.C.O. Vertegaal, and H. Ovaa, *Total Chemical Synthesis of SUMO and SUMO-Based Probes for Profiling the Activity of SUMO-Specific Proteases.* Angew Chem Int Ed Engl, 2018. **57**(29): p. 8958-8962.

4. **Hameed, D.S**., A. Sapmaz, L. Gjonaj, R. Merkx, and H. Ovaa, *Enhanced Delivery of Synthetic Labelled Ubiquitin into Live Cells by Using Next-Generation Ub-TAT Conjugates.* Chembiochem, 2018. **19**(24): p. 2553-2557.

5. **Hameed, D.S**., A. Sapmaz, and H. Ovaa, *How Chemical Synthesis of Ubiquitin Conjugates Helps To Understand Ubiquitin Signal Transduction.* Bioconjug Chem, 2017. **28**(3): p. 805-815.

6. Chojnacki, M., W. Mansour, **D.S. Hameed**, R.K. Singh, F. El Oualid, R. Rosenzweig, M.A. Nakasone, Z. Yu, F. Glaser, L.E. Kay, D. Fushman, H. Ovaa, and M.H. Glickman, *Polyubiquitin-Photoactivatable Crosslinking Reagents for Mapping Ubiquitin Interactome Identify Rpn1 as a Proteasome Ubiquitin-Associating Subunit.* Cell Chem Biol, 2017. **24**(4): p. 443-457 e6.

7. Oualid, F.E., **D.S. Hameed**, D.E. Atmioui, H. Hilkmann, and H. Ovaa, *Synthesis of atypical diubiquitin chains.* Methods Mol Biol, 2012. **832**: p. 597-609.

8. Geurink, P.P., F. El Oualid, A. Jonker, **D.S. Hameed**, and H. Ovaa, *A general chemical ligation approach towards isopeptide-linked ubiquitin and ubiquitin-like assay reagents.* Chembiochem, 2012. **13**(2): p. 293-7.

9. Faesen, A.C., M.P. Luna-Vargas, P.P. Geurink, M. Clerici, R. Merkx, W.J. van Dijk, **D.S. Hameed**, F. El Oualid, H. Ovaa, and T.K. Sixma, *The differential modulation of USP activity by internal regulatory domains, interactors and eight ubiquitin chain types.* Chem Biol, 2011. **18**(12): p. 1550-61.

10. El Oualid, F., R. Merkx, R. Ekkebus, **D.S. Hameed**, J.J. Smit, A. de Jong, H. Hilkmann, T.K. Sixma, and H. Ovaa, *Chemical synthesis of ubiquitin, ubiquitin-based probes, and diubiquitin.* Angew Chem Int Ed Engl, 2010. **49**(52): p. 10149-53.

Curriculum Vitae

Dharjath Ahamed, son of Shahul Hameed, was born on 19th December 1984 in Ambattur, Tamil Nadu in India. In 2006, he finished his Bachelor's degree in Industrial Biotechnology from Government College of Technology, Anna University, Coimbatore (India) with distinction. In 2010, he finished his Master degree in Biomolecular Science (specialization in Cell Biology) from Vrije Universiteit, Amsterdam, the Netherlands. During his Master course, he carried out two internships: the first one in the lab of Prof. dr. Bert de Boer at VU Amsterdam; the second one in the lab of late Prof. dr. Huib Ovaa at the NKI, Amsterdam. It was at the NKI where he was trained in the field of Chemical Biology of ubiquitin proteins. Following the successful completion of the internship project, he continued working as a technician in the spin-off company called UbiQ Bio B.V. at the NKI under the supervision of Prof. dr. Huib Ovaa and Dr. Farid El Oualid. During this time, he was trained in solid-phase peptide synthesis, organic synthesis of peptides possessing unnatural amino acids and in heavy-isotope labelling of proteins using bacterial expression. Besides these, he was also trained in native chemical ligation reactions and in azide-alkyne "click" reactions that are mainly used in the synthesis of diubiquitin molecules. He continued to pursue his PhD in the lab of late Prof.dr.Huib Ovaa under his and Dr. Aysegul Sapmaz's supervision, focusing on further chemical modifications of Ub and in the synthesis of Ub conjugates which were used in solving some outstanding questions in ubiquitin biology. Since the beginning of 2020, he is continuing his research as a post-doctoral fellow in the LUMC lab, focusing on the synthesis of ubiquitin-like protein conjugates and studying the biology behind these proteins. He is also being trained in high-throughput-screening of compounds targeting the enzymes in ubiquitination and deubiquitination process.

Acknowledgements:

I express my deepest gratitude to my late **Prof.dr. Huib Ovaa** for providing me an opportunity to work in this lab and carry out interesting research in the field of ubiquitin biology using chemical tools. He had been a very inspiring mentor who provided me with valuable suggestions and ideas throughout the course of my PhD. In addition, his timely help with scientific publications during my PhD is greatly appreciated. I will miss him dearly and I hope to spread his vision wherever my career takes me to. I also thank **Prof. dr. Sjaak Neefjes** for providing me with excellent motivation and suggestions with my research project. Often, discussions with my supervisors has provided me with out-of-box ideas. Many thanks to **Dr. Aysegul Sapmaz** for motivating and inspiring me to carry-out several challenging aspects of my research and contributing to my publications. Many thanks to my PhD supervisory committee members at the NKI, Amsterdam for providing me with the guidance during the first few years of my PhD. I also thank my PhD evaluation committee members for their time to assess my thesis.

I also thank my former colleagues and current co-workers who helped me with excellent discussions during my PhD work. Without their help in carrying out my experiments and providing me with reagents, this thesis could not have been any better. Special thanks to my collaborators who has shared their projects with me and helped with carrying out several experiments in their lab. Thanks to my paranymphs, **Henk Hilkmann** and **Dr. Alessia Amore** for helping me throughout my PhD and in preparing my thesis and my public defense. Finally, many thanks to my friends and family to have supported and motivated me in this remarkable journey of my PhD.